ISOLATION OF STIGMASTEROL FROM *Piptadeniastrum africanum* (HOOK. F.) AND ITS MODULATORY EFFECT ON MITOCHONDRIAL-MEDIATED CELL DEATH IN LIVER AND COLONIC TOXICITY IN MICE

BY

Folake Olayinka OLOJO

B.Sc. (Hons) Biochemistry (ADO), M.Sc. Biochemistry (Ibadan)

Matric. No.: 152987

A Thesis in the Department of Biochemistry,
Submitted to the Faculty of Basic Medical Sciences
in Partial Fulfilment of the Requirements for the Award of the Degree of

DOCTOR OF PHILOSOPHY

of the

UNIVERSITY OF IBADAN

April, 2023

CERTIFICATION

I certify that this seminar work was carried out by **FOLAKE OLAYINKA OLOJO** with the Matric No: 152987 under my supervision in the laboratories for Biomembrane Research and Biotechnology, Department of Biochemistry, College of Medicine, University of Ibadan. Nigeria.

…….

Supervisor

O. O. Olorunsogo

B.Sc., M.Sc., Ph.D, FNISEB (Ibadan)

Professor and Director, Biomembrane Research Laboratories

Department of Biochemistry

University of Ibadan, Nigeria

……..

Co-Supervisor

C. O. O Olaiya

B. Sc., M. Sc., Ph. D. (Ibadan)

Professor and Director, Nutritional Biochemistry Laboratories,

Department of Biochemistry,

University of Ibadan, Nigeria.

DEDICATION

This Research Work is dedicated to:

The Almighty God, the Most Supreme Being for seeing me through.

My beloved husband, for his strong support and unending love.

My children, for their endurance and tolerance.

ACKNOWLEDGEMENTS

My profound gratitude goes to Almighty God for his mercy, kindness and protection for sustaining me through this programme. May God's name be glorified, amen.

First of all, my sincere appreciation goes to my supervisor, my mentor, tutor and instructor, Professor O.O Olorunsogo for his role in my life, his kindness, intellectual contribution, patience, assistance and for the opportunity given me to run this programme under his tutelage. May your sphere of influence be greater to God's glory and may God crown your efforts with success. Thank you so much sir.

I give God glory for the opportunity to obtain this Doctor of Philosophy under the guidance of the Professor Oyeronke A. Odunola, the Dean in this great Faculty and noble institution. I say a big thank for your usual support, motivation, advise, immense guidance through the course of my programme. Your humility is worthy of emulation. Ma, your motherly role cannot be easily forgotten, may God Almighty bless you. I really appreciate and love you ma.

The unflinching desire to be a better scholar and words of encouragement from Professor E.O Farombi is commendable. Thank you for your kind assistance, great support and training I enjoyed right from Masters class which are very useful towards my career development. May the Lord continue to strengthen you. I am grateful sir.

I cannot but appreciate my teacher and spiritual father, Professor O.A Adaramoye, the Head of this great Department and his family for their love towards me since inception of my programme. May God's goodness and mercy be yours. Thank you, sir. I sincerely appreciate Professor Onasanwo,. The love and efforts from other Professors in the department, Professor M. A Gbadegesin and Professor C.O.O Olaiya cannot be overemphasized. Thank you for your contribution towards the completion of my programme. May God bless you sirs.

I must express my profound gratitude to Dr J.O Olanlokun for his immense contribution, patience, helping hand thank you for always wanting me to be at my best performance throughout my programme. May the Lord you serve increase you in all area. Other lecturers,

Drs. Olubukola T. Oyebode and A. O Olowofolahan work in the Biomembrane Research and Biotechnology Unit., may God bless you and yours for your love and support throughout.

I am grateful to other tutors in the department- Doctors Sarah O Nwoso, A. O Abolaji, Omolola A Adesanoye, Owumi, I. A. Adedara, Oluwatoyin Adeyemo - Salami I. O.Awogbindin, J. O Olugbami, A. M. Adegoke, Esan with Adizsa. God bless you all for your care, support and encouragement towards obtaining a quality research.

I would like to thank Dr (Mrs) Kate Nwokocha, Mr Eric Sabo, Mr Adediran, Mr Okewuyi, Mrs Wuraola Familusi, Mrs Ogunmorokun, Mrs Nwoke, Mr Isiaka Adebiyi, Mr Ajiboye and Mr Bassir for their technical encouragement during my experiments.

My heart goes to the administrative staff- Mrs Bakare, Mr Ogunsola, Mrs Ogunbiyi, Mr Patrick, Mr Akindele and Mr Obadehin for their timely help during my progrogramme.

Special thanks to Professor K. O Adebowale, The Vice Chancellor and Professor Oladosu of Department of Chemistry, University of Ibadan for their efforts towards getting a quality research. I also extend my appreciation to Mrs Grace Egemonu. I am also grateful to my senior colleagues Doctor Adedosu, Temitope Ayeotan, Adejoke Oyedeji, A. Akinrinde, Sade Jemiseye, Olajumoke Nwachefu, Jonah Achem, O.U Oladimeji, Joan Imah-Harry, M. A. Adegoke, O. M. Ogunyemi, B. Ajayi and Isaac Bello for their continuous support to my scientific pursuit.

To other Phd colleagues- Dr A. J Salemcity, Mrs Fatima Musa, Mrs Victoria Opayinka, Mrs Omotunde, Mrs Omosola, Mrs Adeoye, Mrs Ibukun, Mrs Babarinde, Mrs Tosin Obigale and other Biomembrane Postgraduate Students- Yewande, Kelvin, Muiz, Samantha, Tope, your assistance was precious and I really appreciate you all, thanks so much.

I would also like to thank Mr Otegbade, Mr Olaleye, Mr Akinjide (UCH), Mr Adeyemi, Mr Tosin and Mayowa (Pharmaceutical Chemistry), Mr Ayo Habeeb (Pg school), Dr Nestor Johnson, Mrs Victoria (Chemistry), Dr (Mrs) Kike Ilori and everyone at The Polytechnic, Chemistry Department, Ibadan- Mr Anifowose, late Mrs Adegbola, Mr Abiola, Mrs Adegboyega, Dr Olateru, Dr Abiona, Mrs Rasheed-Adeleke, Mrs Olalude, Mr Oketooto, Mrs

Adisa, Mrs Adebayo, Mr Oluwole, Mr alabi, Tola, Zainab, Mariam, Emmanuel, Precious, Queen, Vincentia, Stella, Aanu, Makinde, Dolapo, Ayobami, Lana, Jumoke, Wumi, Dammy, Ebun and others. Thank you all.

My joy knows no bound as I acknowledge with sincere appreciation the love, care, endurance, patience and financial support I always receive from my earthly pillar, my earthly provider, a great man in a trillion husbands - Engineer Samuel A Olojo. Your soothing words and the sacrifices you made really went a long way. May the ground you walk upon produce your increase and we shall live long together to enjoy the fruits of our labour in Jesus name, amen.

My unalloyed gratitude goes to my children- Oluwanifemi, Boluwatife, Oluwafikemi and Oluwasikemi for their understanding, endurance, tolerance, support. Thanks for being there.

I salute the support of my siblings-Bunmi, Adewale, Busayo, Adeniyi, Busola, Adedayo, Adekunle, Seun, Sade, Titi, Folake, Taiwo, kehinde, Elizabeth, cousins, uncles and aunties - Mr Ayo and Romoke Olojo, Dr. K.O Awojobi, Mrs Abayomi and family, Mr Niyi-Fadeyi and family, Mr Doherty and family, Mrs Edun and family, Chief and Mr Akin-Oluwadare and family (Snr and Jnr), Mrs Fagbeja and siblings, Mrs Aina and children, Mr Peter and Ade Odelusi and Families, Mr Dele Ojo and family,

Special appreciation goes to Pst Bamidele Adeniji's family most especially to late Mrs Olubukola Adeniji for engineering my picking up Master's form. May God's presence be with you and the children sir. May the Lord repose the soul of the departed, amen.

My special thanks to my spiritual leaders for their prayers and encouragement, Pst Abisona and family, Prof. (Pst) Ayo Arije and family, Pst Adisa and family, Pst (Mrs) Dayo Jide-Akinrinde, Pst (Mrs) Porter and family, Pst Akinyemi and family, Pst Olayemi and family, Pst Adeola and family, Pst Akinola and family, Pst Afolabi and family, Pst Adesina and family, Pst Popoola and family, Pst Falaye and family, Pst Akinsola and family, Pst Odigie and family, late Pst Adedeji and family, Pst Odeseye and family, Pst Olufemi and family, Pst Johnson and family, Pst Folayan and family, Pst Kehinde and family, Pst Alaka and family, Pst Akintunde and family, Pst Bunmi Ojo and family, Pst Funmi Omotunde and family, A/P Olulegan, A/P Adebisi, A/P Doris, A/P Akinwale and family, Dcn Adedibu and family, Mr

and Mrs Lawal, Mrs Okunubi and family, Holy Ghost Power cathedral members etc to the Adegokes, Isolas, Aladeloye-Odeleyes, Ade-Ojos, Ajalas, Isas, Adeyemos, Funmi, Bola, Bose, Tola, Folake, Seyi, Tope, Kike, Taiwo, Aduke, Abike, Ronke, Tinuade, Favour, Bola, Doyin, Yemisi, Foluso, Risi, Ganiat, Sola, Adeola, Grace, kehinde Baruwa, George, Bernard, Comfort, Tokunbo,…God bless you all.

I must mention my dependable and able colleagues-Ushers Aderemi, Bimbo, Awotoye, Majekodunmi, Abayomi, Fisher, Sanda, Aina, Ayodele, Modupe, Adesina, Esan, Ayeni, Onijala, Rebecca, Ayobami, Callistus, Segun, Blessing, Patience, Funmilayo, Christiana, Bright, Bola, Taiwo, Akanbi, Yemi, Seyi, Wumi, Lekan, Bosede, Abiola, mummy Habeeb, Kujore, Faleye, Adanike and Jolayemi etc. I love you all.

Thank God.

ABSTRACT

Hepatocellular and colonic damage are fatal outcomes arising from liver and colon toxicity. Modulation of mitochondrial-mediated cell death is a strategy in these diseases management. The use of synthetic drugs in the treatment of these diseases presents several side effects. In folklore, *Piptadeniastrum africanum* (PA) is used for the treatment of these disorders but the mechanism has not been explored. This study was designed to investigate the role of bioactive compound(s) purified from PA on liver and colon damage via the modulation of mitochondrial-dependent cell death.

The stem bark of *Piptadeniastrum africanum* was collected from a forest at Ibadan, identified at the department of Botany, University of Ibadan (UIH-22562) air-dried, pulverised and soaked in absolute methanol to obtain its extract (CMEPA). The CMEPA was fractionated using n-hexane, chloroform, ethyl acetate and methanol to obtain their respective fractions (HFPA, CFPA, EFPA and MFPA) which were tested on mitochondrial permeability transition (mPT) pore opening and ATPase activity (*in vitro*). The effects of the fractions of PA on liver and colon tissues were evaluated in study 1. Twenty mice (20±2g; n=5) were grouped and treated as follows, groups 1 (vehicle), 2, 3 and 4 were treated intraperitoneally with 25, 50 and 100 mg/kg of EFPA once daily for 14 days and liver mPT assayed. The EFPA was purified using column chromatography to obtain a pure compound which was characterised as stigmasterol by spectroscopic techniques. In study 2, forty-two mice were grouped (n=7), treated with Dextran Sulphate Sodium (DSS) and Benzo{a}Pyrene (BaP) for 10 days as follows, groups 1 (vehicle), 2 (oral 4% DSS), 3 (125mg/kg BaP), 4 (DSS+BaP), 5 (DSS+BaP and 200mg/kg of stigmasterol) and 6 (DSS+BaP and 400mg/kg of stigmasterol). The mice were sacrificed and colon samples prepared. Tumor Necrosis Factor-α (TNF-α), Interleukin 6 (IL-6), p53, Caspases 9 (C9), Bax, Bcl-2, were performed on the colon using immunohistochemistry. All data were analysed using descriptive statistics and ANOVA at $\alpha_{0.05}$.

In vitro, EFPA had the highest induction of mPT pore opening (3.80, 5.60, 6.40, 8.10 and 8.90 folds) at 20, 60, 100, 140 and 180µg/ml, respectively and enhanced ATPase activity (0.20±0.01, 0.35±0.10, 0.40±0.10, 0.45±0.20 and 5.20±0.80µmole/Pi/mg/protein/min), relative to the vehicle (0.05µmole/Pi/mg/protein/min), respectively. *In vivo*, EFPA caused mPT induction of 2.50, 4.90 and 6.90 folds at 25, 50 and 100mg/kg, respectively. The toxicant groups (DSS, BaP and DSS+BaP), relative to the vehicle significantly increased TNF-α (40.00±1.20%, 30.00±0.90%, 34.00±1.10% vs 15.00±0.70%), IL-6 (160.00±3.50%, 110.00±2.20%, 120.00±1.50% vs 60.00±1.50%) and p53 (80.00±2.30%, 70.00±1.10%, 85.00±2.20% vs 25.00±0.90%) However, stigmasterol (200 and 400mg/kg), relative to DSS+BaP significantly attenuated TNF-α (12.00±0.09%, 13.00±0.10% vs 34.00±1.10%), IL-6 (53.00±1.30%, 50.00±1.20% vs 120.00±1.50%), p53 (40.00±2.20%, 50.00±1.70% vs 85.00±2.20%). The DSS, BaP and DSS+BaP, relative to the vehicle increased C9 (1.10±0.10, 0.90±0.01, 1.10±0.10ng/ml vs 0.01ng/ml), Bax (120.00%, 100.00%, 90.00% vs 110.00%) and reduced Bcl-2 (80.00%, 75.00%, 75.00% vs 90.00%) which were modulated by stigmasterol.

Stigmasterol isolated from the *Piptadeniastrum africanum* modulated mitochondrial-mediated cell death via a decrease in pro-inflammatory cytokines and levels of pro-apoptotic proteins.

Keywords: Colon damage, Cytokines, Liver, *Piptadeniastrum africanum*, Stigmasterol
Word count: 490

TABLE OF CONTENTS

LIST OF FIGURES

LIST OF TABLES

LIST OF PLATES

LIST OF FORMULA

ABBREVIATIONS

AGR	Antigen 5-related
AMP-PNP	ATP analog, adenosine 5'-(beta, gamma-imido) triphosphate
ATP	Adenosine Triphosphate
BAD	Basic-Acidic Dipeptide
BAK	Bcl-2antagonist killer 1
BaP	Benzo [a] Pyrine
BAX	Bcl-2 Associated X Protein
BCL-2	B-cell lymphoma 2
BH	Bcl-2 homology
BH_3	Borane
BID	BH_3 Interacting Death Agonist
BIM	Bisindolymaleimide
BMF	Bcl-2 Modifying Factor
CA^{2+}	Calcium ion
CsA	Cyclosporin A
CYP	Cytochrome P450
CYP1A1	Cytochrome P450 1A1
CYP1A2	Cytochrome P450 1A2
CYP1B2	Cytochrome P450 1B2
CypD	Cyclophilin D
DNA	Deoxyribonucleic acid
DSS	Dextran sulfate sodium
ETC	Electron Transport Cycle
F_0F_1	F-type ATP Synthase
FAD	Flavin Adenine Dinucleotide
FADH	Flavin Adenine Dinucleotide
GC-MS	Gas Chromatography- Mass Spectrometry
GST	Glutathione-S-transferase
H+	Hydrogen
H_2O_2	Hydrogen Peroxide

HCC	Hepatocellular Carcinoma
HCL	Hydrochloric acid
HEP G2	Hepatoma Cell Line G2
HRK	Harakiri protein
IARC	International Agency for Research on Cancer
IMM	Inner Mitochondrial Membrane
KCL	Potassium Chloride
MCL-1	Myeloid-cell leukemia 1
MFO	Mixed Function Oxidase
Mg^{2+}	Magnesium
$MG^{2+/}$ADP	Adenosine Diphosphate
MM	Mitochondria Membrane
MMC-PTR	Mucosa mast cell-
MOMP	Mitochondrial Outer Membrane Permeabilization
NAD	Nicotinamide Adenine Dinucleotide
NADH	Nicotinamide Adenine Dinucleotide
NMR	Nuclear Magnetic Resonance
NOXA	Phorbol-12-myristate-induced protein
nS	nano second
O_2	Oxygen
OSCP	Oligomycin-sensitivity Conferring Protein
OX PHOS	Oxidative Phosphorylation
p53	Tumor protein
PCD	Program cell Death
Pi	Inorganic Phosphate
PPIF	Peptidyl-prolyl cis-trans isomerase, mitochondrial
PPLASE	Peptidyl-prolyl cis-trans isomerase
PTP	Protein tyrosine phosphatases
PUMA	p53 Upregulated modulator of Apoptosis
RF	Radio Frequency
ROS	Reactive Oxygen Species

U	Ubiquinone
UCP2	Uncoupling Protein 2
UV	Ultraviolet

CHAPTER ONE
INTRODUCTION

1.1 Background to the study

Inflammation, a necessary reaction of the body, allows, simultaneously with the restoration of damaged tissues, to get rid of dangerous signals (Farombi, 2011; Chen *et al*., 2018). Inflammation is a defence plan that has gradually evolved in multicellular organisms as a way to respond to aggressive factors such as tissue damage, microbial invasion, and other unpleasant circumstances. This mechanism helps the host cell to repel an aggressive invasion and also triggers the repair of damaged tissues (Chen *et al*., 2018). However, excessive inflammation leads to cell death.

Over the years, accumulating evidence has shown that inflammation is very important in supporting cancer, especially the process of tumor formation (oncogenesis). The inflammatory environment is always important for the development of tumors (deVisser *et al*, 2006). Research shows that cancer cells proliferate easily in an inflammatory microenvironment and also promote mutations related to the formation of reactive oxygen species, which leads to DNA breakage and genomic imbalance (Grievnikov *et al*., 2010). However, it should be aware that not all chronic inflammation leads to cancer. For example, rheumatoid arthritis exacerbates inflammatory bowel disease and chronic liver failure (hepatitis), but not cancer. It can be caused by direct exposure to both dietary and environmental carcinogens such as heavy metals, phalate compounds, and benzo(a)pyrene.

Toxicity of the colon result from inflammation of the colon as a result of infection through environmental factors (chemicals), contaminated water, poor hygiene, etc., manifested by symptoms such as diarrhea, weight loss, blood spots in the anal region (Abegunde *et al*., 2016). A frequent origin of death, such as neurodegenerative diseases is chronic inflammation (Furman *et al.*, 2019), while some orthodox drugs have shown significant

effects through the modulation of apoptosis pathways in experimental animals (Alatize *et al*., 2012; Kim *et al*., 2019). In addition, surgery, chemotherapy, and radiotherapy are also used to treat severe stages of relative inflammation (Chen *et al*., 2018). These applications are related with numerous problems, like high cost of drugs, as well as various side effects associated with chemotherapy or radiotherapy (Arruebo *et al.*, 2011).

Apoptosis, which is the controlled destruction of cells, often occurs to establish homeostasis between cell development and cell death (Hassan *et al*., 2014). Unregulated cell proliferation or an autoimmune syndrome can lead to apoptotic dysfunction. Therefore, apoptosis is very important, starting with the development of the embryo in the body throughout its life, along with tissue renewal and removal of inflammatory cells (Obeng, 2021). It is this activity that is responsible for the necessary removal of old and damaged cells to ensure complete homeostasis of the cellular composition of tissues and organs (Kaina, 2011).

Apoptosis plays a very important role in cell development, differentiation, proliferation (Bergmann, 2010) and it can be activated by DNA damage, stress, or toxin (Lopex and Tait, 2015). Some of the diseases associated with suppression of apoptosis include cancer, autoimmune diseases, ischemia, and others (Xu *et al*., 2019). All cells have been reported to have an intracellular stimulus that can induce death at any time (Lavrik *et al.* 2005). It is a properly regulated and ATP-mediated mechanism that causes the initiation of a class of cysteine proteinases known as caspases, which through their cascade orchestrate cell disassembly, responsible for the proteolytic activity and cleavage occuring during apoptosis at aspartic acid residues.

Several pathways can initiate or inhibit apoptosis, but the two main pathways are the death effector and mitochondrial-mediated pathways also known as extrinsic and intrinsic (Jan and Chaudhry, 2019). The extrinsic pathway depends on the binding of signalling molecules to a receptor present on the surface of the cell membrane, while the intrinsic pathway is initiated by stress, causing damage to the cell, which leads to mitochondrial outer membrane permeability (MOMP), resulting in the release of proteins such as cytochrome c and others. Apoptotic processes are controlled by the Bcl-2 family and caspases, respectively.

Mitochondrial modulation relates to mitochondrial-mediated apoptosis, which leads to a decrease in the potential of membrane and release of cytochrome c (Vianello *et al*., 2012).

Pores openings are activated by calcium overload, oxidative stress and membrane depolarization (Carraro *et al*., 2020). However, the identity of the pore is not known, but it is thought to be opened by the interaction of a number of programmed cell death proteins (Flores-Romero *et al*., 2020). Blender *et al.*, (2017) reported that excessive apoptosis causes tissue inflammation, which is also a pathological condition that occurs when apoptosis is dysregulated (Boehm, 2006).

Therefore, more effective and less toxic strategies needed to be developed (World Health Organisation, 2012). Recently, the progress of possible therapies with medicinal plants has been widely recognized due to their important biological activity, little side effects, as well as their low cost (World Health Organization, 2018). In addition to Western medicine, there is a class of traditional herbal remedies known as folk medicines that have great antitoxic potential. For thousands of years, medicinal plants have been used to treat different diseases, including epidemics. The understanding of their therapeutic properties has transformed over years within and among human communities (Sofowora *et al*., 2013). Bioactive compounds in plant extracts are applied in the treatment of diseases, as well as to develop new dosage forms in the pharmaceutical industry (Singh *et al*., 2007).

Medicinal plants have been used to treat health disorders (Singh, 2015), which contain active ingredients without serious side effects in relation to research studies (Wu *et al* ., 2019; Payab *et al*., 2020). Some traditional medicinal herbs such as *Senna alata* traditionally used in Nigeria in the treatment of bacterial and fungal infections (Seenivasan *et al.* 2010) and *Piptadeniastrum africanum* has been reported to show great pharmacological potential managing malaria and intestinal disorder.

Piptadeniazrtum africanum) is a plant of the Mimosa family, found in different forests of Western Nigeria (Owoeye *et al*., 2018). It is called Kiryar "kurmi" in Hausa, "ofi" in Igbo and "agboyin in Yoruba" (Hutchison and Daiziel, 2015). It contains alternate and bipinnate leaflets (Burkill, 2014). *Piptadeniastrum africanum* can treat diseases such as malaria, toothache and human colon cancer (Mengome *et al.,* 2009; Hutchison and Daiziel, 2015). Mengome *et al*., 2009 reported that it contains biologically active compounds such as

tannins, flavonoids and cardiac glycosides. Several studies on the plant have identified its antibacterial, antiulcer, antiproliferative, antioxidant as well as anti-inflammatory properties (Owoeye *et al*., 2018; Diamini *et al*., 2019).

1.2 Rationale of the study

Plant bioactive components have been identified as agents that have potential therapeutic efficacy against disease (Mensah *et al*., 2019). It is well known that certain pathological conditions such as neurodegenerative diseases and tumor development can results due to dysregulation of programmed cell death (Favaloro *et al*., 2021).

The development of therapeutic approaches based on the control of programmed cell death has recently attracted attention in connection with drug discovery. In particular, manipulation of mitochondrial-mediated cell death is an approach for the effective treatment of conditions related to apoptosis dysregulation (Oyebode *et al*., 2012).

The release of cytochrome c follows the opening of the pore of mitochondrial membrane (Li *et al.,* 2017). For instance, homoisoflavanone-1, a natural compound extracted from *Polygonatum. odoratum*, curing lung cancer cell death (Ning *et al*., 2018). Also, thymoquinone isolated from the seeds of *Nigella sativa* induced apoptosis via mitochondrial pathway in numerous cancer cell lines (Zhang *et al*., 2018).

Studies from our laboratories also provide compelling evidence that certain medicinal plants modulate mitochondria-mediated cell death (Olanlokun *et al.,* 2017, Olowofolahan *et al.,* 2017, Oyebode *et al.,* 2017; Oyebode *et al.,* 2018). Betulinic acid, a natural product in clinical trials, induces apoptosis through mitochondria membrane permeability transition opening (Olanlokun *et al.,* 2021).

This phenomenon has made mitochondrial-mediated cell death a universal strategy for drug development. *Piptadeniastrum africanm* are medicinal plants that are folklorically used to treat colon disorders and other ailments (Mengome *et al.* 2009; Hutchinson and Dalziel 2015).

It is not known whether *P. africanum* modulates mitochondria-mediated cell death. In addition, it has not be identified, the mechanism by which it prevents colonic upset. Thus,

it is pertinent to ascertain if *P. africanum* contains bioactive compounds that can modulate specific cell death in liver and colon diseases.

1.3 Aim

This research, therefore intended to assess whether *P. africanum* has bioactive compounds that can cause mitochondrial-mediated cell death in liver and colon disorder in mice.

1.4 Specific objectives include the following:

i. To screen for the phytochemicals of *P. africanum* stem bark
ii. To evaluate the inductive effect of crude extract and fractions of *P. africanum* on apoptotic biomakers via mPT, cytochrome c, ATPase and mLPO (*in vitro*)
iii. To determine the representative profile of the most potent (Ethyl acetate) fraction on mPT, ATPase, mLPO, caspases 9 and 3 (*in vivo*)
iv. To evaluate the plant (PA) toxicity through haematological parameters, liver function test (LFT), Renal function test (RFT), antioxidant and histological examination)
v. Activity bio-guided assays of the most potent *P. africanum* (Ethyl acetate), will be carried out.
vi. Identification and isolation of the purified compound using Gas Chromatography Mass Spectrometry and Nuclear Magnetic Resonance (GC-MS and NMR)
vii. Modulatory effect of isolated stigmasterol on apoptotic biomakers (mPT, Bcl2, Bax, caspases 9 and 3, DNA fragmentation)
viii. Evaluate the ameliorative effect of stigmasterol on DSS/BaP-induced colon toxicity and inflammatory biomarkers (TNFα, IL-6, p53)

CHAPTER TWO
LITERATURE REVIEW

2.1 Apoptosis

Caspase-mediated cell death, programmed death of cell type 1, can be described as genetically controlled mode of self-destruction. Activation of apoptosis is induced by appropriate internal and external stimuli leading to DNA condensation, membrane swelling and shrinkage of affected cells due to stimulation of the Bcl-2 cascade of caspases (Kroemer *et al*., 2009). Apoptosis occurs in an amazing way, avoiding damage to cells and tissues around the affected cells, which also leads to the stimulation of an immunological response. After enough stimuli, unwanted cells are removed from the body through a process called apoptosis. Activation of the caspase cascade leads to DNA condensation, membrane swelling, and cell contraction.

Therefore, apoptosis prompts the destruction of damaged or contaminated cells. Apoptosis can also be called regulated or programmed death cells. Unlike inflammation, apoptosis does not have a destructive effect on neighbouring cells; it only gently destroys the infected cells and destroys them without disturbing others. It has been reported that if apoptosis is not stopped, diseases such as diabetes mellitus and neurodegenerative can occur. Contrarily, apoptosis is often avoided in various types of cancer (Chen *et al.*, 2019). Thus, it is necessary to decipher the essence of this process in order to develop new ideas about how to deal with various diseases.

2.2 Physiological and patological role of programmed cell death

Apoptosis is a sequential control of cell death, often existing to maintain homeostasis between the rate of cell formation and cell death. It is a sequential order of cell death that occurs regularly to ensure a homeostatic balance between the rate of cell formation and cell death. Apoptosis is controlled in an organized manner to eliminate any defects in cells as

well as tissues. On the other hand, downregulated apoptosis may result in aberrant cell growth or proliferation as well as autoimmune diseases. This demonstrates that apoptosis is essential from the very beginning of embryonic development all the way through the growth of the organism.

Apoptosis is responsible for initiating tissue renewal by getting rid of inflammatory cells. However, if this balancing function is disturbed, it may lead to aberrant cell growth or proliferation as well as other conditions such as autoimmune illnesses. As a result, apoptosis is regarded as an essential process in terms of embryonic development all the way through the growth of the organism.. Apoptosis is responsible for the destruction of cell shrinkage, membrane swelling, DNA protrusion, and DNA fragmentation. The B-cell lymphoma-2 (BCL-2) anti- and pro-apoptotic protein family is responsible for regulating apoptosis pathways. This protein family is split into three subgroups according to its structure and function owing to the presence of conserved areas known as BCL-2 homology domains (motives of BH).

Anti-apoptotic proteins such as (BCL-2, MCL-1, BCL-W, and AI/BFL1) and B\H3-only proteins such as (PUMA, NOXA, BMF), BAX and BAK, as well as proteins with multiple BH domains, are estimated to be the initiators and effectors of apoptosis. These proteins appear as oligomers, which results in mitochondrial outer membrane permeabilization (MOMP), followed by the release of (aspartate-specific cysteine proteases). Programmed cell death PCD is very well structured within the physiological systems that are used to repair any abnormality in cells or tissues (Moujalled *et al*., 2021). Cell shrinkage, membrane swelling, and formation of membrane protrusions and fragmentation are three well-known apoptotic cell disassembly processes. Proteins containing only BH3 (BIM, PUMA, BID, BMF, BAD, HRK, BIK, and NOXA) are critical initiators of apoptosis. Proteins with multiple BH domains (BAX and BAK) are the main effectors of apoptos (Redza-Dutordoir and Averilbates, 2016; Kelly and Strasser, 2020).

Caspases, when triggered, break hundreds of cellular substrates, generating morphological evidence of apoptosis as well as cell demise (Singh *et al*., 2019). In multicellular organisms, the formation of normal tissue and the maintenance of homeostasis are dependent on the organization and stringent regulation of PCD signaling processes. During embryogenesis,

the removal of cells via the process of programmed cell death (PCD) is required to ensure the proper creation of particular tissues. One such example is the production of vertebral digits. The PCD is responsible for the formation of the central nervous system (CNS), which includes the brain and spinal cord. Neural architecture is established as a result of signaling proceedings which carefully controlled at the certain (temporal and spatial) levels.

Apoptosis is the primary mode of programmed cell death that occurs throughout the normal embryonic and postnatal development of the nervous system. Apoptosis can have an effect on many different cell populations, such as neural progenitor cells (NPCs), differentiated postmitotic neurons, and glial cells. This helps to ensure that only cells that are the appropriate size and shape and have established the appropriate connections to their axons and neurites are allowed to survive (Kuan *et al*., 2009).

2.3 Biochemical features of apoptosis

Phagocytic manifestation, cleavage of protein and DNA are some of the many biochemical alterations of apoptotic cells that contribute to the typical pathology that was discussed before. Other biochemical modifications include fragmentation of apoptotic cells' mitochondria (Hengartner, 2000). Caspases are shown in the inactive proenzyme form. Once activated, caspases have the ability to often activate additional procaspases, which in turn allows for the fast start of proteases. The pro-caspases that have been accumulating will eventually become active. This activation proteolytic cascade, in which one caspase might trigger another caspase, contributes significantly to the process of apoptotic transmission and cell death.

Caspases are the enzymes responsible for the proteolytic activity and cleavage that occurs at aspartic acid residues. However, various caspases have distinct relevancies, including the ability to acknowledge surrounding amino acids. As soon as caspases are activated, an apparent irreversible connection to the process of cell death seems to take place. It has been shown that there are a total of ten (10) important caspases, which may be broken down into the following categories: initiating (caspases-2, -8, -9, and -10), effector or executive (caspases-3, -6, and -7), and inflammatory (caspases-1, -4, and -5) (Rai *et al*., 2005).

2.4 Extrinsic pathway

Interactions mediated by transmembrane receptors, which are members of the tumor necrosis factor (TNF) receptor gene superfamily, are included among the extracellular signalling pathways that are responsible for the initiation of a programmed cell death (Locksley *et al*., 2001). The family have extracellular domains that are rich in cystidine and a region in the protoplasm known as the "death domain" that has around 80 amino acids (Ashkenazi and Dixit, 1998). Because of this, an essential role in the process of ignaling death from the cell surface to the intracellular signaling system is eliminated. To this point, the ligands and comparable death receptors that have been found include TNF-/TNFR1, FasL/FasR, and others (Rubio-Moscardo *et al*., 2005).

The result of the programmed cell death may be predicted based on the sequence of events that take place. These processes are indicated using models such as FasL/FasR and TNF-/TNFR1, in which receptors construct a homologous trimeric ligand, adaptor proteins are recruited, and death domains link receptors (Vajant, 2002). The proteins that are produced as a consequence (FADD or TRADD) link to procaspase 8, which results in the formation of a death-inducing signaling complex (DISC) that triggers the autocatalytic tripping of pro-caspase 8. (Hsu *et al*., 1995). The activation of caspase 8 marks the beginning of the execution stage of apoptosis (Hitoshi *et al*., 1998).

2.5 The Perforin / Granzyme way

The T cell-mediated cytotoxicity, also known as CTLs, is a type IV hypersensitivity variation that has the ability to kill chosen cells from the outside. The primary method of CTL-induced apoptosis is the ligand and receptor connection (Kawamura *et al.*, 2019). Granules include a number of serine proteases, the most important of which are grandzymes A and B. (Pardo *et al*., 2004). It has been reported that pro-caspase 10 can enhance death signal through intrinsic apoptotic mechanism by specifically cleaving BID with release of cytochrome c. The activation of pro-caspase 10 was caused by the separation of grandzyme B from other proteins at an aspartic residue, and it has also been reported that this separation triggered pro-caspase 10. (Russell and Ley, 2002). Granzyme B has the ability to trigger

apoptosis by skipping steps in the signaling pathway's ascending sequence, which results in the activation of caspase 3 directly.

Granzyme A induces programmed cell death via caspase-independent routes, in addition to playing a crucial part in cytotoxic T cell-induced cell death. Granzyme A is responsible for the cleavage of DNA by DNase NM23-H1 (Fan *et al*., 2003). This plays an important role in immune surveillance, which helps put an end to cancer by causing apoptosis in tumor cells. Apoptotic DNA is destroyed when SET, the nucleosome assembly protein, is cleaved by grandzyme A protease. This frees up NM23-H1 inhibition, which allows apoptotic DNA to be degraded. In addition to its involvement in M23-H1 inhibition, the SET complex (composed of SET, Apel, pp32, and HMG2) plays an important part in the structure of chromatin and the repair of DNA (Lieberman and Fan, 2003). However, granzyme A's ability to inactivate this complex, which de turn obstructs the preservation of DNA integrity and chromatin structure, is what ultimately leads to the promotion of apoptosis.

2.6 Intrinsic pathway

High size of cytoplasmic calcium, reactive oxygen species (ROS), among other stimuli initiates the mitochondrial-mediated intrinsic pathway (Shoshan-Barmatz and Ben-Hail, 2012). Intracellular signals that can manifest in positive and negative manners are produced by stimuli that strat intrinsic apoptosis pathway. Negative signals bring about apoptosis in the absence of growth factors, cytokines, the death events will be suppressed, hence apoptosis.

The induction by these stimuli results in morphological changes causing opening of mitochondrial permeability transition pore (MPTP). The opening of the pore sequestered pro- apoptotic proteins such as cytochrome c into the cytosol from intermembrane space (Garrido *et al*., 2006). These proteins stimulate proteinase-dependent intrinsic pathway of apoptosis forming “apoptosome” by bonding Apaf-1 alongside pro-caspase 9 (Hill *et al*., 2004). caspase 9 is triggered by its inactive form, pro-caspase 9. Other pro-apoptotic proteases including Smac/DIABLO promotes apoptosis by preventing inhibitors of apoptosis proteins (IAPs) (Schimmer, 2004). It has been revealed that, there are mitochondria proteins that down regulate IAP but an

experiment on gene knock out suggests that only IAP interaction may be insufficient confirmation designating "pro-apoptotic" (Yuan *et al*., 2011)

Other groups of proapoptotic proteins free from inner mitochondria are AIF, endonuclease G, and CAD, which takes effect after cell death. AIF gets to the nucleus and bring about fragmentation of DNA into ~50 – 300kb fragments with condensation of chromatin (Joza *et al*., 2001). The nuclear condensation of this type is known as "stage 1" condensation (Susin *et al*., 2000) Endonuclease G produce oligonucleosomal fragments of DNA by splitting from nuclear chromatin in the nucleus (Li *et al*., 2001). The both of AIF and endonuclease G perform their functions in caspase-dependent order. Furthermore, CAD liberated from the mitochondria fragmented oligonucleosomal DNA after cleaving caspase 3 in the nucleus (Enari *et al*., 1998) giving rise to"stage 11" condensation (Susin *et al*., 2000).

These apoptotic mitochondrial events are controlled and regulated by the Bcl-2 proteinase family (Cory and Adams, 2002). The p53 is an important protein in the management of proapoptotic proteins of the Bcl-2 family; nevertheless, the processes are yet fully understood (Schuler and Green, 2001). These proteins regulate mPT pore and could be anti-survival (Bcl-2, Bcl-x, BCl-XL) or pro-survival (Bax, Bak, Bid), apoptosis.

These are of particular importance because they can determine whether a cell undergoes apoptosis or terminates it. Believing that the course of action of proteins these proteins is the regulation of the release of cytochrome *c* from mitochondria to cytosol by changing the permeability of the mitochondrial membrane. Several possible actions have been explored, but none is conclusively proven. The cleavage between Bid and caspase 8 give rise to mitochondria distruption (Li *et al.,* 1998; Esposti, 2002). At phosphorylation of Bad, it will be taken up by 14-3-3 and isolated in the cytosol, but move to mitochondria to give away cytochrome c if not phosphoryated (Zha *et al*., 1996).

Bad can also heterodimerize with Bcl-X1 or Bcl-2, neutralizing their protective effect and promoting cell death (Yang *et al*., 1995). When Bcl-2 and Bcl- Xl are

not sequestered by Bad obstruct mitochondria from releasing cytochrome c, of which the technique isyet to be understood.

The involvement of Bcl-2 family members, PUMA and Noxa cannot be overemphasized in proapoptosis. PUMA is significant in p53-mediated apoptosis; its overexpression *in vitro* has been shown to follow with increased Bax expression, conformational changes, transferring into mitochondria, release of cytochrome c and decrease in mitochondria membrane potentiality (Liu *et al*., 2003). Noxa when localizes to mitochondria can relate with anti-apoptotic Bcl-2 to give rise to caspase 9 activation (Oda *et al*., 2000). These proteins modulate apoptosis by induction of genetoxic damage and oncogene activation.

2.7 Mechanism of action

Both extrinsic and intrinsic pathways terminate during the execution phase, which is considered the terminal pathway of apoptosis. This phase of apoptosis begins with the activation of executive caspases which in turn switch on cytoplasmic endonuclease and proteinases to destroy nuclear material and cytoskeletal proteins respectively. The executors cysteine proteases 3, 6 and 7 operate by cleaving varieties of substrates such as cytokeratins, PARP in the end produce morphological and biochemical alterations observed in apoptotic cells (Slee *et al*., 2001).

Caspase 3 can be initiated by any initiator caspases and this particularly makes it the most essential among the executor caspases. Caspase-3 categorically trips the CAD endonuclease. In multiplying cells, it forms a complex with its ICAD inhibitor while in apoptotic events, the activated executor caspase 3 splits ICAD to liberate CAD (Sakahira *et al*., 1998). Chromosomal DNA is then damage by CAD causing chromatin condensation in the nuclei. Apoptotic bodies are generated by induction of cytoskeletal reorganization by caspase 3. An actin-binding protein gelsolin activates caspase 3 and normally acts just like a nucleus for actin polymerization, it binds phosphatidylinostitor bisphosphate, cleaves fragments and actin filaments distrupting cytoskeleton and signaling (Kothakota *et al*., 1997).

The final stage of programmed cell death is phagocytic engulment where a distinctive feature of the phase is the asymmetry of phospholipids and the appearance of ‘eat me shock’ phosphatidylserine (PS) on the outer surface. Nevertheless, the mechanism is not entirely clear. Studies show that Fas, caspases-8 and -3 are engaged in the management of emergence of PS on erythrocytes (Ferraro-Peyret *et al.*, 2002; Mandal *et al*., 2005). The showing of PS on outside sheet of the event ease non-inflammatory awareness by phagocytes granting their early pick up and removal (Fadok *et al*., 2001). The activity of prompt and well-mannered absorption without the liberation of cell components ends in little or no inflammation.

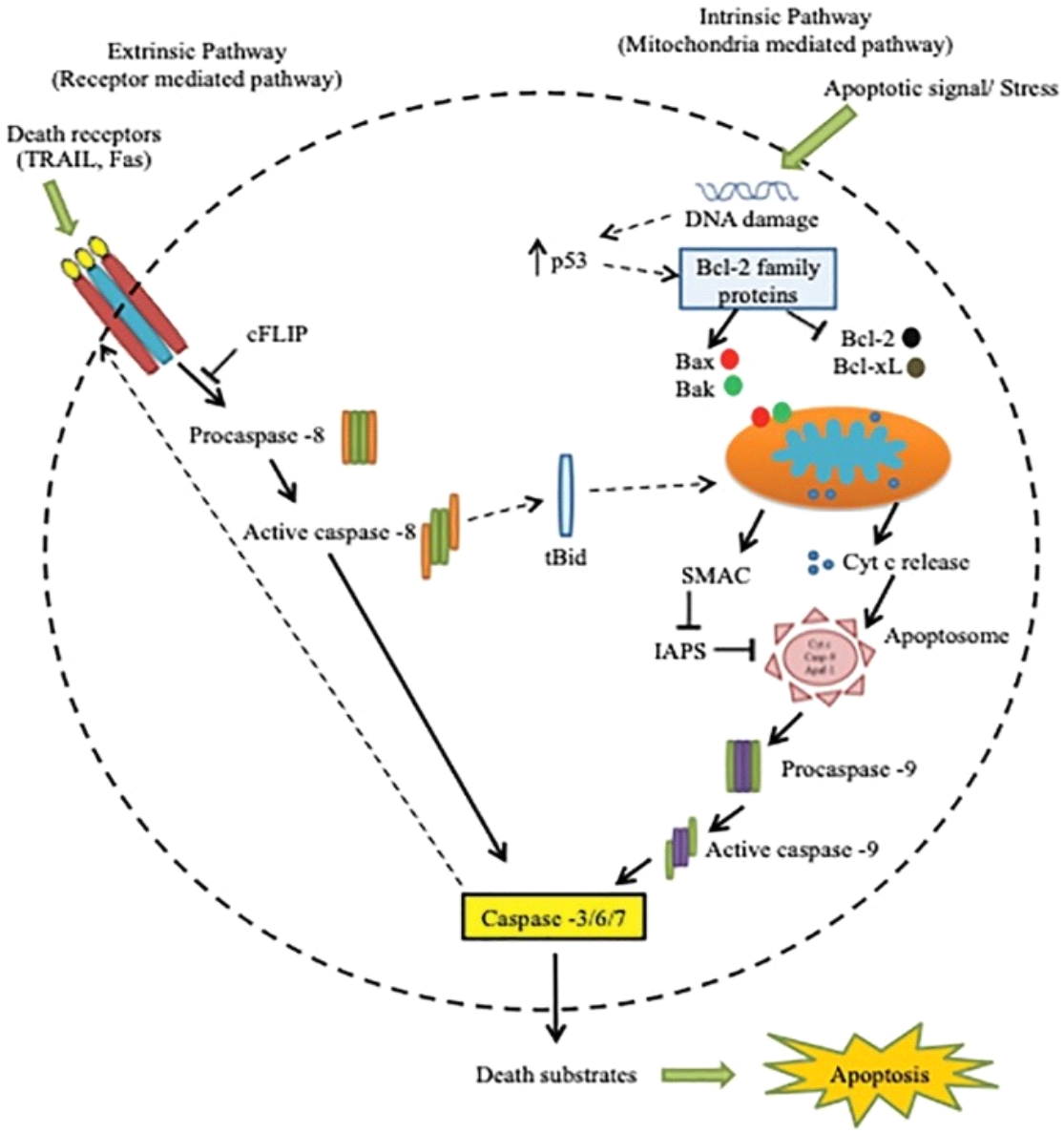

Figure 2.1: Schematic representation of apoptosis events (Yang and Chaudhry, 2019)

2.8 Reactive oxygen species

Reactive oxygen species (ROS), a term that covers all highly reactive oxygen-containing molecules including free radicals. Types of ROS include hydroxyl radical, radical anion superoxide, peroxide hydrogen, singlet oxygen, radical oxide nitrogen, radical hypochlorite and various peroxides lipids. Everything that are able to react with membrane lipids, nucleic acids, proteins and enzymes, as well as others small molecules can lead to damage cells.

However, they are generated in several ways (Jacob, 2008). Therefore, such things like energetic exercises that accelerate cellular metabolism; chronic inflammation, infection and others diseases; impact allergens and presence syndrome elevated intestinal permeability; and toxins such as cigarette smoke, pollution from environments, pesticides and insecticides can enhance oxidative stress.

2.9 Antioxidants

2.9.1. Protective effects of antioxidants

In addition to dietary antioxidants organism relies on the various endogenous defence systems that help protect cells from harm caused by free radicals.

Antioxidant enzymes - glutathione peroxidase, catalase and superoxide dismutase (SOD) and others. Antioxidant enzymes metabolize oxidative damaging intermediate products and require cofactors dietary trace elements such as selenium, iron, copper, zinc and manganese, for maximum catalytic activity. It turned out that inadequate consumption of these trace elements in diet maybe place under threat the efficacy of systems antioxidant defence.

Research also suggests that consumption and absorption of these critical trace elements may be decreased with ageing. Despite addition, rural farms have contributed to significant exhaustion of these critical trace elements in our soils and products food grown in them.

Reduced Glutathione, important water-soluble antioxidant, synthesized from glycine, glutamate and cysteine amino acids. Glutathione directly inhibits ROS, such as lipids peroxide and as well plays important role in metabolism of xenobiotics.

2.9.2 Antioxidant enzymes

2.9.2.1 Glutathione - S – transferase (GST)

Glutathione-S-transferase (GST) represents an enzyme that involved in detoxification of wide spectrum compounds and in the reduction damage red blood cell from free radicals. Enzyme is used as partner for mergers for many recombinant proteins. GST identification is used to carry out Western blotting or, easier speaking, enzymatic analysis. It plays an important role in cellular detoxification, protecting macromolecules from attack by reactive electrophiles, environmental carcinogens, reactive oxygen species and chemotherapeutic agents (Protéga *et al*., 2022). The enzymes prevent cells against toxicants by conjugating them to glutathione, thereby neutralizing their electrophilic sites, and making the products water soluble (Cooper *et al.,* 2010). Most soluble GSTs are active as dimers of subunits of 23–30 kDa with subunits of 199–244 amino acids in length (identical, homodimers or different, heterodimers) subunits, and each dimer is encoded by independent genes as reported by Nissar *et al*., (2017).

2.9.2.2 Catalase (CAT)

Catalase is an antioxidant enzyme present in most aerobic cells. It serves to protect organism from H_2O_2, strong oxidants, which maybe cause intracellular damage. It is found in high concentrations in erythrocytes and liver, and more low concentration found in skeletal muscles, brain and heart. Measurement of the activities of catalase may be useful as tool research at certain diseases such as spicy pancreatitis and some diseases in the liver, at which values elevated. Each unit catalase decomposes 1 μM H_2 O_2 per minute at 25°C and pH 7.0. Analysis of catalase complements antioxidant biomarkers and could then represent one of the useful tools to study oxidative stress. Catalase reacts with known amount of H_2O_2, reaction stop smooth across in one minute with inhibitor catalase.

2.9.2.3 Superoxide dismutase (SOD)

Superoxide dismutase is an enzyme that helps split potentially harmful molecules oxygen in cells. This can prevent damage tissues. Investigation is on, in order to discover its useful significant in ameliorating diseases. It is considered that harmful molecular oxygen plays

good role in the disease management. It catalyses the dismutation of superoxide to hydrogen peroxide:

$O_2^- + O_2^- + 2H^+ \longrightarrow H_2O_2 + O_2$, ……..…….2.1

the hydrogen peroxide will then be removed by catalase or glutathione peroxidase.

2.9.2.4 Reduced Glutathione (GSH)

Reduced glutathione (GSH) is main intracellular low molecular weight thiol, consisting from glutamine acids, cysteine and glycine. Significant roles are palyed by glutathione in cellular protection from redox imbalance in cells mammals. Cellular redox control is crucial in cell-matrix interaction (Rosenberg *et al.*, 2019).

Glutathione may be found in two different states, reduced (GSH) and oxidised (GSSG), inside the boundaries of cellular structures. Less than 10% of the glutathione available in healthy cells and tissues exists in the disulfide form (GSSG), whereas more than 90% of the total glutathione pool is present in its regenerative state (GSH). The glutathione reductase enzyme, which converts GSH from its oxidised form (GSSG), is constitutively active, and oxidative stress further increases its activity. its higher quantity of GSH is explained by these factors. An indication of oxidative stress, the increased ratio of GSSG to GSH is seen. By giving other unstable reactive oxygen species (ROS) regeneration counterparts, the thiol group of glutathione facilitates the repair process in such circumstances. As a consequence, these unstable ROS mix with the unstable GSH to generate stable GSSG molecules, which in turn stabilise as a result of their interaction. Because glutathione is so highly concentrated, this dominating reaction takes place. Under the influence of the enzyme glutathione reductase, GSSG is subsequently converted back into GSH.

Glutathione not only helps the body fight oxidative stress but also is essential for the support of exogenous antioxidants like vitamins C and E. Its presence is essential for the immune system to operate properly and at its best. In addition, glutathione plays important roles in a wide range of metabolic and biochemical processes, such as the production of proteins and prostaglandins, DNA synthesis and repair, maintenance of disulfide bonds in proteins,

enzyme activation, and the transport of amino acids across cellular membranes (Traber and Stevens, 2011).

2.10 Lipids Peroxidation (LPO)

It is a mechanism for cellular damage in both plants and animals and is used as indicator for oxidative stress in cells and tissues. Peroxides lipids unstable and decompose to form row integrated connections, including reactive carbonyl connections. Peroxides polyunsaturated fatty acids decompose to form malondialdehyde (MDA) and 4-hydroxyalkenals (NAE). The MDA measurement was used as indicator of lipids peroxidation. Lipid peroxidation in biological membranes can lead to decreased membrane fluidity and membrane potential, increased permeability to H^+ and other ions, and disruption of organelle or cell integrity (Su *et al.*, 2019). The termination process is the last stage of lipid peroxidation. During this process, LOOs either undergo a reciprocal causal nexus or self-destruct and in this way go on to form non-radical products. Despite their potential to breakdown when exposed to high temperatures or by contact with transitional metal ions, LOOH is a compound which remains stable at physiological temperatures (Suzan *et al*., 2021).

2.11 Phytochemical compounds

2.11.1 Alkaloids

Alkaloids represent the group naturally occurring chemical compounds and they have connections with weak acidic substance. Certain refined structures also classified as alkaloids. Besides carbon, nitrogen and hydrogen alkaloids may contain also oxygen, sulfur and less other elements, for example chlorine, bromine and phosphorus.

2.11.2 Glycosides

Glycoside is molecule in which sugar react with carbohydrate-free part, these may be organic molecule. Glycosides involve in several good roles in the living organisms and they house chemical substances in inactive form of glycosides. The activation is done by enzymatic hydrolysis (Dang *et al*., 2007).

2.11.3 Tannins

Tannin (could also be called vegetable tannin, natural organic tannin or sometimes tanniod, i.e. bimolecular substance, unlike from contemporary synthetic tannin) represents astringent, bitter polyphenolic compound vegetable origin, which binds and precipitate proteins and various other organic connections including amino acids and alkaloids (Anwar *et al*., 2006).

2.11.4 Saponins

These are chemical connections that occur in natural sources commonly found in different types of plants. Precisely, they are grouped phenomenologically on foaming product at shaking in water solution and structurally on their glycosidic fragments in combination with a lipophilic derivative triterpene (Hostettmann *et al.,* 2000).

2.11.5 Flavonoids

Flavonoids (or bioflavonoids) from Latin the words flavus, signifies yellow color in nature, belongs to the class of secondary metabolites plants. Flavonoids were called vitamins group B (probably due to their influence on the permeability capillaries vessels) from the mid - 1930s to early 50s (Huang *et al*., 2015).

2.11.6 Steroids

Steroids form group structurally related to tetracyclic triterponoids, structure which founded on the skeleton of 1,2- cyclopentanophenatrene . From the point of vision of biosynthesis, they are formed as a result enzymatic oxidation of squalene followed by cystalisation. They occur naturally in plant, animals, and fungi, the most famous type animal's sterols is cholesterol, which works efficiently for keeping the structures and integrity of animals membranes and as fat soluble vitamins and steroid hormones (Strobel *et al*., 2003).

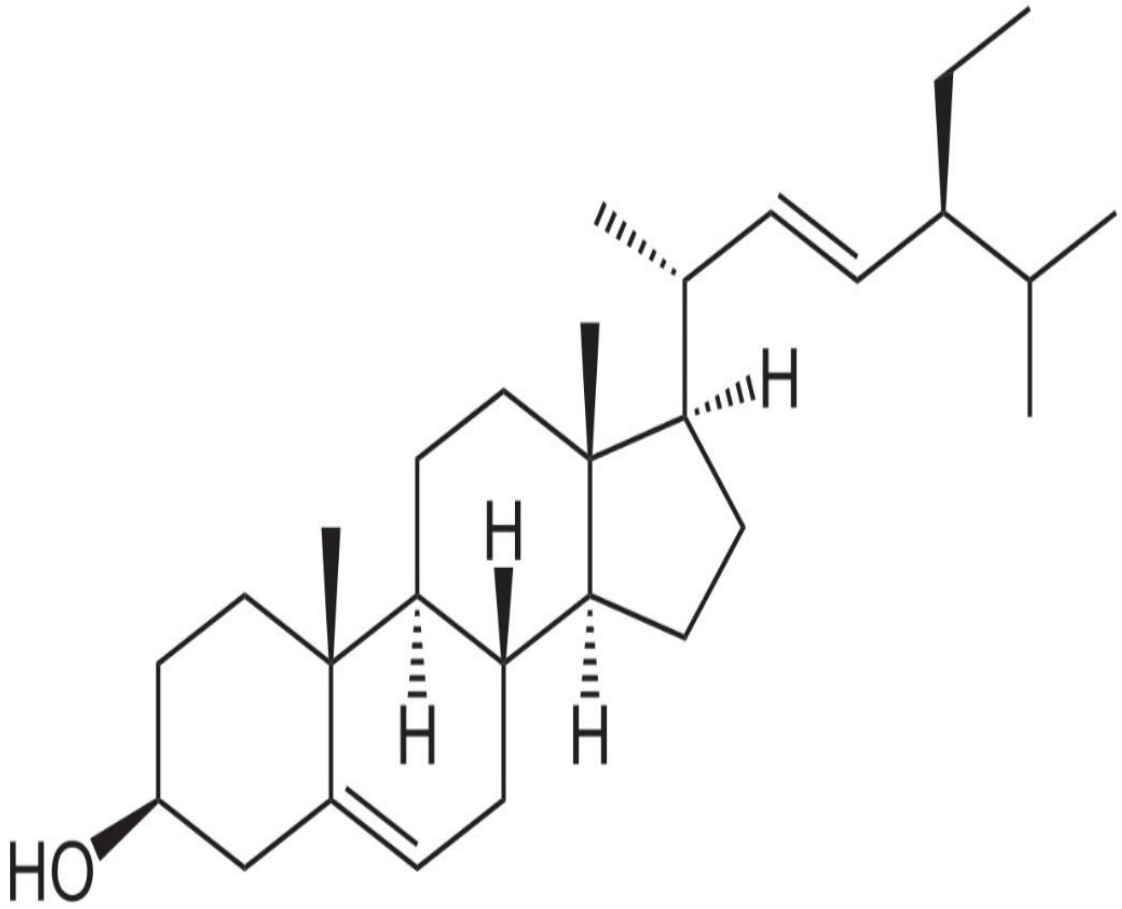

Figure 2.2: Structure of Stigmasterol (Nualkaew *et al*., 2015)

2.12 The Liver

At the beginning of intrauterine life, the liver is the first organ through which many substances enter other tissues (Virtanen, 2023). The liver, a vital organ in vertebrates, carries out a variety of tasks, including digesting, protein synthesis, immunity, and metabolite detoxification. It also creates the biochemicals needed for development and digesting. The liver, which makes up around 2% of the body's weight, is located under the diaphragm, more precisely in the right upper quadrant of the belly. Two basic kinds of liver cells parenchymal cells and non-parenchymal cells are visible when the architecture of the liver is examined under a microscope. A total of two blood vessels feed the liver, with the hepatic artery supplying 25% of the blood and the portal vein providing around 75% of it.

The liver, a recognised specialised biliary tissue, carries cholesterol and bile acids that help break down fat. Among the symptoms and indicators of liver illness include thrombocytopenia, coagulopathy, gastrointestinal bleeding symptoms, and jaundice. There are two different kinds of cells that make up the sinusoids of hepatocytes that line the liver's structure: sinusoidal endothelial cells and phagocytic Kupffer cells. Hepatocytes make up the majority of the tissue in the liver, which is highly specialised and controls a variety of important biochemical processes. Small and complex molecules are created and broken down during these processes, many of which are necessary for maintaining healthy living.

Also, there are many different estimates of the liver's overall number of functions; nonetheless, the literature generally suggests that there are 500 or more. Lack of liver function in the long term cannot be tolerated, although liver dialysis techniques may be used in the short term. An artificial liver is not intended to provide long-term replacement in the absence of a liver. As of 2018, liver transplantation is the only remedy to complete liver failure**.**

.

-

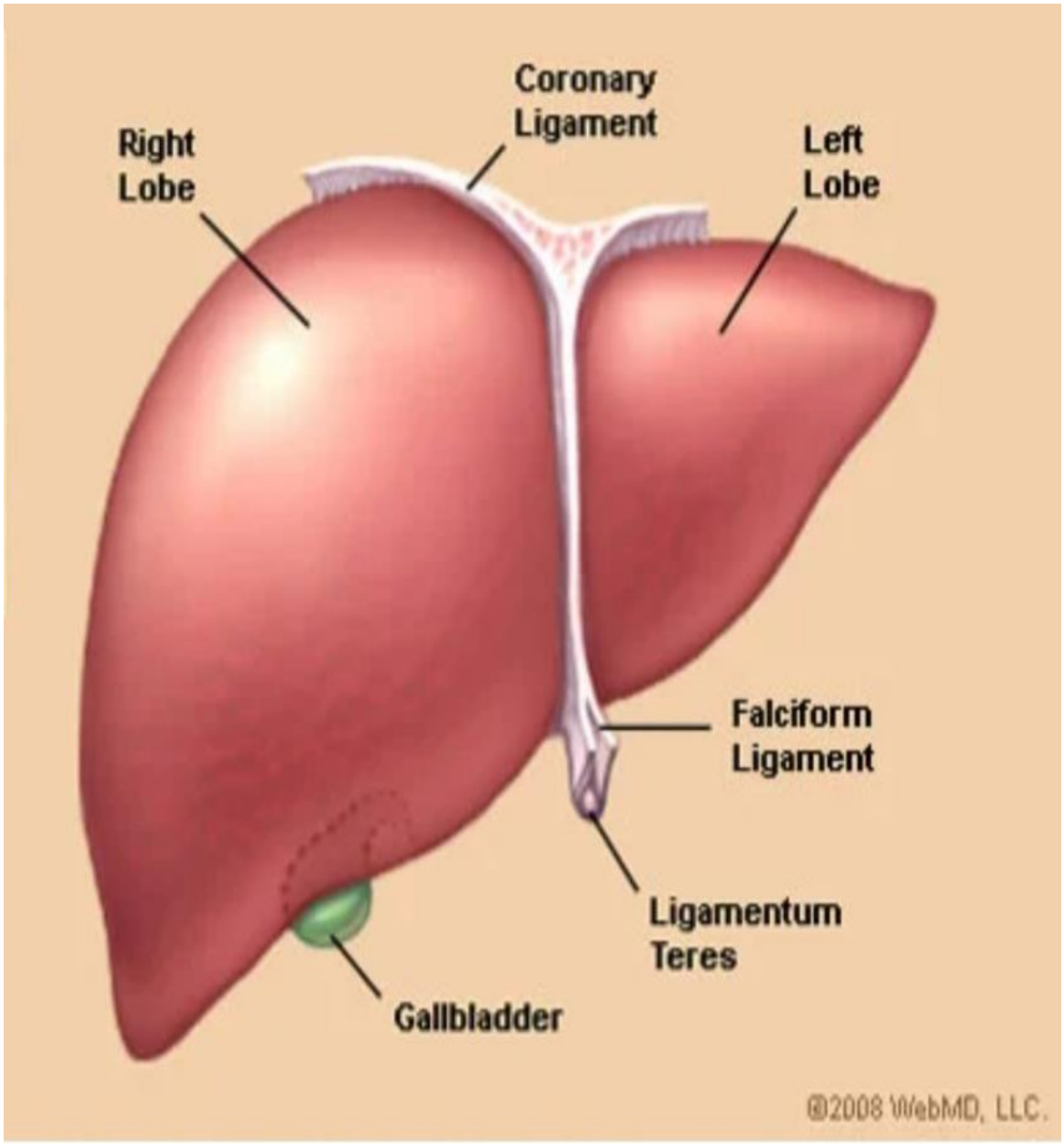

Figure 2.3: Liver structure (Virtanen *et al*., 2023)

2.12.1 Mechanism of hepatotoxicity

Failure in clinical trials leading to drug withdrawal has been associated with hepatotoxicity (David and Hamilton, 2010) and this is evident in animals such as rabbits, cats, monkeys, fish and poultry (Rahman *et al*., 2020), Gossypol, an example was given for juvenile Halibut (Scophthalmus maximus) has been associated with a pro-inflammatory cytokine state as well as activation of many drug promotions in the pharmaceutical industry due to increased toxicity, and the liver is known to be the site of metabolic toxic reactions that are associated with xenobiotic compounds, phases 1 and 2, which are then secreted by phase 3 vectors.

Hepatotoxicity has been reported in ruminants, pigs, rabbits, dogs, cats, monkeys, poultry and fish. In a number of species (especially in sheep, pigs, broiler chickens, rainbow trout and catfish), there is a predominant accumulation of gossypol in the liver (Alexander *et al*., 2008). Feeding of gossypol to juvenile halibut (*Scophthalmus maximus*) has been associated with pro-inflammatory cytokine status, activation of unfolded endoplasmic reticulum protein, cellular stress response, and liver fibrosis (Bian *et al*., 2016).

The most frequent reason novel compounds are removed from consideration for therapeutic development in the pharmaceutical industry is because of their high toxicity. In order to exclude potentially hazardous chemicals from further research and development, it is believed that the field of toxicogenomics would make it easier to discover toxic effects and the molecular processes behind their manifestations during the preclinical testing phase. Combinations of different plants are what make up herbal treatments, and these mixtures are a key source of both heterogeneity and toxicity due to their composition (Hussain *et al.*, 2019). Misidentification of the plant as something else, contamination with pesticides, exposure to heavy metals or organic solvents, microorganisms, or radiation are all potential causes.

Plant foods that have been tampered with on purpose may include chemicals or hormones. Research on medicinal plants that makes use of approaches to the use of omics-based technologies (genomics, transcriptomics, proteomics, and metabolomics) may assist in the identification of the toxicity associated with herbal medicine. Since orally consumed herbal medicines are first processed in the liver by phases I and II enzymes, and subsequently eliminated by phase III transporters, toxic responses in the liver are typical of a large number

of naturally occurring xenobiotic substances. Existing toxicogenomic approaches need to be modified so that they can be applied to toxicology research on medicinal plants. These modifications must be made in terms of appropriate *in vitro* and *in vivo* test models, experimental reproducibility, the development of predictive models, appropriate software tools for data analysis and databases, the identification and validation of biomarkers, and methods for quantitatively modelling association and structure-activity. Despite the fact that toxicogenomics of medicinal plants and herbal products is still in its infancy, omic technologies are interesting tools for predicting the effects of herbal medicine, both the intended and the unwanted consequences.

2.13 Gastrointestinal tract (GIT)

2.13.1 The Colon

The colon is responsible for the absorption of electrolytes, short chain fatty acids, water, and the metabolites of bacteria. The epithelium of the large intestine has far more densely packed cell connections than the epithelium of the small intestine does. Ions cannot redifuse through these substances as a result of this obstruction. Because of this, the enterocytes that line the colon are capable of absorbing sodium ions to a greater degree than those that line the small intestine (Spainhour, 2007). In contrast to the walls in the abdomen and caecum do not contain a continuous layer of longitudinal smooth muscles. Therefore, peristaltic contractions cannot occur in the proximal 85 percent of the colon at this point. There is evidence of rhythmic segmentation in the absence of damage to the orbicularis muscle.

Retropulsion is generated by rhythmic segmentation, but the colon does not undergo peristalsis as a result; this enables the colon to perform its job as a storage organ (Belberg, 2017). The proximal and middle colon both experience orthograde and retrograde contractions (Sarna, 1991). In addition to cytochrome P450 isoenzymes, the human colon also contains uridine diphosphate (UDP)-glucuronosyltransferase (McKinnon *et al.*, 1993: Peters *et al.*, 1991). Through either direct contact or systemic pathways, a variety of medications and therapeutic substances have the potential to modify the colon and/or the function of the colon (Ernest, 2010).

The bacterial alpha-glucuronidase found in the colon is used by the microbiota to hydrolyze some of the hydrolysates and xenobiotics that are still present. Microbes in the gut are responsible for the increased enterohepatic circulation of drugs such as phenytoin, phenacetin, diethylstilbestrol, and warfarin. In addition, these bacteria are responsible for the conversion of methylmercury to its inorganic form. The contents of the colon are slowly moved aborally by the colon, which keeps any leftover material in the distal colon and regurgitates those contents when a person defecates (Sarna, 1991). Because the mucosa of the colon does not have villi, the area available for absorption in the colon is much less than that of the small intestine.

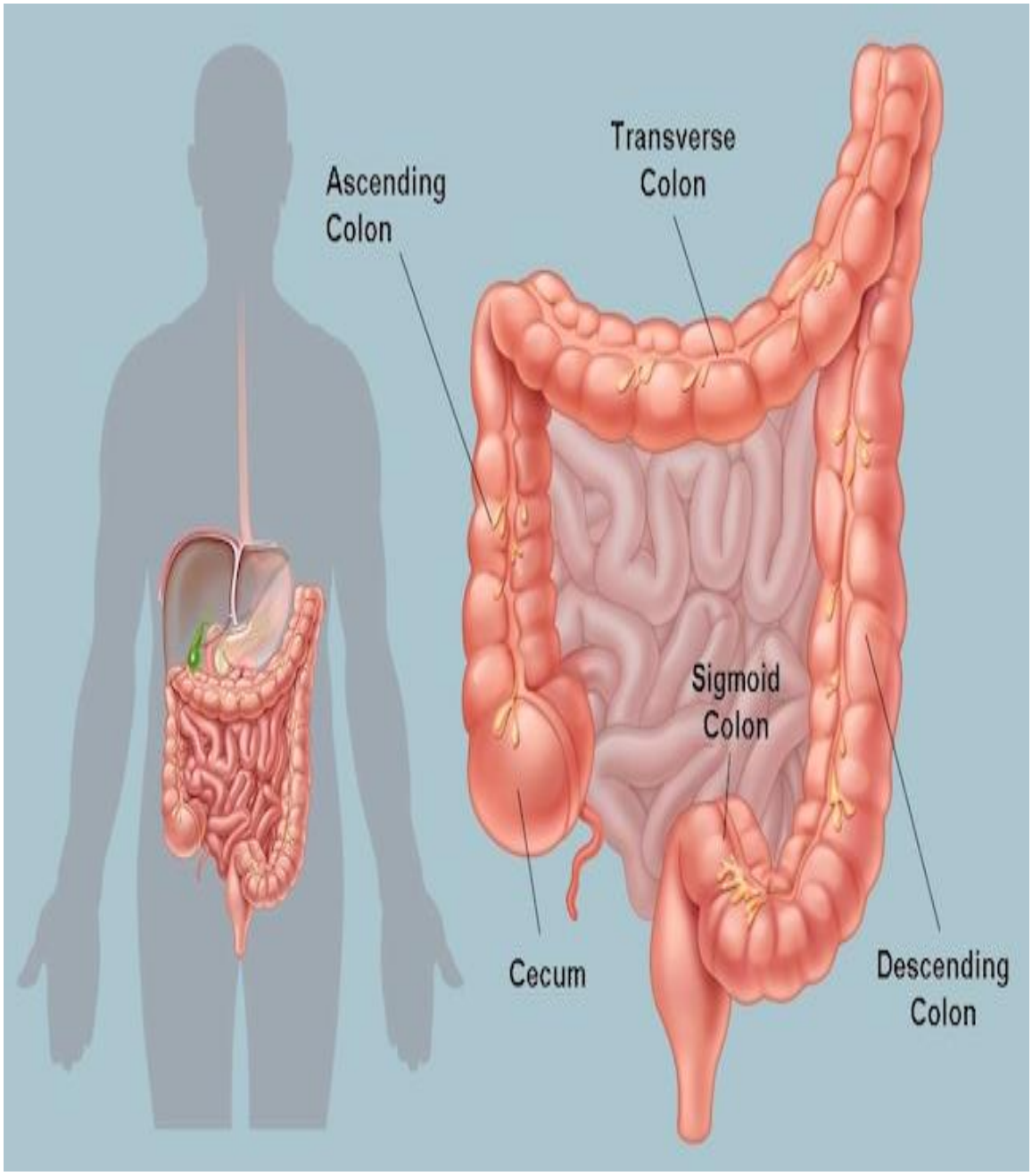

Figure 2.4: Colon Structure (Hoffman, 2020)

2.13.1.1 Types of intestinal cells

Progenitor cells in the crypts create various gut epithelial cell types through Notch signaling (Sander and Powell, 2004). Intercellular communication through Notch pathways regulates embryonic and adult cell development via genes. Enterocyte excision pathways determine whether intestinal epithelial stem cells become secretory or absorptive. The ligand is a transmembrane protein expressed in one cell type that binds to a notch receptor (notch protein) on the cell membrane of another cell type. This binding interaction modifies gene expression in the receptor-expressing cell, enabling its differentiation into an engulfing enterocyte. The ligand-receptor binding appears to organize cells into cell types needed for tissue and organ differentiation.

Enterocyte progenitor proliferation requires Notch and Wnt signalling, but cell type differentiation does not. Wnt-Notch synergy causes intestinal adenomas. Cell turnover is fastest in the intestine. A new born piglet's epithelium renews every 7 days. Mature intestine turnover is 2–3 days. Except for enteroendocrine and Paneth cells, immature cells mature as they slide along the basement membrane to the villous tip extrusion zone, where senescent cells undergo anoikis and become part of the feces.

2.13.1.2 Mechanism of intestinal toxicity

Any colon inflammatory disease may predispose to toxic megacolon (TM), as shown by ulcerative colitis (UC) and chron’s disease (CD). TM is an uncommon but lethal consequence of any colon inflammatory condition. Anticholinergics, electrolyte imbalances including hypokalemia, and diagnostic procedures like barium enema and colonoscopy may also cause TM.

2.14 Toxicants

2.14.1 Benzo{a}pyrene (BaP)

Furan-like polyaromatic hydrocarbon (PAH) with yellow crystals, has hydrocarbons with two or more benzene rings, moderately soluble in water, whereas lipophilic compounds are very soluble. One of the most hazardous PAHs. It may be adsorbed by solid particles. In water or on solid particles, ultraviolet radiation photolyze benzo(a)pyrene. O_2, SO_2, NO_2, and sulfonic acid react with it. It may be degraded by soil microbes.

Air, soil, and water are present in BaP. It is known that benzo(a)pyrene is extensively dispersed in aquatic creatures and comes from crude oil (petrogenic), incomplete combustion of organic matter (pyrogenic), breakdown of organic matter (biogenic), and biotransformation in sediments (diagenetic). It is a category 1 carcinogen according to the IARC.

Benzo(a)pyrene is carcinogenic, teratogenic, neurotoxic, reproductive toxic, and immunosuppressive in animal models. Lipid peroxidation, regulated cell death, and epigenetic alterations may result. Oral or inhaled access is possible. Inhalation causes lung cancer alone, while oral exposure may cause lung cancer and others (von Einem *et al*., 2011).

This toxicant enters the body by inhalation or ingestion and travels to many organs through the circulatory and lymphatic systems. It attaches to the nucleus' aryl hydrocarbon receptor, expressing a mixed-function oxygenase enzyme system, and undergoes both phase 1 functionalization and phase 2 conjugation in the organs. BaP is metabolized by phase 1 enzymes CYP1A1, CYP1A2, and CYP1B1. Epoxides are initially processed by the enzyme. Phenols or dihydrodiols may spontaneously arise from the metabolite. The latter may be converted to mixed function oxidase (MFO) enzymes to generate active optical isoforms of dihydrodiol epoxides, such as anti-BaP 7,8-diol-9,10-epoxy (anti-BPDE). This kind of DNA adduct causes cancers in humans. Sulfate, glucuronic acid, and glutathione may conjugate BaP metabolites during drug metabolism.

Administration method affects this toxicant's absorption. Its hepatic first pass impact reduces systemic blood flow, making oral administration less deadly. The first pass effect is skipped and the toxicant circulates directly in the body through the inhalation and cutaneous pathways, enhancing bioavailability. Its metabolism may also be affected by gene expression of metabolizing enzymes. Polymorphism is genetic.

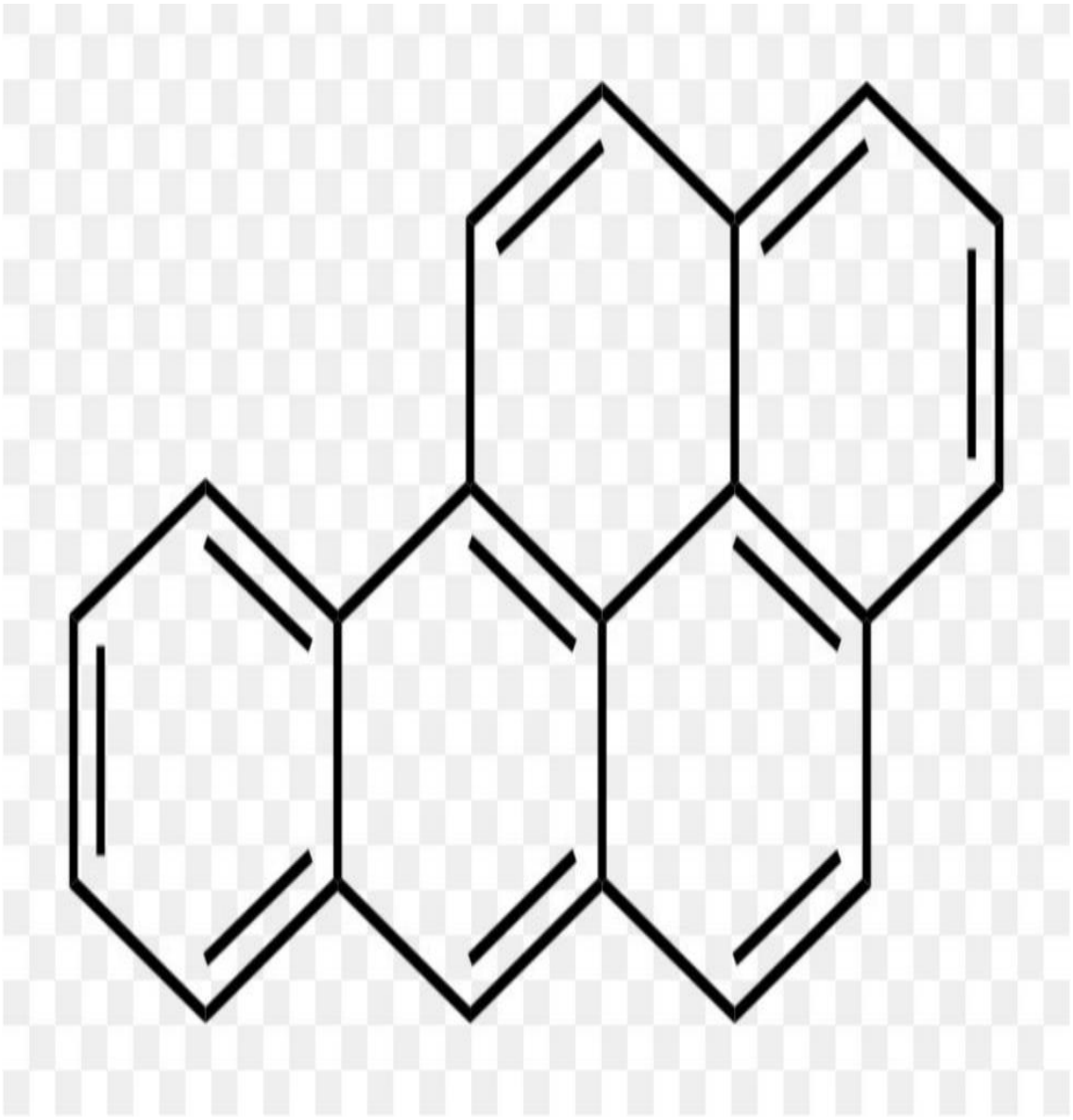

Figure 2.5: Chemical Structure of Benzo {a} Pyrene (Bukowska *et al*.,, 2022)

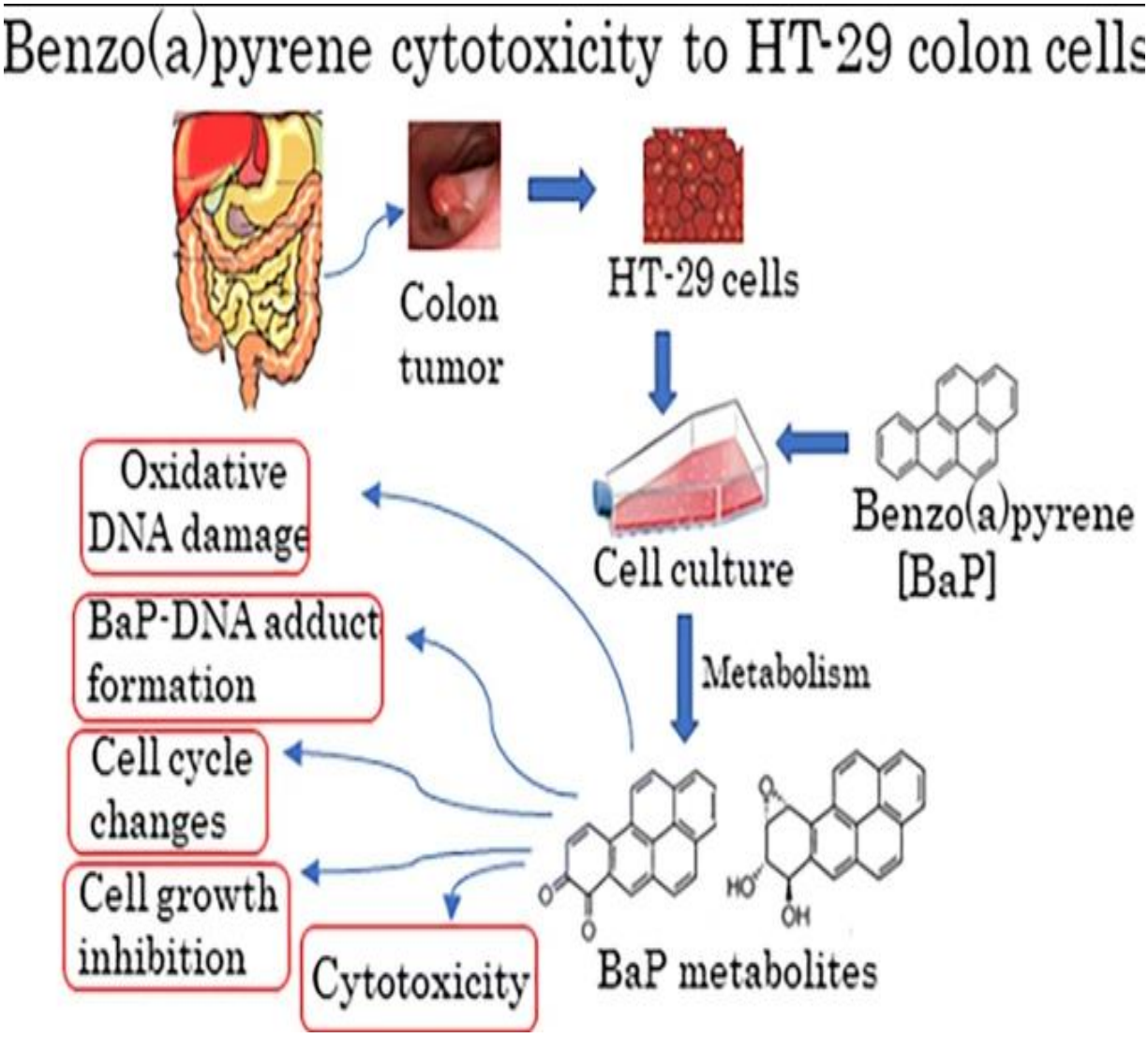

Figure 2.6: Mechanism of BaP action (Myers *et al*., 2021)

2.14.1.2 Source of human exposure

Tobacco smoke is one of the pathways for BaP to enter the environment. It is estimated that the primary smoke inhaled by a smoker contains 1-1.6 µg BaP per pack of cigarettes. Secondary smokers typically consume about 52-95 ng of smoke from a primary smoker. It can also be found in water bodies as a result of water erosion and various industrial activities.

2.14.1.3 Impact of chronic exposure on health

A strong evidence showed that chronic associate with BaP accelerates detrimental wellbeing effects. This occurs as a result of bioaccumulation of the toxicant without significant excretion from the body. These adverse conditions include difficulty breathing, chest congestion, hematemesis, chronic skin injury,

An epidemiological report showed that BaP causes genotoxicity. This toxicant result in the formation of a DNA adduct that causes mismatches and other aberrations in DNA sequences. Effects include chromosomal aberrations, DNA damage and apoptosis. This process of events eventually leads to mutation.

2.14.1.4 Benzo{a}Pyrene epigenetic disorder

Benzo(a)pyrene has been demonstrated several times to have carcinogenic activity in almost all in vivo animal model studies. This potential has been associated with both genotoxic and epigenetic factors. It accounts for 50% of cell mutagen ability of the polycyclic aromatic hydrocarbons (PAH), for example, occupational display in connection with cancers of the mouth, bladder, skin, hemolymphatic vessels, lips (IARC, 2012). So much human health threat propelled the detection its major unsafe mechanisms associated with transcriptional triggering aryl hydrocarbon receptor (AhR) with oxidative stress etc while the final metabolite is benzo(a)pyrene-7,8-dihydrodiol 9,10-epoxide (BPDE) (Miller and Ramos, 2001; Van-Delft *et al*., 2010)

The alteration of gene transcription and moleculaer part have been elucidated using high-efficience methods related to series of cellular models such as lungs, liver, skin (van Delft *et al*., 2010; Jetten *et al*., 2013) . In addition to being involved in some terminal diseases, BaP could be engaged in progress of liver disease, hepatocellular carcinoma (HCC) (El-

Serag *et al*., 2008; Alatise *et al*., 2009). Research data recorded of rodents administered with BaP revealed a relaxed-investigative connection following the occurrence of liver growth (IARC, 2012). Therefore, there is need for comparism between gene expression order with a recently established set of *in vivo* signatures in models with HCC, which includes close to nine thousand (9,000) genes to determine the molecular importance of non-genotoxin substance mechanism of action of BaP on liver carcinogens, (Kayment *et al.,* 2014).

2.14.2 Dextran sulfate sodium (DSS)

This is a common colitogenic chemical known, negatively charged, water-soluble toxicant with a molecular weight of 35 to 50 kDa. dextran sulfate sodium is chemically used in models of induced colitis due to its simplicity; a pair with varying similarities to human ulcerative colitis (Chassaing *et al*., 2014).

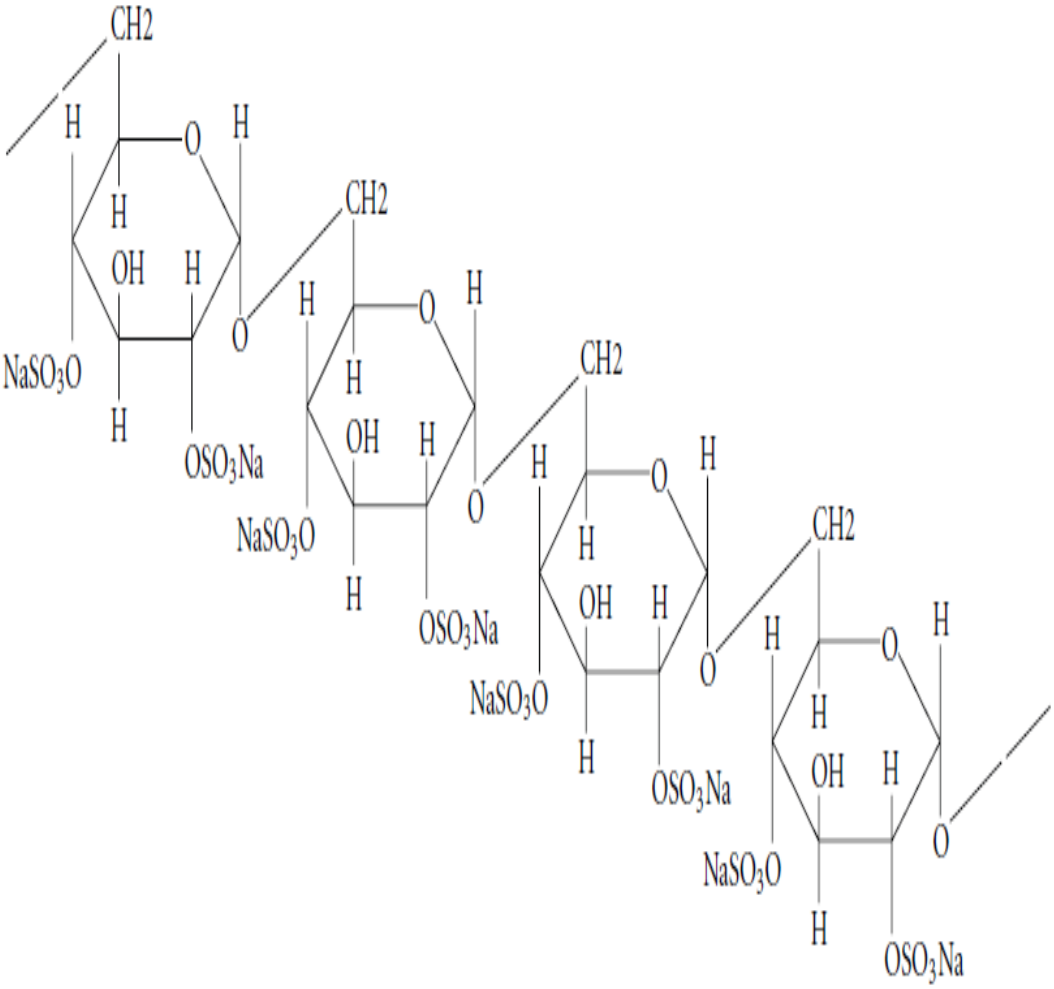
CH2
H
O
H
H
OH
H
NaSO3O
H
OSO3Na
O
CH2
H
O
H
H
OH
H
NaSO3O
H
OSO3Na
O
CH2
H
O
H
H
OH
H
NaSO3O
H
OSO3Na
O
CH2
H
O
H
H
OH
H
NaSO3O
H
OSO3Na

12)

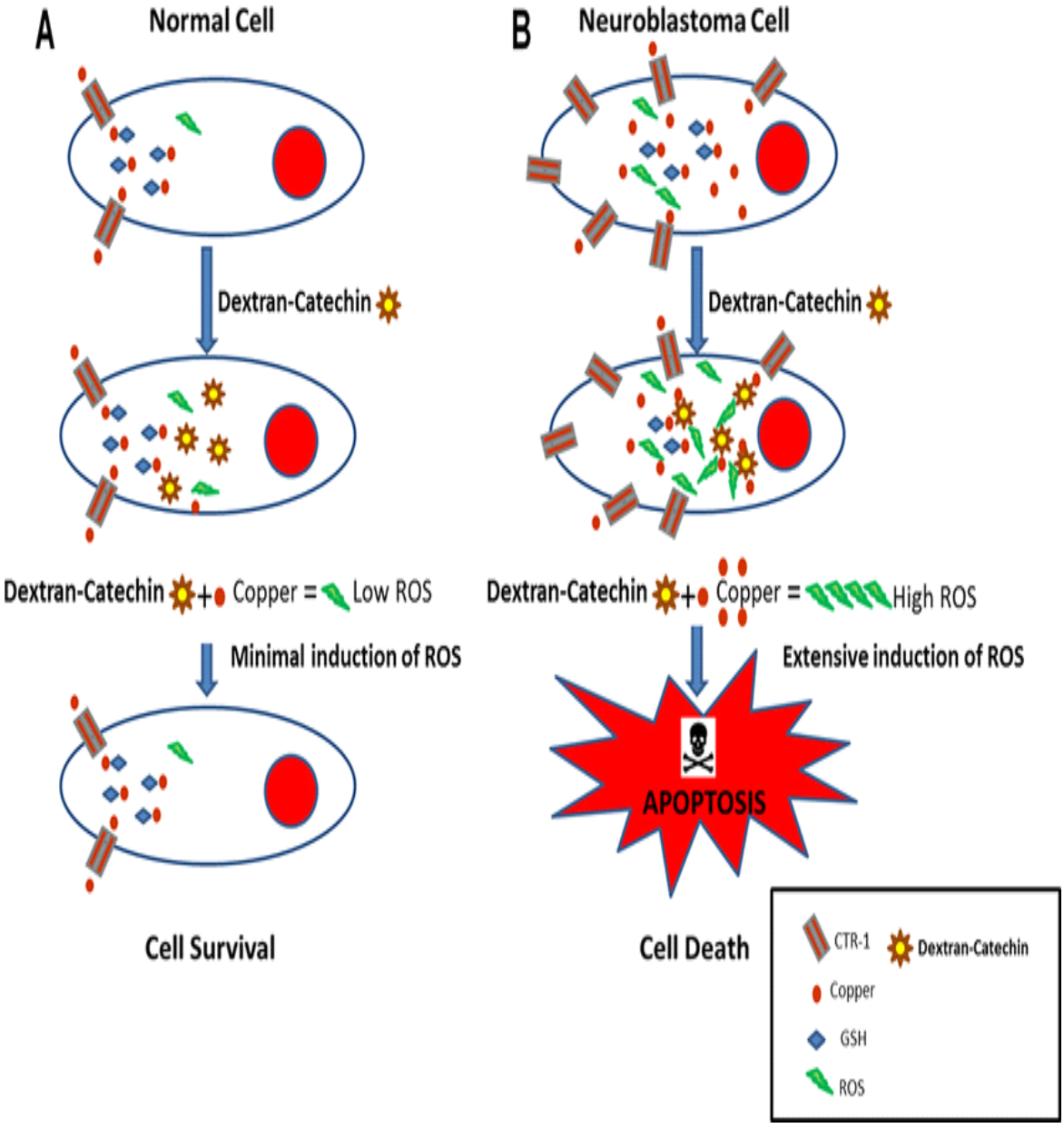

Figure 2.8: Mechanism of action of DSS (Vittorio *et al*., 2016)

2.15 *Piptadeniastrum africanum* (PA)

Piptadeniastrum africanum (Mimosa family) is a plant widely distributed in Senegal, Sudan, Angola and the Democratic Republic of the Congo. The tree spread up to 50 m tall and 2.0 m in diameter above large buttresses, often in drier or more disturbed forests and also alternate and doubly pinnate leaves (Burkill, 1985). Fresh sapwood is pale reddish-yellow or pinkish-white, relatively wide (Tatiana, 2008).

In Nigeria it is called "kiryar kurmi" in the Hausa language, "ofie" in the Igbo language, and "agboin or agboyin" in the Yoruba language (Hutchinson and Daiziel, 1963). Legumes are mainly tropical and subtropical trees and shrubs with about 40 main and 2000 species. The tree sprouts, freeing itself from the stump. Fresh sapwood is pale reddish-yellow or pinkish-white, relatively wide (Tatiana, 2008). It is a strong, tough wood of medium strength and hardness that looks good after polishing and varnishing.The wood is utilised for the production of planks, furniture etc (Burkill, 1995).

In folk medicine, the bark is used in the treatment of dysmenorrhea, bronchitis, headaches, coughs, male impotence, and abdominal pain, hemorrhoids, as a laxative and as a remedy for worms. A decoction of the root and bark is used for enemas, antimalarials, toothache, and human colon cancer (Mengome *et al*., 2009; Hutchinson and Dalziel, 1963). *P. africanum* bark has been shown to have antimicrobial activity against Gram-positive strains of Bacillus substilis, Staphylococcus aureus, and Staphylococcus epidermidis. Gram-negative Pseudomonas aeroginosa, Escherichia coli and Klebsiella pneumonia strains (Akinlami *et al*., 2012)

In Nigeria, the root and bark are prepared for use as an enema, trees are often shown to be cut for antimalarial use, and bark extract is used to relieve toothache (Hutchinson and Dalziel, 1963). According to Mengome *et al*., 2009), the root of this plant is used against human colon cancer cells. Recent phytochemical studies on the root of *Piptadenia africanum* revealed the presence of tannins, flavones, alkaloids, steroids, terpenoids, saponins and glycosides, among others (Mengome *et al*., 2009).

Plate 2.1: ***Piptadeniastrum africanum*** **(2015, 12:30, Ibadan Forest)**

Plate 2.2: Stem bark of *P. africanum* (2015, 12:30, Ibadan forest)

2.15.1 Medicinal value -*Piptadenastrium africanum*

Wood (trade names: dabema, dahoma) is used for maritime construction, bridges, flooring, railway sleepers, mine supports, shipbuilding, vehicle bodywork, interior design, joinery, furniture, gardening, carpentry, sports, turning, fiberboard, chipboard, and pulpwood. It makes hollow boats historically. The wood, known as "African oak" in Europe, is a good alternative for oak (Quercus spp.). It makes charcoal and fuel wood. Bark fibers made carpets. Honey bees' nectar from the blossoms while edible caterpillars eat the leaves.

Folk medicine often uses *Piptadeniastrum africanum* bark, roots, and leaves. Decoctions of the bark are used internally for coughs, bronchitis, headaches, mental disorders, hemorrhoids, urinary infections, stomach pain, dysmenorrhea, male impotence, and as an antidote; externally for fever, toothache, pneumonia, edema, skin diseases, rheumatism, worms and fleas, and as a laxative and abortifacient. The complicated leprosy therapy includes bark decoction. (2007) The bark is used to poison mice with grains, arrows, tests, and fish. Cameroonian and DRC pygmies employ root and stem bark in arrow poison. Mental illnesses, abortifacients, and aphrodisiacs are treated using root maceration.

Enemas for gonorrhea and abdominal illnesses employ crushed leaves and leaf decoction. Leaves poison mice. Coffee, cocoa, and banana farms use the tree as a shade tree during deforestation. Thus, *Piptadenastrum africanum* is a mystical tree in many cultures (Neuvinger *et al*., 2000).

2.16 Mitochondria

Mitochondrion are essential internal organs that, in addition to their role in the making of energy, also engage in other processes, such as apoptosis, mitosis, and necrosis, because of a phenomenon known as the mitochondrial outer membrane permeability transition, or MOMP (Martel *et al*., 2012). Mitochondria are specialized organelles with a double membrane that are responsible for the production of ATP (a kind of energy) and are sometimes referred to as the "powerhouse" of cells (Wallace and Fan, 2010). Mitochondria are singular cytoplasmic cell organelles that are involved in a wide variety of metabolic processes inside the cell.

A wide variety of cellular functions, including as signalling, cell differentiation, and cell death, as well as the control of the cell cycle and cell growth, are only possible when cells have access to sufficient amounts of energy. The significance of mitochondria lies in the fact that they are responsible for the production of almost all of the necessary cellular energy in the form of ATP (adenosine triphosphate). They are able to do this in large part due to the oxidation of substrates that are involved in the Krebs cycle. Because mitochondria are responsible for the oxidation of chemical compounds by enzymes, they are often referred to as the "powerhouses" of the cell. This is because they are the source of the energy (ATP) that is produced by the cell.

Mitochondria have emerged as useful targets for new anticancer medicines, which are collectively referred to as mitocans (Neuzil *et al.*, 2006). Mitochondria are linked to a variety of human diseases, such as mitochondrial abnormalities (Gardner, 2005) and heart failure (Lesnefsky *et al.*, 2001), and there is some speculation that they are also implicated in the aging process. Richard Altman conducted the study that is credited as being the first on mitochondria in the year 1840. After gaining knowledge about them, he gave them the name bioblasts. In the year 1898, Karl Benda came up with the term "mitochondrion." It comes from the Ancient Greek words "mitos," which means "thread," and "chondros," which means "ball." In 1857, Albert von Kolliker was the first person to discover that cells contain mitochondria. He was doing research on human muscle cells when he came across some peculiar granules inside them.

Mitochondria utilize oxygen and oxidative phosphorylation to produce ATP. Mitochondria have two membranes. The inner membrane is impermeable to all molecules, has a huge surface area, and includes oxidative phosphorylation enzymes. Mitochondria's outer membrane shields them. Mitochondria create ATP by passing electrons from tricarboxylic acid cycle intermediates like NAD or FAD, decreasing equivalents. Inner mitochondrial membrane molecular complexes make up the electron transport system (ETS). These complexes transmit electrons, electron transfer transports protons through the inner mitochondrial membrane, raising its potential. F_0F_1 ATP synthase converts protons back to the mitochondrial matrix into ATP. The ultimate electron acceptor is water-forming molecular oxygen.

Electron transport complexes may release electrons. This one-electron reduction of molecular oxygen produces superoxide anion (O^{2-}). Up to 1% of oxygen absorbed may create reactive oxygen species (ROS) such superoxide anions. Mitochondria produce most reactive oxygen species (Ischiropoulos and Beckman, 2003). 2003's Ischiropoulos-Becker study. A substantial proton gradient in the mitochondrial inner membrane (IMM) may impede electron transmission and increase mitochondrial superoxide generation (IMM). An excess of fuel (which creates NADH) or a functional impairment of one or more electron transport complexes (particularly complexes I and III) may cause protons to accumulate (Lenaz, 2001). Lenaz, 2001. Reactive oxygen species (ROS) like hydrogen peroxide (H_2O_2), when mixed with ferrous iron, may cause the Fenton reaction, which produces extremely reactive hydroxyl radicals. Reactive oxygen species (ROS) overwhelm mitochondria's enzymatic and non-enzymatic antioxidant mechanisms, causing cell death and damage.

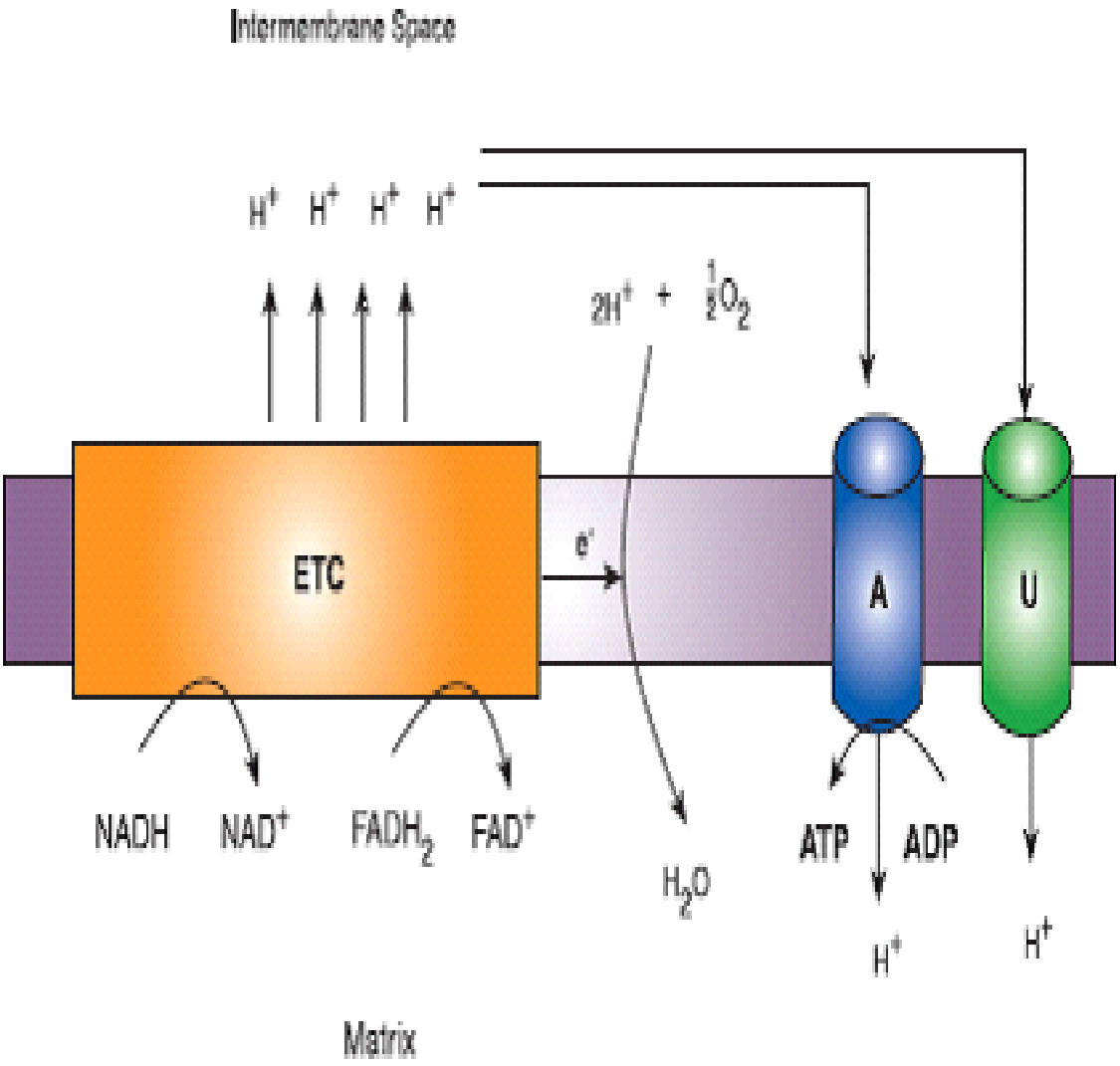

Figure 2.9: Schematic representation of the Mitochondrial Electron Transport Chain (etc.), coupling and decoupling of Oxidative phosphorylation (Bergen *et al*., 2008).

NADH and $FADH_2$ are oxidized in this mechanism. Protons (H^+) are injected into mitochondria's intermembrane space while electrons are transported to the ETC enzyme complexes. The proton motive force, or mitochondrial membrane potential, is high. Using the energy lost when protons re-enter the mitochondrial matrix, the ATP synthase (A) enzyme may create ATP energy from ADP. UCP2 and other uncoupling proteins (U) may return protons to the matrix without ATP.

Apoptotic and necrotic cell death, Ca^{2+}, and iron homeostasis are all controlled by mitochondria. Mitochondria regulate Ca^{2+} and iron homeostasis as well as energy production (Green and Kroemer, 2004). Thus, mitochondria appear to monitor cell vitality. Cell death may be caused by mitochondrial processes such reduced oxidative phosphorylation (OXPHOS-ATP generation), beginning of the mitochondrial permeability transition, increased free Ca^{2+} and bioavailable ferrous iron, and oxidative damage to essential mitochondrial components (Swarup *et al*., 2004). Given what we know about mitochondrial function, mitochondrial oxidative stress and damage are contributors in many illnesses.

Liver disease (alcoholic, iron overload, or non-alcoholic fatty liver disease), ischemia-reperfusion damage, diabetes complications, neurodegenerative illnesses, cancer, aging, and others are among these clinical conditions. (Fariss and Zhang, 2003; Pessayre, 2004) Experimental and clinical data suggests that oxidative damage to mitochondrial lipids, nucleic acids, and proteins is a key event in oxidative stress-mediated disease. Antioxidant mitochondria enrichment also protects cells from oxidative stress. With a greater understanding of mitochondrial molecular pathways that cause deadly oxidative stress, defence strategies for these catastrophic clinical conditions may be established.

2.16.1 Mitochondrial architecture

Power house of the body (Mitochondrion) are typically 0.5–1 μm in width and up to 7 μm in length. It does not matter if they appear like spheres, rods, or filaments; the architecture as a whole stays the same.

The number of mitochondria found in a cell is proportional to the molecule of energy that needs to be produced; tissues that have a high capacity for aerophilic metabolic processes; skeletal muscle or kidneys, possess a greater mitochondria.

Each lobes of mitochondria is made up of a double layer of phospholipids. Mitochondria have two membranes. The physical appearance and physicochemical qualities of the two membranes, which together dictate the metabolic activity of each membrane, could not be more unlike from one another.

Cristae are formed when the inner membrane of the mitochondrial envelope wraps around and coils itself into the matrix of the mitochondria. This serves the purpose of increasing the surface area of the inner membrane, which is responsible for carrying the majority of the enzyme equipment involved in the oxidative phosphorylation process.

Both the inner and the outer membranes have a distinct protein-to-lipid and phospholipid-to-protein ratio, although their phospholipid compositions are quite different. This ratio is around 50:50 for the outer membrane, and the protein is thought to have relatively little enzymatic or transport activity due to its composition, which is approximately 50:50. The inner membrane contains around 80 percent proteins and 20 percent lipids.

Ions and bigger molecules may easily pass through the outer membrane since it has a high permeability. As a result of less permeabilization of mitochondria to ions and sizable molecules than external membrane, categorisation is achieved by physically separating the matrix from the environment of the cytoplasm.

In the process of converting free energy that is produced from oxidizable substrates, this separation is an extremely important step. In reality, the inner membrane of the mitochondria serves as both an electrical insulator and a chemical barrier. Certain compounds are able to traverse this barrier as a result of the existence of sophisticated ion transporters. In order to enable the program of anions back and forth between the cytosol and the mitochondrial matrix, the inner membrane of mitochondria has a number of antiport systems. These transporters specifically replace adenosine diphosphate (ADP) with adenosine triphosphate (ATP).

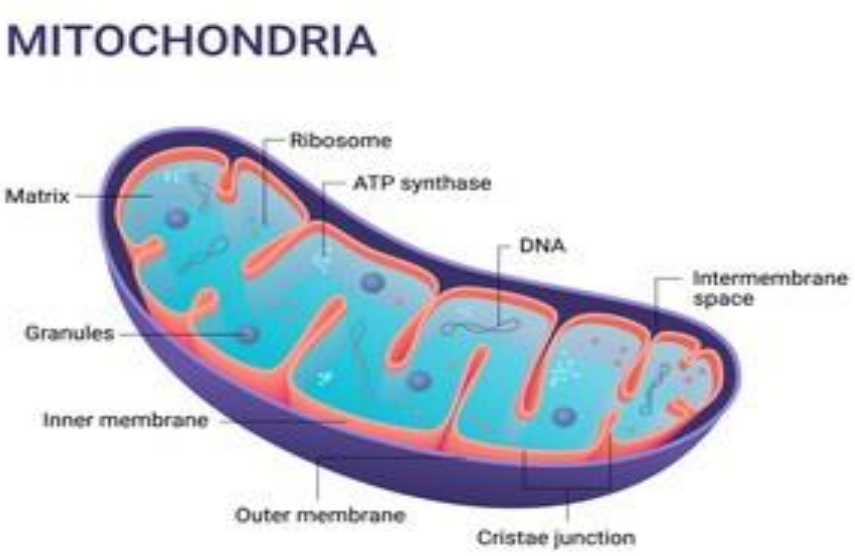

Figure 2.10: Structure of mitochondrion (James *et al*., 2005)

2.16.2 Mitochondrial Permeabilization

The mitochondrial permeability transition (mPT) quickly permeabilizes in response to damaging stimuli like excessive Ca^{2+} (McCommis and Baines, 2012). For molecules up to 1.5 KDa, calcium improves the permeability of the inner mitochondrial membrane.

In normal mitochondria, the onset of inflammation is controlled by cytosolic calcium, inorganic phosphate, fatty acids, and magnesium ions (Raaflaud, 1953). The introduction of the chemiosmotic idea had a detrimental impact on energy conservation (Raaflaud, 1953; Mitchell, 2011). Although the permeability transition was often thought to be an in vitro artifact with dubious significance in physiopathology, some authors now acknowledge its importance in pathophysiology (Rasola and Bernardi, 2007).

Although the physiologic characteristics of the transition are unknown, Haworth and Hunter invented the permeabilty transition in cardiac mitochondria and explained that it was induced by a protein pore opening in the inner membrane. After Peter Mitchell won the 1978 Nobel Prize, the chemiosmotic hypothesis gained widespread acceptance, which may have been attributed to the PT research's lack of focus. The broad adoption of the concept could be to blame for this. The predictions of the chemiosmotic theory were put to the test in studies of energy conservation mechanisms through the examination of mitochondrial ion transport. This was first mentioned in 1999 by Bernardi. In retrospect, the development of a large hole in the inner membrane appears to be a violation of the basic rules of chemiosmosis. (Sokolove and Shinaberry, 1988).

Submicromolar cyclosporin (Cs) A prevents permeability transition activity in mammalian mitochondria, according to Davidson and Haletrap, (1990) discovery. A peptidyl prolyl cis trans isomerase, matrix cyclophilin (CyP) D, interacts to CsA and inhibits PTP (PPIase). According to Takahashi *et al*., (1989) CsA inhibits matrix cyclophilin (CyP) D, an PPIase. (Woodfield *et al*., 1997). The second important finding, made by Sorgato *et al*., (1987) was that mitochondria possess electrophysiologically accessible ion channels. According to Kinnally *et al*., (1989) and Petronilli *et al*., (1989) the inner mitochondrial membrane has a "mitochondrial megachannel" (MMS) with a high conduction channel (1–1.3 inS). Both the mitomycin C (MMC) and the permeability/transition pore (PTP) are obviously two sides of the same molecule.

According to Szabó and Zoratti, (1991) CsA inhibits MMC, and according to Bernardi *et al*., (1993). It exhibits all of the essential PTP regulatory traits. Electrical physiology has assisted in our understanding of the MMC-PTP and adoption of the pore PT theory (Zoratt *et al*., 2005). Twenty five years ago, knowledge of the role of the PT's cell ideath emerged (Crompton and Costi, 1988). Hepatocytes, cardiomyocytes, and isolated hearts were treated with oxidative stress, anoxia, or ATP and showed early support (Griffiths and Halestrap, 1995).

Only after it was discovered that cytochrome c, apoptosis-inducing factor, and other effector phase proteins cytosol after being released (Liu *et al*., 1996) did it significantly increase the amount of experimental research on PT as a cell effector mechanism. (Siemen and Ziemer, 2013) Permeability transition molecular basis are sporadic. There have always been models and working hypotheses available. These models and theories have been unable to discriminate between invading species due to oxidant stimulation, a large number of "inductors" missing common structural features, and a lack of selectivity and a smaller but considerable inhibitor (Gunter, Pfeiffer, 1990).

2.16.3 Adenine Nucleotide Translocator and Voltage-dependent anion channel (VDAC)

Adenine nucleotide translacator (ANT) causes permeabilization to rise while being prevented by the voltage-dependent anion channel (VDAC) and atractylate, ANT is thought to be the cause. It has long been understood that adenine inucleotides prevent mitochondrial development. Brdicka and his associates discovered the structures where two membranes connect with one another intimately to produce protein-protein interactions. Kottke *et al*., (1988) claim that permeabilization occurs inside the membrane. Creatine and nucleoside phosphate kinases are found in the organs that make these proteins, together with Hexokinase on the cytosolic surface, VDAC in the outer membrane, and ANT in the inner membrane. of the mitochondria may channel adenine nucleotides into and out of the mitochondria (Bucheler *et al*., 1991).

The same team observed that N-methylval-4-cyclosporine inhibits channels with PTP-like iconductivity and liposome permeability in fractions that are high in hexokinase in 1996. This year, there was a connection between hexokinase and PTP (Beutner *et al*., 1996).

According to Beutner *et al.*, (1996) atractylate blocked currents but did not comprise the active fractions VDAC or ANT. It also contained a number of proteins. This prevented the activation of species-specific channels. Instead, atractylate enhanced MMC currents. The Bcl-2 family of proteins was examined using the same fractions enriched with hexokinase in a prior work by Marzo *et al*. (1998).

As part of the PTP/VDAC/ANT hexokinase paradigm, these fractions also included the Bcl-2 family of proteins and the TSPO outer membrane, formerly known as the peripheral Bz receptor. Zamzami and Kroemer (2001) were the first to identify the peripheral Bz receptor. Although the exact element(s) in charge of controlling channel activity and membrane permeability have not yet been identified, the general "structure" of PTP may be used as a model.

2. 16.4 Alternative models of permeability transition pores (PTP)

With the Ca2+-CyPD bonding and ANT heterodimerization, discoveries will emerge. An anion-selective channel with a 40 pS average iconductance was revealed to be active in patch-clamp research employing a working mitochondrial Pi carrier. This technique involves both genetic and reparative testing. These tests demonstrated the operation of an anion-selective channel (the conductance of PTP typically ranges between 1.0 and 1.3 inS; the channel is not anion-selective). PTP was decreased by lowering the Ca^{2+} and Mg^{2+} currents to 25 S. Pi blocks channels without the need for ADP, in contrast to pores (Herick *et al*., 1997).

According to a novel model for permeabilization, oxidative stress and other stressors harm integral membrane proteins, causing them to band together and generate holes. This approach, advanced by Kowaltowski *et al*., (2001) and He and Lemasters (2002), contends that the pore development is caused by the integration of damaged proteins. He and Lemasters argue that proteins with chaperone-like properties, such as CyPD, Ca^{2+}, and CsA, regulate the production of misfolded protein clusters. Protein clusters dominate chaperones, leading to "unregulated" gaps in the membrane.

Fatty acids and 3-hydroxybutyrate/polyphosphate activate PT-like channels that require Ca^{2+} but are not sensitive to CsA. These channels are activated by 3HBP (Pavlov *et al*., 2005; Morinova *et al*., 2001). The second is that fatty acids increase the growth of the mitochondria. PTP was found during the experiment (Scorrano *et al*., 2001; Bernardi *et al*., 2002).

According to Leung *et al*., (2008), the most recent PTP model from Halestrap Lab considers the existence of Pi carrier holes. The interaction of Ca^{2+} and CyPD promotes PTP production, whereas ANT heterodimerization promotes opening. The synthesis of PTP improves both. Anion-selective channel function with an average iconductance of 40 pS was suggested by patch lamp experiments using a functional mitochondrial pi carrier, but this has to be confirmed by irepair and genetic approaches.

Studies have shown that an ion-selective channel exists (normal PTP conductance is 1.0–1.3 inS; the channel does not demonstrate ion selectivity). When Ca2+ and Mg2+ current conductance was decreased to 25 pSm, PTP's ability to operate was inhibited. ADP has an interesting effect on channel activity, but Pi does not (Herick *et al*., 1997). Pi media might be a entrant for remote PTP regulation because of these special qualities.

According to reports, the pore is produced by integral membrane proteins that are misfolded and have been damaged by oxidative and other stressors. He and Lemasters claim that clusters of misfolded protein may prevent current conduction. Chaperone-like proteins like CyPD, $Ca^{2+,}$ and CsA are examples of these. This paradigm is quite different from earlier PTP ideas (Kowaltowski *et al*., 2001; He and Lemasters, 2002). Chaperones lose out to protein clusters, which causes "unregulated" membrane gaps to emerge.

The essential aspects of PTP, such as its interaction with calcium and how voltage, the matrix pH, and adenine nucleotides affect these two substances, are not taken into consideration by this model (Bernardi, 1992; Nicolli *et al*., 1993). Methods that depend just on increased protein permeability are insufficient to explain these characteristics. Fatty acids and 3H-butyrate/polyphosphate have been shown by Pavlov (2005) to activate Ca^{2+}-dependent PT-like channels that are insensitive to CsA. Fatty acids have also been shown

to increase mitochondrial size, which connects them to PTP (Scorrano *et al*., 2001; Bernardi *et al*., 2002).

2.16.5 Cyclophiline D, CyP, F_OF_1, ATP, and Synthase

PPIase proteins with a large range include cyclophiline D proteins, which comprise a 109-amino-acid domain. According to Wang and Heitman (2005), sixteen human CyPs serve as a model for cytosolic CyPA and include a CyP-like domain. Walsh *et al*. (1992) and Clipstone and Crabtree (1992) claim that CsA/CyPA suppresses the immune system by regulating cytosolic calcineurin phosphatase after binding to its target.Mammalian mitochondrial CyPD can be found. Genetic removal of Ppif illuminates PTP control (which encodes for CyPD), according to research. CyPD controls PTP. According to Nagawa *et al*., (2012) this lacks mitochondrial structural pores.

According to earlier research Bernardi *et al*., (2006) CsA increases PTP's resistance to Ca^{2+} and PPI opening. Rather than "desensitizing" it, CsA prevents PTP. With Ca^{2+}-Pi loadings that are twice as high in wild-type mitochondria, opening the pores is made simpler. This demonstrates that PTP null alleles do not exist in CyPD-null mitochondria (Ppif-/-). Absence of CsA sensitivity does not show PTP is not active as CsA desensitizes but does not inhibit PTP, therefore, the lack of CsA sensitivity does not necessarily mean that PTP is not participating in the relevant event.

It is crucial to remember that CsA, like CyPD, desensitizes PTP but does not block it while evaluating CsA data. Only mitochondria that express CyPD can react to CsA because muscle denervation alters the expression of CyPD (Csukly *et al*., 2006). For acidic pH and high ionic strength, additional (de)PTP sensitizers can trigger CyPD association or dissociation. No inactive endogenous CsA mimics exist. CyPD. The phosphorylation, acetylation, and nitrosylation of CyPD have been observed to affect the trend of PTP opening, similar to findings by Rasola et al. (2010) and Kohr *et al*., (2011). Numerous proteins interact with CyPD, including Hsp90, TRAP-1, Bcl-2, ERK-2/GSK-3, and possibly p53 (Vaseva *et al*., 2012; Giorgio *et al*., 2009).

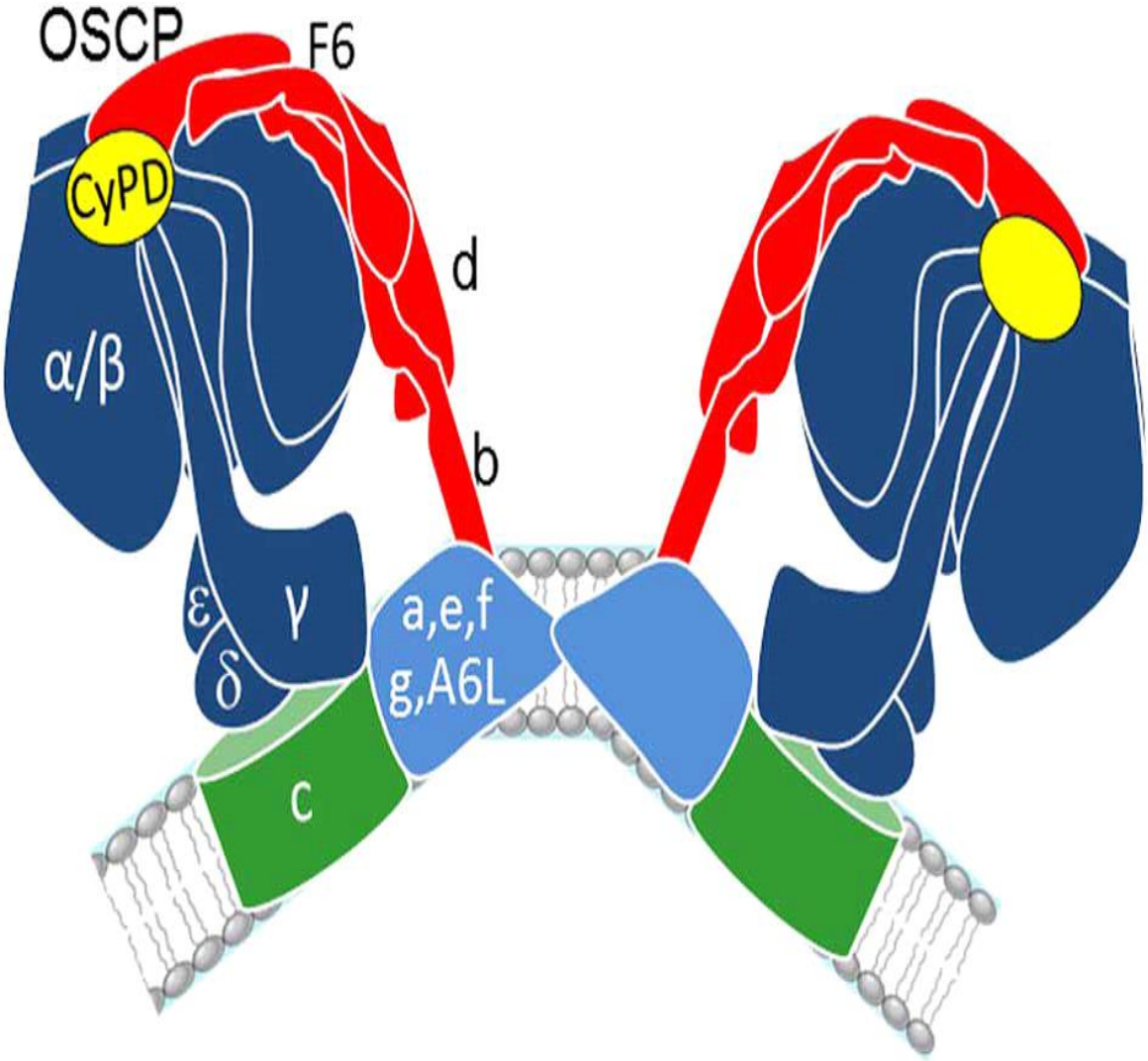

Figure 2.11: Schematic representation of ATP synthase dimers F_0F_1 (Bernadi, 2013).

Structural analysis shows F1 – dark blue; F0 -green and cyan, and stalk subunits (red). CyPD binds the lateral trunk of complex V 1:1:1:1 to oligomycin-sensitivity conferring protein (OSCP) subunits b and d. (2009). CsA displaces CyPD, reactivating the enzyme, whereas CyPD binding to ATP synthase partially inhibits its activity and requires Pi. CyPD mediates CsA's enzyme catalysis stimulatory effect in mitochondria with a Ppif-/- mutation. ATP synthase assembly is unaffected by CyPD lack. Despite the evident parallels between PT and PTP regulation (dependence on Pi, sensitivity to CsA), the answer to whether CyPD and the V complex interact for PT was not known until recently.

2.16.6 Dimers F_0F_1 ATP Synthase form channels indifferent from MMC–PTP

We have convincingly established that the relationship between ATP synthase and aOSCP is largely driven by electrostatic forces. This observation was acquired through meticulous characterization of the precise location where CyPD binds to ATP synthase. By utilizing modeling tools, we thoroughly analyzed the surface potentials and isopotential curves, revealing the interaction between CyPD and OSCP in a region spanning helices 3 and 4. This discovery holds immense significance. It is noteworthy that Bz-423, a extensively studied inhibitor of F0F1 ATP synthase, also binds to this same site (Johnson et al., 2005; Stelzer et al., 2010). As anticipated, the activation of PTP by Bz-423 underscores the significance of CyPD interactions for PTP.

However, the presence of Pi may diminish the inciting influence by enhancing CyPD binding to OSCP. The complex V's involvement in PTP means that reducing OSCP levels decreases the pore's need on Ca2+. When ATP is exploited as an energy source, mitochondria take Ca2+, but PTP opens at only half the rate. This shows that OSCP influences the likelihood of pore opening. Moreover, enzymatic catalysis impacts the Ca2+ affinity of PTP, further highlighting the important involvement of ATP synthase in this process. Mitochondria that hydrolyze ATP require twice as much Ca2+ compared to ATP-synthesizing organelles requiring CsA (Giorgio *et al*., 2013).

To examine the production of PTP, dimers separated by native blue electrophoresis were introduced into azolectin bilayers, and current flow was detected after applying a potential difference. These experiments conclusively revealed that FO F1 ATP synthase generates

PTP. Bz-423 creates highly conductive channels in the presence of Ca^{2+}, while AMP-PNP and Mg^{2+}/ADP block these channels (non-hydrolyzable analogues of ATP). Although ATP synthase monomers lack channel activity, they possess the same subunit composition as the dimers. The reconstructed pores exhibited identical characteristics to MMC-PTP and displayed chordal conductance ranging from 1.0 to 1.3 nS in a symmetrical KCl solution of 150 mM.

Multiple subconductivity phases were also observed. Both Ca^{2+} and Pi sensitized PTP, even in the absence of CyPD, and were responsible for generating PTP currents in dimers formed with 10 mM Pi. These findings are consistent with the features of mitochondrial MMS Ppif-/- (De Marchi *et al*., 2006) and provide support to the concept that the preparations did not comprise CyPD. CsA-insensitive channels contrast with the successful activation of channels by both Bz-423 and boncreic acid, although tratyloside does not enhance channel opening. These statistics show that the preparations lacked either ANT or VDAC. A careful analysis of a human phage display library indicated that Bz-423 induces mortality through cell mitochondria (Blatt *et al*., 2002). Apoptosis is started by Bz-423 via mitochondria, with OSCP as the target. Bz-423 selectively acts on OSCP, probably generating ATP synthase dimer channel activity, while having no influence.

This disproves the hypothesis that unidentified protein contamination created the currents seen by Giorgio *et al*., (2013). Bz-423 may potentially boost ATP synthase dimer channel activity. PTP is indirectly induced by Bz-423 and CyPD, acting through OSCP in the lateral stalk of the matrix. This generates a change in the inner membrane's permeability. Both chemicals act in the same manner, and PTP generated at the membrane border between neighbouring F0 sectors has the potential to compensate for the effects of fatty acids. This is our postulation (Bernardi *et al*., 2002). Both compounds act using the same manner. The compensatory influence of fatty acids may be achieved by PTP generated at the membrane barrier between nearby F_0 sectors. This is our theory (Bernardi *et al*., 2002).

We hypothesised that OSCP would affect the accessibility of Ca^{2+} to the F1 catalytic sector's metal binding sites. The presence of Ca^{2+} in the matrix performs a critical function in PTP formation. The power of this subunit to change metal binding site accessibility in ATP

synthase impacts the matrix's ability to displace Mg^{2+} and open PTP. We hypothesise that OSCP serves as a "negative" modulator, which may be counteracted by adding a "positive" CyPD effector (increasing PTP's apparent affinity for Ca^{2+}). Supporting this hypothesis, binding to a "positive" CyPD effector improves PTP's apparent affinity for Ca^{2+}. We hypothesise that CyPD binding to OSCP or the deletion of OSCP will produce analogous conformational changes, eventually boosting PTP opening. This theory warrants deeper testing.

In the "bound" state, the dimers bind Mg^{2+}-ADP/ATP, and the levels of free Ca^{2+} and Pi are insufficient to induce PT (Panel A). The binding of CyPD facilitated by Pi should alter the accessibility of metal binding sites through conformational changes. This reduced accessibility results in a decrease in the influx of Ca^{2+} into the matrix, which is required for PT. In the absence of CyPD binding, higher levels of Ca^{2+} would be necessary for exchange. Mg^{2+} for calcium (Panel C). Oxidation of thiols enhances metal binding site availability and the likelihood of PT for a given Ca^{2+} load, whereas reduction reduces site accessibility. Chelating Ca^{2+} with EGTA entirely abolishes PT, restoring Mg^{2+} binding and dimer structure (Petronilli *et al*., 1994). Ions and solutes penetrate at the contact location of the c-ring (Panels C, D).

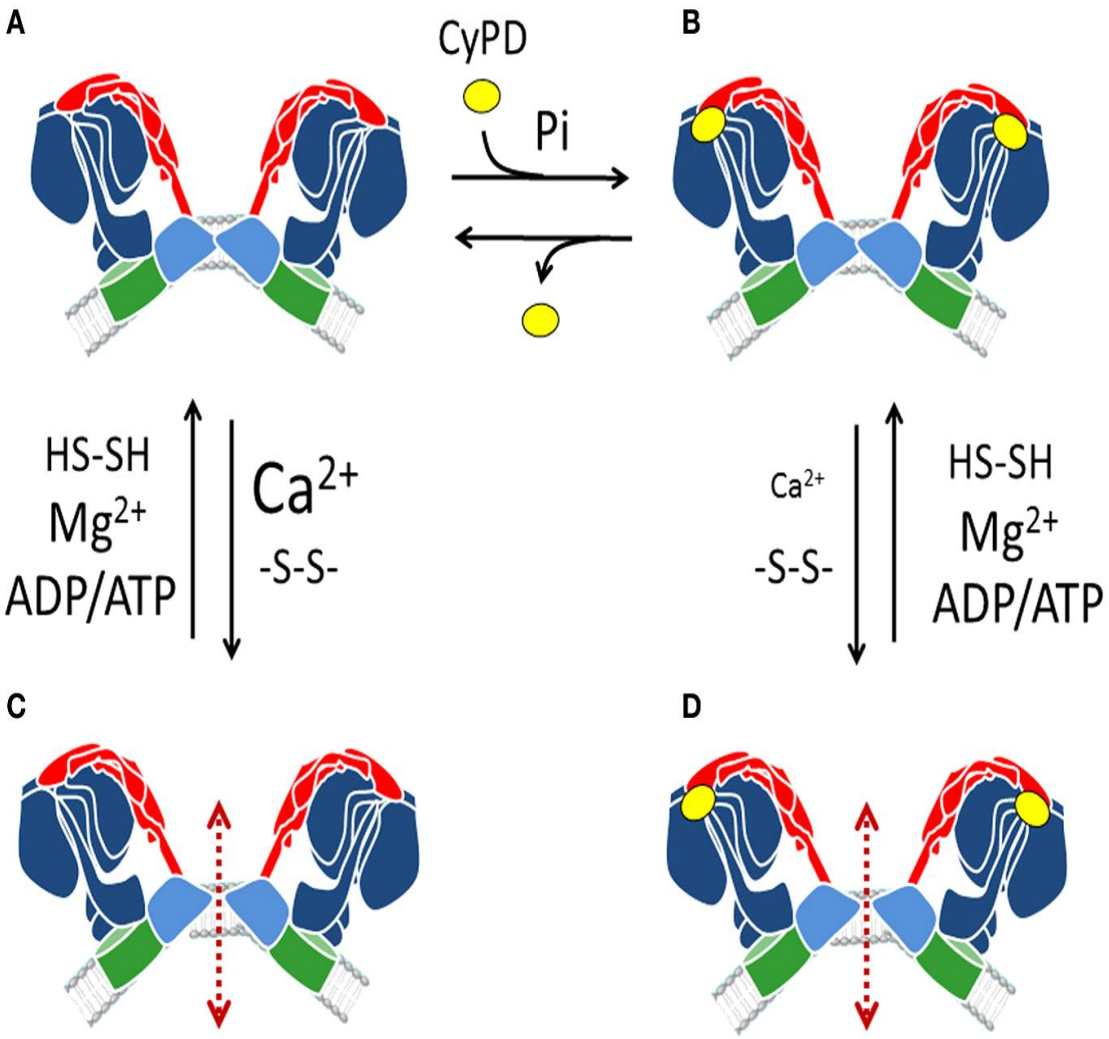

Figure 2.12: Hypothetical conversion of F_0F_1 dimers of ATP Synthase to PTP (Bernadi,2013)

It is possible for dimers of ATP synthase (A) to form PTP through a reversible process that is facilitated by thiol oxidation. This occurs when Ca^{2+} binds at catalytic sites rather than Mg^{2+}. Oxidation of thiols might be of assistance (C). Pi-assisted CyPD binding (B) results in an increase in the number of metal binding sites, which enables PT to form at lower Ca^{2+} concentrations (as seen by face typed, which has a more compacted appearance) (D). The production of phosphotransferase is hampered by the presence of adenine nucleotides and Mg^{2+}. (PTP). A pathway for the diffusion of solutes between F_0 subunits is shown by the red lines.

2.16.7 Role of the outer diaphragm

Mega channel events occur as a result of the actions of complex 5 dimers, as outlined by Urbani et al. in 2019. The modulation of permeability transition pores (PTP) is regulated by the outer membrane. Lê-Quoc and Lê-Quoc originally made a suggestion by establishing that substituted maleimides increase PTP across the cell's outer membrane. Our independent establishment of the outer membrane's "sensitizing" role came from irradiating mitochondria with visible light following hematoporphyrin treatment. This technique produces singlet oxygen, which, depending on the strength of light received by the mitochondria, may either deactivate or reactivate PTP, as explained by Riccelli et al. in 2011.

Permeabilization becomes inactive due to the degradation of histidyl residues under low-light situations, blocking cysteine oxidation on the matrix side. Conversely, light oxidizes the cysteine present in the outer membrane of PTP, therefore activating it. Mitoplasts, on the other hand, display full resistance to PTP induction driven by high light concentrations, indicating that the outer membrane may promote PTP opening via a mechanism that remains unexplained (Ricchelli et al., 2011).

The activation of PTP is regulated by proteins from the Bcl-2 family present in the plasma membranes (Forte and Bernardi, 2006). When activated, Bid triggers the opening of PTP, while Bcl-2 enhances resistance to PTP by reducing the activity of Hile, Bax, and/or Bad. Extensive research investigations have focused on this topic. Although CsA was ineffective in preventing the release of cytochrome c in one of the studies involving Bid, it remains

controversial whether the cells produced CyPD and were susceptible to CsA inhibition (Scorrano et al., 2002; Gracia-Perez et al., 2012).

The attachment of Hexokinase II to the outer membrane negates the stimulatory effects of Bax, thereby restricting the development of PTP (Chiara et al., 2008; Pastorino et al., 2002). Bcl-2 proteins interact with various targets. The Bid-mediated CsA-dependent remodeling of the cristae enhances the availability of intermembrane cytochrome c. Furthermore, even in the presence of an intact outer membrane, Bax can delay the PT-dependent release of cytochrome c by blocking the mitochondrial potassium channel Kv1.3 in the inner membrane (Szabó et al., 2008; Scorrano et al., 2003)

2.16.8 Permeability transition pore (PTP) as calcium exhaust channel

Permeability transition pore (PTP), functioning as a calcium release channel, can abruptly open as a mitochondrial calcium exhaust channel under normal conditions (Hüser et al., 1998; Hüser and Blatter, 1999). Altschuld et al. (1992) observed that CsA significantly enhanced calcium uptake and reduced calcium efflux in isolated cardiomyocytes, as evidenced by radiolabeled 45Ca2+. This effect was attributed to a distinct mitochondrial activity that did not affect cell morphology or viability. The evidence provided in their study supports this concept, as CsA had no impact on cell viability or shape. Recently, three experiments conducted on Ppif-/- cells and animals further support this hypothesis.

Age-related cardiac phenotypes in Ppif-/- animals comprised a loss of contractile reserve, increased shortening and relaxation periods, and a longer decay of cytosolic Ca2+ transients, resulting in a decreased heart rate (Elrod et al., 2010). Ppif-/- hearts exhibited a 2.6-fold increase in mitochondrial Ca2+. CsA-treated myocytes revealed higher mitochondrial Ca2+ transients. Desensitizing PTP with CsA lowered Ca2+ buildup during continuous pacing and lengthened recovery time, suggesting that PTP works as a Ca2+ release mechanism to prevent calcium overload. Consistent with this hypothesis, a cytosolic rise in [Ca2+] caused by ATP or depolarizing dosages of KCl triggered a comparable short-term increase in mitochondrial [Ca2+] in adult neurons in the cerebral cortex of wild-type mice and Ppif-/- animals. But when the two stimuli were administered together, Ppif-/-

neurons had significantly greater mitochondrial [Ca2+], indicating that PTP activation was involved.

These findings suggest that PTP opening and CyPD may be particularly manage Ca2+ homeostasis during high mitochondrial Ca2+ loading (Barsukova et al., 2011). Mutant versions of superoxide dismutase 1, related to amyotrophic lateral sclerosis, lead to motor neuron damage in mice (Gurney *et al*., 1994). Genetically deleting the Ppif-/- gene restored Ca2+ retention in the spinal cord mitochondria of these mice long before motor impairment and neuronal death occurred (Damiano *et al*., 2006). Improved mitochondrial Ca2+ buffering, ATP generation, edema, glia activation, spinal cord misfolded SOD1 aggregates, and motor neuron death were lowered by this intervention, however survival did not increase (Parone *et al*., 2013).

2.17 Procedures for purifications of extract, fractions, subfraction, partially purified subfractions and purified compound of *Piptadeniatsrum africanm* stem bark.

2.17.1 Extraction of *Piptadeniastrum africanum*

When separating desired natural products from their basic ingredients, the initial procedures that must be taken are known as purification and extraction. Isolating and purifying biological samples may be accomplished via the use of a variety of different approaches. Before beginning the extraction process, the most important prerequisite is having a clear understanding of what exactly is to be extracted and then purified, followed by the application of a range of analytical techniques that make use of the distinctive physicochemical characteristics of the substance in order to separate it. (Acille *et al*., 2019).

The most common techniques of extraction include separation/solvent extraction, distillation, and a broad range of chromatographic methods including thin layer, vacuum liquid, high performance, and gas chromatography. Other common extraction methods include ion exchange and ion exchange chromatography. Extraction often involves a number of different chemical processes being carried out in tandem with one another. The goal has always been to select a method or set of methods that will most appropriately separate the compound in question from any other substance that may be present in the mixture. This can be a challenge because there are many possible substances that could be

present in the mixture. When purifying biological macromolecules, it is essential to know for certain and provide assurance that the structure of the compound being separated will not be altered as a result of the purification methods that are being used (Abubakar and Haque, 2020).

2.18 Stigmasterol

The primary function of the extremely common plant sterol known as stigmasterol is to preserve the structure and physiology of cell membranes. They are sometimes used to increase the phytosterol content of foods in order to decrease the amount of bad cholesterol and, as a result, reduce the risk of developing cardiovascular disease. Stigmasterol, as a factor involved in plant cell processes, may perform a significant function in plant reacting to anxiety, metabolism, and functions of enzymes engaged during the biosynthesis of plant cell membranes (Ferrer *et al*., 2017). In addition, stigmasterol is known to possess pharmacological activities such as anti-angiogenic and anti-cancer potentials through the regulation of TNF-α and VEGFR-2 (Kangsamaskin *et al*., 2017).

CHAPTER THREE

MATERIALS AND METHOD

This chapter will proceed by looking at objectives and methods that cut across these objectives. Therefore, for this study, some of the objectives employed more than two to three methods, which also are being employed in another objectives.

3.1: Extraction of *Piptadeniastrum africanum* stem bark extract and fractions

The therapeutic efficacy of the medicinal plant is as a result of the presence of several bioactive compounds that have been established through phytochemiacl screening including saponins, tannins, flavonoids among others (Wuthi, 2010). *Piptadeniastrum africanum* is a very important plant due to its wide range of ethnobotanical uses, including domestic, medicinal, social and agricultural benefits (Owoeye *et al*., 2018).

3.1.1: Collection, Authentication and Isolation of stem bark of *Piptadeniastum africanum.*

Freshly collected P. africanum plant stem bark was found in a forest near Ibadan, Oyo State., identified and authenticated at the Department of Botany of the University of Ibadan with voucher number: (UIH-22562) and the stem bark of the plant was deposited in the herbarium. The plant was washed thoroughly with distilled water and air dried at room temperature for four (4) weeks in the laboratory to lose moisture, then ground to a fine powder, weighed and kept for further use.

A crude methanol extract of *P. africanum* stem bark was prepared by adding 10 litres of distilled methanol (Sigma Aldrich Chemical) to a 5 (five) kg sample of air-dried *P. africanum*. stem bark all over the glass jar. The stirred concoction was kept 72 hours, after which filtration take place using Whatmann No 1 filter paper. A rotary evaporator at 40°C was used to concentrate the filtrate to give a crude extract which was subjected to dryness on a water bath to obtain a solvent-free crude extract

Principle of column chromatography: Separations of samples mixed are done by column chromatography which is based on the different solubilities of the constituents in the immoble state. The addition of the movable phase and the mixtures to be parted at the topmost preparation aparatus causes idividual components to move at a different speed. The solvent-free crude methanol extract was fractionated by dispensing 500ml of dil. H_2O to the crude methanolic extract (ME), adding (50g) to 1L dividing chamber, followed by the addition of 100% n-hexane to degrease extract to the point of exhaustion. The pomace is then washed with chloroform, ethyl acetate, and methanol solvent to remove ethyl acetate, chloroform, and methanol-soluble solvents, respectively, using vacuum liquid chromatography (VLC) to give n-hexane (HFPA), chloroform (CHFPA), ethyl acetate (EAFPA) and methanol (MFPA) fractions, respectively. Thus, the yield percentage of each fraction was calculated;

$$\text{Percentage Output} = \left(\frac{XY}{Z}\right) \times 100 \quad \ldots\ldots 3.1$$

Where the mass of fractions and dishes, only dishes and only fractions were X, Y and Z respectively.

Based on the control of biological activity, the most potent substances were further fractionated using a graduated elution system to collect subfraction, which was then purified using column chromatography with increasing solvent polarity to obtain purified *P. africanum*.

Plate 3.1: Identification and authetification voucher of *P. africanum* stem bark

3.2: Phytochemical screening of *P. africanum* stem bark

3.2.1: Qualitative phytochemical analysis of *P. africanum*

The different fractions have been tested for phytochemicals with respect to Ayoola. *et al.*, 2011 and Hussain *et al*., 2011.

Foaming is obtained by shaking 0.1g of each *P. africanum* extract and fraction with 5ml of distilled water in a test tube. It is known that saponins cause foaming in an aqueous solution, as well as hemolysis of erythrocytes, persistent foaming when heated indicates the presence of saponins.

Chloroform (2mL) with concentrated H_2SO_4 was added to 5ml of an aqueous extract of *P. africanum*; the appearance of a reddish color in the lower chloroform layer indicates the presence of steroids.

The plant extract (0.5g) and fraction was added to a few drops of 0.1% ferric chloride. The physical appearance of a brownish-green color indicates the presence of tannins.

Few drops of 1% ammonia (NH_3) were added to 0.1g of the extract. This caused a yellow coloration in the solution indicating the presence of flavonoids.

Piptadeniastrum africanum stem bark crude extract (0.1g) was dissolved in 5ml of 1% aqueous hydrochloric acid in a water bath. Filter paper was used to sieve the solution. To 1ml of Gradendov's reagent, 1ml of the filtrate was added with a reddish-brown color indicating the presence of an alkaloid.

Addition of 0.5ml of the extract and 0.4ml of glacial acetic acid were mixed with 10% ferric chloride solution and 0.5ml of concentrated sulfuric acid (H_2SO_4). Presence of a blue stain confirmed the presence of cardiac glycoside.

3.2.2: Quantitative analysis of *P. africanum*

Mixture of 0.25g of the extract and plant fractions were approximately mixed together with 10 ml of 1N hydrochloric acid and kept for 4 hours. Filtration was carried out to obtain an ethereal phase by adding petroleum ether and drying by evaporation as soon as the

temperature had dropped to about 270°C. The solute was reconstituted with 2.5ml of acetone/ethanol and 0.2ml of this solution was dispensed into three different tubes with 3ml of $FeSO_4$ solution and 1ml of concentrated H_2SO_4 acid. Absorbance was measured using spectrophotometer at 490nm after vigorous stirring for 10 minutes (Oloyede, 2005).

This was accessed using the Folin-Ciocalteu (FC) reagent (Singleton, 1999) colorimetric method with some modifications from Dewanto (2002). However, Dewanto, (2002) did some modification. About 0.5mL of the plant extract (*P. africanum*) was added to 0.5mL of FC reagent (1:1 diluted with distilled water). This was allowed to incubate for 5 minutes at 22^0C, after which 2mL of 20% Na_2CO_3 and kept at 22^0C for 90min while the absorbance was taken at 650nm. Gallic acid was used as the standard

The immensity of tannins is estimated through spectrophotometric method. Ratio of extract and distilled water was obtain in the order of 1:100 and this was perturbed for 1h in 50mL final volume. The supernatant was filtered into a 50mL standard flask and filled up to the meniscus. 5mL of this was scooped and made to react with 2mL of 100mM HCl together with 8mM Fe $(CN)_6.3H_2O$. The readings were determined spectrophotometrically before 20 minutes expires at absorbance of 395nm wavelength.

Total flavonoid was measured by the colorimetric approach (Dewanto et al., 2002; Jia et al., 1999). About 0.25ml of the diluted extract and fractions of P. africanum was added to 1.25ml of distilled water, as well as to 0.075ml of 5% sodium nitrite solution, and was let to react for 5minutes, after which 0.15ml of 1M aluminum chloride was added, too. The solution was let to react for 5 minutes before adding 0.5ml of 1M sodium hydroxide. Distilled water was then added to bring the total volume of the mixture to 3ml. Absorbance compared to prepared blank was measured at 510 nm.

3.3: Experimental Animals

Twenty-five (25) swiss mice weighing 18±2g, that were purchased from the pre-clinical vivarium of the University of Ibadan, Ibadan, Nigeria, were employed for in vitro examination in this work. They were housed in well-ventilated cages and left to acclimatise

for two weeks, and provided ad libitum access to animal feed until the beginning of the testing.

3.3.1 Ethical approval

The clearance for this study undertaking was obtained by Animal Care and Use study Ethics Committee with **UI-ACUREC/411120/13.**

3.3.2: Experimental designs (*in vivo* studies)

Thirty (30) animals were grouped into six different divisions (n=5) and treated orally for 30 days with *P. africanum* extract as stated below:

a) Group 1: control mice (corn oil).
b) Group 2 : 25 mg/kg bw P. *africanum*
c) Group 3 : 50 mg/kg bw P. *africanum*
d) Group 4 : 100 mg/kg bw *P. africanum*
e) Group 5 : 200 mg/kg bw *P. africanum*
f) Group 6: 400 mg/kg bw *P. Africanum*

Forty-two (42) mice were divided randomly into 6 different groups containing 7 mice each as follows:

a) Group 1: control mice + corn oil
b) Group 2: 4% dextran sulfate sodium (DSS) in drinking water.
c) Group 3: Benzo {a} pyrene (BaP) at 125 mg/kg bw.
d) Group 4 : DSS + BaP
e) Group 5: D SS + BaP + *P. africanum* at 200mg/kg body weight.
f) Group 6: D SS + BaP + *P. africanum* at 400mg/kg body weight.

Groups 2, 4, 5 and 6 were fed with DSS for 10 days to induce colitis while BaP was administered to groups 3, 4, 5 and 6 after stopping DSS for 10 days to cause severe colon damage.

3.4: Inductive apoptotic consequences of crude extract and fractions of *P. africanum* via mPT, mATPase, (in vitro and in vivo)

3.4.1: Separation of mice hepatocyte

The protocol of differential pelleting involved in mice liver isolation in accordance with the process outlined by Johnson and Lardy, (1967).

Principle :The underlying principle of this procedure demonstrates that whenever a mitochondrion swells, the mitochondrial outer membrane ruptures, releasing the components contained in the mitochondrial inner membrane, while the matrix's volume increases. This phenomenon is quantified by the light scattering method at 540 nm due to an increased dilution, which is estimated as

Reagents: 210 mM mannitol, 70 mM sucrose, 5 mM HEPES-KOH, pH 7.4, 1 mM EGTA make up buffer C.

HEPES- 0.12 g melted in 3.83 g of mannitol and seventy milliliters of diluted water. 2.4 grams of sugar with 0.038 grams of 2-aminoethylene ester ethylene glycol bisA pH 7.4 solution was also added using base potassium hydroxide. In a typical volumetric flask, the solution was diluted to 100ml, then cooled.

210 mM mannitol, 70 mM sucrose, 5 mM HEPES-KOH, and 0.5% BSA make up buffer D. 3.83 grams of mannitol and 0.12 grams of zwitterionic sulfonic acid buffering agent are added. In 70mL of distilled water, 2.4g of sugar and 0.5% BSA dissolved. KOH was used to change the pH to 7.4. A 100ml buffer was adjusted, then put in the fridge.

Buffer for swelling: (two hundred and ten millimeters Mannitol, 70MM Sucrose, 5MM HEPES-KOH, with 0.12g of HEPES, dissolved in 60 ml of distilled water at a pH of 7.4. Then, a HEPES-KOH solution was used to dissolve 2.4g of sucrose and 3.83g of mannitol. leveling to the reaction to 100 ml and raise the pH to 7.4, KOH was used.

Sucrose, dissolved in distilled water, then added to a standard volumetric vessel until it reached a volume of 1 liter yielding 0.25 M Sucrose. After that, the remedy was kept in a refrigeration unit.

Method for isolating mitochondria: Animals were slaughtered by shifting their cervical vertebrae. The liver was swiftly removed and trimmed. After being blotted using absorbent

paper, the liver was weighed. After weighing it, it washed off with an isolation buffer, chopped into tiny fragments with scissors, and then homogenized with a Potter Elvehjem glass homogenizer in 10% w/v ice-cold solution. It went through a centrifuge at 2300 rpm for a five-minute period to separate the nuclear fraction and cell debris from the resulting homogenate at 4°C in an MSE centrifugal.

In order to get a mitochondrial pellet, this step was performed again. The resulting supernatant was then centrifuged at 13,000 rpm for 10 minutes. The resulting pelletized was cleaned and spun in 10 minutes at 12,000 rpm in buffer D. The mitochondrial fraction was re-aliquoted into Eppendorf flasks and immersed in MSH buffer after six hours and utilized. For the sake of maintaining the mitochondria's integrity, all of these studies were conducted on ice. According to the method described earlier, mitochondria were collected and used for the investigation of mitochondrial ATPase enzyme activity.

3.4.2: Mitochondrial protein determination

Using this test, we assessed the occurrence of oligopeptides in the assay to measure the quantity of amino acids in mitochondria. The underlying hypothesis rests on the behavior of tyrosine and tryptophan, two amino acids bearing phenolic groups. These amino acids reduce the phosphorus-18-molybdic complex, resulting in a blue hue in the alkaline pH of the solution. When amino acids are present, the phosphorus-18-molybdenum-tungsten complex declines, giving the substance a blue hue. The absorbance reading is collected at 750 nm. The experimental procedure followed the methods outlined by Lowry *et al*. (1951), utilizing Bovine Serum Albumin (BSA) as a standard of reference.

To prepare the chemical solutions, Reagent A was created by dissolving 2 grams of Sodium trioxocarbonate (IV) and 4 grams of sodium hydroxide granules in a sufficient amount of distilled water in a standard 100 ml volumetric flask. The solution was then diluted with distilled water to reach the 100 ml mark.

Reagent B was prepared by dissolving 2 grams of Sodium Potassium Tartrate in 70 ml of distilled water and adjusting the volume to 100 ml with distilled water.

Reagent C was made by dissolving 1 gram of Copper (II) tetraoxosulphate (VI) pentahydrate in approximately 50 ml of deionized water and then diluting it to the 100 ml mark using distilled water.

Reagent D was created by mixing reagents A, B, and C at a ratio of 100:1:1, respectively and finally;

Reagent E: the Folin-Ciocalteau reagent, was utilised with a stock solution ratio of 1:5. During the experiment, 10 milliliters of Bovine Serum Albumin (BSA) at a concentration of 4 mg/milliliter from Sigma Aldrich Inc. was employed. The technique required adding 3 ml of Reagent D to the protein samples and allowed them to rest for 10 minutes at room temperature. Next, 0.3 ml of Reagent E was violently mixed with the mixture to ensure thorough blending. Stirring was maintained for 30 minutes to develop color, following which the optical density was measured at 750 nm using a CamSpec M106 spectrophotometer. The absorbance values were plotted against relevant BSA absorptions or concentrations.

Table 3.1: Protocol for Protein Determination

Test tubes in triplicate	Blank	1	2	3	4	5
BSA standard solution (µl)	-	100	200	300	400	500
Distilled water (µl)	1000	900	800	700	600	500
Reagent D (ml)	3.0	3.0	3.0	3.0	3.0	3.0
Stand 10 minutes						
Reagent E (ml)	0.3	0.3	0.3	0.3	0.3	0.3

Table 3.2: Summary of mitochondria swelling assay at 540nM protocol

Sample	Buffer (µl)	Rotenone (µl)	Spermine (µl)	Mitochondria (µl)	$CaCl_2$ (µl)	Succinate (µl)
Blank	2440	10	-	-	-	50
NTA	2410	10	-	30		50
TA	2385	10	-	30	25	50
INH	2322	10	62.5	30	25	50

NTA: No Triggering Agent. TA: Triggering Agent. INH: Inhibitor

3.5: Valuation of mPT Pore opening in intact mitochondria of mice

Ca^{2+}-accumulating mitochondria can be stimulated to go through a permeability transition. According to Lapidus and Sokolove (1993) and extremely non-selective permeation of the inner membrane to tiny molecules (1500Da). Isolated mitochondria during permeability transition exhibit substantial amplitude colloid osmotic swelling, which reduced 540 nm photometric absorption. A number of experimental PT were evaluated by monitoring the size of the mitochondria, keeping track of corresponding rise or fall in absorbance.

Principle: When the mitochondrial membrane is permeable and the mitochondria are well-positioned so that they scatter less light, the refractive index of the membrane changes (Lapidus and Sokolove, 1993). Reduction in absorbance taken spectrophotometerically at 540 nm.

Components for making mitochondrial swelling: 80 µM Rotenone: Rotenone (0.32mg) was built up to the mark of 100mL after being slightly diluted in distilled water. A dark (or amber) bottle was then used to preserve it because it is light-sensitive. 4mM Spermine was dissolved in distilled water at a concentration of 8.09 mg (Sigma Aldrich Inc., USA) and leveled up into the mark of 10ml, store in a dark container.

12mM $Cacl_2.2H_2O$: Calcium chloride (176.4mg) (Sigma Aldrich inc., USA) was dissolved in 8 ml of distilled water and leveled up to 10 ml with distilled water. 250mM Sodium succinate: Sodium succinate-675.3mg (Sigma Aldrich inc., USA) was dissolved in 8ml of distilled water and leveled up to the 10ml mark.

Procedure for mitochondrial swelling assay: In the presence of 0.8µM rotenone (10µl) and swelling buffer (2200µl), mitochondria were incubated for 3minutes, following addition of 250mM sodium succinate (50µl), kept for 30seconds to evaluate the mitochondria's structural integrity. The mitochondria were initially incubated with rotenone and MSH buffer for a period of three minutes when extracellular calcium was employed as a trigger, and then 12 mM calcium chloride (25µl) and 250 mM sodium succinate were introduced to excite the mitochondria.

Using a CamSpec M106 spectrophotometer set to 540 nm, the absorbance change was read as a result of light scattering. Mitochondria were treated with MSH buffer (2200 µl), 8 mM

rotenone (10 µl), and 4 mM spermine (62.5 µl) for 3 minutes to examine the inhibitory impact of spermine. Calcium (25 µl) was incorporated after three minutes had passed, and after thirty seconds, sodium succinate (50µl) was administered. Spectrophotometric analysis was used to measure the absorbance change.

3.6 Cytochrome c release measurement

As a committed stage in mitochondrial-mediated cell death, or a moment where apoptosis must take place, cytochrome c is always released when the mitochondrial pore opens.

Principle

It is based on the concept that when the mitochondrial permeability transition pore opens, the mitochondrial intermembrane releases cytochrome into the cytosol. At the Soret peak, which is detected using an ultraviolet (UV) spectrophotometer, the heme-containing protein fragments emit the highest intensity. The amount of cellular pigment released from the isolated mitochondria was measured using the technique described by Appaix et al. (2000) by measuring the Soret peak value for cytochrome c at 414 nm (= 100mM-1cm-1).

For the preparation of Buffer C (1mM EGTA coupled with KOH, pH 7.4), 0.12g of HEPES, 3.83g of mannitol, 2.4g of sucrose, and 0.038g of 2-aminoethyl ester-N,N,N',N-tetraacetic acid ethylene glycol were dissolved in a volume of 100 ml in a volumetric flask. The pH was adjusted to 7.4 using KOH, and the solution was frozen. To create Buffer D (210 mM mannitol, 70 mM sucrose, 5 mM HEPES-KOH, and 0.5% BSA), HEPES ethanesulfonic acid (0.12g) was dissolved in 70 ml of distilled water, along with 3.83g of mannitol, 2.4g of sucrose, and 0.5% bovine serum albumin.

The pH was adjusted to 7.4 with KOH. The solution was then increased to a volume of 100 ml and stored in the refrigerator until needed. A solution containing HEPES (0.12g), 3.83g of mannitol, and 60 ml of distilled water was also included of distilled water as a swelling buffer. The combination comprises 5mM HEPES, KOH PH 7.4, 70mM sucrose, and 210mM mannitol. 2.4 grams of sucrose were scattered in the solution within a flask with a flat bottom, 100 ml of KOH was diluted after using KOH to elevate the pH to 7.4.

85.6g of sugar were dissolved in 1L of distilled water to create 0.25M sucrose in a typical volumetric flask. The final product was chilled before use. 12mM $Cacl_2.2H_2O$- Calcium chloride (0.1764g) dehydrate (Sigma Aldrich Inc., USA) was dissolved into 8 ml volume of distilled water and was later made up to 10 ml using distilled water.

Procedure: One milligram (1 mg) (protein/ml) of mitochondria was first incubated in a solution of 0.8 M rotenone in a medium comprising 210 mM mannitol, 70 mM sucrose, and 5 mM HEPES KOH (pH 7.4). for 30min at 27°C. Which proceeded in the presence of a fraction of various concentrations using 24mm calcium as standard. Upon incubation, the mixture was centrifuged at 15,000rpm for 10minutes. The absorbance of the supernatant was measured at 414nm, corresponding to the ɤ peak of cytochrome c.

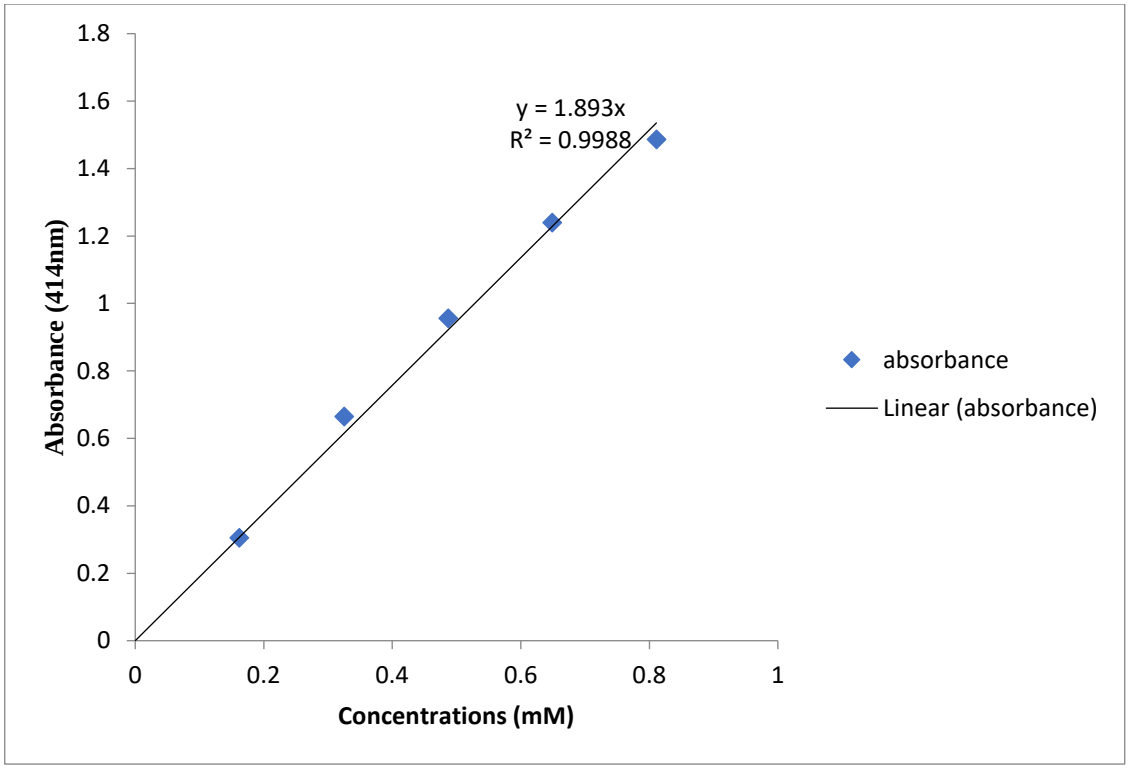

Figure 3.1: Standard curve of cytochromec c released

3.7: Assessment of mitochondrial ATPase (mATPase) activity

ATP synthase, a complex v in respiratory chain catalyses the synthesis of ATP in a normal condition but the enzyme works in reverse manner in a certain condition, thereby hydrolysing ATP to ADP and Pi (inorganic phosphate-PO_4) and cumulation of Pi may induce induction of mPT pore and the structure of the pore is not known. However, Paulo Bernadi proposed the enzyme was the pore. ATPase assay measures the activity of efflux transporters indirectly and was determined by the method of Lardy and Wellman (1953) as modified by Olorunsogo and Bababunmi (1979).

Principle: When mPT pore opens, making a dip in the potential of the membrane. This causes mATP synthase, which is tangled in the creation of ATP, to hydrolyze ATP (using an enzyme called ATPase) (ATPase). ATP, which is a substrate, binds with an enzyme, which is called ATP synthase, to produce an enzyme-substrate complex. This complex then leads to the synthesis of ADP and inorganic phosphate.

This is dependent on the formation of a complex chemical when molybdate is combined with inorganic phosphate (Pi) that has been treated with ascobate, a reducing agent. This results in the production of a blue hue, the intensity of which is proportional to the amount of inorganic phosphate (Pi) present in the mixture (Pi).

Procedure**:** A modified version of the Wellman (1953) method was described by (Olorunsogo and Malomo, 1985) was utilized in order to evaluate the amount of mitochondrial ATPase activity. In this study, a protein concentration of 1 mg/ml was used rather than a concentration of 2 mg/ml of mitochondrial protein. According to the data, each reaction mixture had a concentration of 25mM sucrose, 1mM ATP, 0.5mM KCL, and 65mM Tris-HCl buffer at a pH of 7.4. Through the utilization of distilled water,there was an increament of the reactant volume to an entire or a whole milliliters of 2.

The reaction was kicked off by adding a mitochondrial suspension, which was then placed in a water bath at a temperature of 27 degrees Celsius for thirty minutes while being shaken. The reaction was terminated by adding 1 milliliter of a solution containing 10% sodium dodecyl sulfate. The preparation of a time zero tube began with the addition of mitochondria

to a reaction vessel, which was followed by the addition of SDS to halt the reaction. This was done while the reactions in other vessels were halted at intervals of 30 seconds.

Reagents- TRIS-Hcl-0.01M (pH 7.4): After dissolving 1.21 grams of tris (hydroxymethyl) aminomethane (made by Sigma-Aldrich Inc. in the United States of America) in 60 milliliters of dilH_2O and bringing the pH (7.4), bringing the completing volume to 100 milliliters by adding more distilled water. The container was stored in the refrigerator.

Sucrose (0.25M) : 6.56 grams of sucrose manufactured by Sigma-Aldrich Inc. in the United States were dropped in 60 milliliters of distilled water before the measurement was filled to 100 milliliters.

KCL (1M): After dissolving 7.45 grams of potassium chloride (KCl) manufactured by BDH Chemicals in England in 60 milliliters of distilled water, the volume was brought up to 100 milliliters with more distilled water.

ATP (0.01M): After dissolving 0.062g of ATP disodium salt (Sigma Aldrich Inc., USA) in a small amount of dil. water, the total contents was brought to 10ml, adding more distilled water. After that, kept in the refrigerator.

Ascorbic acid (2 %): Ascorbic acid (2g) manufactured in England by BDH Chemicals were solvated in 80 milliliters of water (distilled) before levelling volume to milliliters of 100.

Ammonium molybdate (5%) In 80 milliliters of 6.5% hydrogen peroxide, 5.0 grams of ammonium molybdate were dissolved. The volume was brought up to the 100 ml level using the same solvent, and then it was placed in a plastic bottle and kept at ambient temperature. Trichloroacetic acid (10%) :The 10 grams of trichloroacetic acid that were purchased from BDH Chemicals in England were dissolved in 80 milliliters of distilled water before being diluted with more distilled water until the volume reached 100 milliliters. Following that, it was preserved in the refrigerator.

3.7.1 Determination of mitochondrial inorganic phosphate concentration

Principle: When inorganic phosphate is exposed to molybdic acid, a yellow color is produced. This yellow color may be changed to a blue hue by adding ascorbic acid, and the strength of the color that is produced is proportional to the amount of inorganic phosphate present. The inorganic phosphate release concentration was examined as described by Bassir (1963) and the graph can `be found in appendix.

Reagents-Na_2HPO_4(10mM): One hundred and forty-two (142) milligrams of disodium hydrogen phosphate from Sigma-Aldrich Inc. in the United States were dissolved in 60 milliliters of distilled water, and the volume was brought up to 100 milliliters with more distilled water.

Ammonium molybdate (1.25%) in 6.5% H_2SO_4: Hopkins and Williams Ltd. in England provided the ammonium molybdate (6.52g), which was thawed inside 450ml of 6.5% H_2SO_4, and the volume of the total mixture was brought up to 500ml with additional 6.5% H_2SO_4 (which was H_2SO_4 added to a little water and brought to 500ml). The molybdate solution that was obtained was kept at a temperature of 25 degrees Celsius in a container made of plastic.

Ascorbic acid (9%): After dissolving 22.5 milligrams of ascorbic acid from BDH Chemicals in around 160 milliliters of distilled water, the volume was brought to 250 milliliters, dispensing more water.

Procedures: For the purpose of generating a conventional inorganic phosphate release curve, disodium hydrogen phosphate at a concentration of 1 mM was utilized. For the standard curve, many different concentrations of 1mM Na_2HPO_4 were used. After incubating the sample at room temperature for thirty minutes, the absorbance was measured at 660 nm. The blank was made up of distilled water.

Table 3 .3: Protocol for inorganic phosphate content

Test tubes in Duplicates	Blank	1	2	3	4	5	6	7	8
1 mM Na_2HPO_4 (µl)	-	20	40	60	80	100	120	200	300
Distilled water (µl)	1000	980	960	940	920	900	880	800	700
1.25% ammonium molybdate (ml)	1	1	1	1	1	1	1	1	1
9% ascorbate (ml)	1	1	1	1	1	1	1	1	1

3.8: Measurement of Lipid Peroxidation (*in vitro* and *in vivo*)

This is the chain of reactions of oxidative degradation of lipids. A process that takes up electrons from the lipids in cell membranes causing the damage of the cells. Some products of medicinal plants may have dual facets effects which may be both antioxidant and pro-oxidant effects, when its pro-oxidant, they induce free radicals and peroxidation of mitochondria membrane lipid. This study was conducted to ascertain that the induction observed was not as a result of reactive oxygen species but by bioactive present in the plant.

Principle: According to the method described by (Ruberto *et al.*, 2000), lipid peroxidation was determined. The product; Malondialdehyde (MDA), formed during lipid peroxidation, reacts with thiobarbituric acid forming a pink product. Butanol is used to extract the colored product and is measured on a spectrophotometer at 532 nm.

Reagents: Thiobarbituric acid(0.8% : Thiobarbituric acid (0.8g) (BDH Chemicals Ltd, Poole, England) was dissolved in a volume of 50 ml distilled water and adjusted to the 100 ml mark with distilled water in a volumetric flask.

Sodium dodecyl sulphate(1.1%) **:**Sodium dodecyl sulfate (8.1g) (BDH Chemicals Ltd, Poole, England) was dissolved in 80ml distilled water and the solution was adjusted to the 100ml mark in a volumetric flask using distilled water. Equal volumes of TBA and SDS were mixed and used in the assay.

Ferrous sulphate(60µM) **:**Ferrous sulfate heptahydrate ($FeSO_4.7H_2O$) (Sigma Aldrich Co. St Louis USA) of 0.8341g was dissolved in a small amount of distilled water and the resulting solution was adjusted to 50 ml.

Acetic acid(20%): Twenty (20ml) of glacial acetic acid (BDH Chemicals, Ltd, Poole, England) was added to 80 ml of distilled water.

Procedure (*in vitro*): Two (2mg/ml) of mitochondria obtained from rat liver and fractions of various concentrations (50–800 µg/ml) were added to each tube and adjusted to 1ml with distilled water. 0.05ml of 60µM $FeSO_4$ was added to the reaction medium and incubated for almost half an hour at 37°C. 1.5ml of 20% acetic acid and 1.5 ml of TBA were added in SDS, mixed on a vortex machine

and heated to 95°C for 1 hour. Afterwards, it was allowed and thoroughly mixed with 3ml of butan-1-ol and centrifuged at 3000rpm for 10 minutes. The optical density of the upper organic layer was measured at 532nm.

Percent inhibition of lipid peroxidation = Ao-A1/ Ao x 100…….……..3.2

Where:

Ao = absorption of control; A1 = sample absorbance

Reagents for Lipid peroxidation (LPO) *in vivo*

1. 30% trichloroacetic acid (TCA)
   4.5g trichloroacetic acid (TCA) (CCl_3COOH) was dissolved in distilled water and adjusted to 15ml with the same solution.
2. 0.1M hydrochloric acid (HCl)
   Addition of 13µl conc. form of 36.5 – 38 % of hydrochloric acid in DH_20 and made to 15ml.
3. 0.75% thiobarbituric acid (TBA)
   0.1125g thiobarbituric acid (TBA) was dissolved in 0.1M HCl and made up to 15ml with 0.1M HCL. Dissolution was aided by stirring in a hot water bath (50°C).
4. 0.15M Tris-KCl buffer (pH 7.4)
   0.559g potassium chloride (KC) and 0.909g Tris base were dissolved in 45ml distilled water. The pH of the solution was adjusted to 7.4 with HCl and the volume was leveled up to 50 ml with water.

Procedure: An aliquot of 0.4ml of the test sample was mixed with 1.6ml of Tris-KCl buffer, and 0.5ml of 30% TCA was added. Subsequently, 0.5ml of 0.75% TBA was also added and the resulting solution was incubated in a water bath for 45min at 80°C. It was then cooled in ice to room temperature and centrifuged at 3000rpm for 10minutes. The clear supernatant was collected and the absorbance was measured against a standard control sample using distilled water at 532nm.

LPO Calculation : Extinction coefficient of $0.156\mu M^{-1}cm^{-1}$ was employed to determine the MDA level (Adam-Veasey and Sergi, 1982).

Lipid peroxidation (nmol MDA/mg protein) =

absorbance x volume of mixture

$E_{532\ nm}$ x sample volume x mg protein/mL…….3.3

3.9: Caspases 9 and 3 levels

Cysteine-aspartic proteases play essential role in programmed cell death. They cleave a target protein only after an aspartic acid residue, they are synthesised as a single zymogen and they are activated by a specific initiator caspase.

Principle: The basic idea behind the sandwich ELISA technique used is to measure, concentration of a particular amino acid that are particular to the one combined with a colorimetric substrate that the strength is proportional to the concentration of the specific one under study.

Multiple secondary antibodies will bind to the primary antibody, leading to signal amplification, when the protein-specific secondary antibody (caspases 9 and 3) that is biotin-bound recognizes and binds to the primary antibody recognizes and surrounds the desired protein in the cell lysate. Both monoclonal and polyclonal antibodies can be employed in sandwich ELISA systems to capture and detect antibodies. Monoclonal antibodies recognize just one epitope, making it possible to detect and quantify even minute variations in an antigen with accuracy. A polyclonal antibody is frequently used.

When utilized to bind the biotin-bound secondary antibody, the streptavidin-HRP complex (horseradish peroxidase) was known for its streptavidin moiety. The HRP's substrate is hydrogen peroxide. The oxidation of the hydrogen donor, which occurs during the reaction, is related with the splitting of hydrogen peroxide, which results in a change in color. The HRP domain reacts with the added TMB substrate. A colorful product is created as a result, and the chromogenic signal is detected at 450 inm using the plate reader (ChroMate-4300, Florida, USA). An inhibitor solution, which is normally acidic, was then added to block the process (Engvall, 1972; Schmidt *et al*., 2012).

To prepare the samples and test Caspases 9 and 3 using the Elisa Technique, rat livers were dissected, weighed, and thoroughly washed with phosphate-buffered saline until a clear wash solution was obtained. The liver was then homogenized on ice, and the resulting homogenate was centrifuged at 8000 rpm for 5 minutes. The resultant supernatant was transferred to sample tubes and frozen. After two days of freezing, the samples were allowed to thaw, expediting cell disintegration. This technique was conducted twice before testing the samples for Caspases 9 and 3.

The procedure for the Elisa process follows the guidelines published by the manufacturer (Elabscience kit). Samples or standards (50 µl) were added to the wells, followed by 50 µl of the antibody mixture/cocktail (a component of the Elabscience kit). The microplate was closed and incubated for one hour at room temperature (25°C) on a plate shaker running at 400 rpm. The wells were then cleaned three times to eradicate loose particles, achieving 100% liquid evacuation at each step. After the last wash, the microplate was spun and wiped with a clean paper towel to remove excess liquid. Next, 100 µl of TMB substrate was added and incubated for 10 minutes in the dark. The process was terminated by adding 100 µl of stop solution, causing the hue to transition from blue to yellow. The absorbance was measured at 405 nm.

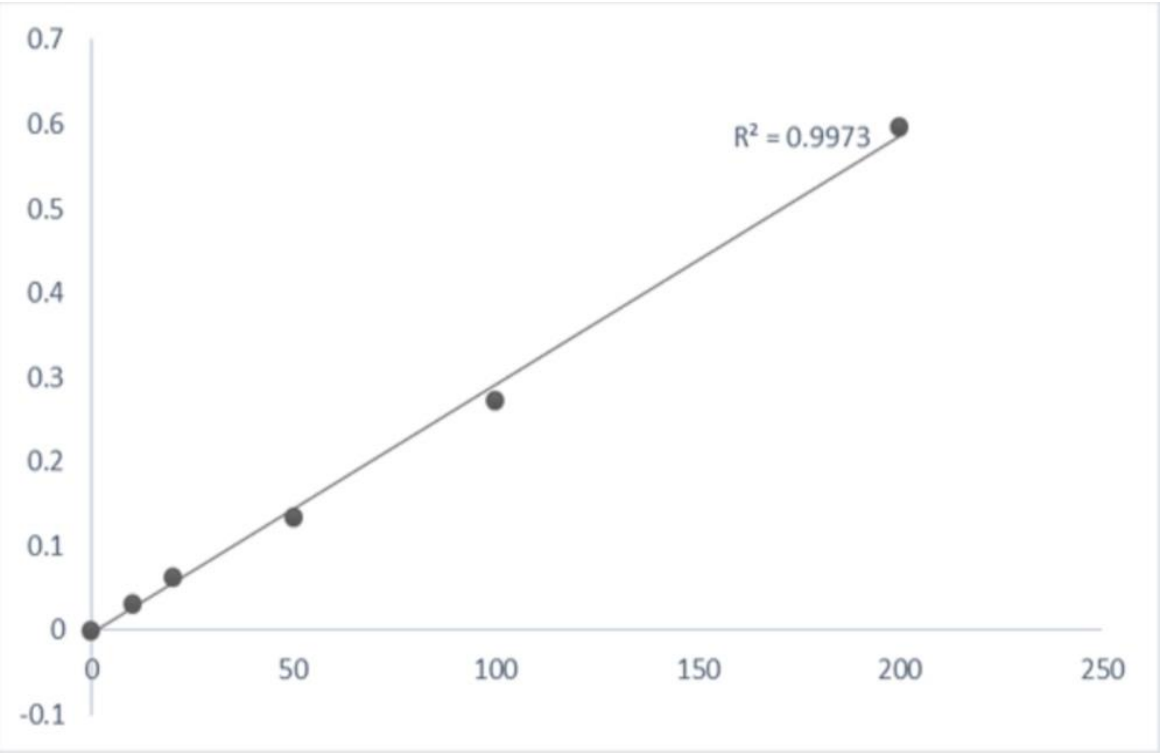

Concentration mg/kg

Figure 3.2: Caspase Standard Curve

3.10: Toxicity Assays

Pathological situations are influenced by changes in haematological parameters, liver enzymes etc since the World Health Organisation (WHO, 2012) has documented that most complications in diseases result from haematological changes in the required cells such as erythrocytes, leukocytes etc (Baahubali, 2013). Haematology tests help to diagonise anemia, infection or a general blood disorder, inflammation among others.

3.10.1: Haematological parameters

The resulting serum was separated from the clotted blood with a Pasteur pipette and used for hormonal analysis (Henry, 1979; Thavasu, 1992).

Tissue preparation: The silver and colon were rapidly removed, dissected, and with 10% formalin for approximately five days to ensure complete fixing. They were then rehydrated in increasing concentrations of isopropyl alcohol over the course of one hour. Organs that had been dehydrated were cleansed in xylene and transplanted in two shifts using vaseline oil. Ehrlich's hematoxylin was used to stain tissue sections for eight minutes. Following this, the sections were rinsed using regular water, then submerged in abrasive alcohol to get rid of any leftover spots. It was then positioned for micro photography after being counterstained with 10% aqueous eosin (Hopwood, 1996). A counterstained with 10% aqueous eosin (Hopwood, 1996).

Experimental animal preparation: Twenty-four hours following the final treatment, the animals were murdered by cervical dislocation and the blood samples were obtained by heart puncture. The blood samples for haematological parameters-red blood cell (RBC) count, white blood cell (WBC) count, platelet count, packed cell volume (PVC), hemoglobin etc were collected into EDTA bottles and analysed as follows:

Volume of the packed cell was measured by collecting blood sample into non-heparinized tubes, sealed with plasticine and spun in hematocrit centrifuge at 250g for 5min. PVC was then read using a hematocrit reader. To evaluate the white blood cell count, the whole blood sample was mixed with 380µl of Turk solution and allowed to settle for 2 minutes. The

resulting samples were then placed in a Newbaur counting chamber and placed in a humid room for 1 minute. The samples were observed under a microscope using a ax10 objective.

For platelet count, the complete blood samples were mixed with 380µl of an ammonium oxalate solution, settled for 2 minutes, and then placed in a counting chamber within a humid chamber for 1 minute. The count was performed using a x40 objective.

To determine the differential white blood cell count for lymphocytes, monocytes, eosinophils, and neutrophils, a thin film of whole blood was created on a grease-free slide. The slide was air-dried and stained with Leishman stain for 5 minutes. The stain was then diluted with phosphate buffered saline on the slide and allowed to stain for an additional 10 minutes. After washing and mopping the slide, the differential count was performed, air-dried and read under a microscope using an oil immersion objective.

3.10.2 Liver function tests

3.10.2.1: Aspartate amino transferase (AST) activity

This enzyme catalyses the reversible transfer of an α-amino group between aspartate and glutamate and, as such is an important enzyme in amino acid metabolism. Its activity was determined via RANDOX AST test kit.

Principle: AST is a measured by monitoring the concentration of oxaloacetate hydrazine formed with 2,4 dinitrophenylhydrazine.

α-oxologlutarate + L-aspartate →L-glutamate + oxaloacetate……..3.4

Reagent 1:100mmol/1 of phosphate buffer pH 7.4

100mmol/1 of L-aspartate

2 mmol/1 α-oxoglutarate

Reagent 2:2, 4 dinitrophenylhydrazine

0.4 mol/1 sodium hydroxide solution

4g of sodium hydroxide was dissolved in distilled water and made up to 100mL

Table 3.4: Protocl for determination of AST activity

	Reagent blank	**Sample**
Sample	--------	0.1mL
Solution 1 (R 1)	0.5mL	0.5mL
Distilled water	0.1mL	-------
The samples were mixed and incubated for 30mins at 37^0C		
Solution (R 2	0.5mL	0.5mL
Samples were mixed and allowed to stand for 20mins at 25^0C		
Sodium hydroxide	5.0mL	5.0mL
Samples were mixed and absorbance was read against after 5mins at 546nm with a microplate reader.		

Note: 200µL of the reaction mixture was pipette into microplate before taking the absorbance readings.

3.10.3 Assessment of Antioxidant Indicators

Since liver enzymes often scavenge free radicals, it is crucial to quantify their scavenging activity. They shield and defend cells from free radicals, which can help in the treatment of diseases.

Principle: The three intracellular anti-free radical proteins SOD, catalases, and peroxidases all work by converting O_2 into H_2O_2, while SOD converts H_2O_2 into water. However, direct toxicity occurs and glucose absorption is further inhibited when H_2O_2 removal is altered by inhibiting these intracellular antioxidant enzymes, leading to a chemically reduced status of glucose deprivation and hydro peroxidation that will eventually be disrupted.

3.10.3.1: Glutathione-s-transferase (GST) indices

The GST activity was measured in 1974 using the Habig *et al*. (1974) approach.

Principle: Since all known glutathione-S-transferases have reasonably high activity when employing 1-chloro-2,4-dinitrobenzene as the second substrate, the classic glutathione-S-transferase activity assay uses 1-chloro-2,4-dinitrobenzene as the second substrate. When conjugated with reduced glutathione, the substance's absorption maximum shifts to a higher wavelength. The new 340nm wavelength at increased absorption enables for a direct assessment of the enzyme process.

Reagents preparation: 1-Chloro-2,4-dinitrobenzene (CDNB): Reduced glutathione (3.37 mg) was dissolved in one 1mL of ethanol to make 20 mM CDNB.

Reduced Glutathione (0.1M): Reduced glutathione (30.73mg) was mixed in 1mL of phosphate buffer in the test tube.

Phosphate buffer (0.1 M; pH 6.5): A capacity of 1000mL was made with distiled water of K_2HPO_4 (4.96 g) and KH_2PO_4 (9.73 g) with a pH of 6.5.

Procedure: In the test tube containing 0.2ml of 1mM GSH, 0.025ML of 1mM CDNB and 0.1ml of homogenate in a total volume of 2ml for GST analysis was added 1.67ml of sodium phosphate buffer (0.1M, pH 6.5). Absorbance was taken at 340nm spectrophotometerically and the enzyme activity was calculated as n moles of CDNB conjugates formed min^{-1} mg^{1} protein using molar extinction coefficient of 9.6×10^3 M^{-1} cm^{-3} (Mannervik, 2010).

3.10.3.2 Lipid Peroxidation Assay

Tissue Preparation : The tissues were weighed, cut into small pieces, and homogenized in a 9:1 ratio on ice. For 10 minutes, the tissue homogenate was centrifuged at 1000 g rpm. The supernatant was kept on ice for future research.

Procedure After adding 0.1mL of the reagent mix to the standard test tube and 0.1mL of absolute ethanol to the blank test tube, the procedure was completed. The sample test tube and the control test tube each received 0.1ml of the sample solution. Then, 0.1 ml of reagent was applied to each test tube (blank standard, sample, and control). Additionally, each solution received 3.0ml and 0.1ml of (R x 2) and (R x 3) additives, respectively.

One (1.0ml) of 50% glacial acetic acid was added to the control and then mixed thoroughly. The tube was fastened with the plastic film and a small hole was then pierced with a needle. However. 40 minutes of 95°C water bath incubation were followed by 40 minutes of running water cooling for the test tubes. With the spectrophotometer adjusted to zero using double-distilled water, the mixture was spun at 3100 rpm for 10 minutes. The supernatant was then collected, and the value was measured at 532 nm using a cuvette with a 1 cm diameter.

3.10.3.3: Determination of Reduced Glutathione Activity (GSH)

Beutler et al method was used to measure GSH level (1963)

Principle: For the determination of reduced glutathione activity (GSH), the Beutler et al method from 1963 was used. This method relies on the reaction of GSH with 5,5'-dithiobis(2-nitrobenzoic acid) (Ellman's reagent) to produce 2-nitro-5-thiobenzoic acid, which has a molar absorption at 412 nm. The optical density at 412 nm is proportional to the level of reduced glutathione in the sample.

Preparation of Reagents:

1. Glutathione Working Standard

Phosphate buffer (0.1M; 100 mL; pH 7.4) was used to solvated 40 g of GSH.

2. Buffer (0.1M Phosphate at pH 7.4)

a. $Na_2HPO4.2H_20$ (7.1628 g; mol. Wt. 358.22) was mixed in dH_2O (200 mL capacity) to make $Na_2HPO4.2H_20$ (0.1M; mol. Wt. 358.22).
b. $NaH_2PO_4.2H_2O$ (1.5603 g; mol. Wt. 156.03) was dissolved in dH_2O (100 mL capacity) to make 0.1M $NaH_2PO_4.2H_2O$ (mol. Wt. 156.03).
3. Finally, by mixing solutions (a) and (b) and positioning the pH to 7.4, 0.1M phosphate buffer was created.

Ellman's Reagent [5,5'-dithiobis-(-2-nitrobenzoic acid) DTNB]

A total of 40 mg of DTNB was dissolved in 0.1M phosphate buffer and filled to a capacity of 100 mL.

Precipitating Solution: Sulphosalicyclic acid (4g) in dH2O of 100 mL capacity ($C7H6O6S.2H2O$, Mol Wt. 254.22) to yield 4 % sulphosalicyclic acid.

Procedure: To achieve 1 in 10 dilutions, the test sample (0.1 mL) was diluted with H2O (0.9 mL). To deproteinize the diluted test sample, and addition of 4 % sulphosalicyclic acid solution (3 mL precipitating solution) was applied. At 3000 g, centrifugation was observed for 10mins, mix the supernatant (0.5mL) with 0.1M phosphate buffer (4ML), afterwhich Ellman's Reagent (4.5 mL) was injected. Blank made from 0.1 M phosphate buffer (4 mL), 0.5 mL of the diluted precipitating solution (made by mixing 3 mL of precipitating solution to 2 mL of distilled water), and 4.5 mL of the Ellman's Reagent combination. After applying Ellman's Reagent, the samples were read at 412 nm within 5 minutes with the unstable colour produced. Reduced glutathione, or GSH, has a linear relationship with absorbance at 412 nm.

3.10.3.4: Superoxide Dimutase (SOD) Activity Measurement

This was carried out according to the technique of Mistra and Fridovich (1972).

Principle: The measurement of superoxide dismutase (SOD) activity was carried out according to the technique of Mistra and Fridovich from 1972. This method is based on the ability of SOD to inhibit the autoxidation of epinephrine at pH 10.2. An aliquot of the diluted sample solution was mixed with sodium carbonate buffer at pH 10.2. A blank was prepared using distilled water and the sodium carbonate buffer. The reaction was initiated by adding adrenaline solution, and the absorbance was measured against the blank.

Preparation of Reagents:

Carbonate buffer (0.05M, pH 10.2): In 900 mL of dH_2O, $Na_2CO_3.10H_20$ (14.3 g) and $NaHCO_3$ (4.2 g) were dissolved. After adjusting the pH to 10.2, 1000 mL of distilled water was added.

Epinephrine (0.3M): Freshly prepared soltion, epinephrine (0.0137 g) dissolving in dH_20 (200 mL).

Procedure: The ratio of the first dilution (1) to the ninth dilution (9) was obtained from a serum sample of 1 mL coupled with distilled water. An aliquot of 0.2 mL from the diluted sample solution was combined with 2.5 mL of a pH 10.2 anhydrous sodium carbonate (Na2CO310H20) buffer, which has a concentration of 0.05 M. To make the blank, 2.5 mL of the anhydrous sodium carbonate buffer was pipetted into a test tube along with 0.2 L of distilled water, and the test tube was then mixed. The addition of freshly made 0.3 nM adrenaline solution to the combination, which was quickly mixed using the inversion approach, started the reaction mixture. One cuvette was filled with one millilitre of the sample solution, and another cuvette was filled with one millilitre of the blank solution. The data set was then compared to the blank using a UV/visible spectrophotometer, and the absorbance at 480 nm was measured and recorded every 30 seconds for 150 seconds.

Calculation of SOD: Change in optical density per minute

$$= \frac{A_f - A_i}{2.5}$$

A_i = initial optical density

A_f = final optical density

$$\% \text{ Inhibition} = \left(\frac{\text{Increase in sample optical density}}{\text{Increase in blank optical density}} \right) \times 100 \ldots\ldots\ldots\ldots\ldots\ldots 3.5$$

The amount of superoxide dismutase required to block the oxidation of adrenalin by at least 50% is defined as a unit of superoxide dismutase activity.

3.10.3.5: Catalase (CAT) activity Measurement

Claiborne *et al* technique was used to determine catalase activity (1984).

Principle: The basis of this protocol, is the reduction of absorbance at 240nm when catalase spilts hydrogen peroxide. Although hydrogen peroxide has no optical density maximum at this wavelength, its optical density corresponds well enough with concentration to be used in a quantitative analysis. The extinction coefficient (Noble and Gibson, 1970).

Preparation of Reagents: Phosphate buffer (0.05 M, pH 7.4): A hundred (100mL) of dipotassium hydrogen phosphate (0.696 g) and potassium dihydrogen phosphate (0.265 g) dissolved in dH_20 (90 mL) at pH 7.4

Hydrogen peroxide (19mM):This solution was made by dissolving 30 % H_2O_2 in 50 mL phosphate buffer and filling to 100 mL.

Procedure: In a 1 cm quartz cuvette, sample (50µl) was pipetted into 19 Mm hydrogen peroxide (2.95 mL) mixture. After quickly inverting the mixture to mix it, it was placed in a spectrophotometer. Every 5 minutes, the absorbance was measured at 240nm.

3.11: Purification of subfraction -*Piptadeniastrum africanum* stem bark

Two phases are used for the removal of impurities from plants, the mobile (solvent system) and the stationary (silical gel) and bioactive compounds are separated based on their to desires for the phases. The migration features their affinity for the phytochemicals present in the plant.

Principle:A gas chromatography/mass spectrometer, or GC/MS separates chemical mixtures (using the GC component) and identifies the components of the mixture at the molecular level (MS component). When a mixture is heated, the GC method relies on the principle of breaking the mixture down into its component parts. The heated gaese travel through a column that is filled with an inert gas (eg helium) pass through the entrance of the column and the compounds to be separated are brought into the mass spectrometer. The mass of the analyte molecule is used as the identifying factor for chemicals in mass spectrometry.

Materials:

1. Glass chamber having a button
2. Silica gel (immovable/stationary phase)
3. Mixture of solvents - absolute chloroform/ methanol (mobile phase)
4. cotton wool

Protocol : Dry mesh silica gel (60-200) was packed in the column as a immobile state, while the moveable phase was added to the column. It was then preliminarily adsorbed by silica gel in a ratio of 1:1 prior to stationary phase. The pre-adsorbed mixture was washed away using varieties of solvent systems madeaccording to the polarity. The pooling of those with the same Rf values on the thin layer chromatography plate was done.

A line 1 cm long was drawn to the bottom of a chromatographic plate measuring 10 cm by 5 cm. The line was spotted with each fraction using a capillary tube and dropped into a chromatographic chamber containing a mixture of chloroform and methanol in a ratio of 3:2. Migration of the solvent occurred up the plate and a line was drawn indicating the volume of the solvent, air dried and viewed in the short ultraviolet range of 254 nm and the long ultraviolet range of 365 nm. The high purity eluents were then subjected to GC-MS and NMR analyses.

For the gas chromatography assessment of P. africanum stem bark, an HP-5890 gas chromatograph equipped with HP-Wax and HP-5 capillary columns was used. The oven temperature was programmed from 60°C to 220°C at a rate of 5°C per minute. Helium was used as the carrier gas at a flow rate of 2mL/min. A Varian CP-3800 gas chromatograph coupled with a Varian Satum 2000 ion trap mass detector was used for gas chromatography coupled with mass spectrometry (GC-MS) analysis. The injector and transfer line temperatures were 220°C and 240°C, respectively.

The gas chromatography oven temperature range was programmed from 60°C to 240°C at a rate of 30°C/min. Helium was used as the carrier gas at a flow rate of 1mL/min. The identification of the plant was established by comparing the retention time and retention indices of the constituents with those of reference standards. Mass spectra were also compared with published spectra and reference standard compounds. The concentration of each component was determined by measuring the gas chromatography peak areas.

3.12: Physical Appearance (Loss in body weight)

The mice's total body weight was determined daily using a weighing balance throughout the entire study, starting from the beginning and continuing until the validation of colitis symptoms.

3.13: DNA Fragmentation

Principle: The measurement of fragmented nuclear waste involved utilizing the DNA fragmentation method developed by Wu *et al*., (2005). This method relies on the extraction of highly fragmented double-stranded DNA from chromosomal DNA through centrifugation sedimentation.

In an acidic environment, a light-sensitive molecule called diphenylamine (DPA) reacts with d-2-deoxyribose in DNA, resulting in the formation of a blue-colored complex. The absorbance at 620 nm and the percentage of fragmented DNA were determined based on the amount of intact DNA molecules.

Reagents: To prepare the TRITON buffer (TET), a solution was made by dissolving 5 mM Tris and 20 mM EDTA, pH 8.0 Tris-HCl (0.61 g) and 7.45 g EDTA in a small amount of

distilled water. Then, 2 mL of Triton-X100 solution was added, and distilled water was added to make the final volume 1 L after adjusting the pH to 8.0. For the TE buffer, 20 mM Tris-HCl (0.61 g) and 7.45 g EDTA were dissolved in a small amount of distilled water, and distilled water was added to reach a final volume of 1 L in a volumetric flask. The pH was adjusted to 8.0.

Diphenylamine (DPA) solution: 0.1 L of acetic acid and 1.5 g of diphenylamine were combined. Afterward, 1.5 mL of saturated H_2SO_4 was added to the solution.

Procedure for tissue homogenate: The mice were put to death by cervical dislocation, and their livers were then chopped into little pieces, cleaned, and weighed. Following that, the tissues were homogenised by combining them with 10 litres of pH 8.0 TET buffer. The intact chromatin precipitate was separated from the disturbed supernatant by centrifuging the homogenate at 27,000 g for 20 minutes. To resuspend the intact chromatin pellet, TE buffer was added. Five millilitres of each sample were transferred to separate tubes. Each tube received 3 mL of freshly made diphenylamine solutions, which were then incubated in the incubator for 20 hours at 37 degrees Celsius. Measurements were made of the absorbance at 620 nm.

Calculation of DNA fragmentation: The fragmented DNA was calculated thus;
The broken % of DNA = B / (A+B) x 100…….…….3.6
However, A- (complete DNA) while B - (fragmented DNA)

3.14 Immunoassays

Mice were slaughtered 24 hours after the final dose by dislocating their cervical vertebrae after receiving intraperitoneal injections of P. africanum for 10 days. They were swiftly dissected, and blood was drawn from the heart and placed in flat tubes for the manufacture of the serum. The whole blood clot was spun down at 3000 rpm for 10 minutes after 30 minutes.

3.14.1: Immunodetection of apoptotic and inflammatory biomakers

Principles: Immunohistochemistry (IHC) is a way to find foreign substance (antigens) in the cells of liver and colon sections by using the way vaccines (antibodies) bind to antigens in these tissues. Their binding is performed in diverse ways. Enzymes, horseradish peroxidase (HRP) was used to speed up the color-making process (Clifon, 2011) most of the time.

3.14.2: Preparation of Immunohistochemistry samples

The approach entails immersing specific sections of liver and colon tissues in a solution of 10% formalin for a predetermined duration. To conduct Immunohistochemistry investigations, several reagents were utilised. Absolute Ethanol was manufactured by decreasing a specific quantity of absolute ethanol until it occupied exactly 100 ml, resulting in ethanol of varying grades at 10%.

Phosphate buffered saline with a pH of 7.4 (PBS, pH 7.4) was created by mixing distilled water with exact amounts of KCl, NaOH, kH2PO4, and sodium hydrogen phosphate.

By adding phosphate-buffered saline to 125 mL of 40% formalin to create a final volume of 500 mL, a 10% buffered formalin solution was created. Ten millilitres of 30% hydrogen peroxide were dissolved in one thousand millilitres of phosphate-buffered saline to create a 0.3% hydrogen peroxide solution.

The technique used in the study, also known as the avidin-biotin-immunoperoxidase method, is known as the avidin-biotin complex (ABC) approach. Each antibody marker has a 1:100 dilution factor applied to it. Using a rotary microtome, 2 micron-thick slices of liver and colon tissue were cut, and they were then heated on a hot plate at 70 degrees Celsius for at least an hour. The slices were ultimately submerged in water after being treated with xylene and alcohol.

The tissue slices were heated for five minutes and then chilled to remove antigens. The sections were covered with a 3% hydrogen peroxide solution, which was left to work for 15 minutes as part of the peroxidase-blocking procedure. The sections were washed in

phosphate-buffered saline, and for 15 minutes, avidin was employed to prevent protein binding. Endogenous biotins were blocked for 15 minutes in the tissue by biotin application, followed by three more blocking sessions. The sections were then washed with phosphate-buffered saline and exposed to the relevant primary antibody at the proper dilution for an hour.

The sections were exposed to the secondary antibody for 15 minutes after excess antibodies had been eliminated by washing with phosphate-buffered saline. The sections were washed, and then a secondary antibody that had been coupled to horseradish peroxidase (HRP) was used. A DAB substrate solution was then used after the sections had been washed with HRP PBS for at least five minutes. In regions with high readings, in particular, a brown colour response began to emerge. Water was used to wash away extra DAB solution and precipitates. Hematoxylin solution was used to counterstain the sections for at least two minutes, producing a brief blue stain. Following alcohol-induced dehydration, the sections were cleaned with xylene before being mounted with DPX. The targeted antigenic sites were deemed present in cells that displayed different shades of brown in the cytoplasm, cell membrane, or nucleus. Negative scores were given to cells that had no brown pigmentation when hematoxylin stained them.

3.14.3: Histopathology

This approach aids in better understanding the link between antibodies and antigens.

Method: The strategy depends on externally tagged antibodies to identify or monitor specific antigens in tissue sections that represent distinct disease states. These antigens could be either defined or specific.

Procedure: The samples were fragmented and kept in a 10% formaldehyde solution before collection. Dehydration of the samples entailed soaking them in various alcohols at separate sampling points. Pure alcohol was applied for fixation for three hours, followed by transfer to xylene for seventeen hours. The samples were then sliced into smaller pieces and positioned on a wooden board for rectification using a microtome. The previously introduced wax was utilised for embedding. Each histology sample was sectioned using a

microtome, resulting in slices with a thickness of five micrometers. Subsequently, the fragments were floated in warm water to unfold the tissue samples. Afterward, the samples were dried on a hotplate and stained with hematoxylin and eosin (HE).

3.14.4: Immunohistology

After the blocking step, the samples were separated by dipping slides into xylene twice for a total of five minutes each, and then the slides were submerged into absolute alcohol twice for a total of three hours. The next procedure included submerging the sample in alcohol at a concentration of 95% twice and 70% just once, each for a duration of three minutes. In order to execute antigenic recapturing, the samples were washed in washing buffer twice for a total of five minutes. This exposed the antigenic epitope in the samples. Other stages were completed as described in the reference, and a chromogenic color stain was noticed on the antibody using a microscope.

3.15: Statistical Analysis

Determination of the mean, standard deviation, and confidence interval for 95% were performed using The Turkish exam in order to make group comparisons and determinations. The Graphpad Prism program was used to do a number of different comparisons. All data were analysed using descriptive statistics and ANOVA at $\alpha_{0.05.}$

CHAPTER FOUR

RESULTS

4.1 Determination of Qualitative and Quantitative Phytochemical Screening of *P. africanum*

Table 4.1.1 offers a qualitative phytochemical assessment of the crude methanol extract (CM), chloroform fraction (CF), ethyl acetate fraction (EAF) and methanol fraction (MF) of *P. africanum* stem bark. Outcome revealed reveals the presence of cardiac glycosides, saponins, phenol, tannins, flavonoids and steroids are present in the crude extract, but the chloroform fraction contains a large amount of alkaloids, tannins, flavonoids and steroids, while alkaloids, phenol, flavonoids and steroids are abundant in the ethyl acetate. Methanol fraction, contains a large amount of cardiac glycosides, saponins, phenol flavonoids and steroids. However, alkaloids are absent in the methanol fraction

Table 4.1.1: Qualitative Phytochemical Screening of *P. africanum* stem bark

Phytochemicals	**Crude Methanol Extract**	**Chloroform Fraction**	**Ethyl Acetate Fraction**	**Methanol Fraction**
Alkaloids	+	++	++	-
Cardiac Glycoside	+	+	+	++
Saponins	+	+	+	++
Phenol	+	+	++	++
Tannins	+	++	++	+
Flavonoids	+	++	++	++
Steroids	+	++	++	++

Present + Absent – Abundant ++

Quantitative phytochemical screening of crude and stem bark fractions of *P. africanum* revealed the presence of tannins, cardiac glycosides, saponins, phenol, flavonoids, and steroids, as shown in Table 4.1.2. The results showed that ethyl acetate has the highest percentage of flavonoids, which is 4.529 ± 0.11, the methanol fraction has the highest percentage of phenolic compounds and saponins, which are 1.574 ± 0.01 and 2.394 ± 0.03, respectively, and ethyl acetate has the highest percentage of tannins, which is 8.450 ± 0.21.

Table 4.1.2: Quantitative Phytochemical Screening of *P. africanum* stem bark

Phytochemicals	**Crude Methanol Extract**	**Chloroform Fraction**	**Ethyl acetate Fraction**	**Methanol Fraction**
Flavonoids %	0.251±0.05	1.037±0.04	4.529±0.11	0.393±0.02
Phenols %	0.736±0.08	0.072±0.01	0.597±0.03	1.574±0.01
Saponins %	2.310±0.12	0.556±0.04	0.426±0.01	2.394±0.03
Tannin %	1.196±0.08	1.113±0.04	8.450±0.21	1.990±0.06

4.2: Assessment of crude extract of *P. africanum* on apoptotic biomakers

4.2.1 Assessment of Mitochondrial integrity

The data presented in Figure 4.1 revealed the baseline alteration in uptake caused by non-addition of calcium was low, indicating no definite different in the normal succinate-respiring mitochondria when rotenone was added for twelve (12) minutes. With the addition of calcium pore opening activator, an increase in swelling amplitude by 7.5 times was observed, which was significantly ($p<0.05$) reversed by an inhibitor, spermine from 81%

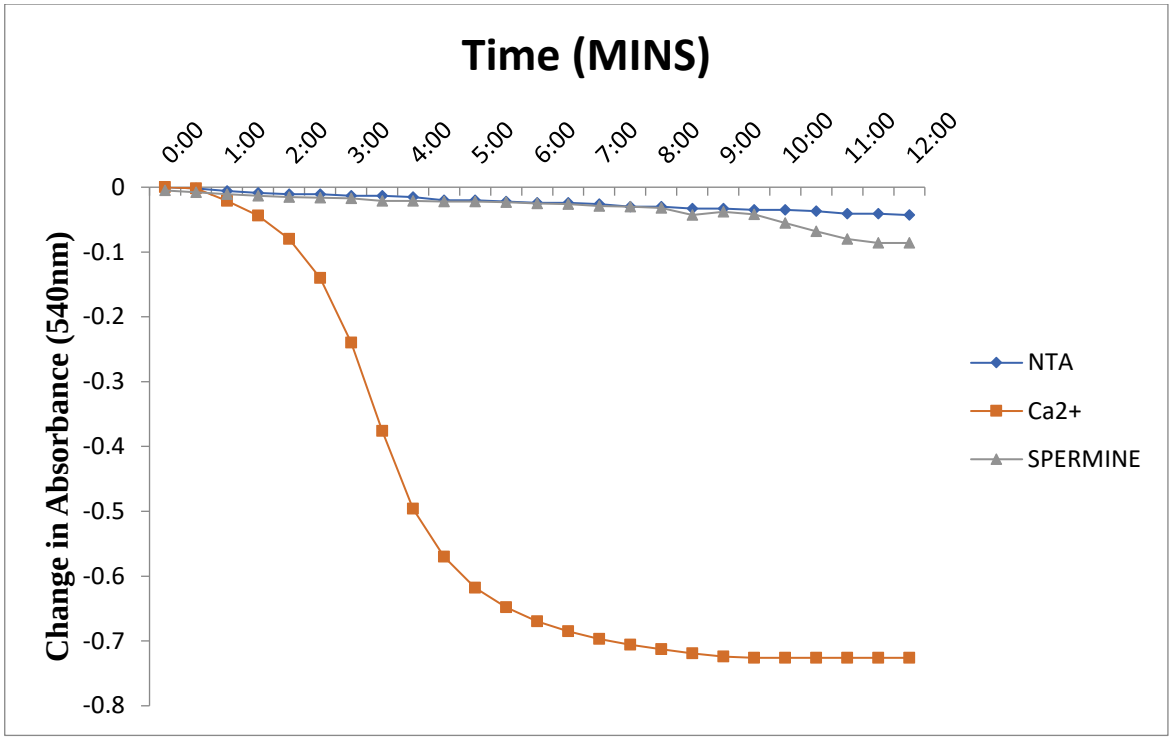

Fig 4.1: Evaluation of the impact of spermine and ca^{2+} on mice mPT Pore.

4.3: Inductive Effect of varying concentrations of crude methanol extract of *P. africanum* stem bark on mPT (*in vitro*)

4.3.1 Assessment of the effect of varying concentrations of crude methanol extract of *P. africanum* stem bark on Mitochondrial Membrane Permeability Transition Pore opening in the absence and presence of Ca^{2+} (*in vitro*)

The results showed that crude methanolic extract of *P. africanum* stem bark was found to open mitochondrial-membrane permeability transition pore with inductions of 3.4, 4.9, 6.1 and 6.3 folds in the absence of calcium in figure 4.2 together with this 8.5, 7.7, 7.0 and 6.6 folds when calcium was present at 20, 60 100, also 140 µg/mL in figure 4.3, respectively. However, addition of calcium (a standard trigger agent) further enhanced the induction process. Maximum induction of 6.3fold was observed at140 µg/mL in the absence of the trigger-agent while the highest induction of 8.5fold was observed at the lowest concentration of 20µg/mL in the presence of calcium.

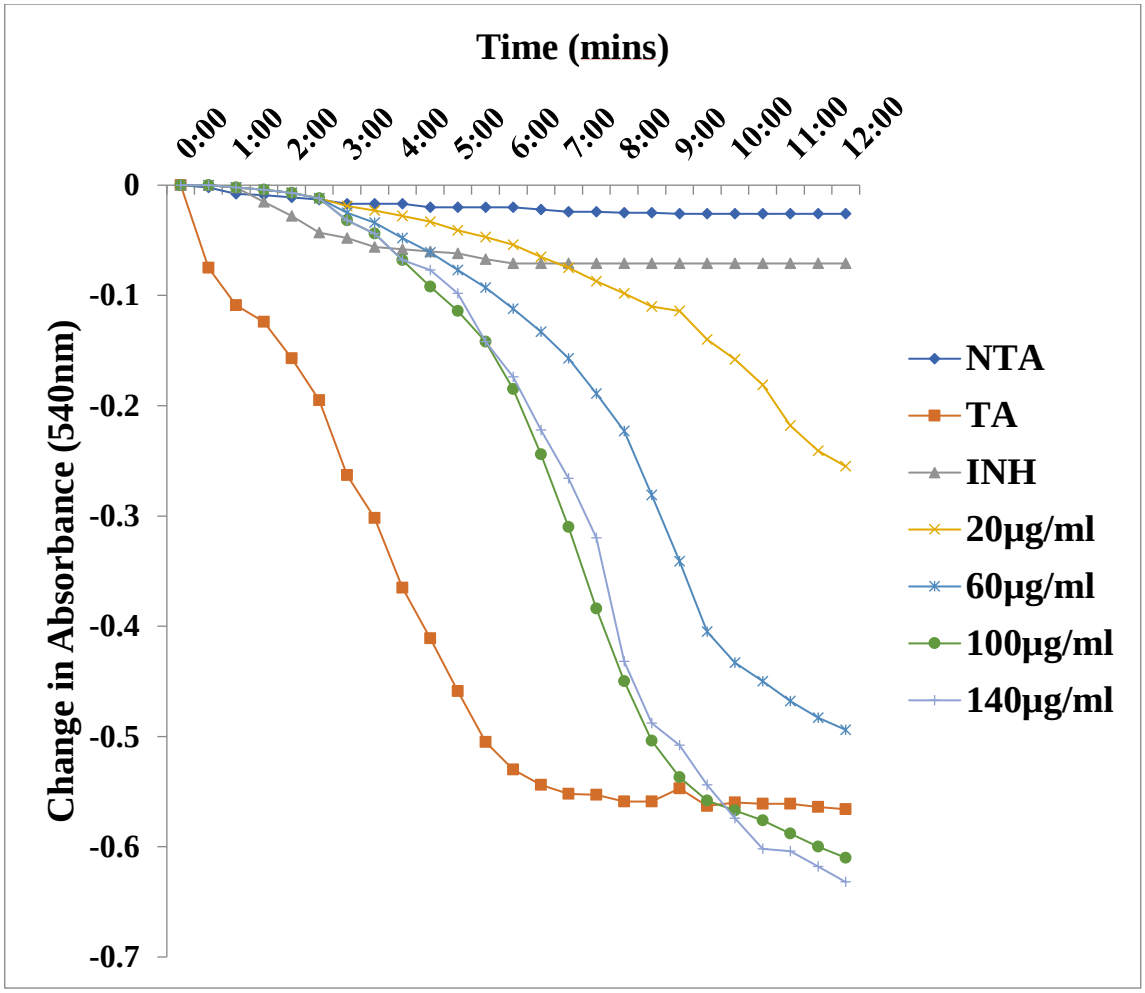

Figure 4.2: Effect of varying concentrations of crude methanol extract of *P. africanum* stem bark on mitochondrial membrane permeability transition pore opening in the absence of ca^{2+}Induction fold (Absence of Ca^{2+} -3.4, 4.9, 6.1 and 6.3)

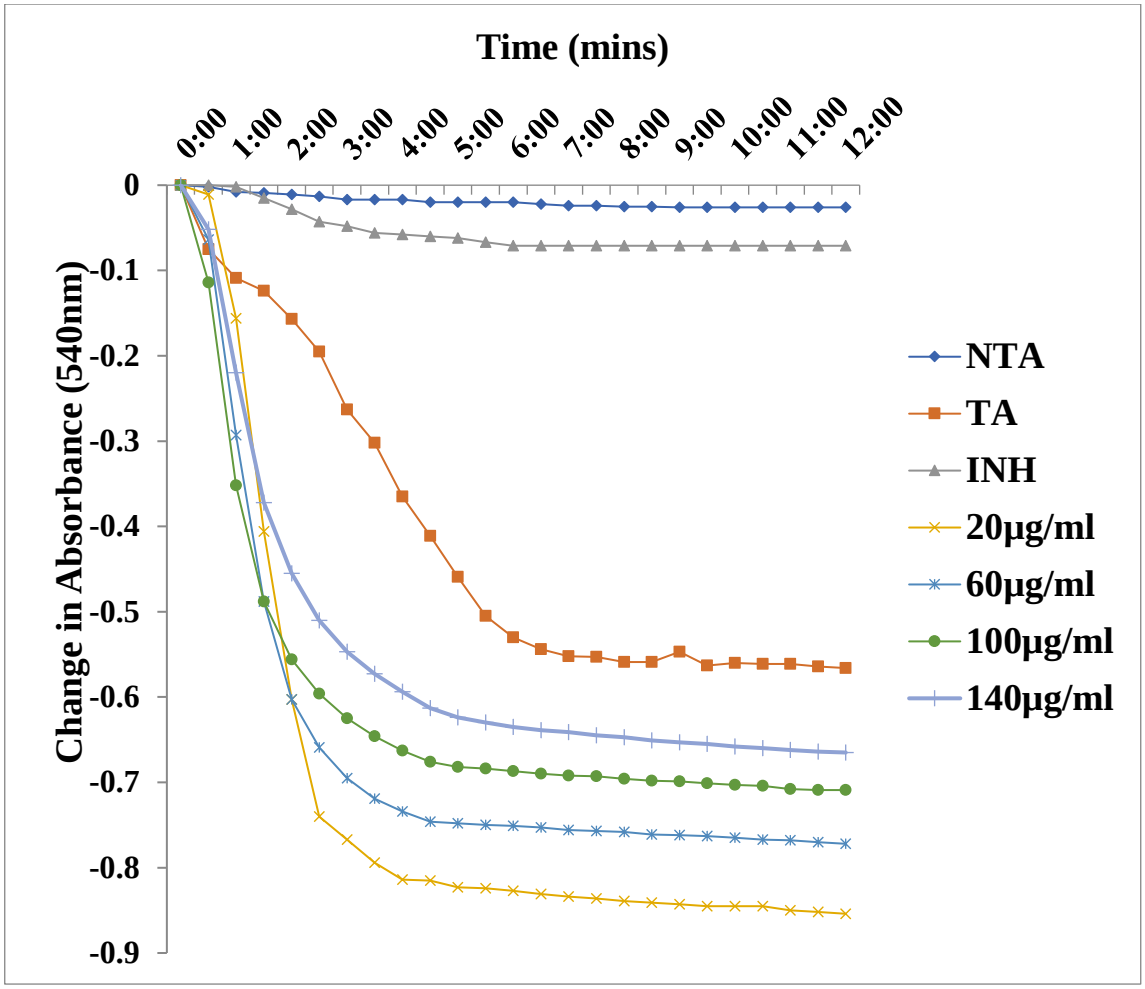

Figure 4.3: Effect of varying concentrations of crude methanol extract of *P. africanum* stem bark on mitochondrial membrane permeability transition pore opening in the presence of Ca^{2+}. Induction fold (Presence of Ca^{2+}- 8.5, 7.7, 7.0 and 6.6)

4.4: Assessment of the potency of *P. africanum* stem bark fractions on apoptotic biomarkers.

4.4.1: Assessment of the potency of varying concentrations chloroform, ethyl acetate and methanol fragments of the stem bark of *P. africanum* mitochondrial-mediated with and without ca^{2+} *(in vitro)*.

From a previous study, a crude methanolic extract of *P. africanum* was found to open mitochondrial pores, and the plant was also shown to have certain biologically active agents responsible for opening pores. The mPT (*in vitro*) assay was performed using various concentrations of three fractions of chloroform, ethyl acetate and methanol. Figure 4.4 showed the effect of chloroform and there was no induction in the absence of ca^{2+} while the presence of calcium in figure 4.5 potentiated the calcium induced opening in a reversed order with induction of 9.1, 7.4, 7.1 and 6.3 folds.

However, figure 4.6 revealed that ethyl acetate fraction had significant inductions of 3.8, 5.7, 6.0 and 8.0 while figure 4.7 divulged that addition of calcium disclosing decreased inductions with increase in concentrations 5.7, 5.4, 5.2 and 3.6, folds respectively. Methanol fractions opened the pore of mitochondria but had the highest (5.0) induction at 100µg/mL in the absence as shown in figure 4.8 had 2.3, 2.5, 5.0 and 4.6, the triggering agent opened the pore in a reversed manner with 8.0, 7.3, 7.2 and 5.4 in figure 4.9, all concentrations at 20, 60, 100 and 140 µg/mL, respectively. The result showed that highest mPT pore opening was observed with ethyl acetate having highest induction of 8.0-fold 140µg/ml.

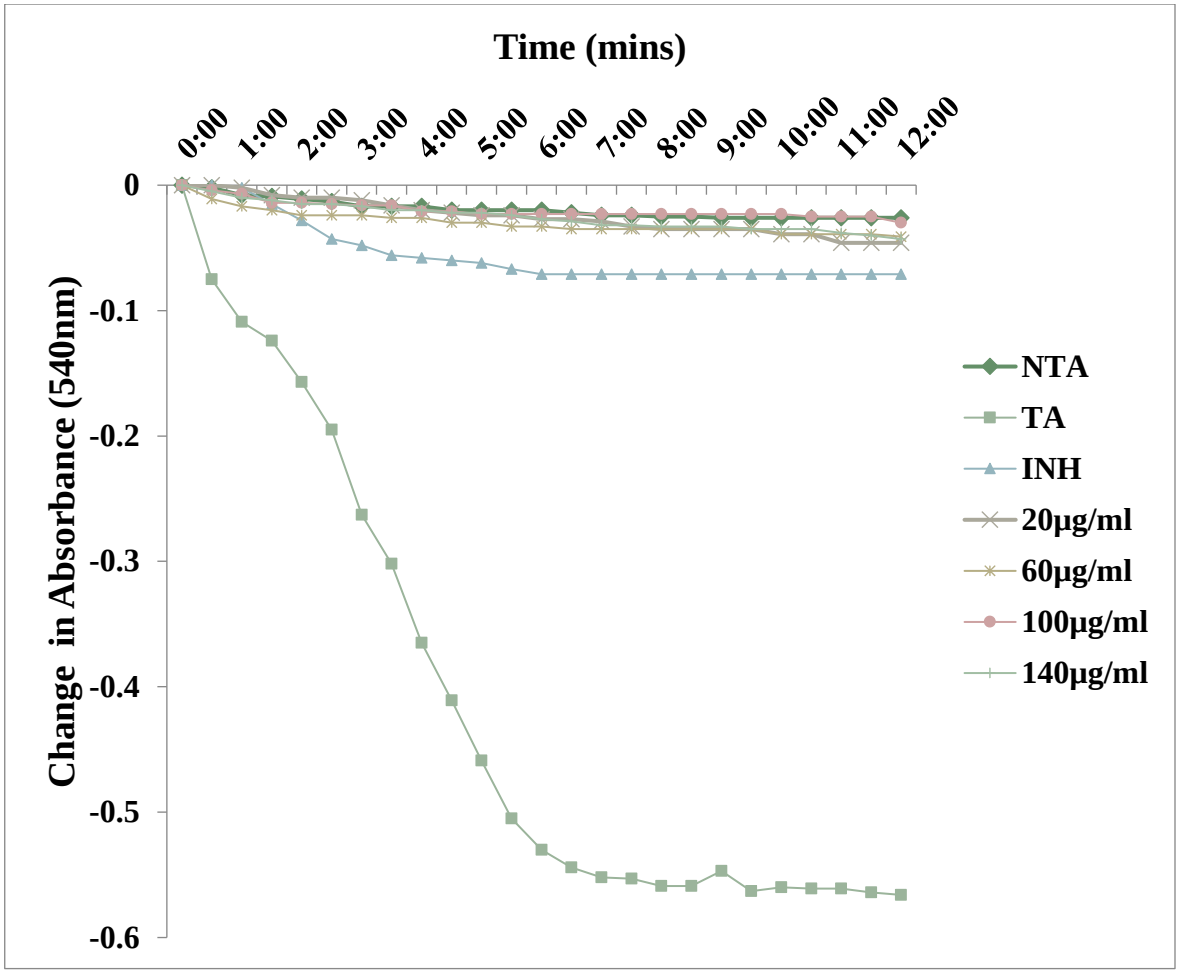

Figure 4.4: Effect of different chloroform fraction concentrations on mitochondrial membrane permeability transition pore opening in the absence of Ca^{2+} *(in vitro)*. Induction fold*:* No induction

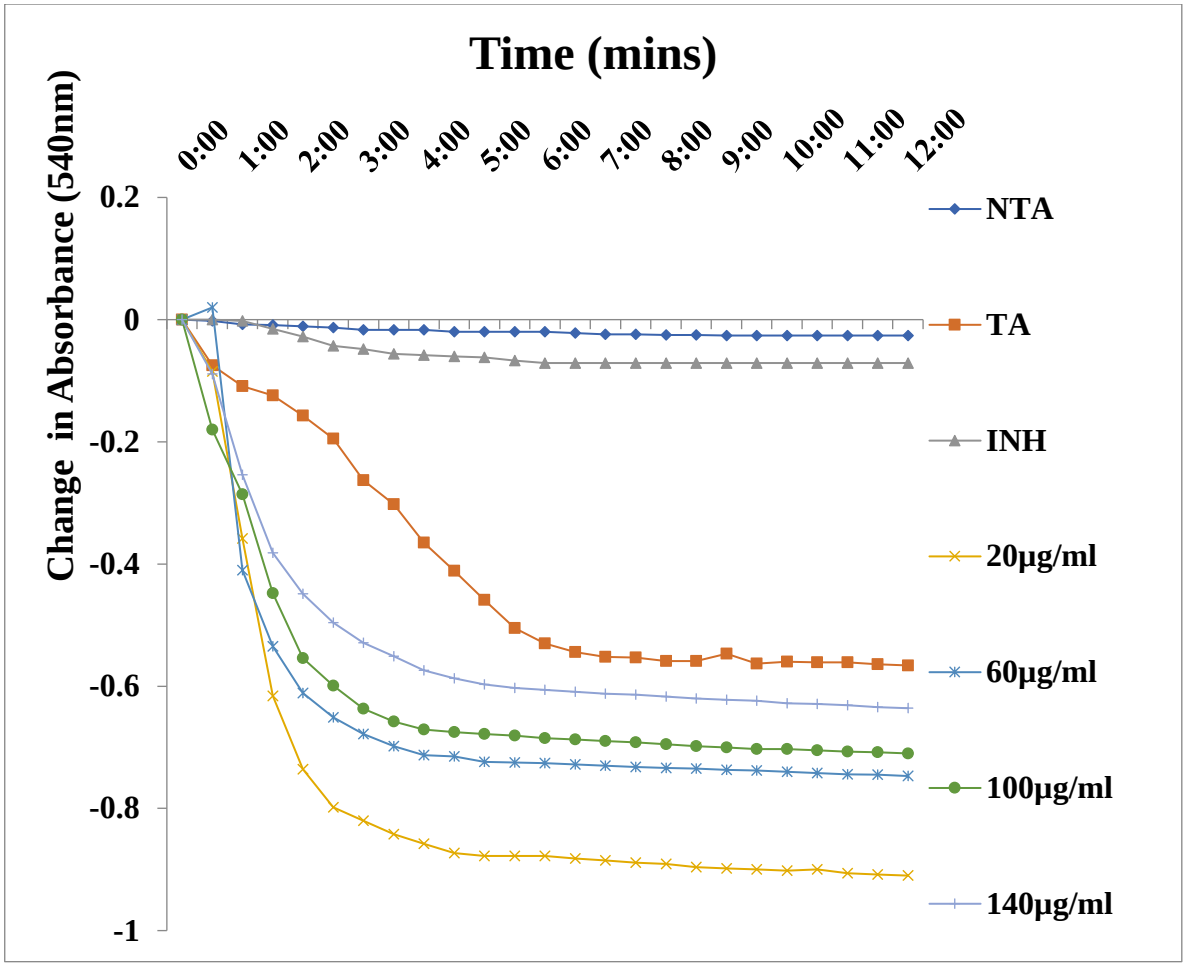

Figure 4.5: The impact of various chloroform fraction concentrations on the opening of the mitochondrial membrane permeability transition pore in the presence of Ca^{2+} *(in vitro)*. Induction fold*:* 9.1, 7.4, 7.1 and 6.3

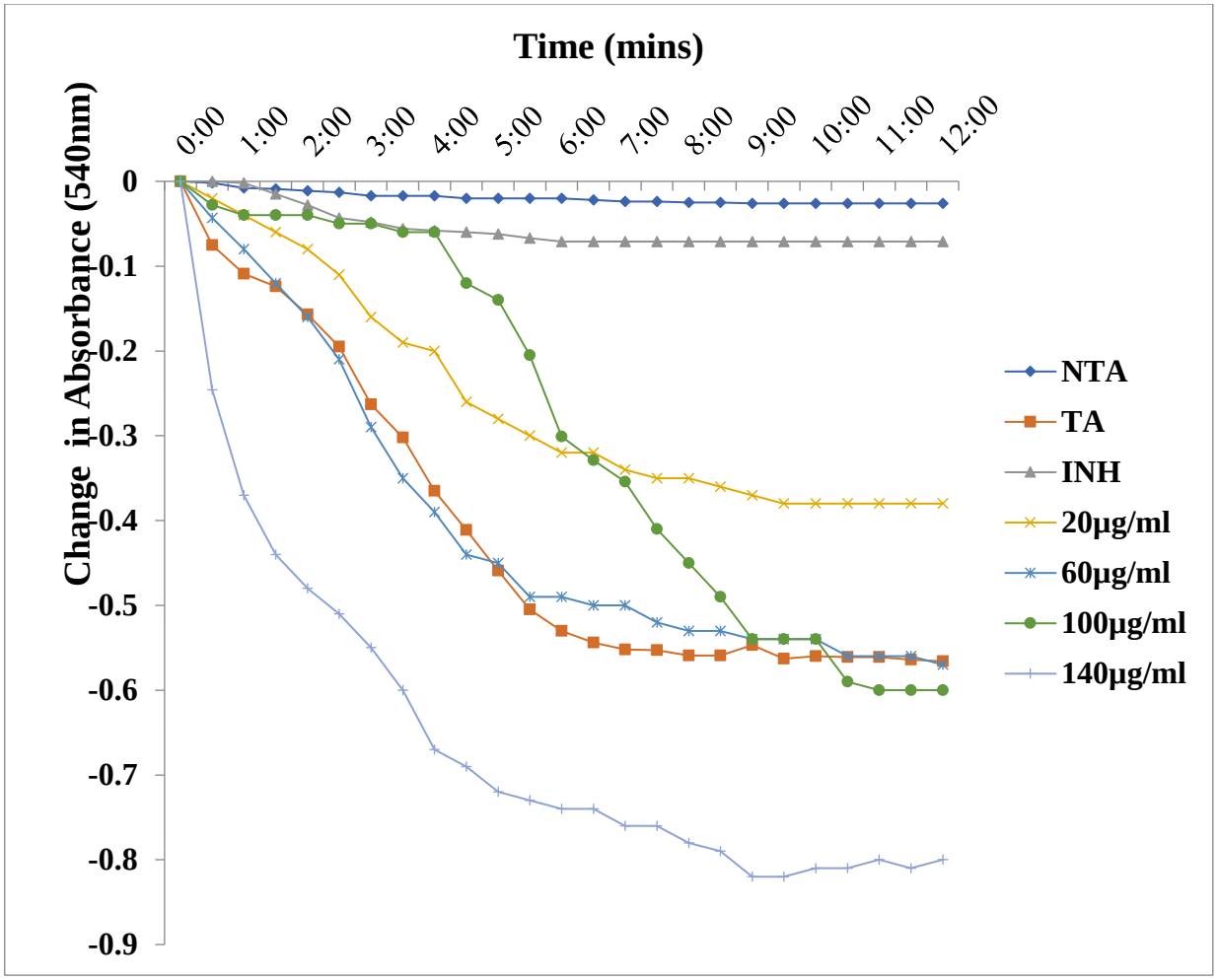

Figure 4.6: Effect of varying concentrations of ethyl acetate fractions of *P. africanum* stem bark on mitochondrial membrane permeability transition pore opening in the absence of Ca^{2+} *(in vitro)*. Induction fold*:* 3.8, 5.7, 6.0 and 8.0

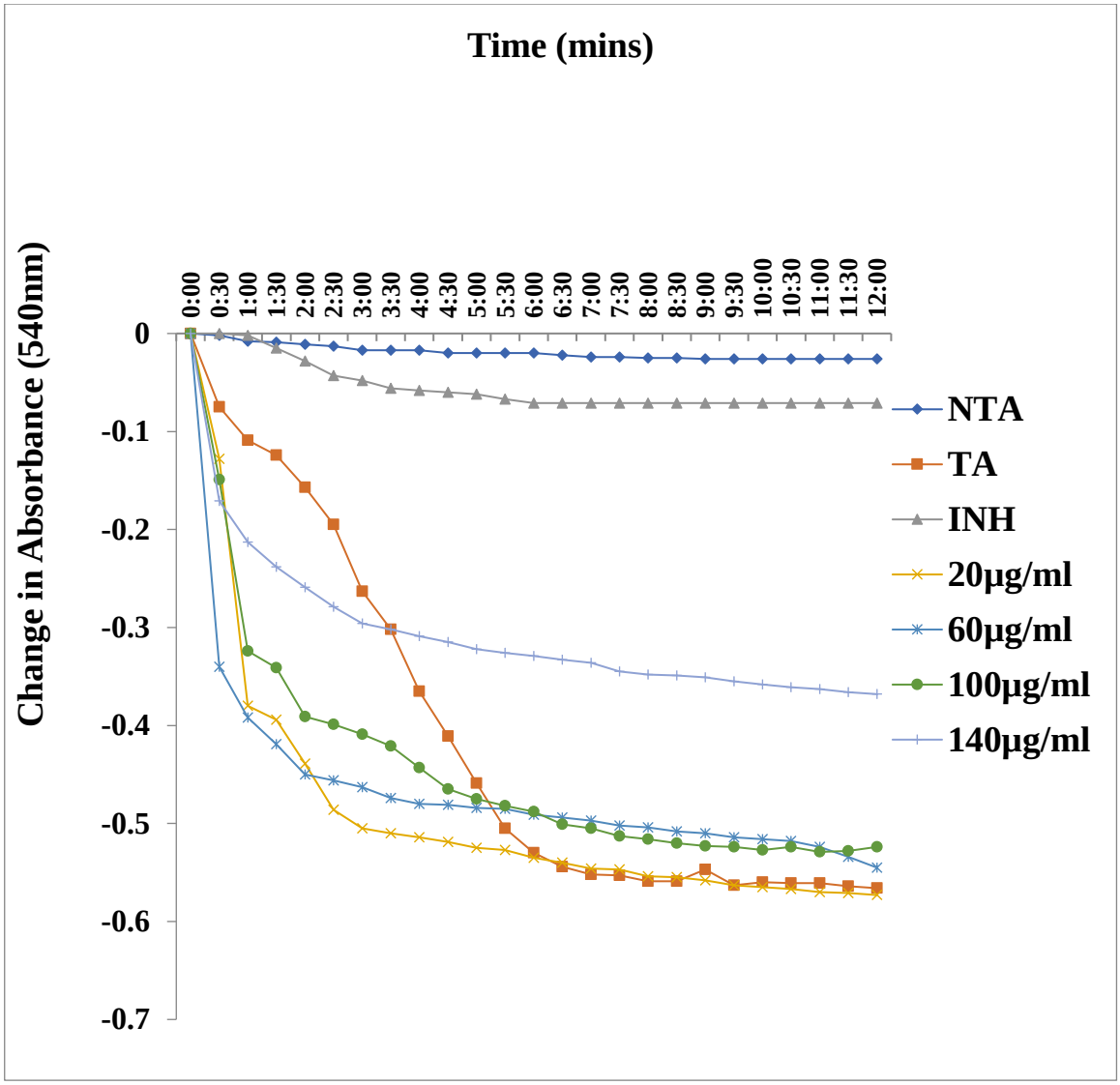

Figure 4.7: Effect of varying concentrations of ethyl acetate fractions of *P. africanum* stem bark on Mitochondrial Membrane Permeability Transition Pore opening in the presence of Ca^{2+} *(in vitro)*. Induction fold*:* 5.7, 5.4, 5.2 and 3.6

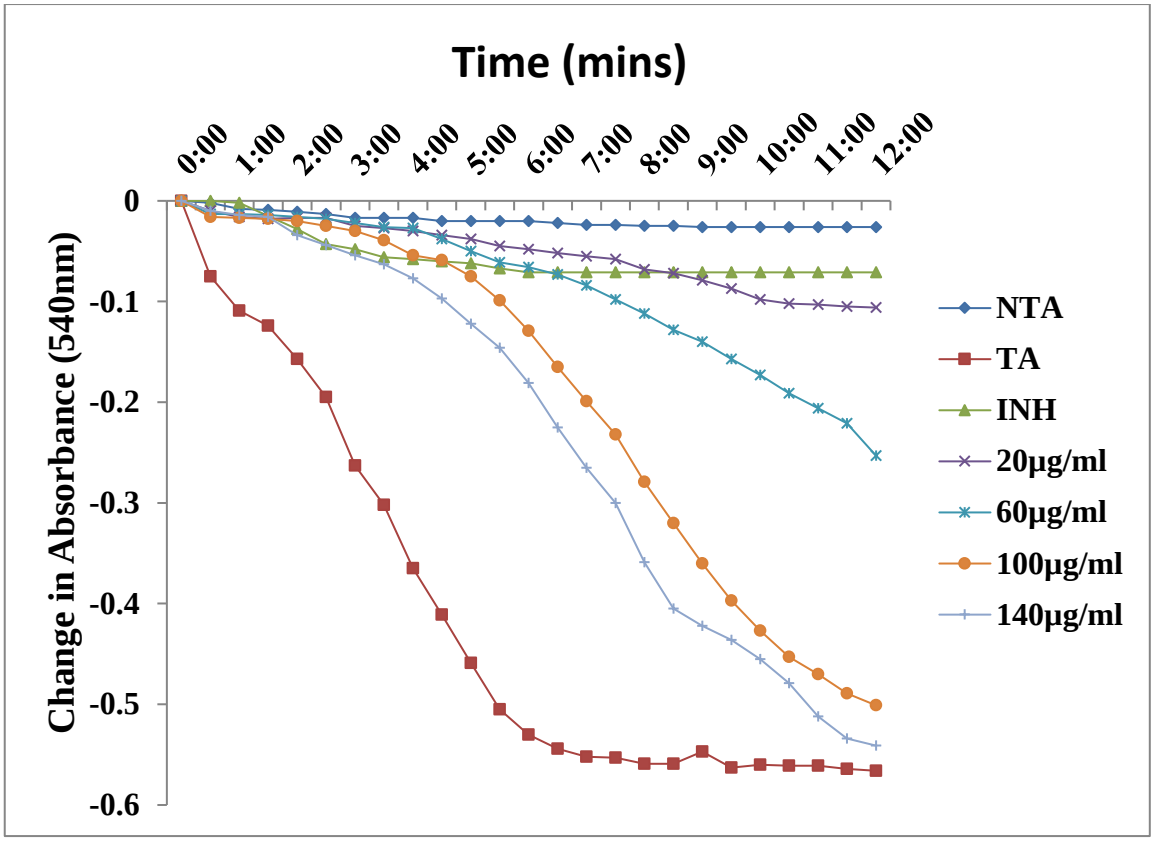

Figure 4.8: Effect of varying concentrations of methanol fractions of *P. africanum* stem bark on mitochondrial membrane permeability transition pore opening in the absence of Ca^{2+} *(in vitro)*. Induction fold*:* C-2.3, 2.5, 5.0 and 4.6

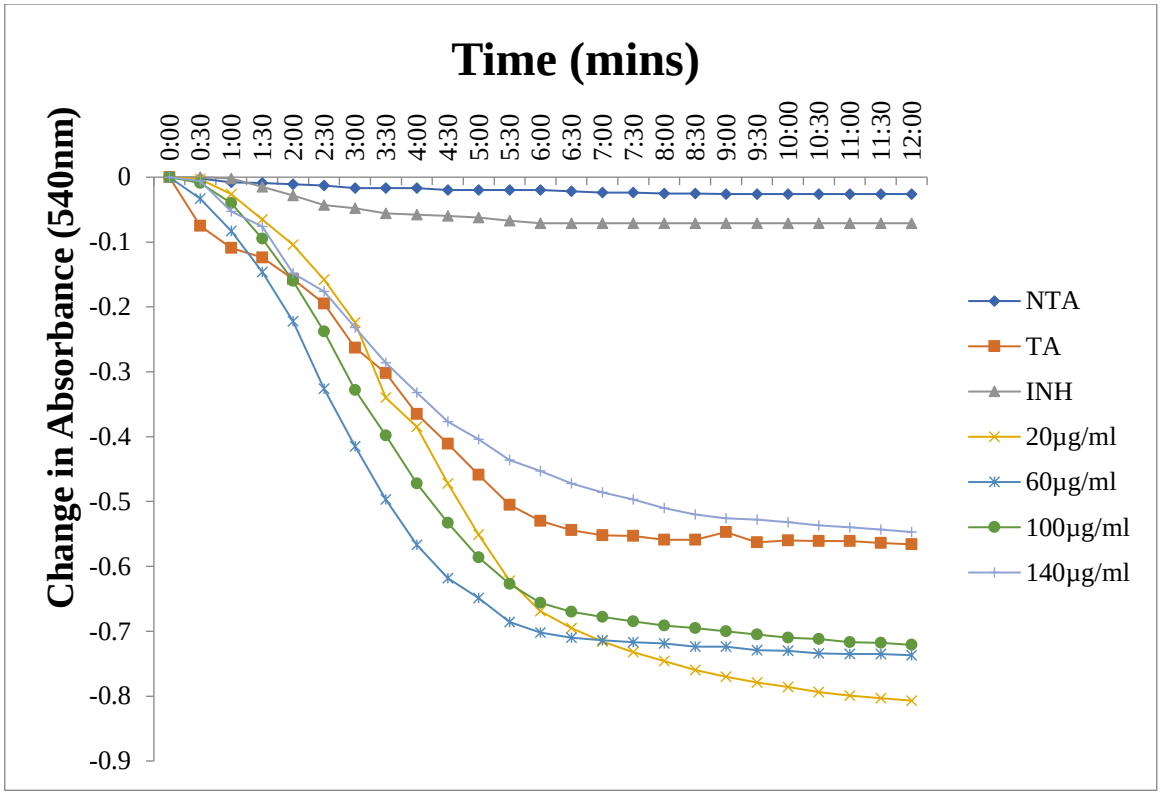

Figure 4.9: Effect of varying concentrations of methanol fractions of *P. africanum* stem bark on Mitochondrial Membrane Permeability Transition Pore opening in the presence of Ca^{2+} *(in vitro)*. Induction fold: 8.0, 7.3, 7.2 and 5.4

4.4.2: Effect of varrying concentrations of extract and fractions of the stem bark of *P. africanum* on Cytochrome C release (*in vitro*)

The outcome of the result in figure 4.10 shows that cytochrome c was released significantly from both the crude methanol extract and its fractions (chloroform, ethyl acetate and methanol fractions). The amount of cytochrome C that was released was highest in the ethyl acetate fraction, then in the methanol fraction, and then in the crude methanol extract. There was no release of cytochrome c observed by chloroform fraction when compared to the control. Ethyl acetate had the highest release at 180µg/ml which proved that mPT pores were opened.

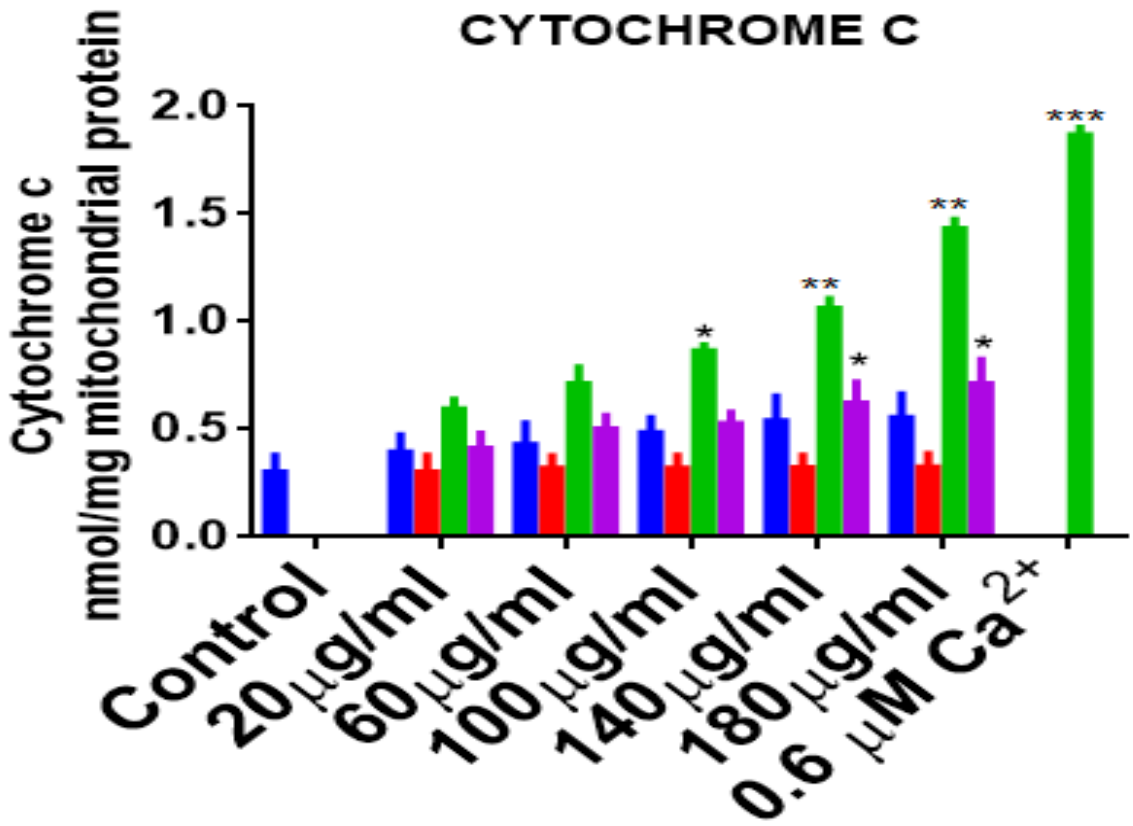

Key

CRUDE METHANOL
CHLOROFORM FRACTION
ETHYL ACETATE FRACTION
METHANOL FRACTION

Figure 4.10: Effect of various concentrations of extract and fractions of the stem bark of *P. africanum* the stem bark of *P. africanum* on cytochrome c release of mice liver mitochondria at pH 7.4

Significant differences from the control are indicated by: * ($p < 0.05$), ** ($p < 0.01$), * ($p < 0.001$) and **** ($p < 0.0001$)**

4.4.3: The impact of various amounts of crude extract and fractions of *P. africanum* stem bark on ATPase activity (*in vitro*)

Figure 4.11 revealed the effect of various concentrations of the fractions and extract of *P. africanum* on the ATPase action of mitochondria of the mice liver. The data obtained showed that there was a statistically distinct activity ($p<0.05$), and the greatest increase of mitochondrial ATPase activity was discovered to be enhanced by ethyl acetate fraction, methanol fraction, crude methanol extract, and chloroform with ethyl acetate having the highest enhancement at a concentration of 180 μg / mL and this was observed in concentration dependent manner.

The results obtained here are consistent with mPT result and cytochrome c. There was improvement of ATPase action and phosphate accumulation which result in metabolic alterations that helps mPTP formations causes the uncoupling of mitochondria making it to work in a reverse manner so as go hydrolyse ATP, with the reduced ATP levels, the cells lack structural and functional integrity, resulting in irreversible damage and cell death.

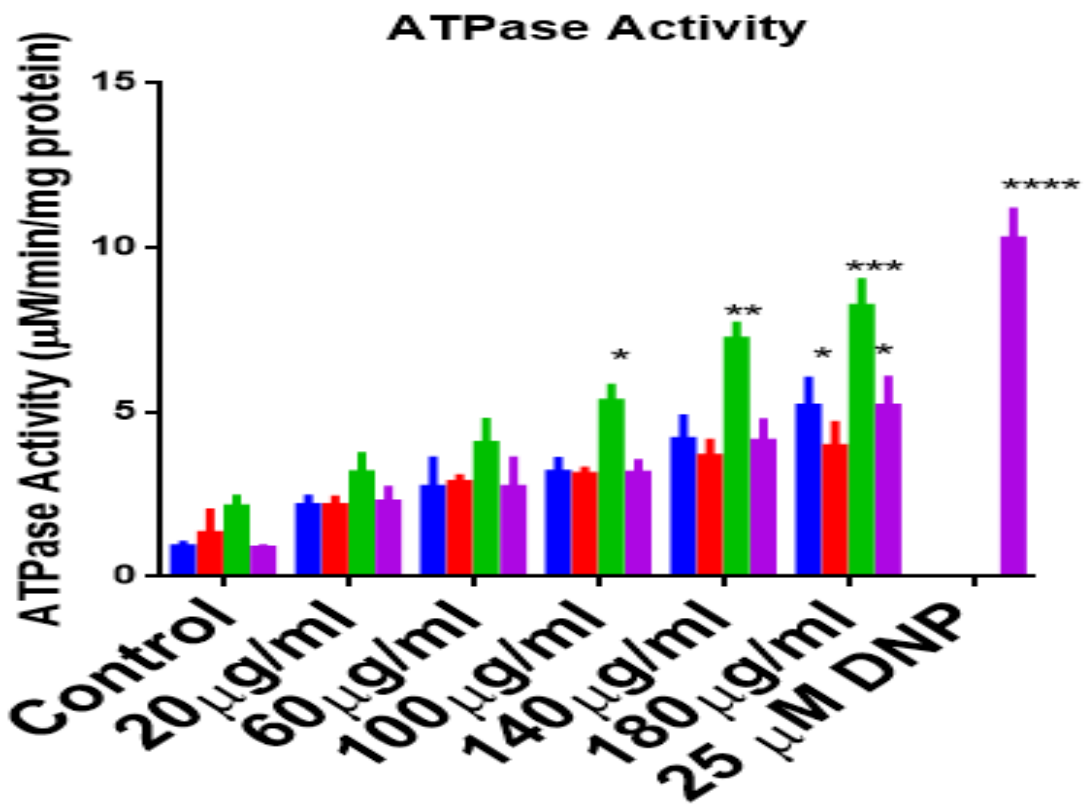

Figure 4.11: Effect of using fractions and extract from the stem bark of *P. africanum* at various concentrations on ATPase activity of mice liver mitochondria at pH 7.4

Significant differences from the control are indicated by: * ($p < 0.05$), ** ($p < 0.01$), * ($p < 0.001$) and **** ($p < 0.0001$)**

4.4.4: Effects of different amounts of extract and fractions of *P. africanum* stem bark on lipid peroxidation caused by Fe2+ using Mitochondria as Lipid-rich medium (*in vitro*)

The outcome of the crude methanol crude extract and *P. africanum* fractions on iron-induced lipid peroxidation is manifested (Figure 4.12). The results showed, pore opening by the solvent fraction was not as a result of membrane damage. The results also showed that ferrous-induced lipid peroxidation was ameliorated by the stem bark of *P. africanum* crude methanol extract and fractions when compared to the control in concentration dependent order. The highest inhibition was seen by chloroform at 180 μg / mL.

Ethyl acetate was manifested as the most potent fractions via the permeabilization of the membrane of the mitochondria, release of cytochrome c, enhancement of ATPase activity and inhibitory activity which was not as a result of membrane damage. The result also showed a concentration-dependent in of Fe^{2+}-induced lipid peroxidation by extract and fractions of *P. africanum* revealing that the plant contains bioactive compounds that can act as free radical scanvengers.

.

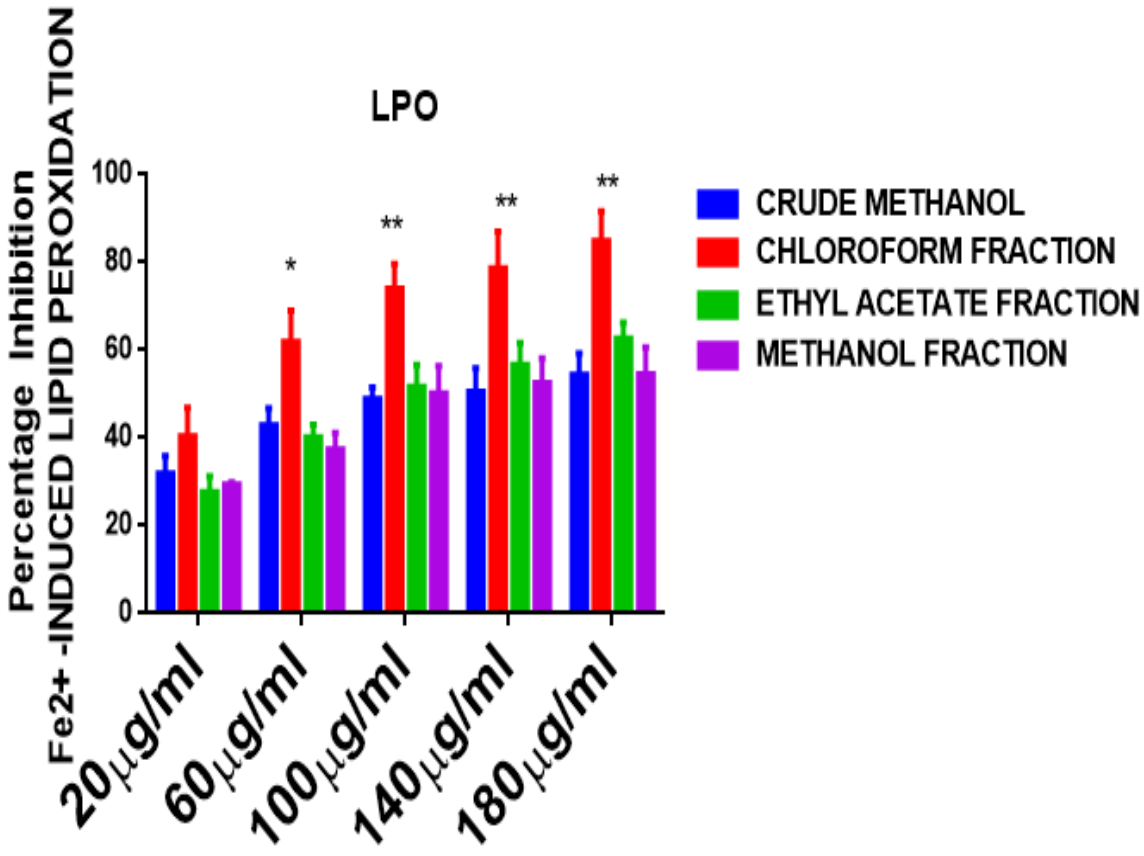

Figure 4.12: Effect of various extract and fraction concentrations of *P. africanum* stem bark on Fe^{2+}-induced lipid peroxidation (C) of mice liver mitochondria at pH 7.4

Significant differences from the control are indicated by: * ($p < 0.05$), ** ($p < 0.01$), * ($p < 0.001$) and **** ($p < 0.0001$)**

4.5: Representative profile of the most potent (ethyl acetate) fraction mPT (*in vivo*)

4.5.1: Representative profile of the effects of varying doses of *P. africanum* stem bark of ethyl acetate fraction on the opening of mitochondrial membrane permeability transition pores (*in vivo*)

The integrity of mitochondria for induction depends on the intactness, suitability and uncoupling of the mitochondria with calcium as the triggering agent and spermine a significant reversal agent. It was evidenced that the mitochondria used in this study were intact, suitable and not uncoupled according to figure 4.13. Figure 4.14, which shows the effect of ethyl acetate measured spectrophotometrically at 540 nm for 12 minutes at 30 seconds, and a distinct increase in pore opening was observed ($p<0.05$), with induction of 2.5, 4.9 and 6.9 folds at 25, 50 and 100mg/kg body weight respectively. The maximum opening of 6.9 induction fold was observed at the highest dose of 100 mg/kg body weight.

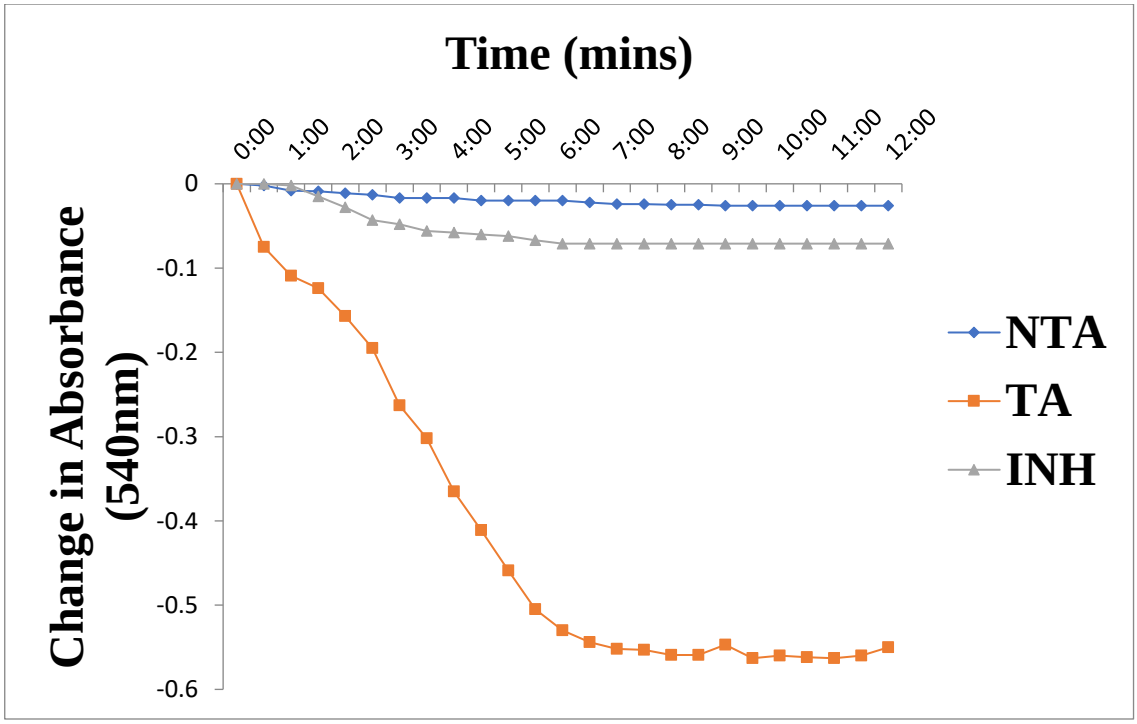

Figure 4.13: Calcium-induced mitochondrial membrane permeability transition pore opening in normal mice liver mitochondria and its reversal by spermine.

TA: 5.5 Induction **Inhibitor: 87% inhibition**

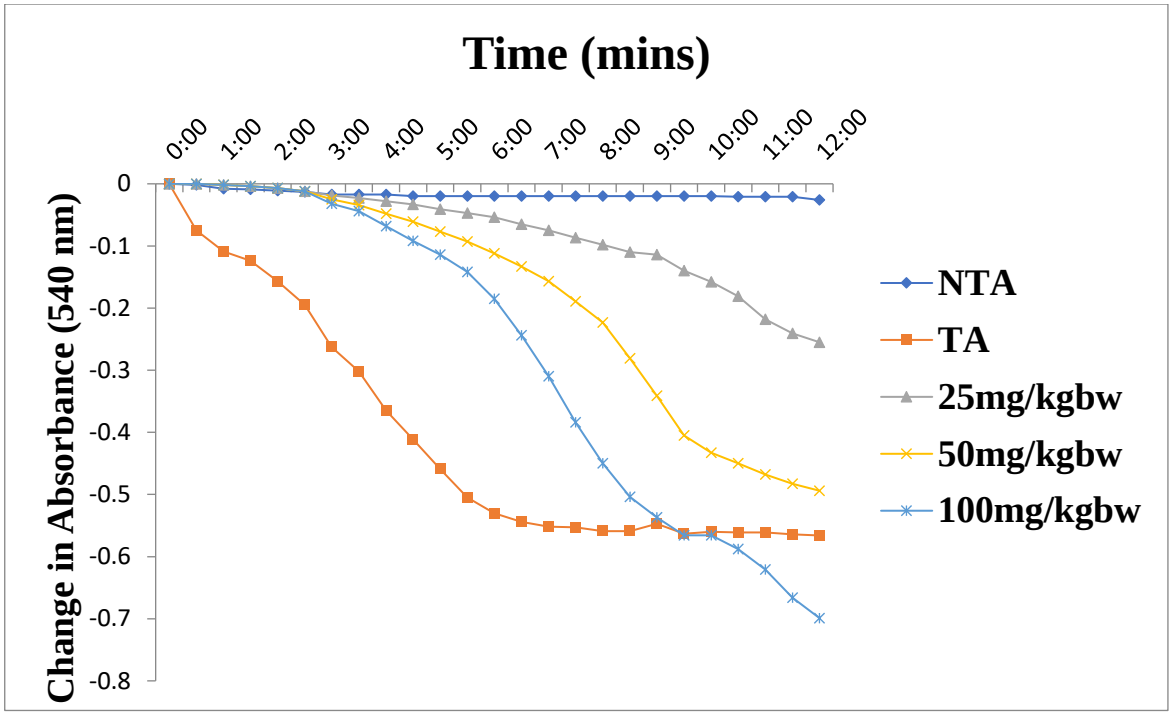

Figure 4.14: Representative profile of the effects of varying doses of ethyl acetate portion of *P. africanum* stem bark on the mitochondrial membrane permeability transition pore opening (*in vivo)*

NTA: Non-triggering agent; TA: t= Triggering agent;

Induction fold -2.5, 4.9 and 6.9

4.5.2: Effect of varying doses of ethyl acetate fractions of the stem bark of *P. africanum* on ATPase activity

There was significant enhancement of ATPase activity in the values obtained 30%, 45% and 65% by varying concentrations of ethyl acetate at 25, 50 and 100 milligrame/kilogramme body weight in dose dependent manner in relation to control of 10% and the highest was viewed at 100mg/kg bw.

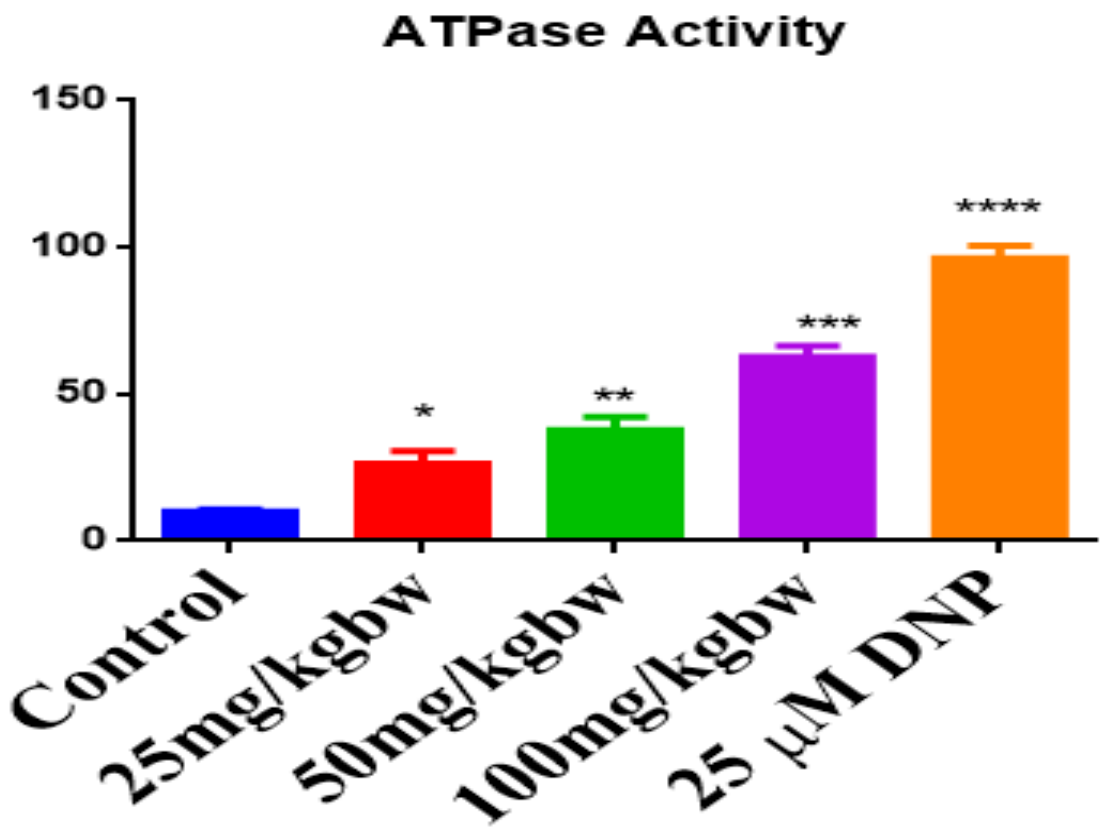

Figure 4.15: Effects of varying doses of ethyl acetate fraction of the stem bark of *P. africanum* on ATPase activity at pH 7.4 (*in vivo*)

Values are expressed as mean ± standard deviation. Significant differences from the control are indicated by: * ($p < 0.05$), ** ($p < 0.01$), * ($p < 0.001$) and **** ($p < 0.0001$)**

4.5.3: Determination of varying doses of ethyl acetate fractions of the stem bark of *P. africanum* on Lipid Peroxidation

Figure 4.16 shows that there was no significant difference in the results obtained with varying doses of ethyl acetate fractions of the stem bark of *Piptadeniastrum africanum*

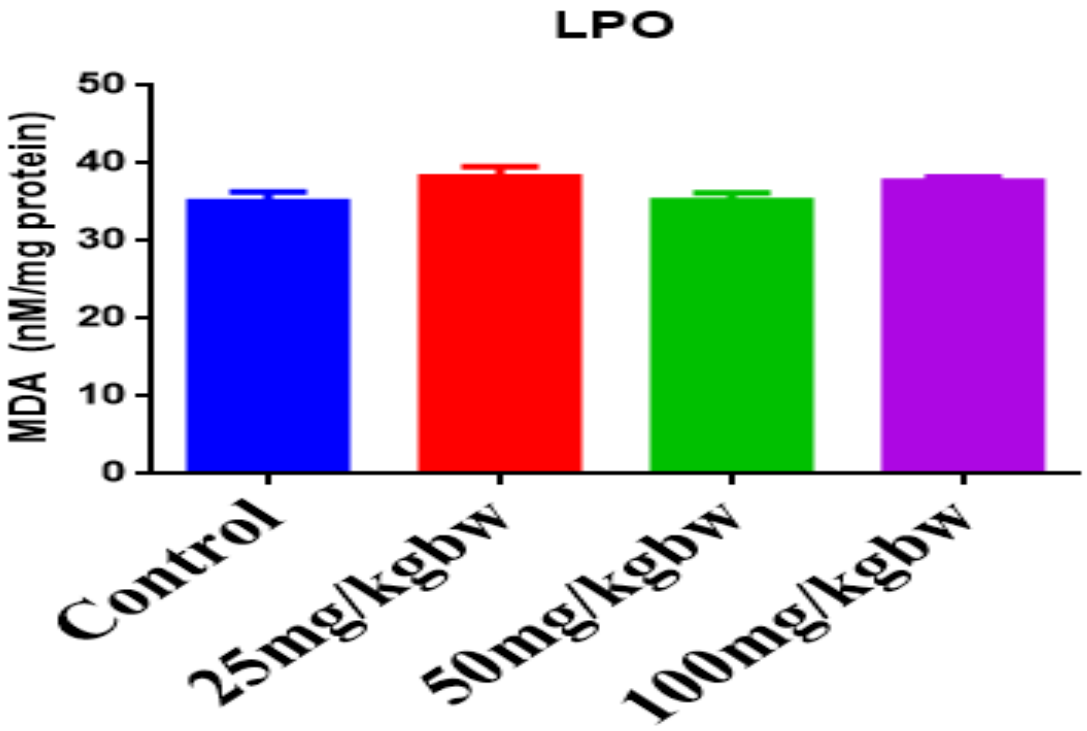

Figure 4.16: Effects of various dosages of the stem bark of *P. africanum* ethyl acetate form on Lipid Peroxidation at pH 7.4 (*in vivo)*

Values are expressed as mean ± standard deviation. Significant differences from the control are indicated by: * ($p < 0.05$), ** ($p < 0.01$) and * ($p < 0.001$)**

4.5.4: Effect of different doses of ethyl acetate fraction of the stem bark of *P. africanum* using the Elisa Technique on Caspases 9 and 3

There was a relevant increase in caspases 9 and 3 levels with the *in vivo* administration of the ethyl acetate fraction of *P. africanum.* This was observed in a dose-dependent manner as shown in figure 4.17. The ethyl acetate *P. africanum* causes induction in the levels of caspase 9 activity by 30%, 55% and 76% related to 30% (control) and caspase 3 activities by 25%, 45% and 68% against control of 10% at 25, 50 and 100 mg/kg body weight respectively. The result confirmed that the ethyl acetate fraction of *P. africanum* is a modulator of mitochondria-mediated apoptosis through the activation of caspases 9 and 3 levels. The increase in caspases 9 and 3 activities in all the doses indicates that the plant supports apoptotic process.

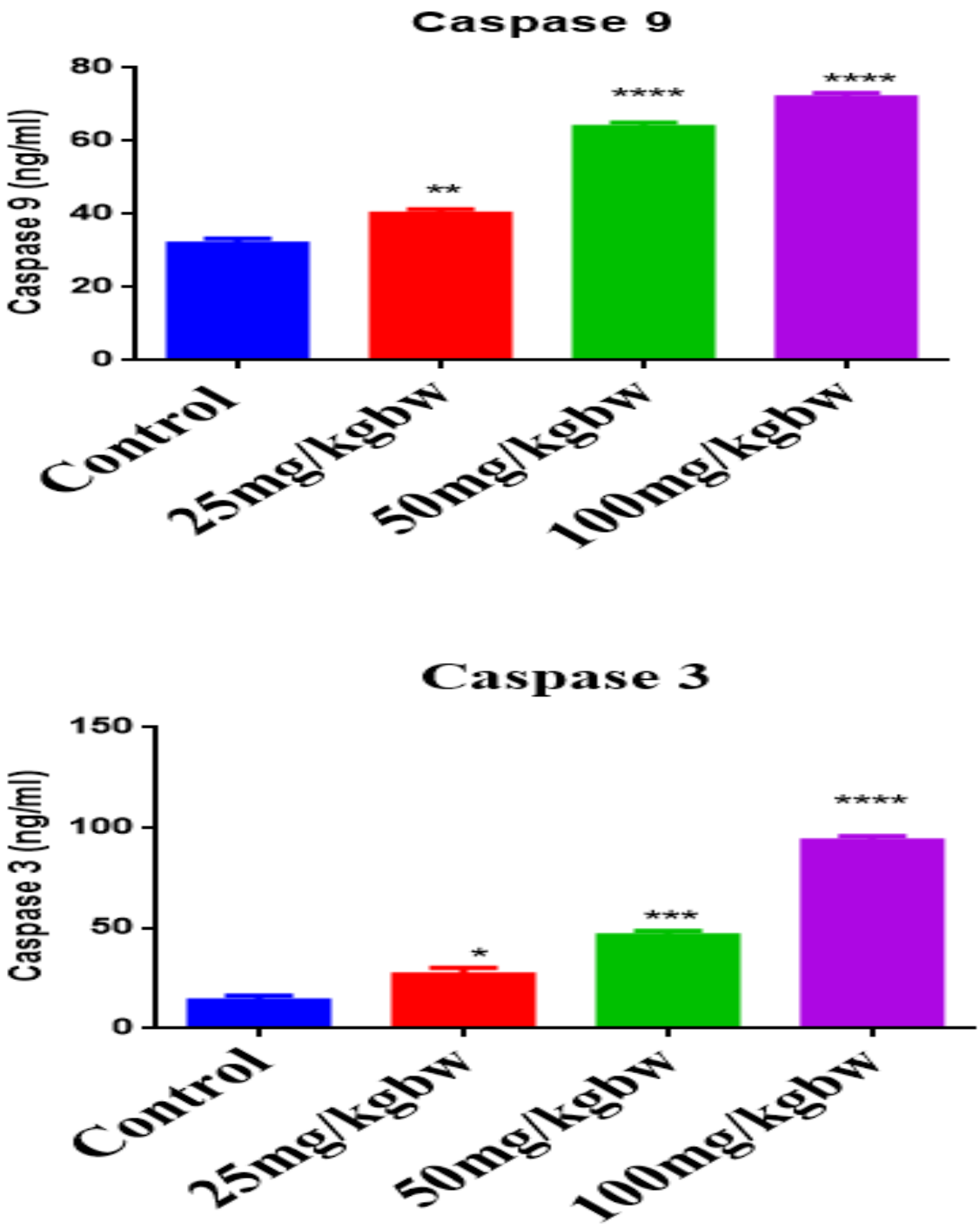

Figure 4.17: Effects of different ethyl acetate fraction dosages of the stem bark of *P. africanum* on the levels of Caspases 9 and 3 at pH 7.4 (*in vivo*).

Values are expressed as mean ± standard deviation. Significant differences from the control are indicated by: * ($p < 0.05$), ** ($p < 0.01$), * ($p < 0.001$) and **** ($p < 0.0001$)**

4.6: Evaluation of *Pipatdeniastrum africanum* stem bark Toxicity

4.6.1: Assessing the toxic effect on some hematological parameters of mice orally exposed to ethyl acetate fraction stem bark of *P. africanum*.

The effect of the administration of the *P. africanum* stem bark on twenty mice (20±2g) grouped into four (4) with five (5) mice in each treated interperitoneally with group one (vehicle), groups 2, 3 and 4 received 25, 50 and 100mg/kg body weight respectively for 14 days and samples were taken for toxicity analyses which revealed that there were no significant differences in all the parameters (haematological, LFT, RNT and antioxidants) measured when compared with the control as indicated below.

4.6.1.1 Hemoglobin concentration

Heamoglobin (HB [g/dl]) - the results obtained are 11.40±0.74, 12.20±1.04, 11.37±0.03, 11.00±1.13 and 11.11±0.32 in relation to 10.10±0.32 at 20, 50, 100, 200 and 400mg/kg body weight. This result supported other results that there was no difference between the doses of the plants administered to the experimental animals in relation to that of control.

Mean corpuscular volume (MCV [fL]) has 60.39±0.52, 62.04±2.08, 58.20±1.43, 61.08±2.34 and 61.57±0.23 in comparison to 61.89±2.2 at 25, 50, 100, 200 and 400mg/kg body weight in comparison to the control.

4.6.1.2 The Red Blood Cell (RBC) has 5.96±0.38, 6.03±0.59, 5.36±0.41, 5.91±0.86 and 5.97±0.77 versus 5.03±0.33 at 25, 50, 100, 200 and 400mg/kg body weight versus control. This result specified that no sustantial alteration in the doses when compared to the control.

4.6.1.3 Packed cell volume - (PCV [%]) reveals 36.30±16, 36.30±3.85, 32.70±0.47, 34.65±5.20 and 35.65±20 versus 31.00±2.16 at 25, 50, 100, 200 and 400mg/kg body weight versus the control and it shows that there was no distinct difference between the results obtained at various doses compared to the control.

4.6.1.4 Mean corpuscular hemoglobin (MCH [pg]) – The data obtained from this study are 19.78±0.18, 19.80±0.41, 19.16±0.42, 18.95±0.32 and 18.88±0.23 while 19.49±0.24 was obtained for the control at doses of 25, 50, 100, 200 and 400mg/kg body weight.

4.6.1.5 Mean corpuscular hemoglobin concentration (MCHC [gm/dL])-There was no significant difference in the data derived from the study when compared to the data derived from the control. The doses at 25, 50, 100, 200 and 400mg/kg body weight have 32.75±0.23, 32.45±0.57, 31.81±0.40, 31.95±0.50 and 32.03±0.55 compared to 32.33±0.23 of control.

Table 4.6.1: Hematological Parameters

Parameters	Control	25mg/kgbw	50mg/kgbw	100mg/kgbw	200mg/kgbw	400mg/kgbw
RBC	5.03±0.33	5.96±0.38	6.03±0.59	5.36±0.41	5.91±0.86	5.97±0.77
PCV%	31.00±1.24	36.30±2.16	36.30±3.85	32.70±0.47	34.70±5.24	35.65±5.20
HB(g/dl)	10.10±0.32	11.40±0.74	12.20±1.04	11.37±0.03	11.00±1.13	11.11±0.32
MCV (fL)	61.89±2.24	60.39±0.52	62.04±2.08	58.20±1.43	61.08±2.34	61.57±2.22
MCH (pg)	19.49±0.24	19.78±0.18	19.80±0.41	19.16±0.42	18.95±0.32	18.88±0.23
MCHC (gm/dL)	32.33±0.23	32.75±0.20	32.45±0.57	31.81±0.40	31.95±0.50	32.03±0.55
LYMPHOCYTES	68.70±2.05	65.00±1.41	68.30±3.85	66.00±2.16	67.30±3.68	67.55±3.33
NEUTROCYTES	27.66±2.49	29.33±1.24	28.33±4.78	28.00±1.63	29.30±4.10	28.98±2.45
MONOCYTES	2.31±0.47	2.30±0.47	1.66±0.47	1.66±0.47	1.30±0.42	1.35±0.47
EOSINOPHILS	2.00±0.82	1.83±0.94	2.30±0.47	1.86±0.47	2.00±0.82	2.05±0.78

4.6.2: Determination of the effects of ethyl acetate fraction of *P. africanum* stem bark on liver and renal function test in mice

In the figure 4.18 below, it was found that ethyl acetate *P. africanum* has no toxic effect in relation to the control. No significant ($p < 0.05$) difference was found in all the parameters measured on both the liver function assays -Alkaline phosphatase (ALP), Aspartate amino transferase (AST), Alanine amino transferase (ALT) and renal function test – Urea (UR), creatinine (CRT) and Total protein which shows the plant is not toxic.

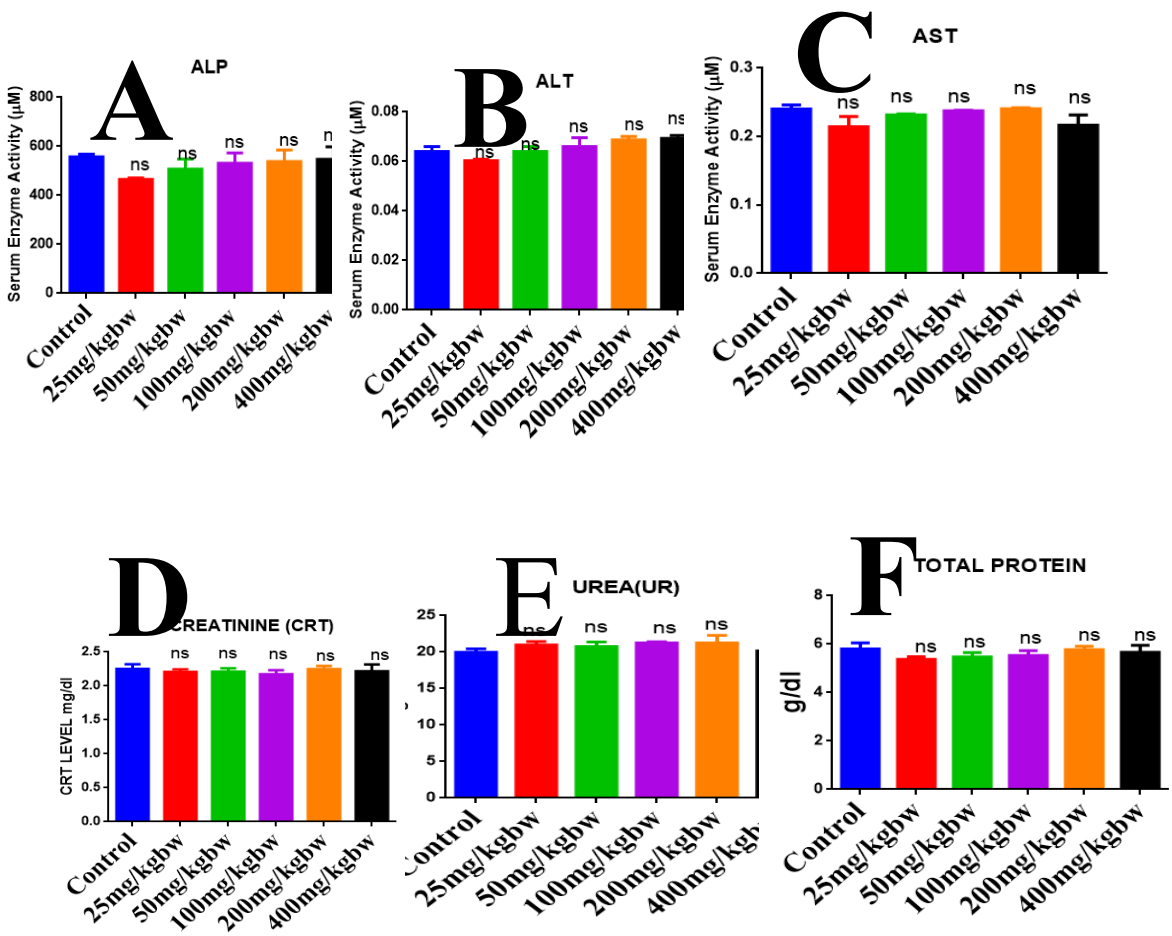

Figure 4.18: Effects of ethyl acetate fraction of *P. africanum* stem bark on liver function test- serum {A-alkaline phosphatase (ALP), B-alanine amino transferase (ALT), C-aspartate amino transferase (AST); Renal function test: D-urea (UR), E- creatinine (CRT) and F- Total protein} b and ns-Significant difference relative to control ($p < 0.05$)

4.6.3: Validating the effect of ethyl acetate fraction of *P. africanum* on antioxidant enzymes in mice

The results of this study as reported in figure 4.19 showed significant differences at ($p < 0.05$) with dose of 400mg/kg body weight in all the parameters when compared to the control, A- superoxide dismutase (SOD), B- catalase (CAT), C- glutathione-s-transferase (GST), D- reduced glutathione (GSH) in figure 4.19. However, E- lipid peroxidation (LPO) showed a significant decrease in MDA level. Ethyl acetate has shown antioxidant activity through its ability to enhance GSH, SOD, GST, total protein and inhibit lipid peroxidation to maintain cellular homeostasis. The plant demonstrated antioxidant activity by its ability to enhance GSH, SOD, GST, total protein and its inhibitory ability on lipid peroxidation in the tested animals.

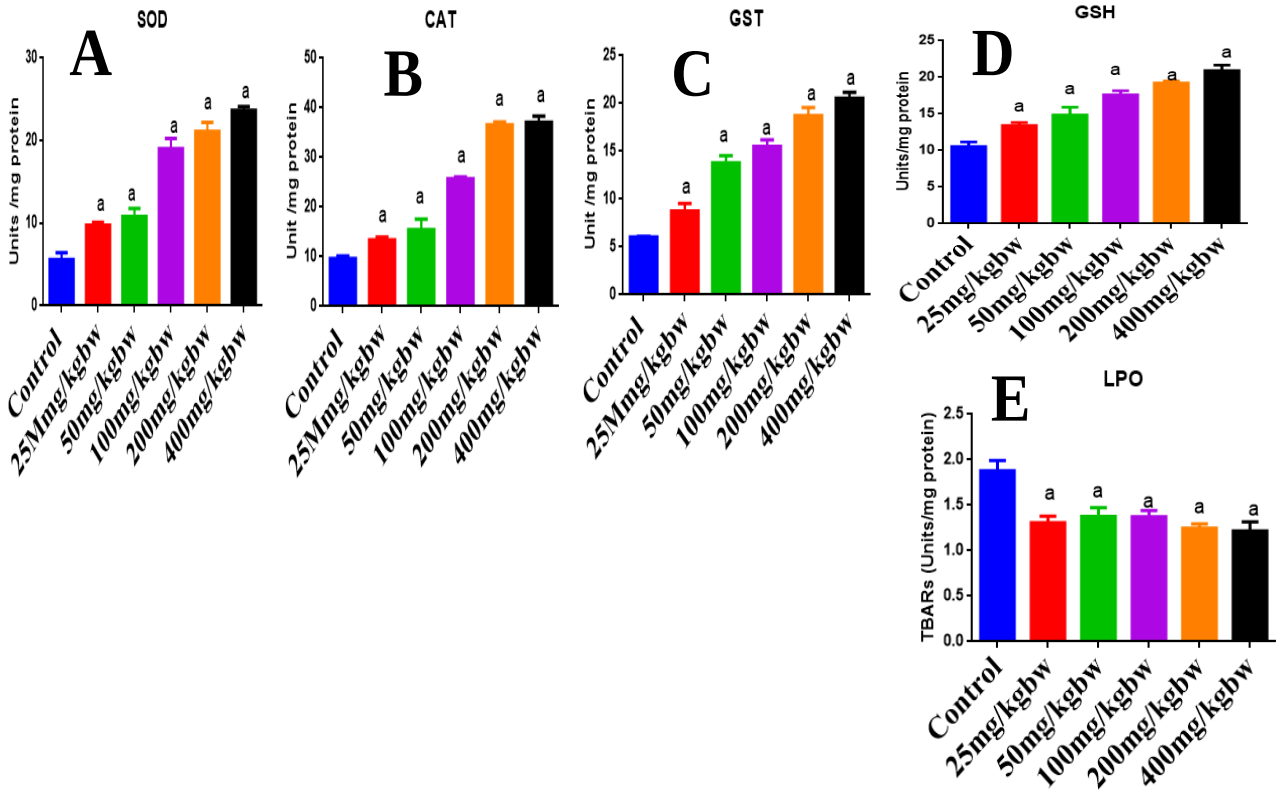

Figure 4.19: Effects of P. africanum stem bark ethyl acetate fractions on mice lipid peroxidation and antioxidant status

Key SOD(A) = Superoxide dismutase; CAT(B) = Catalase; GST (C)= Glutathione-S-transferase GSH (D) = Reduced Glutathione; LPO (E)= Lipid peroxidation a-significant difference relative to control; ns-no significant difference relative to control ($p < 0.05$)

4.6.4: Evaluation of the histological examination of the mice liver

The histology data reported on plate 4.1 reflected the outcome of the investigation. In the control group, normal central venules and portal tracts were discovered, depicted by the white arrow. The hepatocytes demonstrated normal morphology, as indicated by the blue arrow, while the sinusoids appeared normal and were not invaded, as revealed by the thin arrow. No bleeding or suspicious lesions were identified. At a dose of 25 mg/kgbw, normal hepatocyte morphology was found, however there was an enhanced focal area of fat degradation visible, represented by the black arrow. The central venules and sinusoids appeared normal and were not invaded. The identical pattern happened at a dose of 50 mg/kgbw, where hepatocyte morphology remained normal, and sinusoids appeared normal without infiltration.

In the group given a dose of 100 mg/kgbw, normal central venules and portal tracts were detected. However, hepatocytes revealed substantial microvesicular steatosis, with apparent fatty vacuolizations in the cytoplasm (blue arrow). The sinusoids appeared normal and were not invaded. In the 200 mg/kgbw group, central venules appeared normal without congestion (white arrow), while the portal tract revealed denser connective tissue (black arrow). The sinusoids appeared normal and were not invaded. However, in the 400 mg/kgbw group, hepatocyte morphology partially appeared normal with small vacuolations (blue arrow), and sinusoids showed normal without infiltration. No bleeding was noted, and no morphological abnormalities were seen. Overall, the data revealed that there were no substantial morphological abnormalities in the studied samples.

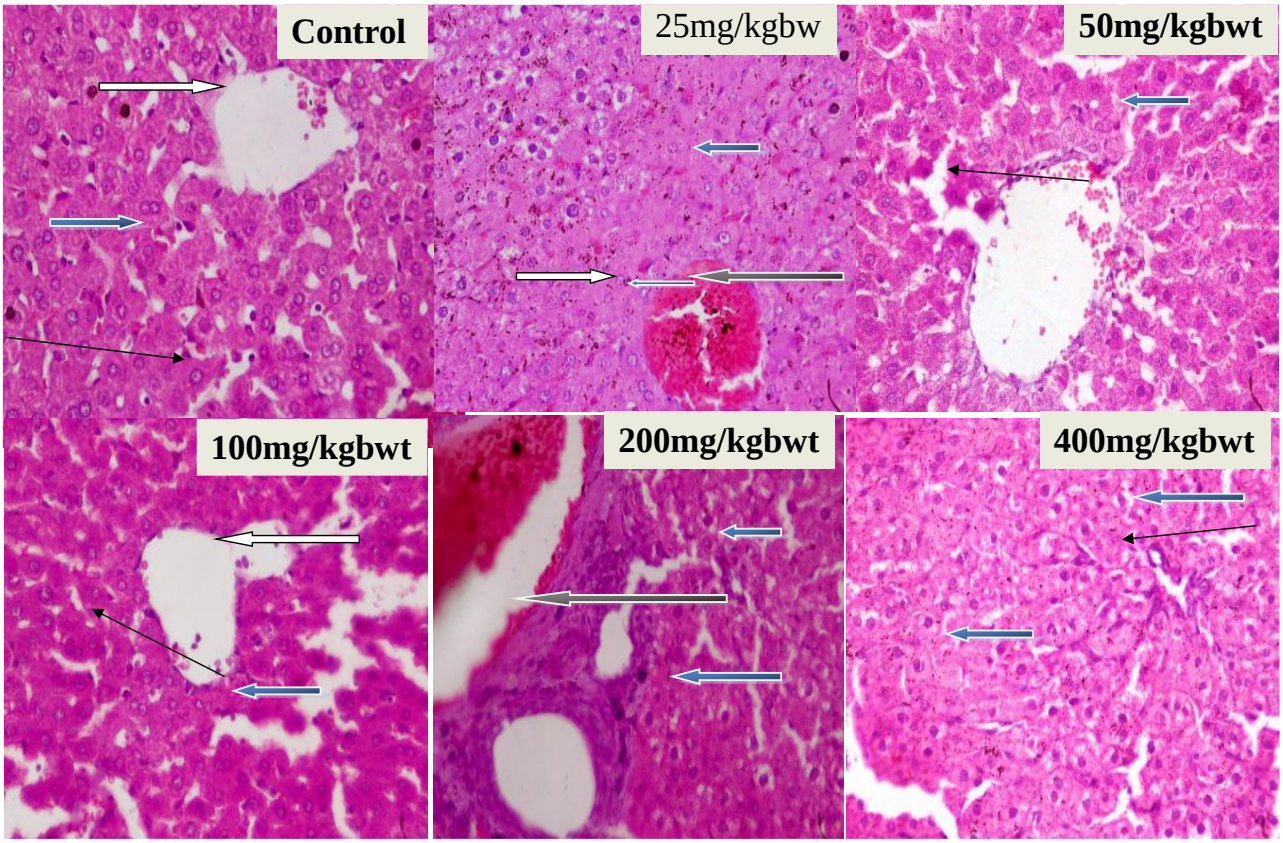

Plate 4.1: Assessing the bioactivity guided assays

Table 4.7.1: Pooled subfraction in ratios of the most potent subfraction of ethyl acetate of *P. africanum* stem bark.

SUBFRACTIONS	SOLVENTS
100% ETHYL ACETATE SUBFRACTION	A
80% ETHYL ACETATE: 20% METHANOL SUBFRACTION	B
60% ETHYL ACETATE: 40% METHANOL SUBFRACTION	C
40% ETHYL ACETATE: 60% METHANOL SUBFRACTION	D
20% ETHYL ACETATE: 80% METHANOL SUBFRACTION	E
100% METHANOL SUBFRACTION	F

4.7.2: Modulatory effect of various concentrations of ethyl acetate subfractions (in ratios) of the stem bark of *P. africanum* on MPTP opening to confirm the most potent subfaction (*in vitro*)

The results obtained in all the groups (A, B, C, D, E and F) in figure4.20 demonstrated that there were distinct modulations of mPT pore opening and the trend of the opening were not consistent in some groups resulting in reversal of the opening and the concentrations used were 20, 60, 100, 140 and 180µg/mL, respectively. In group A, the opening of the pore observed were 1.2, 4.5, 6.6, 4.5, 7.9 folds, the reversal occurred at 140µg/mL. Group B caused significant opening of mitochondrial pore having inductions of 1.7, 4.5, 6.7, 8.0 and 7.9 folds, it reversed at the highest concentration of 180µg/mL.

There was significant opening of the pore in group **C** with the following induction folds 3.7, 5.4, 5.7, 5.4 and 5.4, it was discovered that three different concentrations (60, 140 and 180 µg/mL had the same induction fold of 5.4. At group D, opening of the pore was experienced only at the highest concentration of 180 µg/ml having 5.0 induction fold in comparison with the triggering agent (TA) while highest induction of 5.9 -fold was noticed at the lowest concentration (20 µg/mL) in group E which was further potentiated down the concentrations. However, there was a large amplitude swelling of mitochondria in group F. The induction folds were 3.8, 5.6, 6.4, 8.1 and 8.9 and they were discovered in concentration manner. Group F was found to be the most potent due to 8.9 times the induction of all groups.

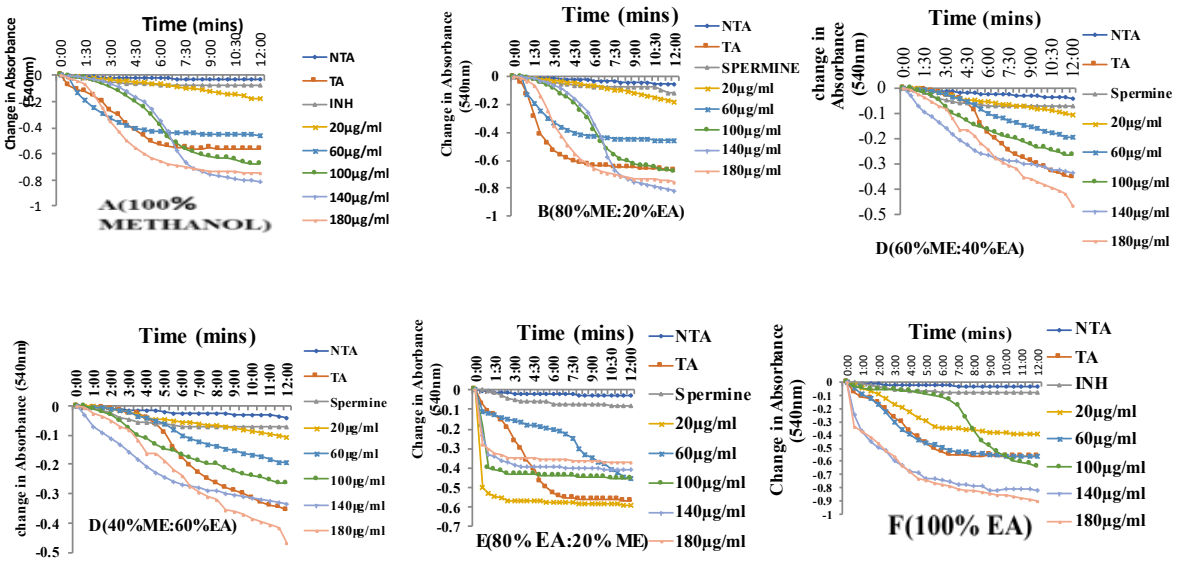

Figure 4.20: Effect of various concentrations of ethyl acetate subfractions (in ratios) of the stem bark of *P. africanum* on mPTP opening to confirm the most potent subfractions

Table 4.7.2: Purification- Pooled samples (ratios) from Column Chromatography

POOLED FRACTIONS	ELUTING SOLVENT SYSTEM	SUBFRACTIONS
1-16	100% Chloroform	A
17-26	90% Chloroform : 10% Ethyl Acetate	B
37-41	80% Chloroform : 20% Ethyl Acetate	C
42-47	70% Chloroform : 30% Ethyl Acetate	D
48-59	50% Chloroform : 50% Ethyl Acetate	E
60-69	100% Ethyl Acetate	F
60-80	90% Ethyl Acetate :10% Methanol	G
81-94	80% Ethyl Acetate :20% Methanol	H
95-111	70% Ethyl Acetate :30% Methanol	I
112	50% Ethyl Acetate :50% Methanol	J
113– 125	50% Ethyl Acetate :50% Methanol	K
126-144	100% Methanol	L

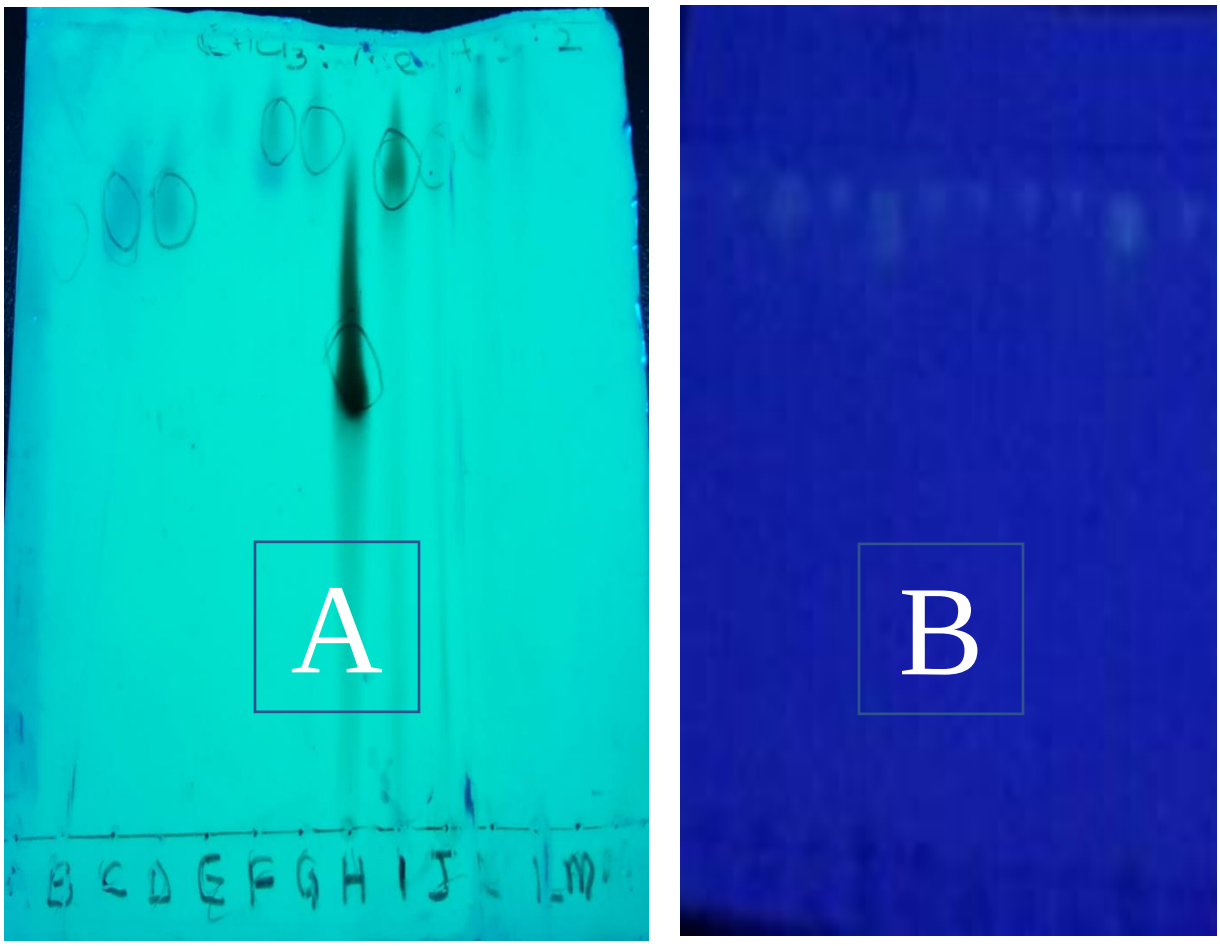

PLATE 4.2: Spotted Pooled Subfractions on Thin Layer Chromotography (TLC) Key: viewed at short (A) UV-254nM and long (B) UV-365nM (ELUTING SOLVENT: CHLOROFORM: METHANOL-3:2)

Table 4.7.3: Pooled, Partially Purified Samples from Column Chromatography

TUBES	ELUTING SOLVENT	PARTIALLY PURIFIED SUBFRACTIONS
1-13	CHL: MET 3: 2	A
14-20	CHL: MET 1: 1	B
21-29	CHL: MET 3: 3	C
30-59	CHL: MET 1: 4	D
60-144	CHL: MET 4: 1	E

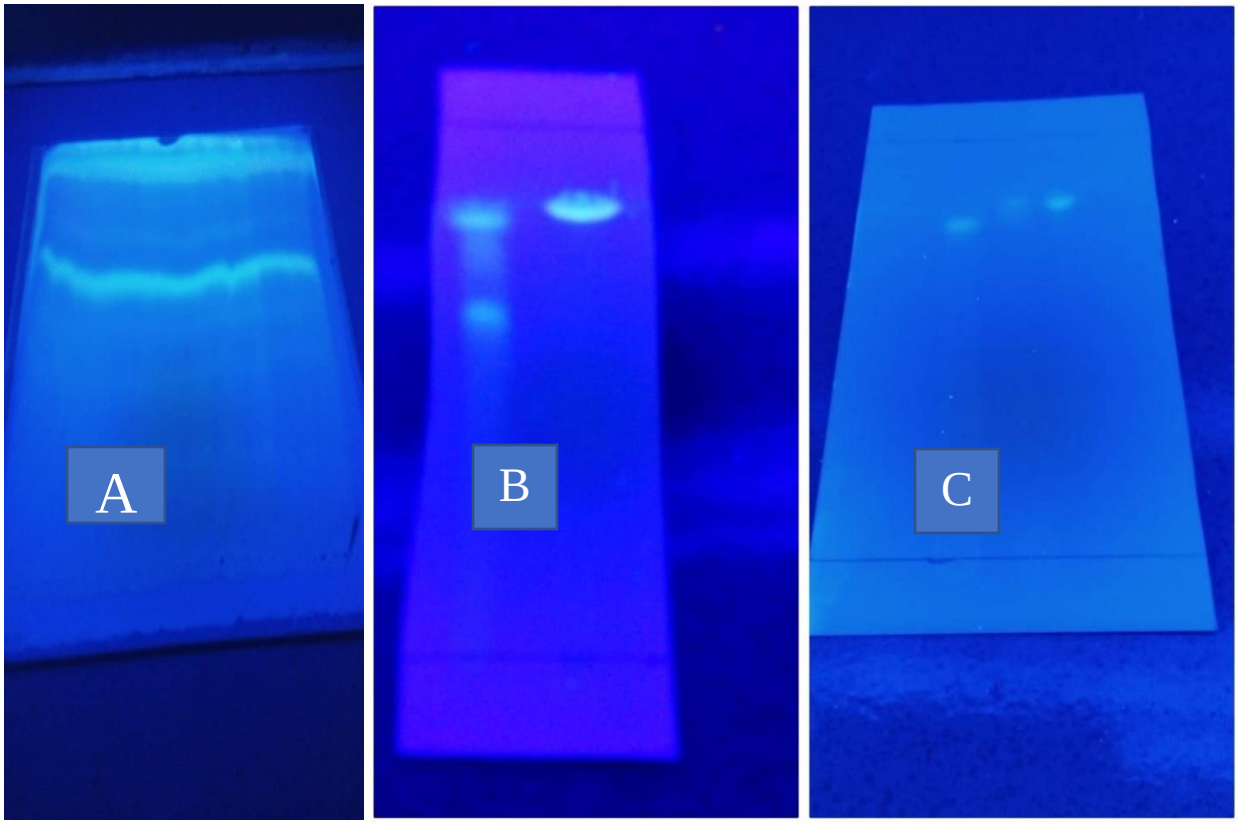

Plate 4.3: Identification of the Plant via Column Chromatography

Key: Partially purified ethyl acetate subfraction on prep Thin Layer Chromatography (TLC) Plate (A)

Purified fraction of ethyl acetate subfraction of *P. africanum* on TLC Plate

Viewed at 365nM (B), 254nM (C)

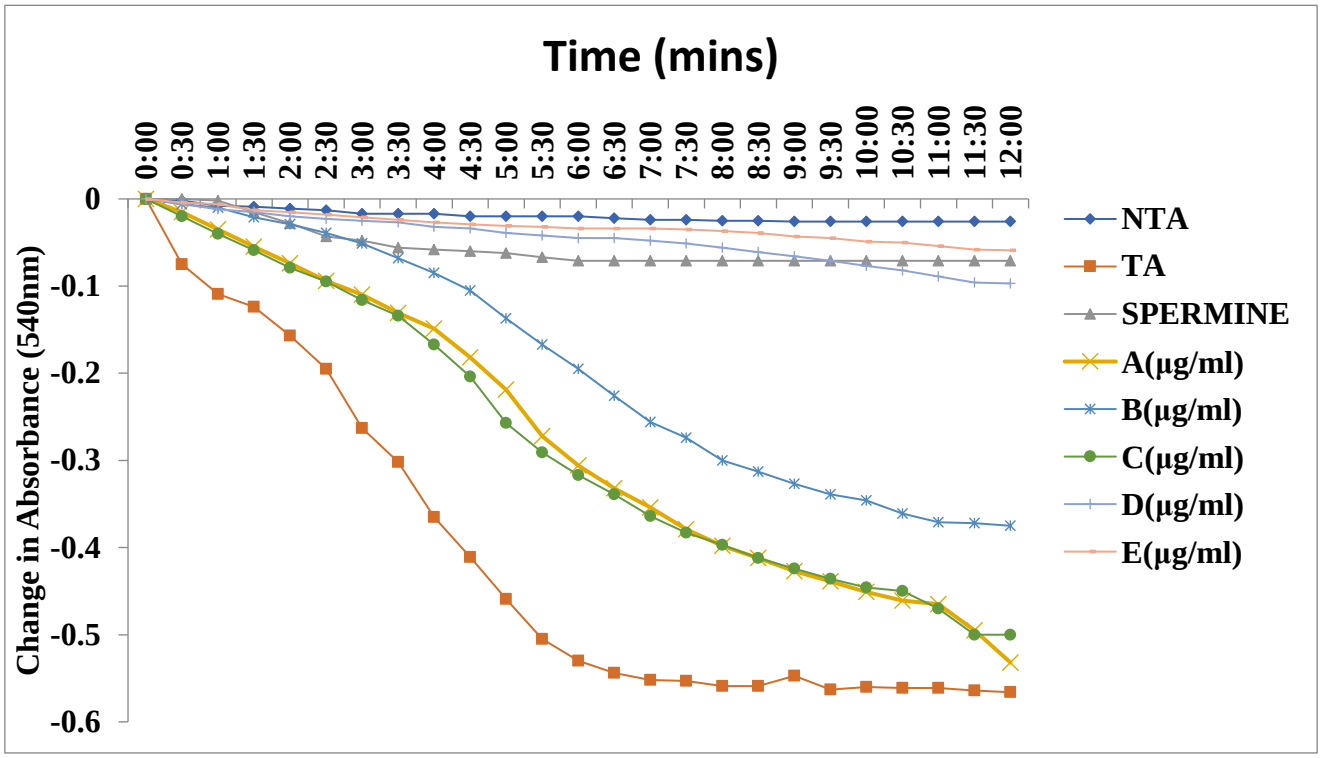

Figure 4.21: Effects of partially purified pooled ethyl acetate subfractions of *P. africanum* on mPTP opening (*in vitro)*

NTA- Triggering TA – Triggering agent.

(Eluting Solvent- Chloroform: Methanol (A-3: 2, B-1: 1, C-3: 3, D- 1: 4 and E- 4: 1)

4.8: Identification of purified compound (GC-MS)

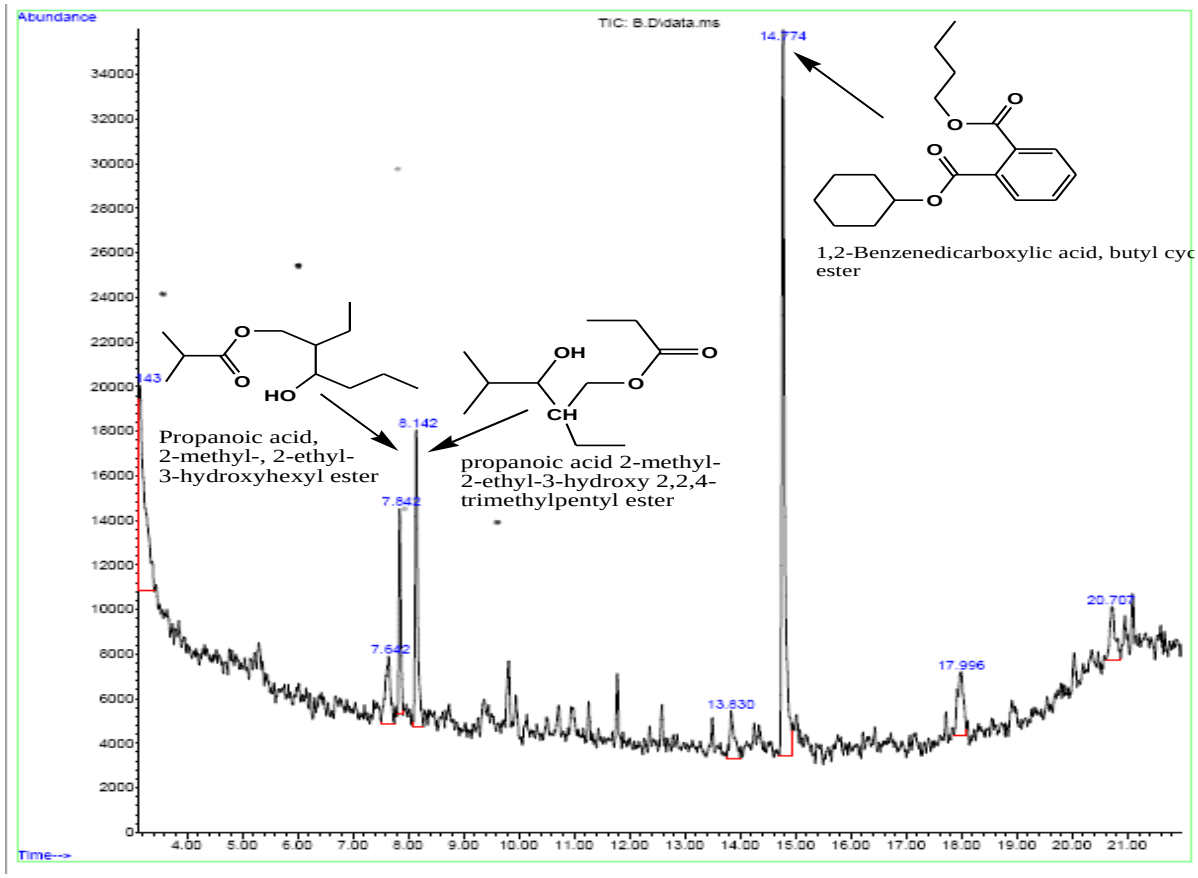

Figure 4.22: Total ion chromatogram of purified ethylacetate fraction of *P. africanum* stem bark

Table 4.8.1: GC-MS analysis of the purified ethyl acetate fraction of PA

S/N	Suspected Compounds Identified	% Area	RT	Reported Bioassays	Chemical Class	Molecular Formular
1	1,2-Benzendicarboxylic,butylcyclohexyl ester	91	14.774	It is acknowledged to possess noticeable pharmacological activities, including antineoplastic, antimicrobial and antiviral activities also, possesses anti-cancer activities.	Benzoic acid ester	$C_{17}H_{24}O_3$
2	Propanoic acid, 2-methyl-, 2-ethyl-3-hroxyl-2,2,4-trimethylpentyl ester	78	8.142	It is an example of non-steroidal anti-inflammatory drugs (NSAIDs) used in the treatment of inflammation associated with tissue injury.	Carboxylic ester	$C_{17}H_{24}O_3$
3	Propanoic acid, 2-methyl-, 2-ethyl-3-hroxylhexyl ester	72	8.142	Also, an example of non-steroidal anti-inflammatory drugs (NSAIDs) used in the treatment of inflammation associated with tissue injury.	Isobutyric acid	$C_{17}H_{24}O_3$

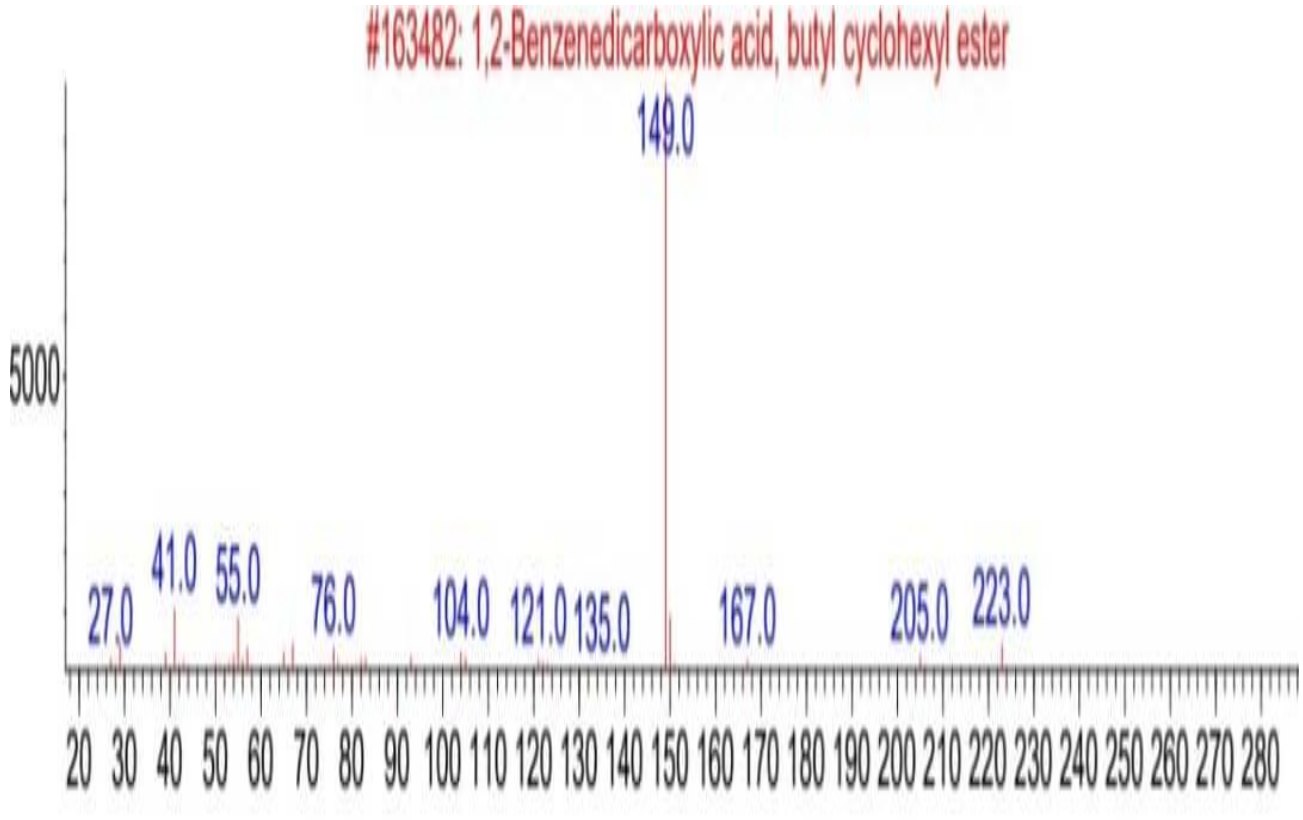

Figure 4.23: GC-MS spectra of 1,2-Benzendicarboxylic, butylcyclohexyl ester

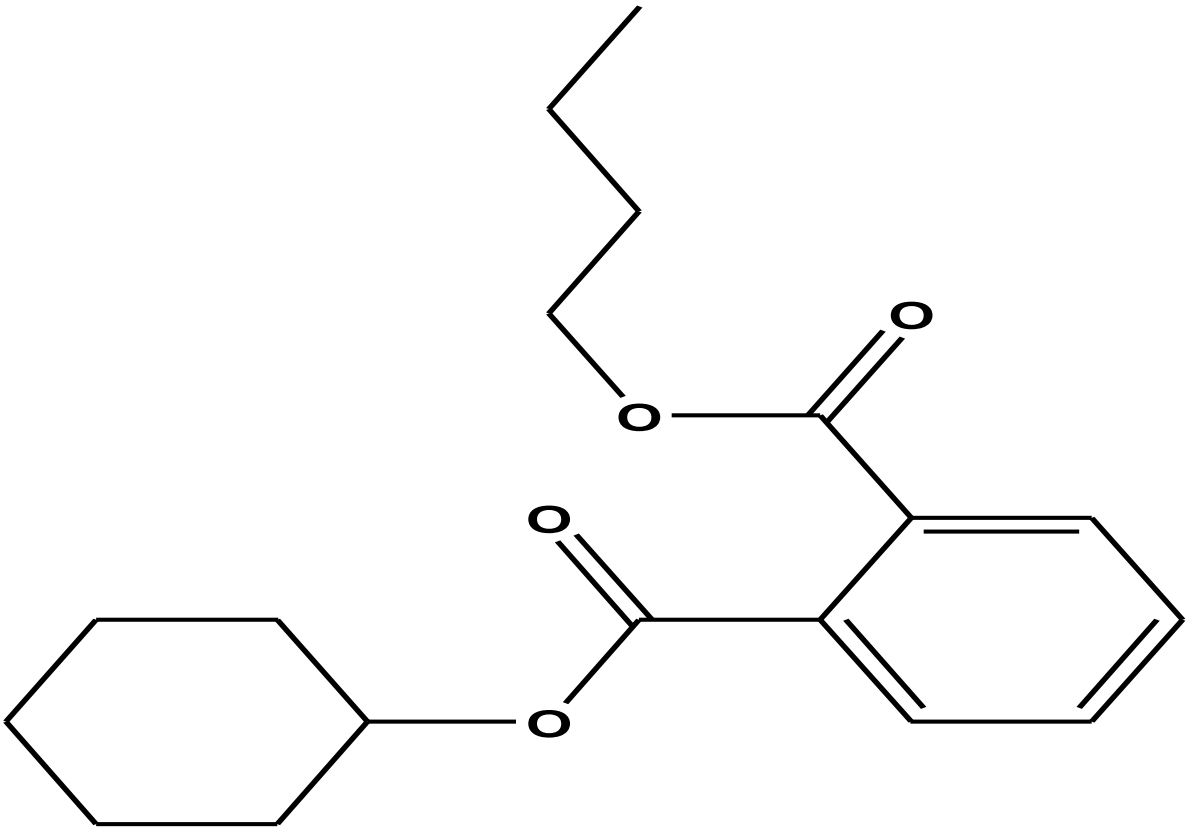

Figure 4.24: Mass Spectrometry of 1,2-Benzendicarboxylic, butylcyclohexyl ester

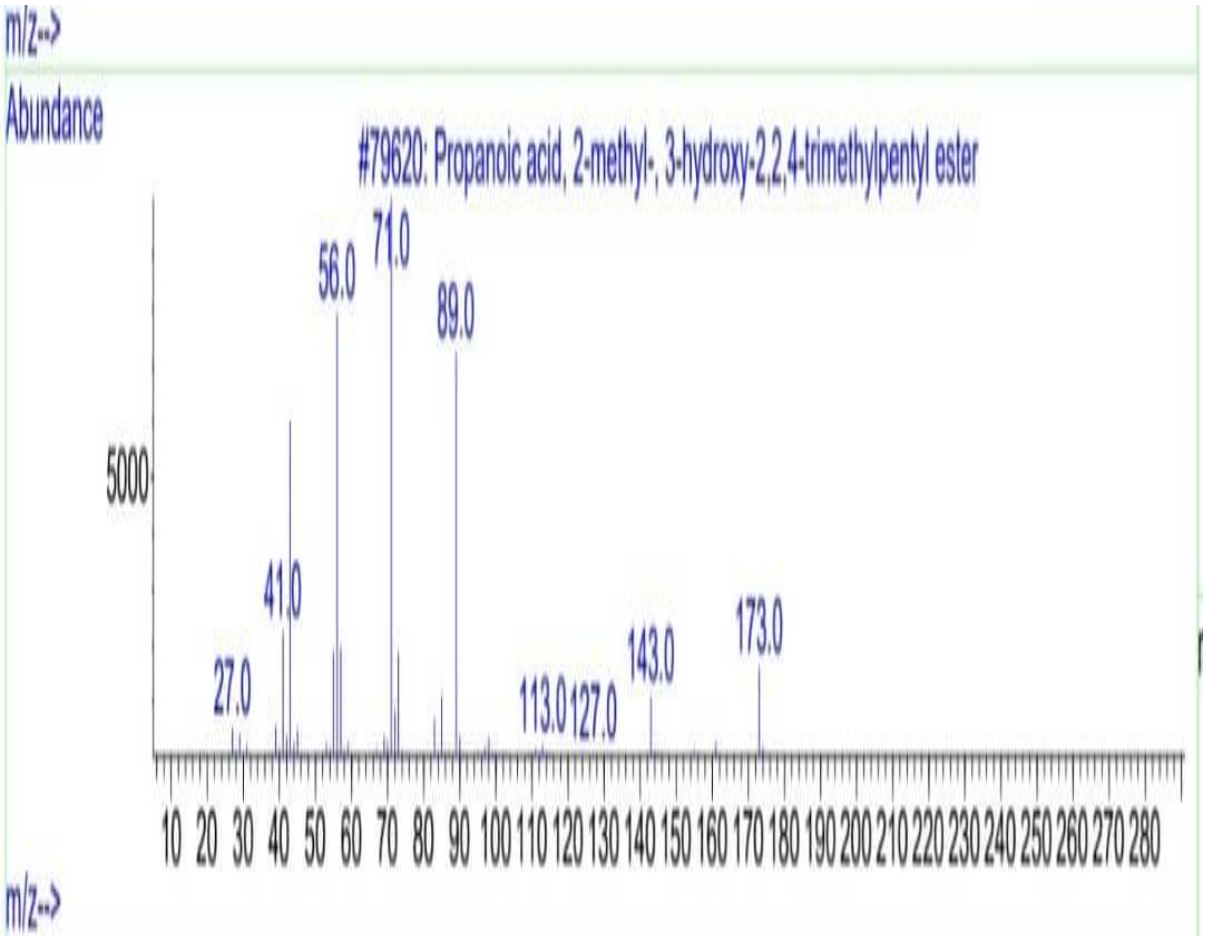

Figure 4.25: GC-MS spectra of Propanoic acid, 2-methyl-, 2-ethyl-3-hroxyl-2,2,4-trimethylpentyl ester

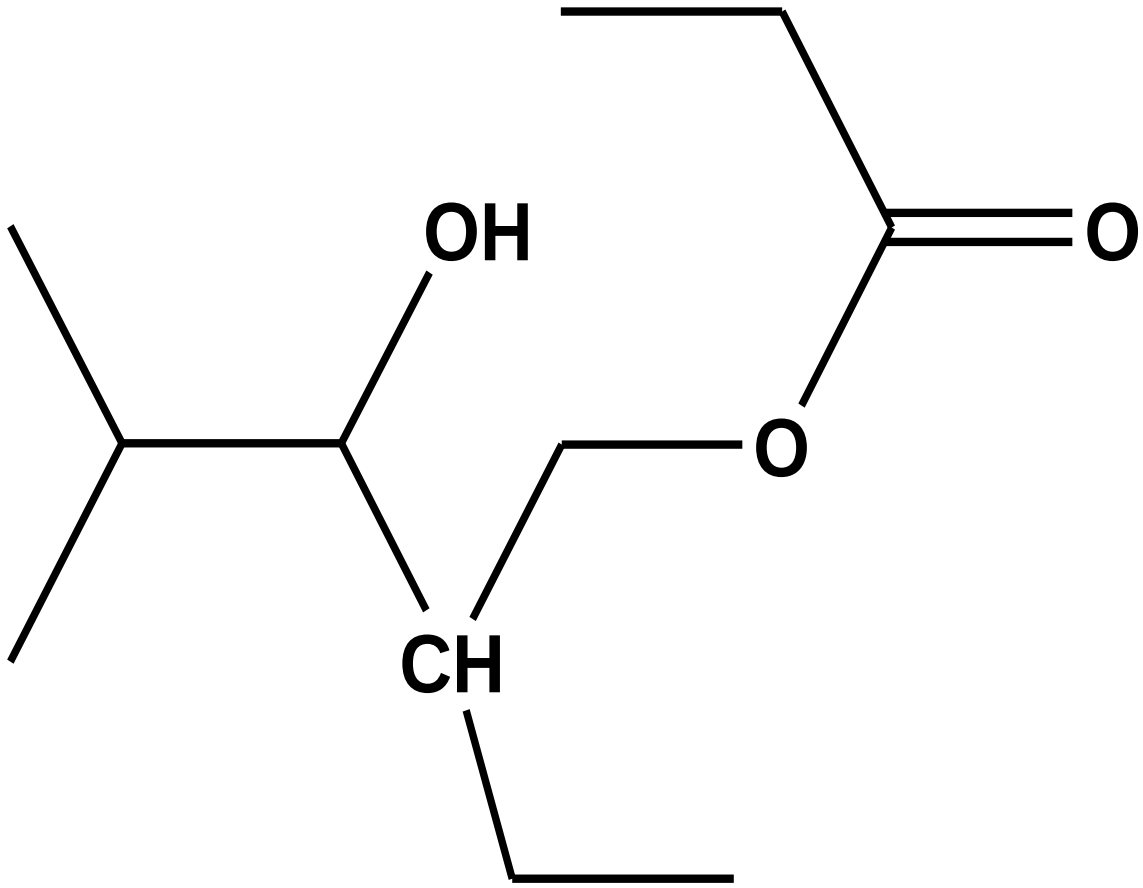

Figure 4.26 Mass spectra of Propanoic acid, 2-methyl-, 2-ethyl-3-hroxyl-2,2,4-trimethylpentyl ester

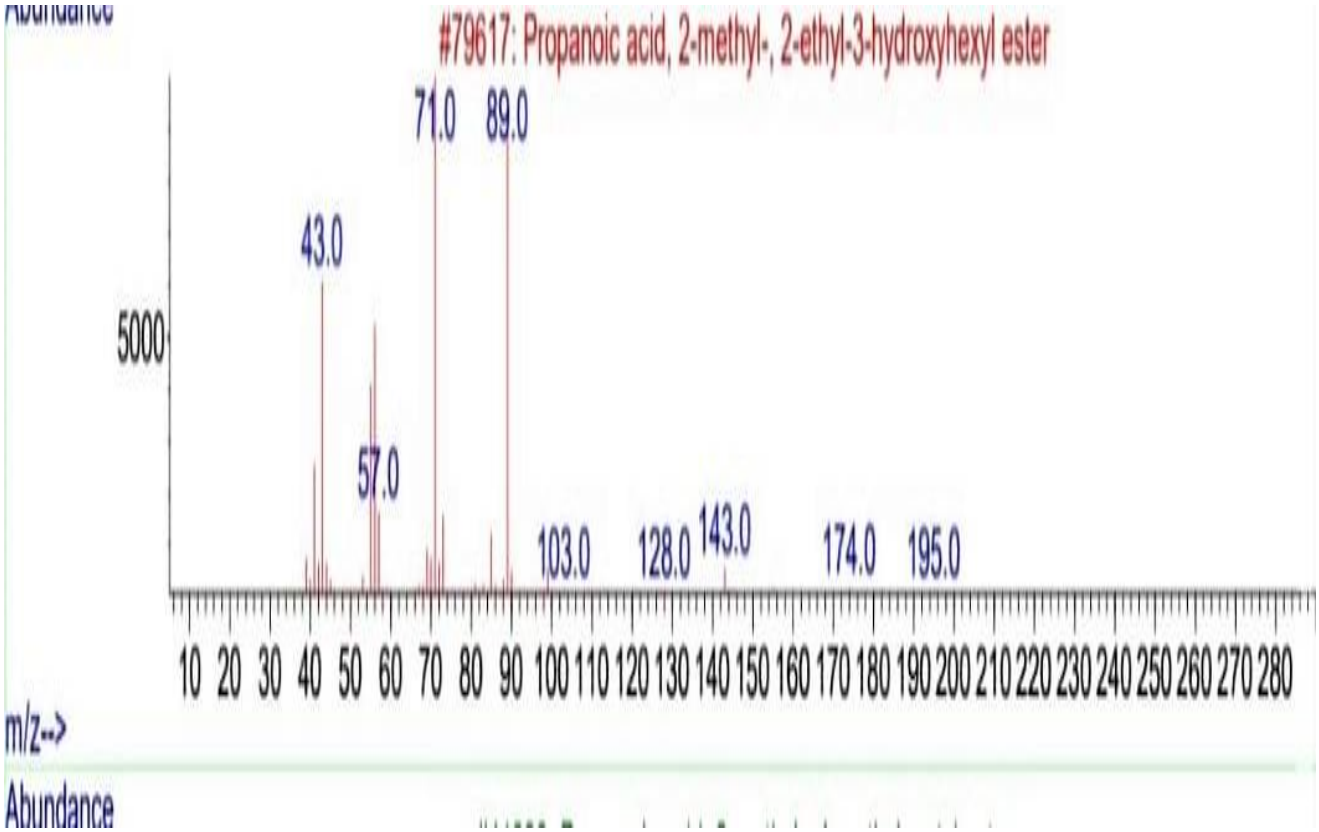

Figure 4.27: GC-MS spectra of Propanoic acid, 2-methyl-, 2-ethyl-3-hroxylhexyl ester

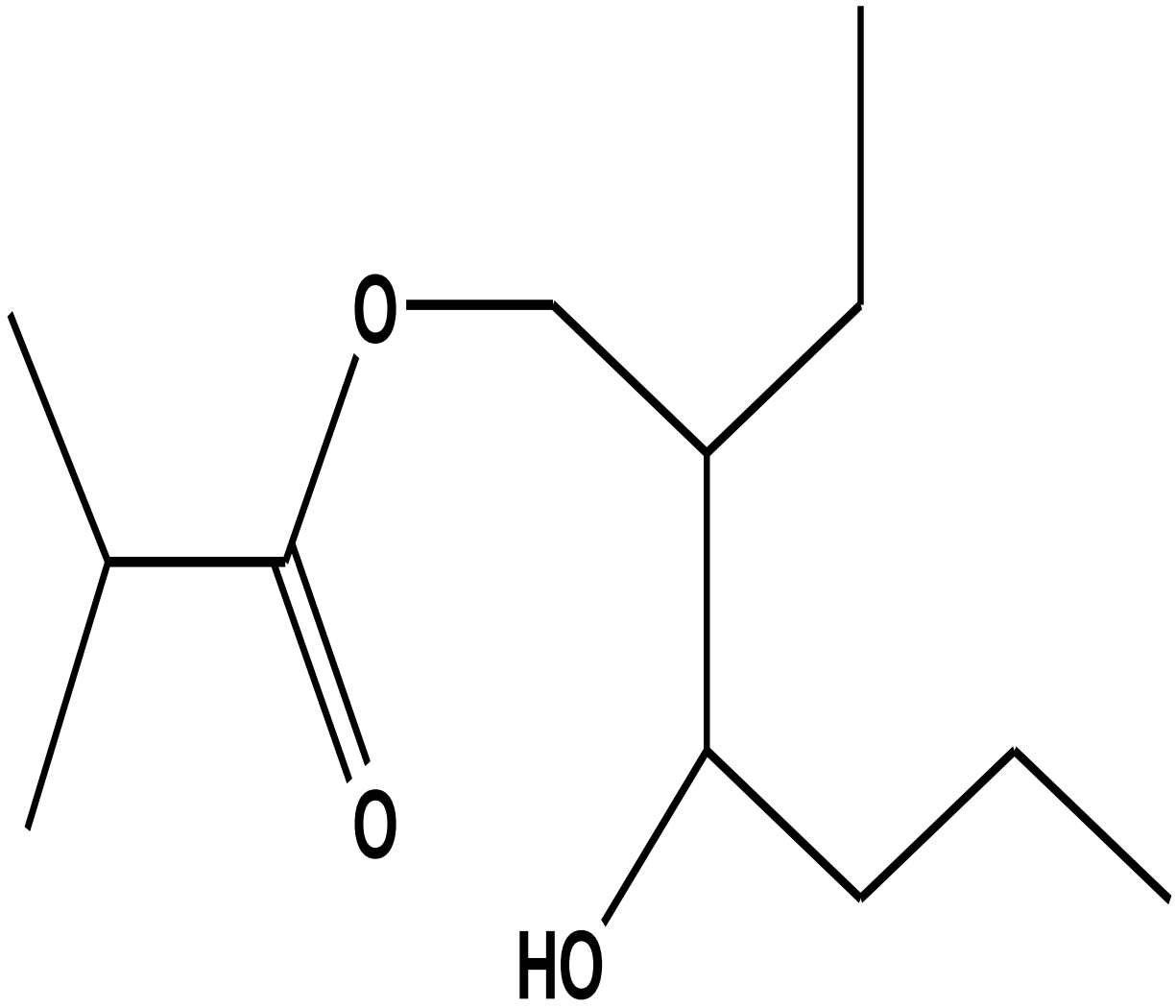

Figure 4.28: Mass Spectrometry of Propanoic acid, 2-methyl-, 2-ethyl-3-hroxylhexyl ester

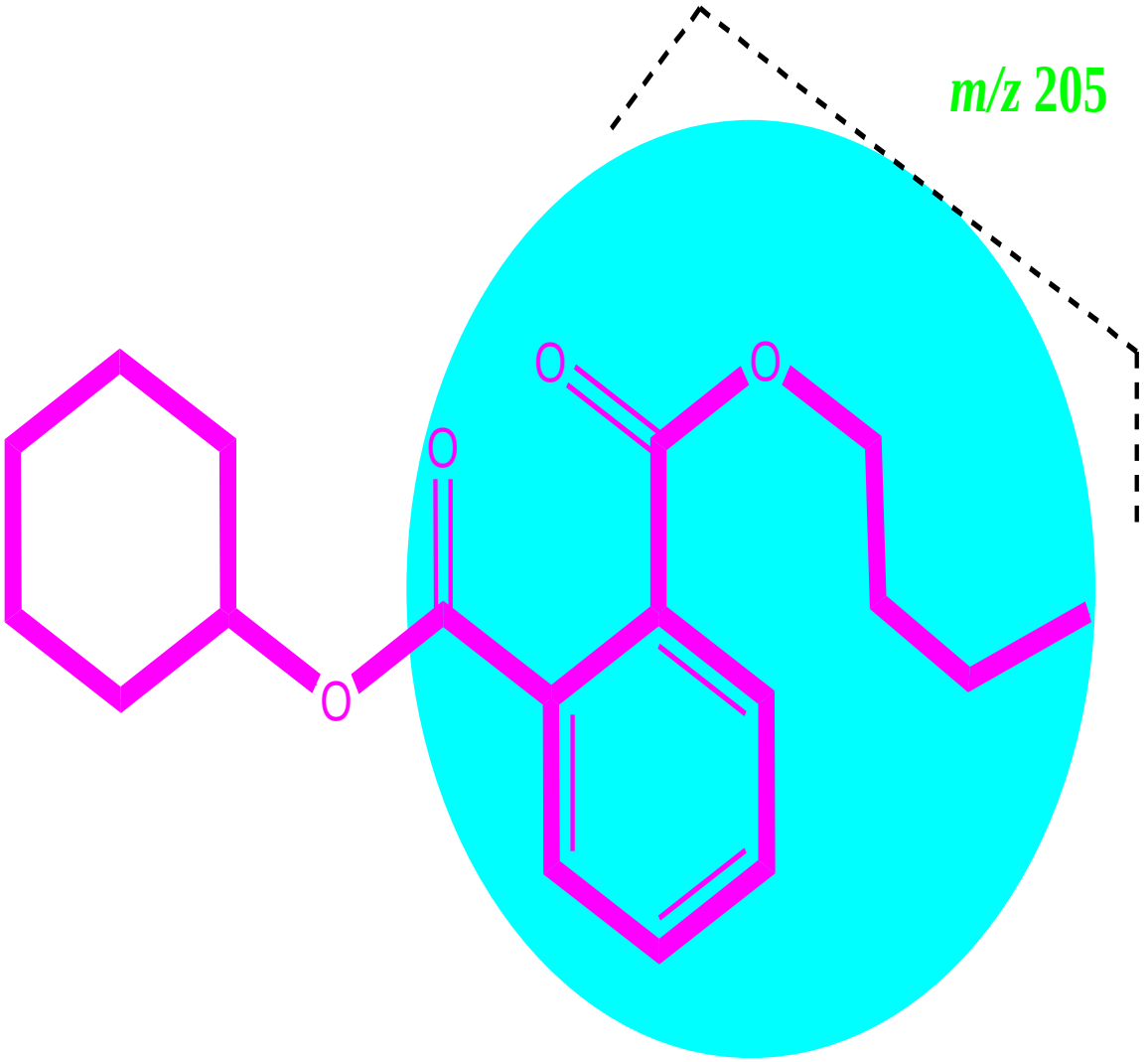

Figure 4.29: Fragmentation pattern of 1,2-Benzenedicarboxylic acid, butyl cyclohexyl ester

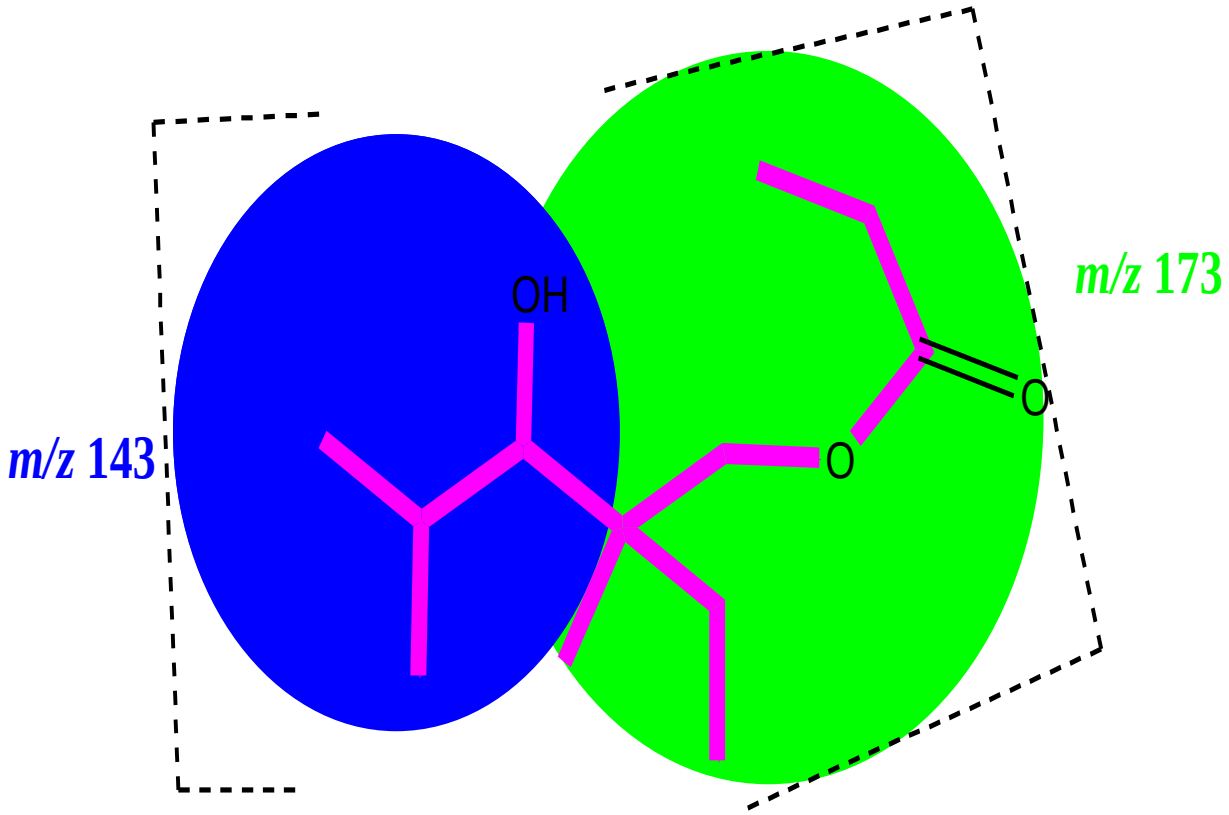

Figure 4.30: Fragmentation pattern of Propanoic acid 2-methyl- 2-ethyl-3-hydroxy 2,2,4-trimethylpentyl ester

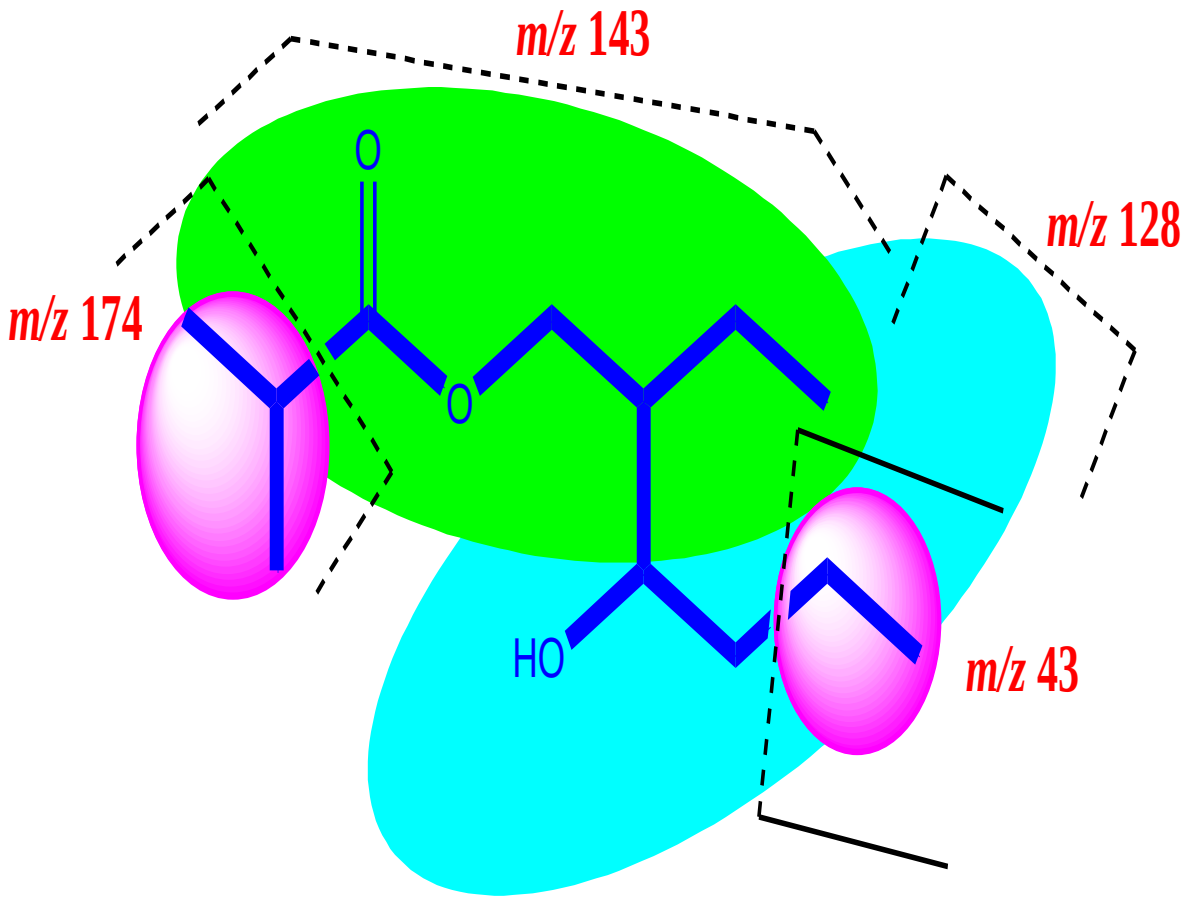

Figure 4.31: Fragmentation pattern of Propanoic acid, 2-methyl-, 2-ethyl-3-hydroxyhexyl ester

4.8.1: Nuclear Magnetic Resonance result of purified compound (Stigmasterol)

Figure 4.32 revealed the structural elucidation of stigmasterol in ethyl acetate subfraction of *P. africanums* and it could be responsible for the pharmacological benefits observed in the treatment of liver and colon damage in this research.

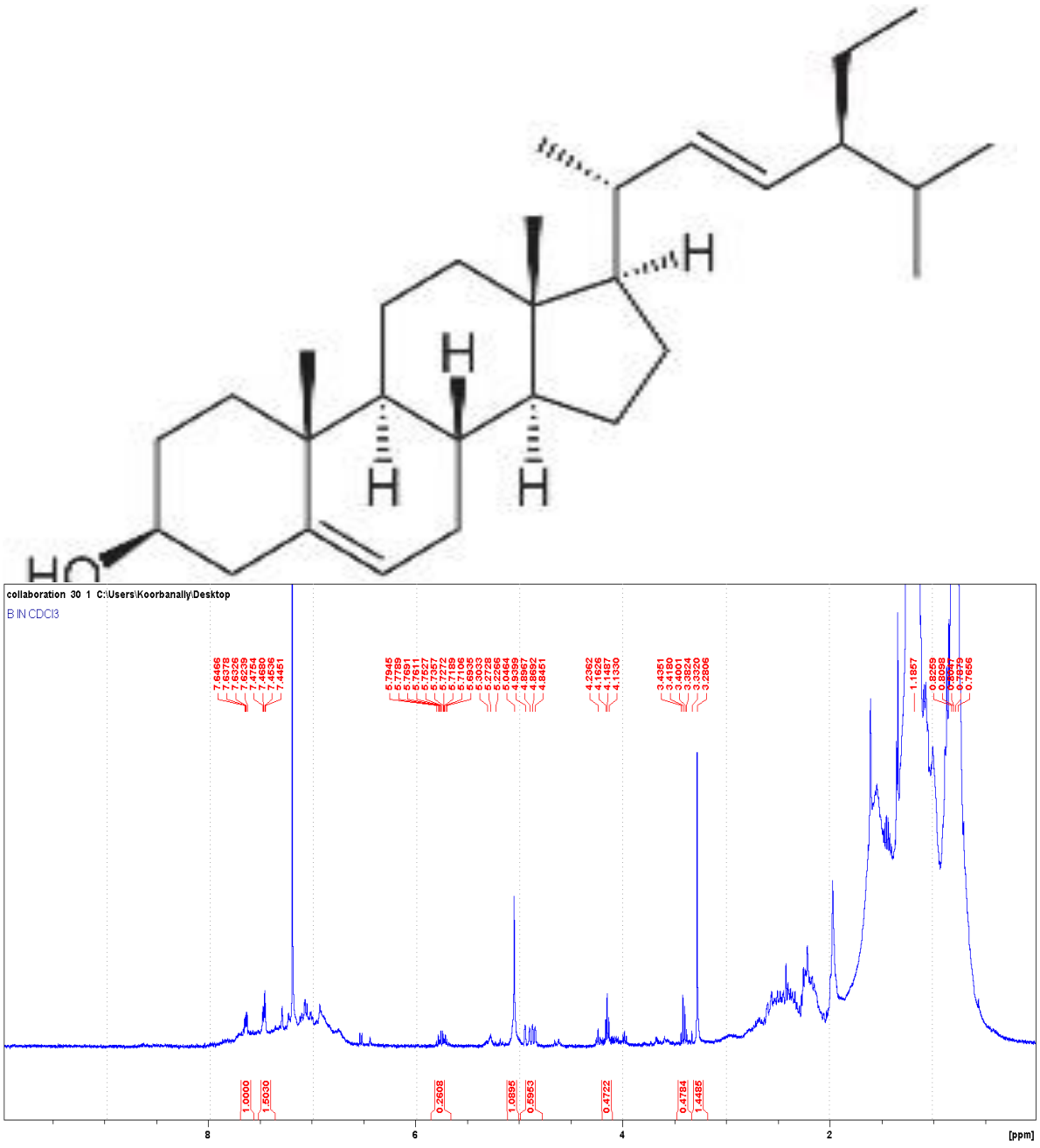

Figure 4.32: Spectrometry of Stigmasterol

4.9: Modulatory effects of stigmasterol isolated from the stem bark of *P. africanum* on Mitochondrial-Mediated Cell Death in colon of experimental mice.

4.9.1: Apoptotic inductive effect of Stigmasterol in colon (mPT)

Stigamasterol has an inductive effect on the liver, although it does not have an inductive effect on the apoptotic biomarkers examined in DSS+ BaP-induced colonic injury, confirming the previous mPT results of stigmasterol, as shown in Figure 4.33. However, *P. africanum* extract and fractions increased ATPase activity (3.80, 5.60, 6.40, 8.10, and 8.90-fold) at 20, 60, 100, 140, and 180 µg/mL, respectively, and increased ATPase activity (0.20±0.01, 0.35±0.10, 0.40±0.10, 0.45±0.20 and 5.20±0.80 µmol/Pi/mg/protein). /min) relative to vehicle (0.05 *µmol* /Pi/mg/protein/min), respectively as reported in Figure 4.11

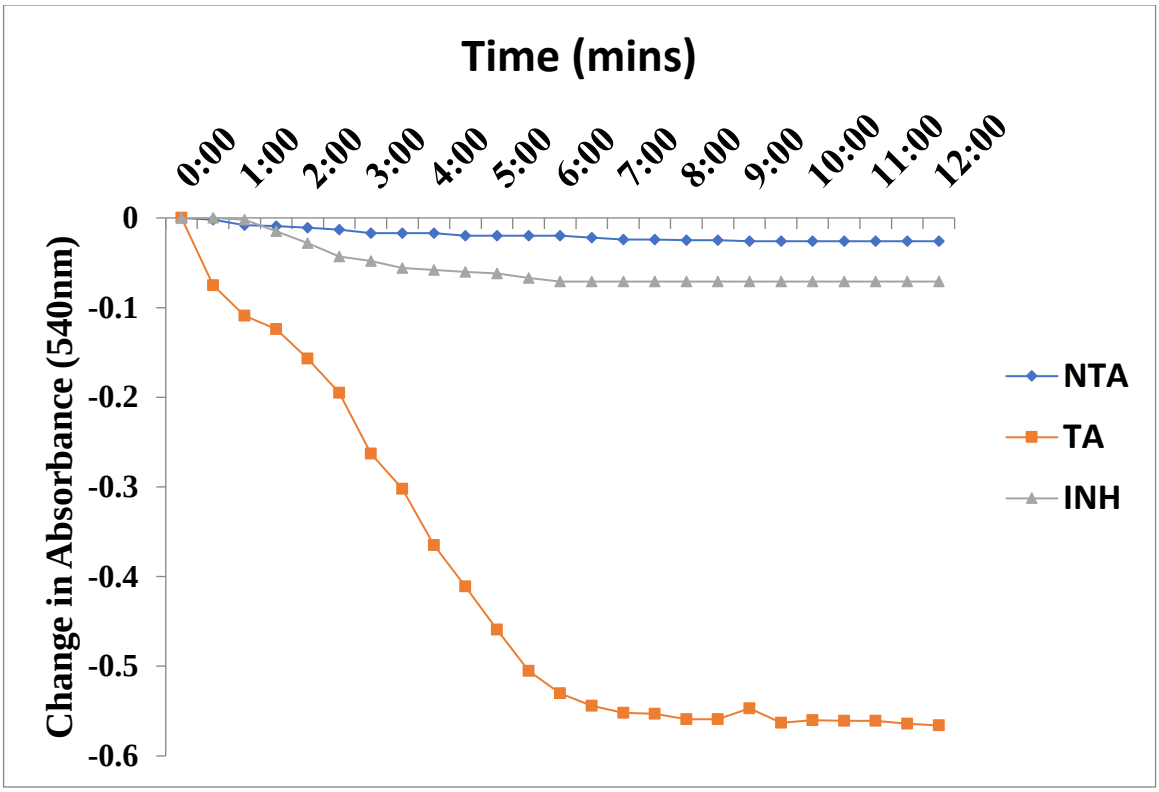

Figure 4.33: Calcium-induced mitochondrial membrane permeability transition pore opening in normal mice colon mitochondria and its reversal by spermine. TA: 5.6 Induction Inhibitor: 71% inhibition

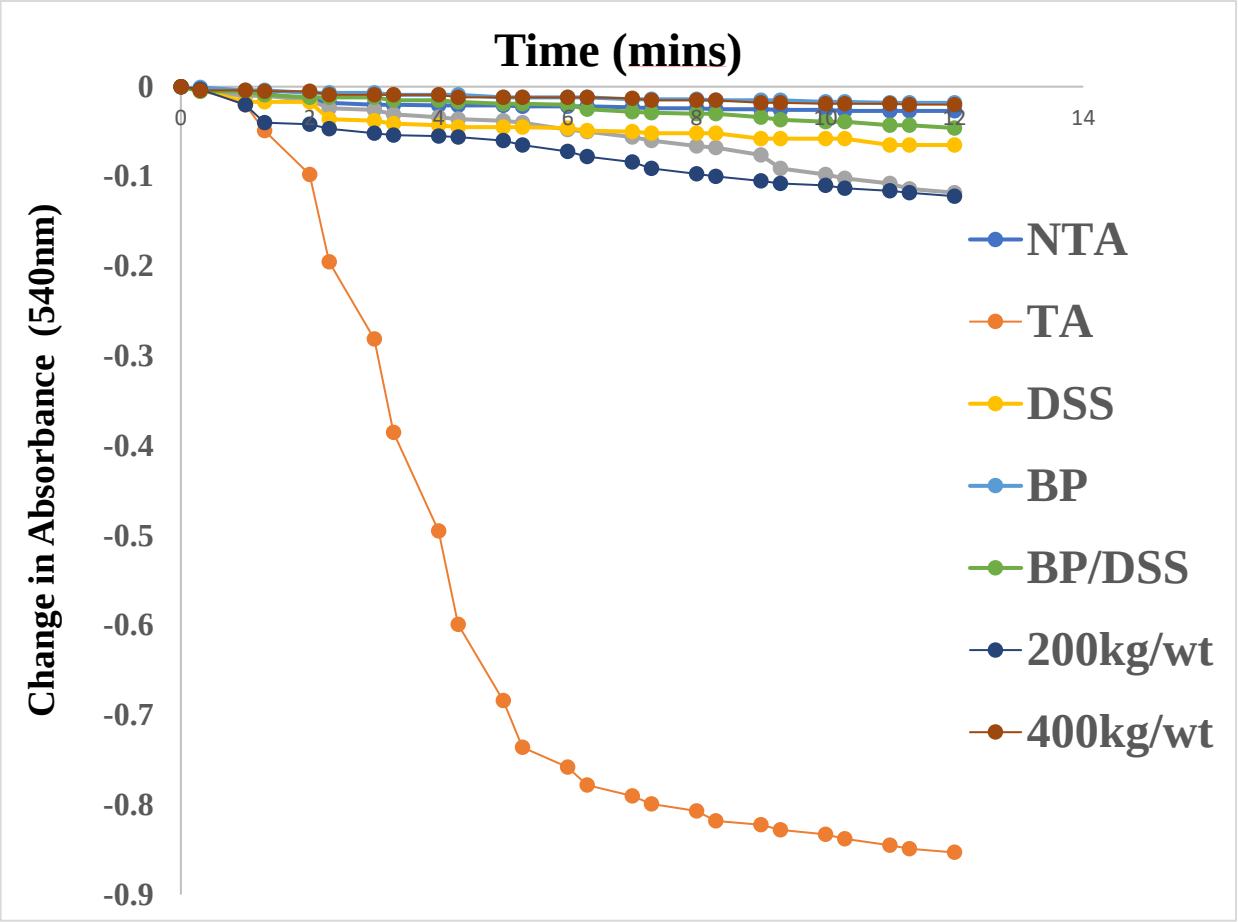

Figure 4.34: Effects of purified fraction *P. africanum* on colon of experimental mice NTA-triggering. TA – Triggering agent, DSS- Dextran sulfate sodium, BaP – Benzo{a}pyrene

4.9.2: Sensitivity of stigmasterol to apoptotic biomakers in the colon, including Caspases 9 and 3, cytochrome c, Bax, and Bcl-2, as well as DNA fragmentation

The level of DNA fragmented when exposed to the toxicant groups (DSS and/or BaP), produced significant difference when compared with the control groups while there was distinct reduction when the groups treated with stigmasterol compared to DSS+BaP groups (figure 4.35). There were no significant differences in level of caspase 9 (figure 4.36) (1.10±0.10, 0.90±0.01, 1.10±0.10ng/ml vs 0.01ng/ml) and also no distinct difference experienced with the levels in caspase 3 when compared with the control group and also when the toxicants groups were compared to the groups that were treated with stigmasterol (Figure 4.37). The DSS, BaP in Bax (120.00%, 100.00%, and 90.00% vs 110.00%) and DSS+BaP, relative to the vehicle increased reduced as indicated in figure 4.38, Bcl-2 (80.00%, 75.00%, and 75.00% vs 90.00%) which were modulated by stigmasterol. However, stigamsterol has no significant effects on the expression of Bcl-2 and cytochrome c as indicated in figure 4.39 and 4.40.

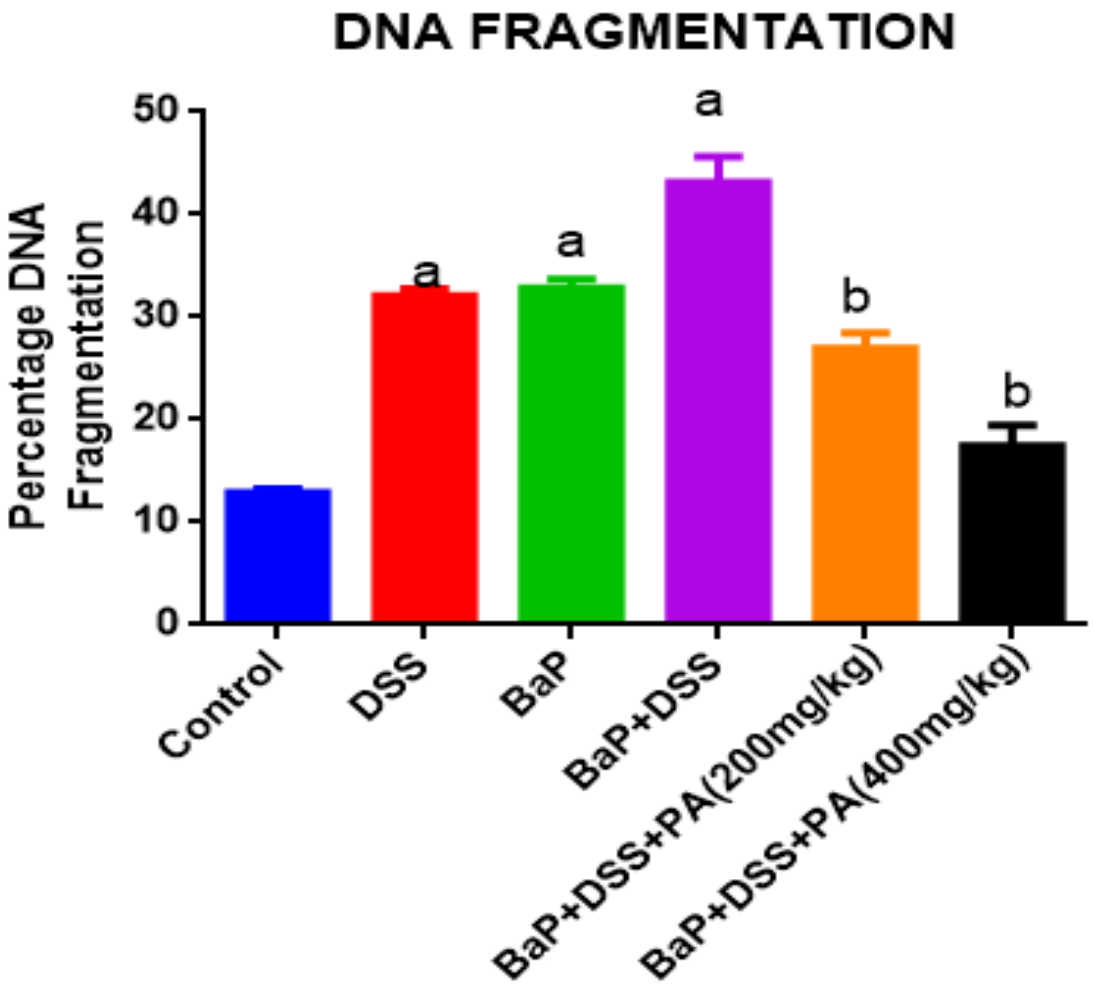

Figure 4.35: Effects of purified ethyl acetate of *P. africanum* stem bark on DNA Fragmentation

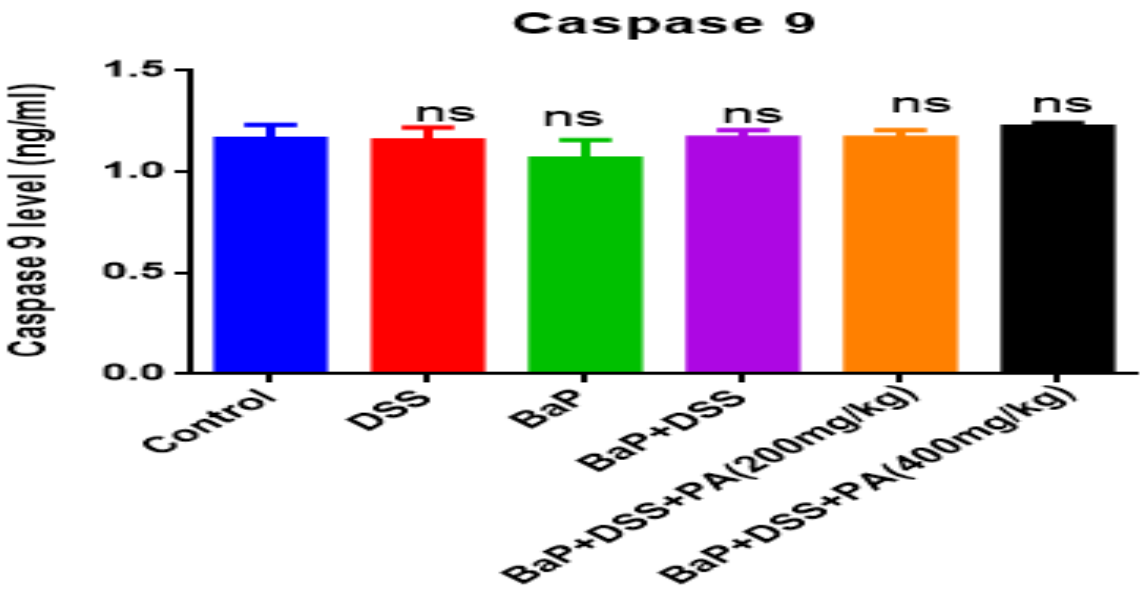

Figure 4.36: Assessment of the levels of caspases 9 on colon values are expressed as mean ± standard deviation significant differences from the control are indicated by: * (P < 0.05) (A-Significant relative to control, B-Significant relative to DSS/BaP, NS-No significant)

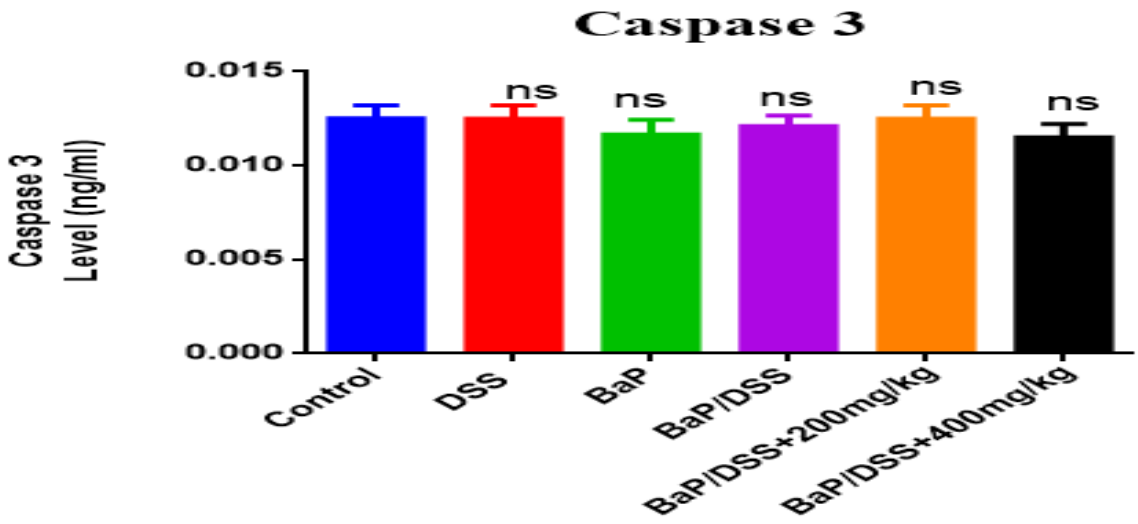

Figure 4.37: Assessment of the levels of caspases 3 on colon values are expressed as mean ± standard deviation significant differences from the control are indicated by: * (P < 0.05) (A-Significant relative to control, B-Significant relative to DSS/BaP, NS-No significant)

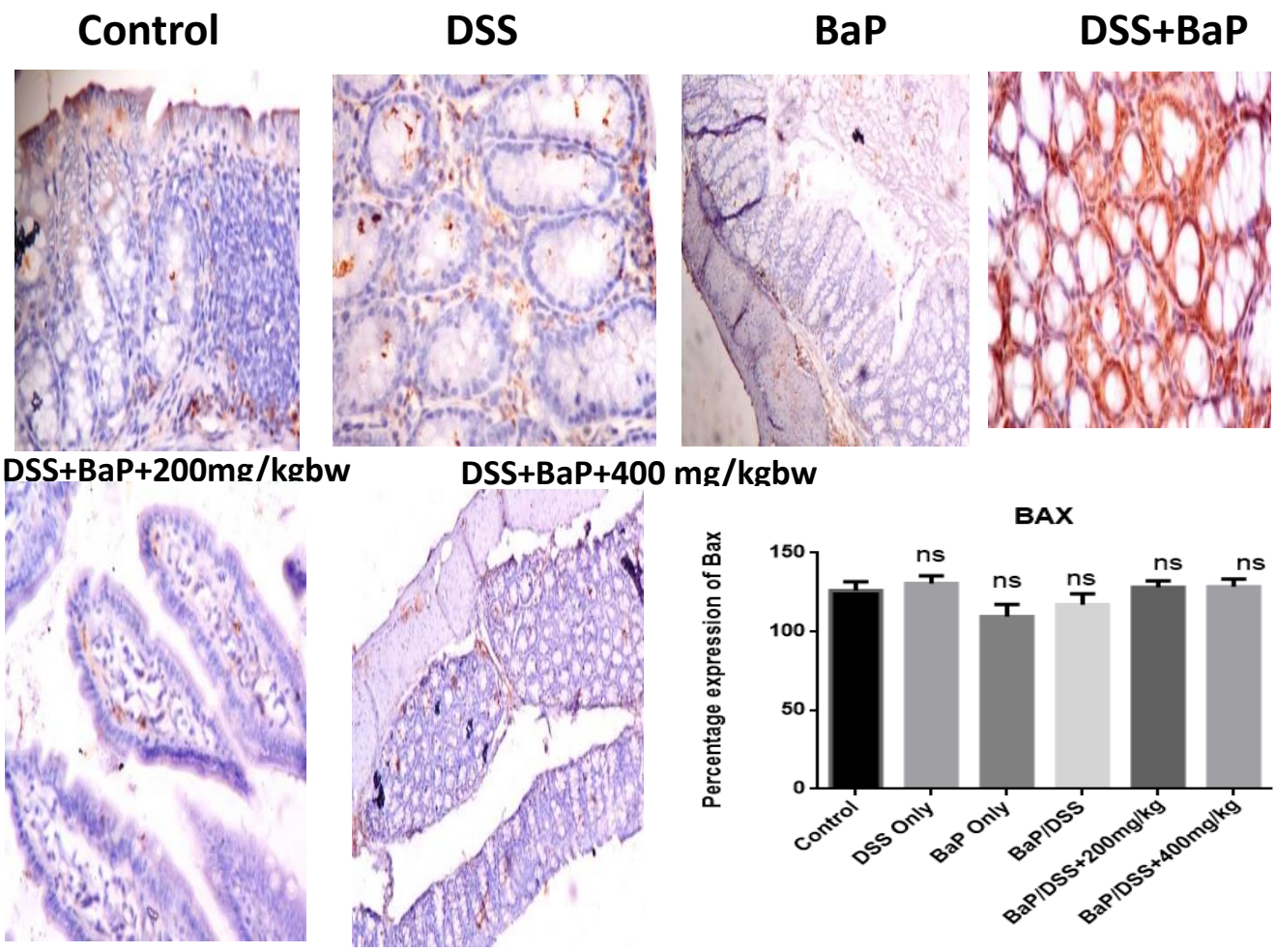

Figure 4.38: Expression of Bax protein in the colon after exposure to DSS and BaP by immunohistochemical method (x400) (a-significant relative to control, b-significant relative to DSS/BaP, ns-no significant.

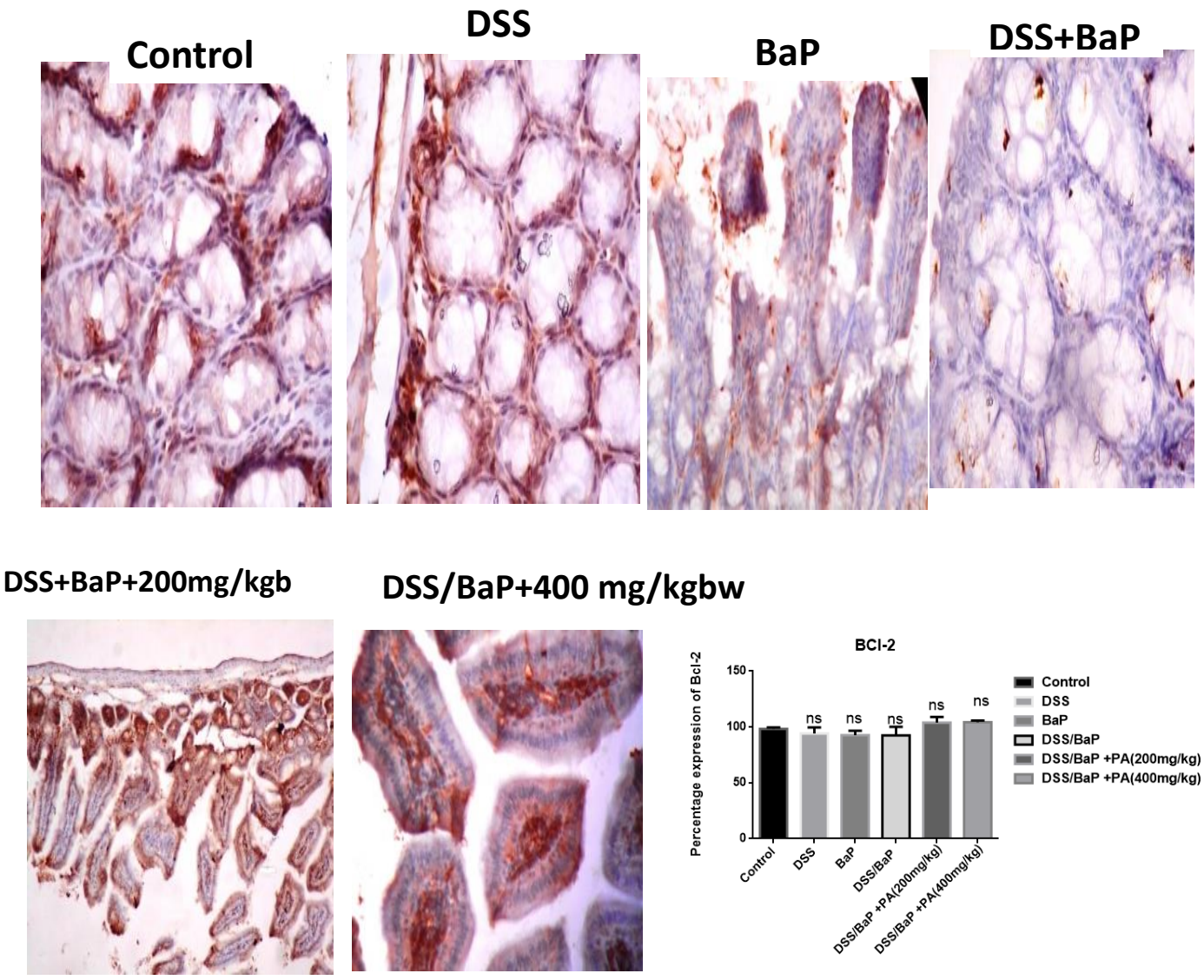

Figure 4.39: Expression of Bcl-2 protein in the colon after exposure to DSS and BaP by immunohistochemical method (X400) (a-Significant relative to Control, b-Significant relative to BaP/DSS, ns-No Significant)

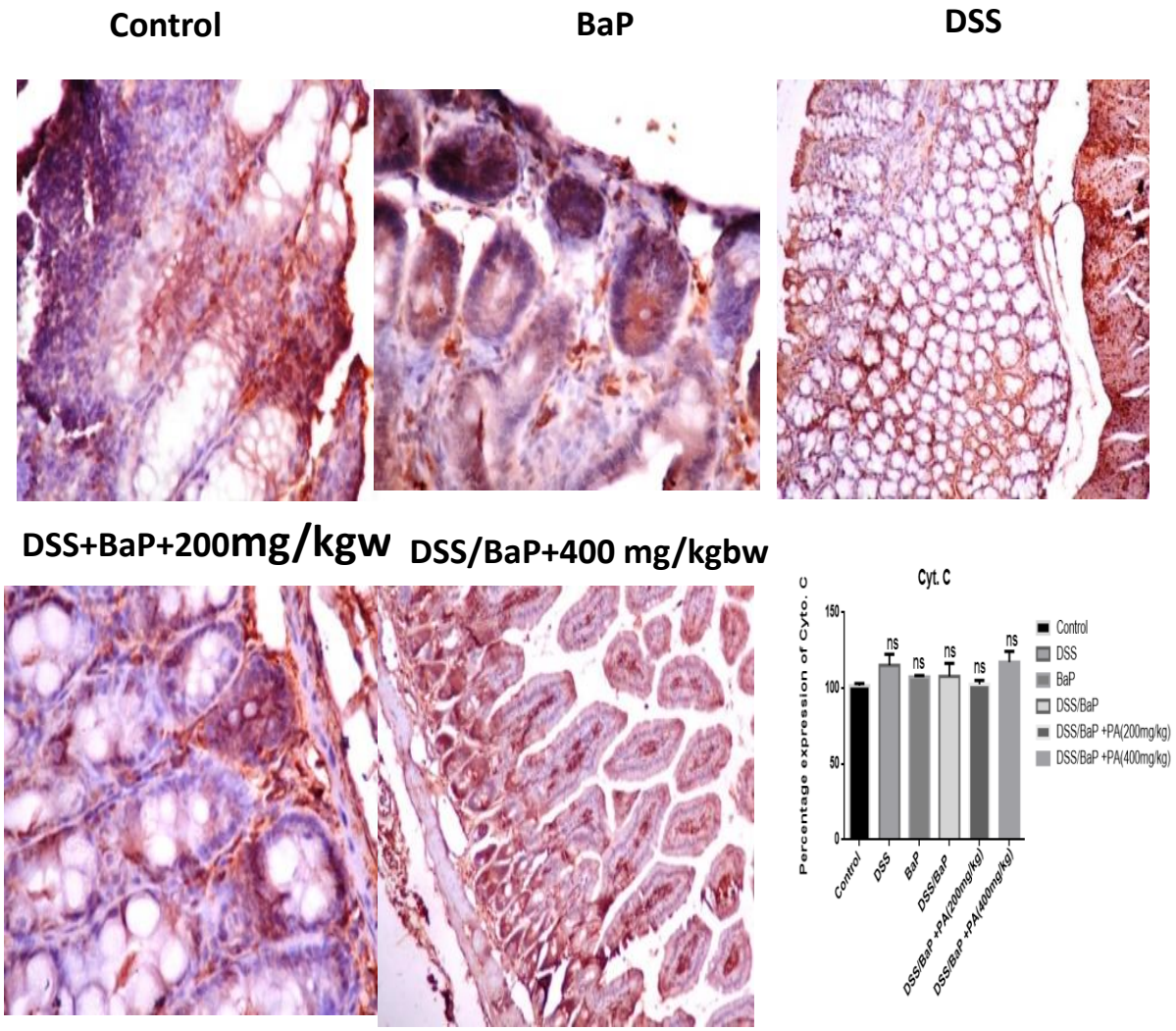

Figure 4.40: Release of cytochrome c in the colon after exposure to DSS and BaP by immunohistochemical method (X400) (a-Significant relative to Control, b-Significant relative to DSS/BaP, ns-No Significant).

4.10: Ameliorative effect stigmasterol on DSS/BaP-induced colon toxicity and inflammatory biomarkers (physical appearances, TNFα, IL-6, p53)

4.10.1: Effect of stigmasterol on physical appearance of DSS/BaP-induced colon toxicity.

In all groups exposed to DSS (DSS, DSS+BaP, and the treatment groups), there was an initial gain in body weight until the third day. However, afterwards, there was a steady reduction in weight until the conclusion of DSS induction, which was then replaced by water and followed by the arrival of colitis, as shown in figure 4.41. Interestingly, majority of the animals demonstrated amazing recovery from the initial weight reduction, as indicated in figure 4.42.

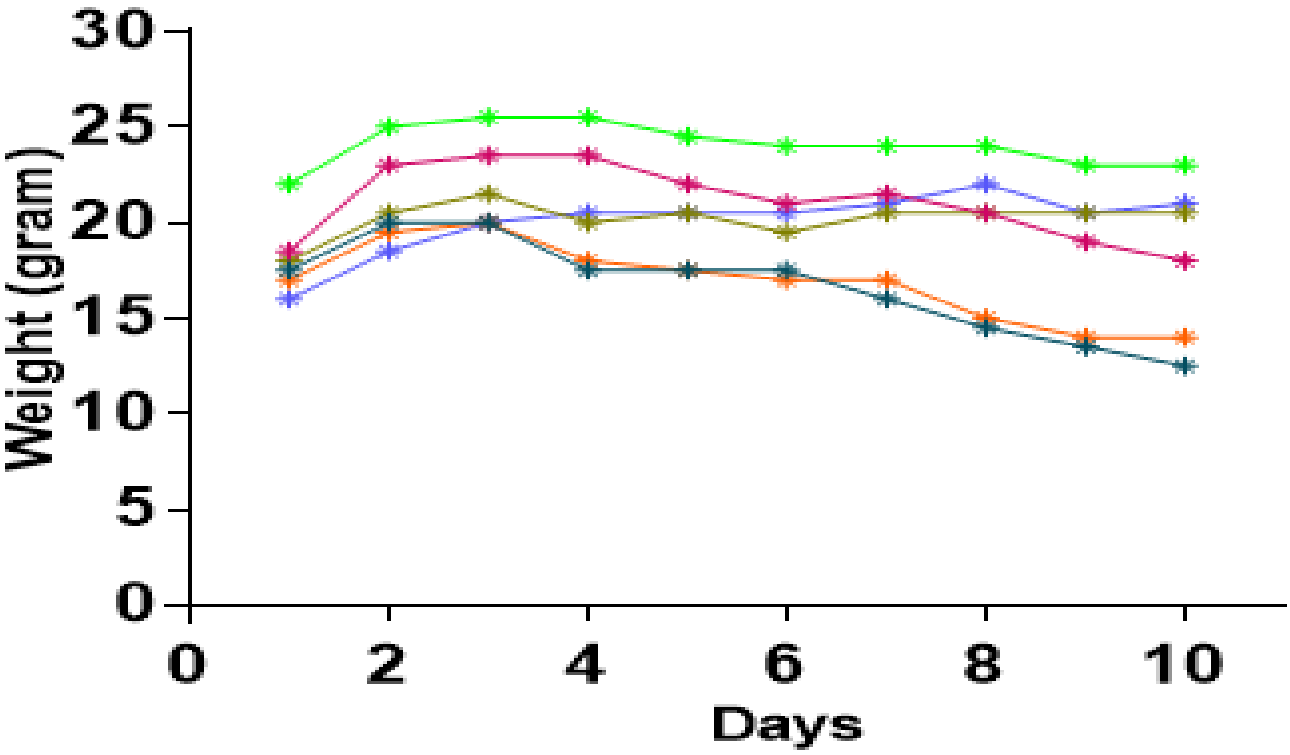

Figure 4.41: Weight of experimental animals during *i*nduction with DSS

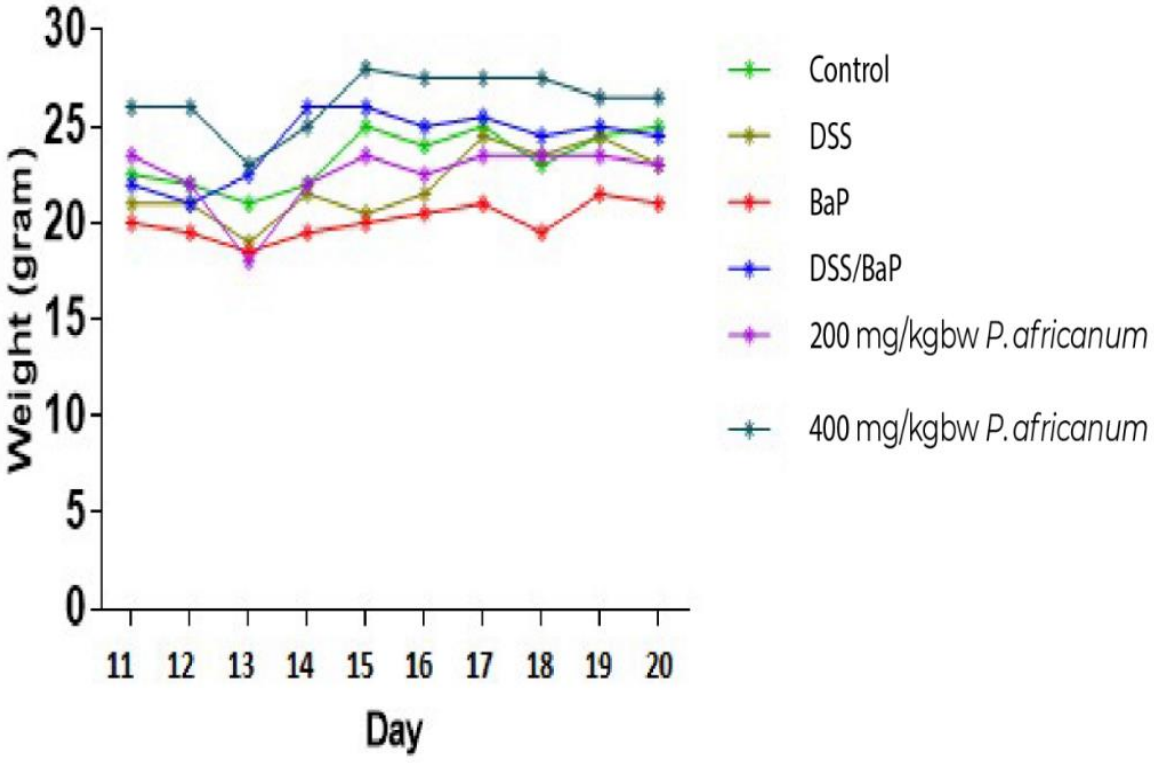

Figure 4.42: Weight of experimental animals after termination of DSS

4.10.2: Effect of stigmasterol on alterations of DSS/BAP-induced on the mice anal region

There were appearances of faeces on the anal region of the animals after the tenth day, this implies that faecal materials have developed into diarrhetic faeces and these were softened with appearances of blood stains at the anal region indicating haemorrhages in the gastrointestinal tract. Ten (10) days 4% oral administration in drinking water of mice from day 5, resulted in the presence of diarrhea and grossly bloody stool as seen in figure 4.43 and figure 4.44 respectively.

Figure 4.43: Sign of diarrhea in colon damage after day 5 of induction by DSS

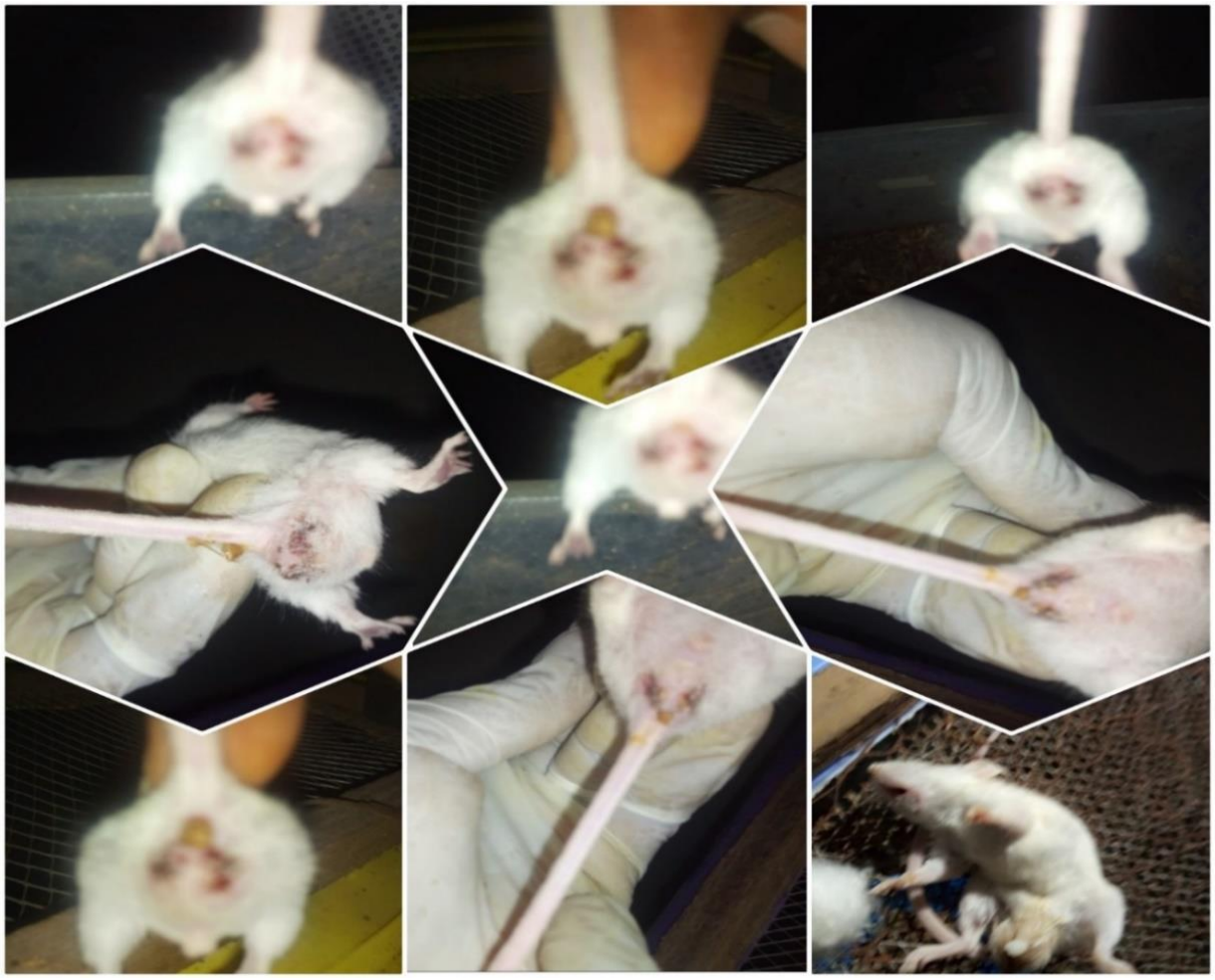

Figure 4.44: Anal region appeared haemorrhagic

4.10.3: Assessment of purified fraction (stigmasterol) of *Piptadeniastrun africanum* stem bark on DSS/BAP-induced colon toxicity (liver function test, antioxidant parameters)

4.10.3.1: Stigmasterol prevents oxidative Stress burden in Ulcerative Colitis in Mice

Overexpression of reactive oxygen species plays a key role in the pathological conditions of the liver and colon. As shown in figure 4.45. Liver enzymes (AST, ALP, ALT and total proteins) activity levels in the colon of toxic mice were distinctly increased than in the control group ($p < 0.05$), which were attenuated by stigmasterol. However, there was a significant reduction in the levels of antioxidants SOD, GSH, GST, GSH, which increased significantly during treatment with stigmasterol (Fig. 4.46).

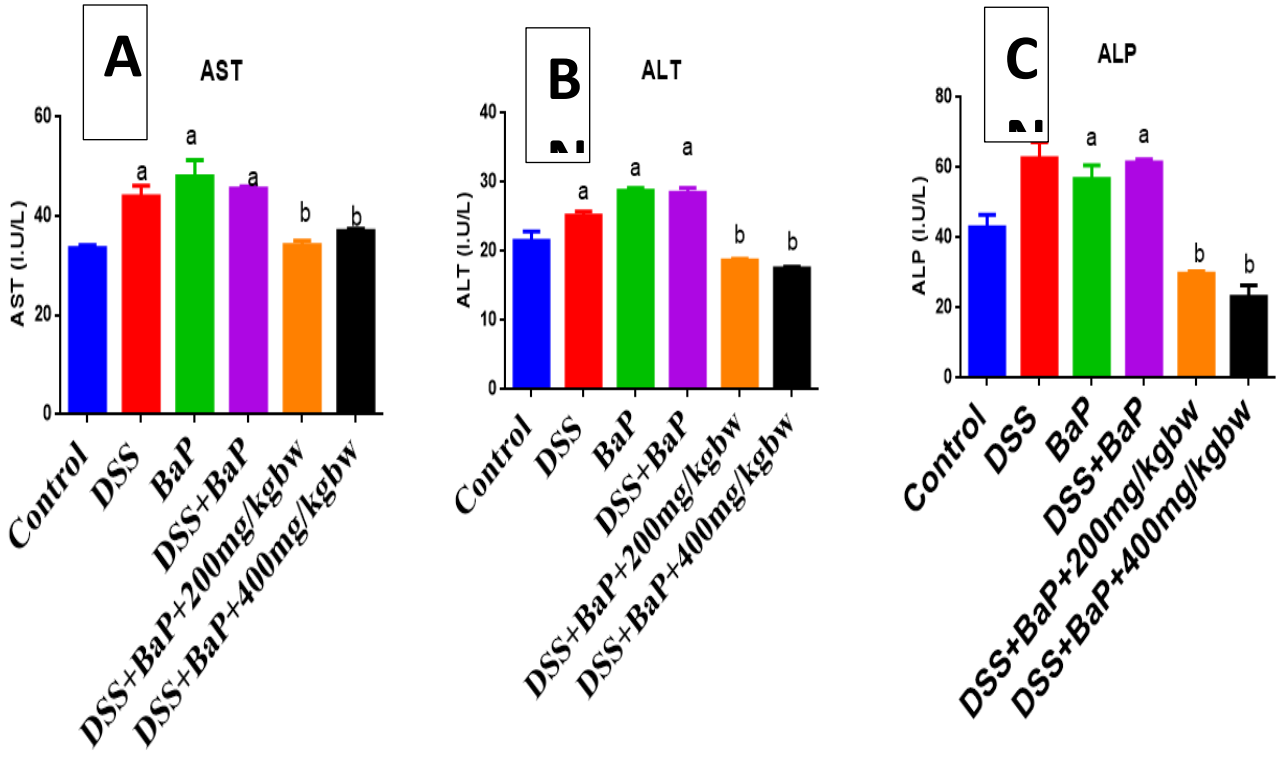

Figure 4.45: Effects of purified fraction (stigmasterol) of *P. africanum* stem bark on liver enzymes {A-aspartate amino transferase (AST), B- alanine amino transferase (ALT) and C- alkaline phosphatase (ALP)}.

a-significant difference relative to control, b-significant difference relative to control ns-no significant difference relative to control and DSS/BaP ($p < 0.05$)

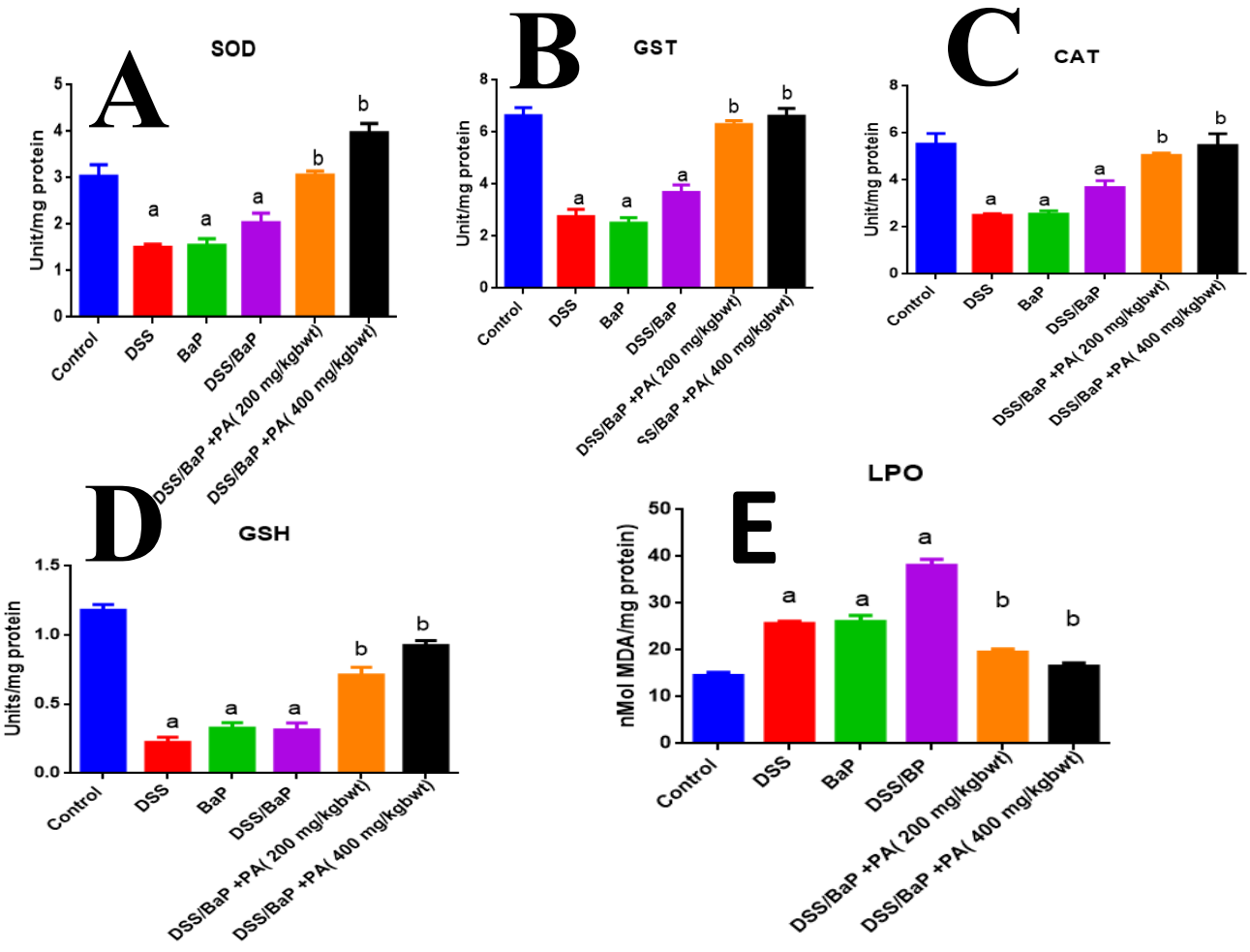

Figure 4.46: Effects of purified fraction (stigmasterol) of *P. africanum* stem bark on antioxidants status and lipid peroxidation

Key:

SOD(A) = Superoxide dismutase; GST(B) = Glutathione-S-transferase; CAT(C) = Catalase; GSH = Reduced Glutathione. LPO(D) = Lipid peroxidation. a-significant difference relative to control, b-significant difference relative to DSS/BaP ($p < 0.05$)

4.10.4: Stigmasterol ameliorates histological damage in Dextran sodium sulfate/ Benzo[a]Pyrene-induced Ulcerative Colitis in Mice

The result in plate 4.4 showed that the mucosal of the epithelium (white arrow) and glands were normal and not inflamed (red arrow). The severe damage caused by DSS/BaP on colon was mitigated by purified fraction of *P. africanum* showing its anti-inflammatory potential.

CONTROL-Epithelium (white arrow) and glands were not inflamed (blue arrow), and the submucosal appear normal and not infiltrated (thin blue arrow).

DSS-Poorly preserved mucosal epithelium (white arrow). The lamina propria shows moderate fibrosis (blue arrow). Several normal villi and mildly infiltrated inflammatory cells within the propria (slender arrow).

BaP-Moderate infiltration by inflammatory cells (slender arrow) and the glandular epithelial cells show atypical cells of adenocarcinoma (black arrow).

BaP+DSS-The glandular epithelial cells show well differentiated adenocarcinoma (red arrow) and hyperplasia (white arrow). Moderate to severely necrotic

BP+DSS+PA at 200mg/kgbw- Infiltration of lamina propria by inflammatory cells (slender arrow) areas of glandular hyperplasia without adenomas (white arrow)

BP+DSS+PA at 400mg/kgbw-Poorly preserved mucosal epithelium (white arrow), glandular hyperplasia without adenomas (red arrow)

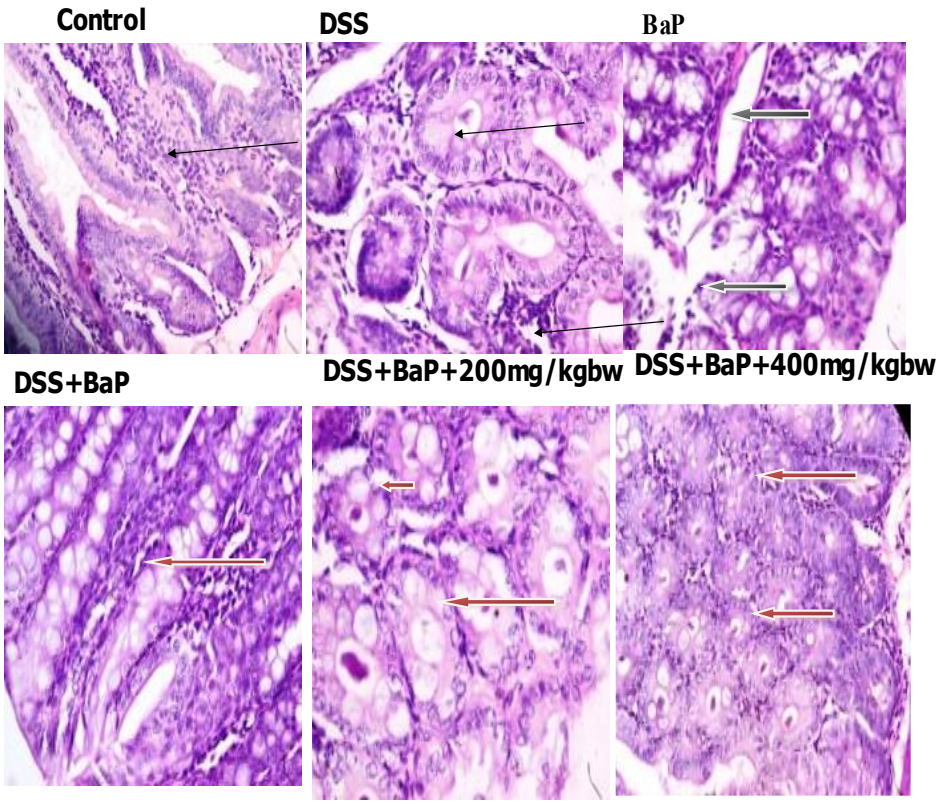

Plate 4.4: Photomicrograph of a Colon damage (X400)

Table 4.10.5: Effects of stigmasterol on anti-inflammatory cytokines in dextran sulfate sodium/benzo{a}pyrene-induced ulcerative colitis

Table 4.10.5.1: Haemotology Parameters of stigmasterol on colitis

Sample ID	PCV %	HB g/dL	RBC 106µl	WBC 103µl	PLAT ELET	LYMP %	NEUT %	MON %	EOS %
Control	24.5± 0.71	11.2± 0.07	5.30± 0.08	4700± 70	135500 ±707	78.5± 0.71	37.5± 0.71	2±0	0.5±0. 001
DSS	18±1. 41*	5.3±1 .27*	1.54± 0.28** *	3800± 70.7**	122500 ±707*	44.5± 0.71**	26.5± 0.71**	1.0±0.7 0*	3±0.04 1***
BaP	15.5± 0.71*	4.3±1 .41**	2.03± 0.01*	3125± 35.4**	118000 ±707**	57.5± 0.71*	29.5± 0.71*	1.01±0. 71*	2±0.04 1***
DSS+BaP	12.5± 0.71**	6.9±0 .28*	4.35± 0.05	4000± 70.7*	47025± 353***	41.5± 0.71** *	33.5± 0.71*	1±0*	2.5±0. 071**
DSS+BaP+200mg/kgbw	27.5± 0.71	7.25± 0.78*	7.21± 0.06	5150± 70.7	133500 ±707	65.5± 0.71*	35.5± 0.71	2.5±0.7 0	1.2±0. 071*
DSS+BaP+400mg/kg/bw	30.5± 0.71*	8.5±0 .14*	8.22± 0.17*	5675± 35.4*	130000 ±353	66±1. 41*	38.5± 0.71	2±1.41	1±0.002*

4.10.6: Stigmasterol inhibits inflammatory responses to TNF-α, IL-6 and p53 in Dextran Sulfate/Benzo{a}Pyrene-induced Ulcerative Colitis

The injection of Dextran sulfate sodium (DSS) and Benzo[a]pyrene (BaP) induced damage in the colon, but the effects were alleviated by stigmasterol isolated from P. africanum. This indicates the anti-inflammatory qualities of the plant, as seen in figures 4.47, 4.48, and 4.49. The groups treated to the toxicants (DSS, BaP, and DSS+BaP) demonstrated considerable increases in TNF-α levels compared to the vehicle group (40.00±1.20%, 30.00±0.90%, 34.00±1.10% versus 15.00±0.70%). Similarly, greater levels of IL-6 (160.00±0.70%, 3.50%, 110.00±2.20%, 120.00±1.50% compared 60.00±1.50%) and p53 (80.00±2.30%, 70.00±1.10%, 85.00±2.20% versus 25.00±0.90%) were detected. Conversely, the vehicle group revealed lower levels of TNF-α, IL-6, and p53 (13.00±0.10% compared 34.00±1.10%, 53.00±1.30%, 50.00±1.20% vs 120.00±1.50%, 40.00±2.20%, 50.00±1.70% versus 85.00±2.20%, respectively).

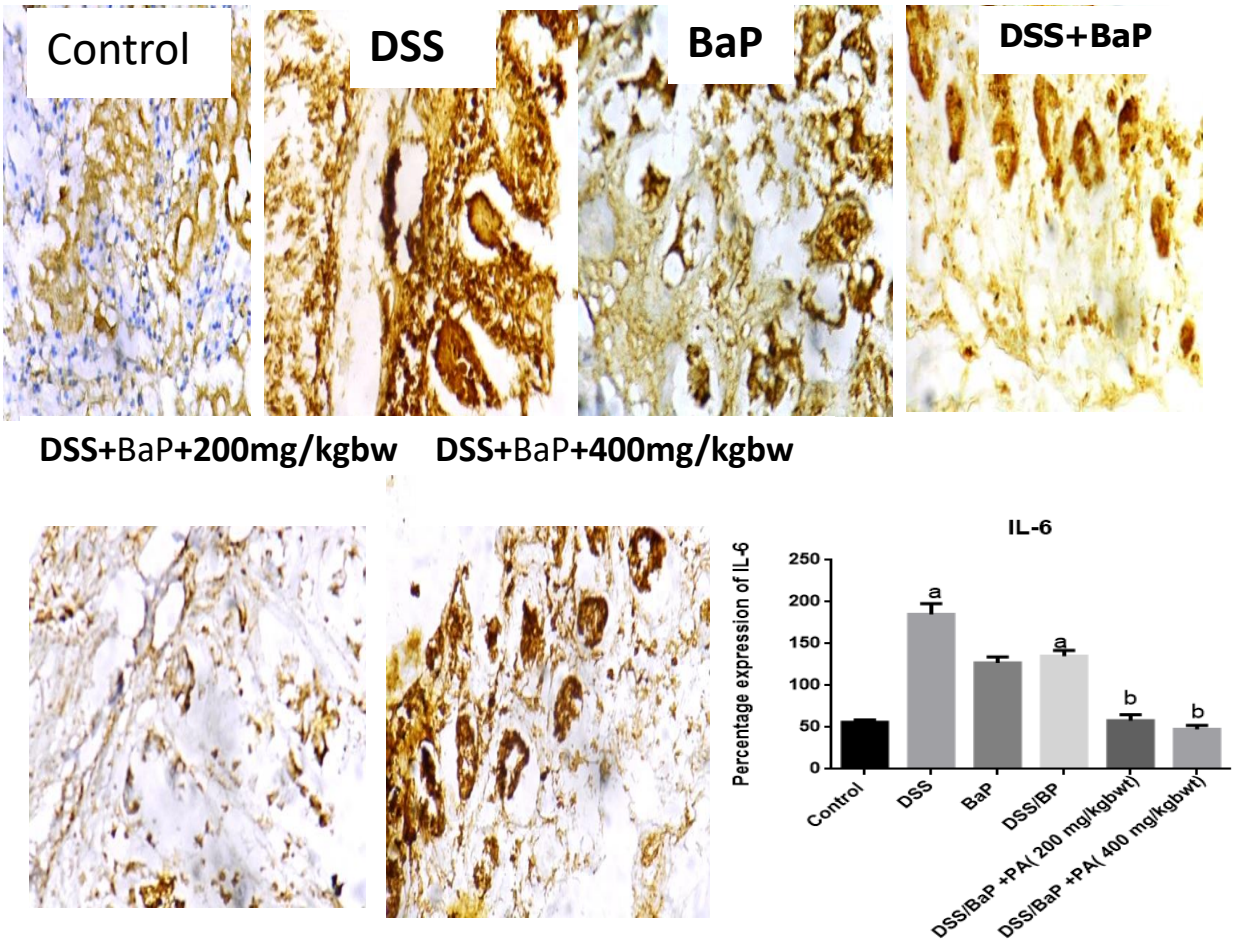

Figure 4.47: Photomicrograph of immuno assay for the colonic section showing abundant expression of interleukin 6 on DSS while others are moderately expressed (x400) (a-significant relative to control, b-significant relative to DSS/BaP ns-no significant

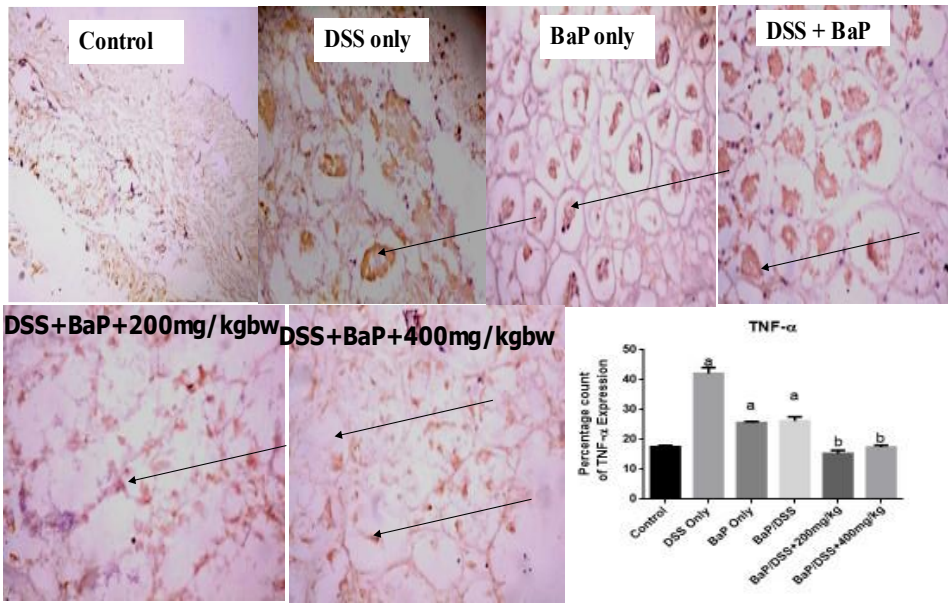

Figure 4.48: Photomicrograph of immunohistochemistry assay for the colonic section showing abundant expression of TNF-α (X400) (a-Significant relative to control, b-significant relative to DSS/BaP, ns-no significant

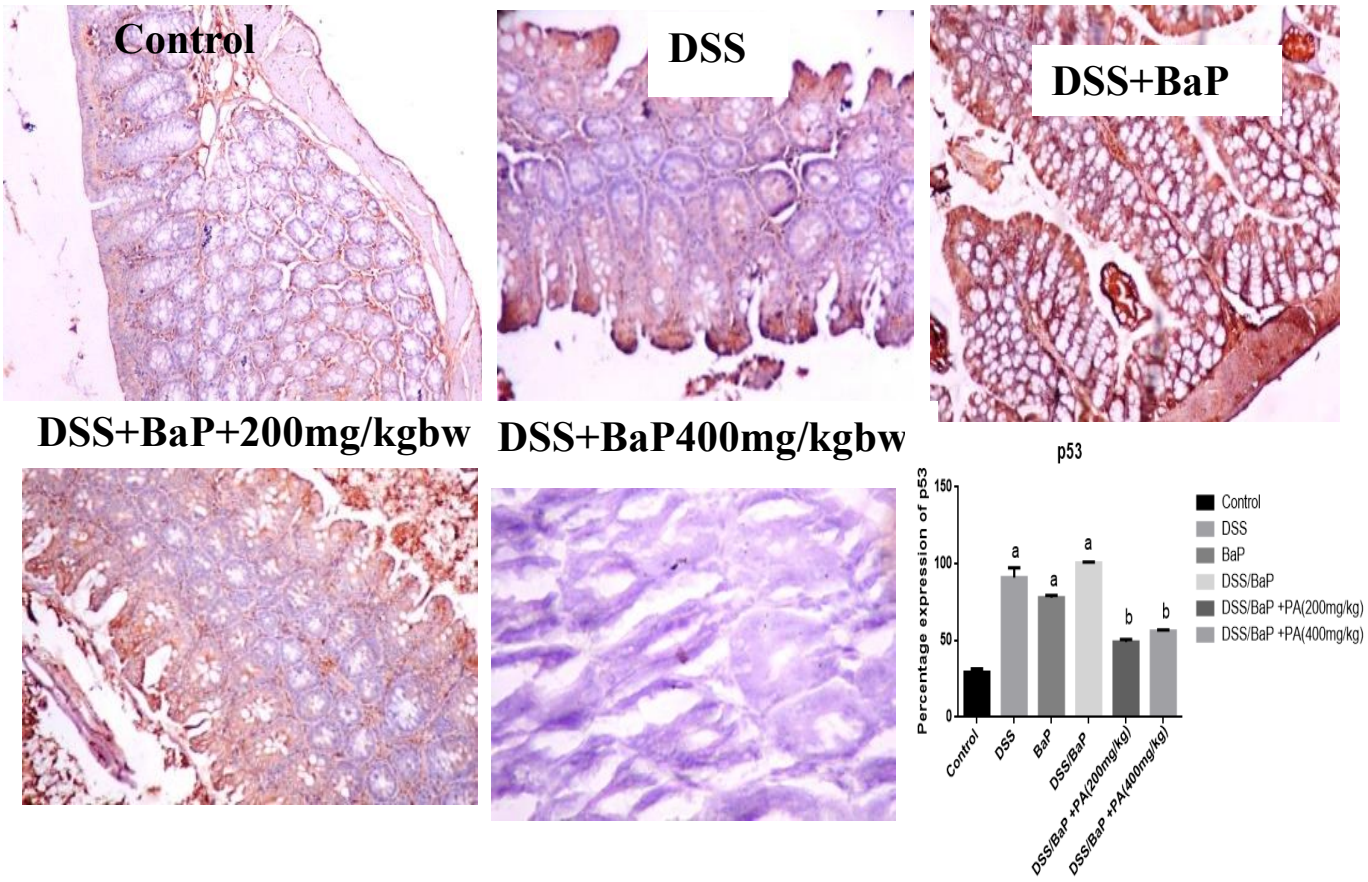

Figure 4.49: Expression of p53 protein in the colon after exposure to DSS and BaP by immunohistochemical method (X400) (a-Significant relative to Control, b-Significant relative to BaP/DSS, ns-No Significant)

CHAPTER FIVE

DISCUSSION

Advances in research in recent years has extended the understanding of mitochondrial functions beyond the energy production with which they are historically associated. Research has established a remarkable role of mitochondria in ion homeostasis, apoptosis, cellular response, antioxidant and redox regulation, participation in various biosynthetic pathways, etc. (Singh *et al*., 2019). In addition, the presence of self-DNA (mtDNA) in effective coordination with the nuclear genome determines their importance for cell physiology (Giacomello *et al*., 2020). Therefore, dysregulation of key mitochondrial signals is associated with dysfunction ranging from tissue wasting, cancer, neurodegenerative diseases, inflammation, and metabolic disorders (Zhu *et al.*, 2019).

5.1 Biological compounds of the stem bark of *P. africanum*

In recent years, research has demonstrated the use of dietary phytochemicals to heal diseases such as diabetes, cardiovascular trouble, cancer and other connected problems (Delshad et al., 2021). These phytochemicals have a therapeutic impact on a range of clinical conditions by modulating various signaling pathways (Feldman et al., 2019; Anifowose et al., 2020). Preliminary phytochemicals screening in this investigation indicated the presence of alkaloids, cardiac glycoside, saponins, phenols, tannins, flavonoids and steroids in crude methanol extract, chloroform and ethyl acetate fractions of P. africanum (Table 4.1.1). However, alkaloids are missing in methanol fraction.

These phytochemicals are non-nutritional but biochemically active components inherent in the plant. They have been shown to play important roles in the biological system. For instance, flavonoids and other phenolics have been discovered to exhibit antioxidant, anti-inflammatory and other health-boosting efficacies (Favazza, 2020). Flavonoids are known to lower the tendencies of cancer development in the body and also prevent onset of cardiovascular disease

because of their ability to halt lipid peroxidative event (Manach *et al*., 2005). Several researches have shown the potency of flavonoids in preventing cancer cell line proliferation (Appaih *et al*., 2023). Some flavonoids which include quercetin, luteolin and its glycoside derivative, garlangin and nargarin among others have been shown to possess anti-bacterial activity (Swaminathan *et al*., 2012). Research has shown that concentration of cardiac glycosides, alkaloids and other polyphenols in plants can be linked to their ability to prevent turmorigenesis and gastrointestinal inflammatory process. This may not be unconnected with the engagement of *P. africanum* as trado-medical intervention for diseases.

Alkaloids were not present in methanol fraction of *P. africanum* stem bark extract. The absence of this phytochemical may result from the solubility of some phytoconstituents in some solvent and its inability to dissolve others. specific solvent and its inability to dissolve others. This is substantiated by the research done by Osei et al., (2017) which indicated that the isolate of Ficus exasperata lack the presence of flavonoids, phenols and tannins and were included in the crude extract.

The quantitative phytochemical analysis showed that ethyl acetate fraction has the highest quantity of flavonoids and tannins which are known to play vital biological significance in the cells. Bagyalakshmi *et al.* (2019) reported that tannins can decrease digestibility of some protein molecules by complexing with them. This mechanism is also employed against bacteria by forming tough complex with the carbohydrate moiety of their cell walls and inhibiting enzymes responsible for digestion, thus, preventing the bacteria from releasing its cytoplasmic content to take over the host DNA synthesizing machinery.

Tannins were reported to prohibit microbial degradation of semen proteins (Mohan and Savithramma, 2019). The health-improving effects of these bioactive compounds were as well observed in their ability to scavenge free radicals, prevent ulceration of the gastrointestinal tract and halt peroxidative tendencies in myocardiac mitochondria (Ajayi *et al*., 2018; Muhammed *et al*., 2012). The reported results of the bioactive components are indicative of the pharmacological potential of *P. africanum*.

Phytochemicals are beneficial and integral to the drug development process due to their wide spectrum of activity and potential (Ogboru *et al*., 2015; Salaudeen *et al*., 2023). These

secondary metabolites protect cells from the damaging effects of radicals generated when exposed to harsh environmental conditions (Sivakumar and Balasubramanian, 2020). Medicinal plants with potent biologically active compounds influence mitochondrial apoptosis via mPT pore modulation, especially in relation to the effective and selective improvement of pathologies characterized by suppression or enhancement of apoptosis (Oyebode *et al*., 2018; Olowofolahan *et al.*, 2020. An example is *Callandra portoricensis*, a flowering plant belonging to the subfamily *Mimosacea*, which is reported to have anti-apoptotic, anticonvulsant, antioxidant, and antipyretic effects (Aguwa *et al.*, 1988; Oyebode *et al*., 2020).

5.2 Inductive effects of extract and fractions of *P. africanum* (*in vitro*)

Studies have shown that certain solvent fractions of the stem bark of *P. africanum, a* plant of the Mimosaceae family, are used to treat diseases such as constipation, stomach ulcers, meningitis, malaria, and colon cancer (Jiofack, 2008; Mengome *et al*., 2009; Teinkela, 2020). Previous experiments with *P. africanum* showed antibacterial (Pathak *et al*., 2009), anti-inflammatory (Diffoum, 2012), ulcer-healing properties (Assob *et al.,* 2011), with no toxicological effects at a dose of 5 mg/kg in rats (Mengome *et al*., 2009). The combination *of Piptadeniastrum africanum, Petersianthus macrocarpus, Cissus* and *Dieffenbachia* has shown anti-proliferative potential against human colon cancer (Mengome *et al*., 2009) by stimulating mitochondrial-mediated apoptosis, and this may be beneficial in pathological situation when apoptosis desires to be upregulated and enhanced (Olanlokun *et al*., 2020).

However, it is unconfirmed if phytochemicals present in *P. africanum* will have a modulating effect on mitochondrial-mediated apoptosis through opening mitochondrial permeability pores. Previously, *in vitro* study revealed that, mitochondrial integrity was confirmed through the induction of exogenous calcium-induced pore opening, a process which was significantly returned by the potent inhibitor, spermine. This confirmed the integrity of mitochondria and made them appropriate for further usage (Lapidus and Sokolov, 1993).

Treatment of normal mitochondria with various concentrations of crude methanolic *P. africanum* stem bark extract (CRMEPA) without calcium, the standard triggering agent (TA), caused significant pore opening compared to the non-trigger agent (NTA). The addition of

calcium (a standard triggering agent) further potentiated the induction in reverse manner. However, pore opening was significantly altered by spermine, suggesting that induction with crude methanolic extracts of *P. africanum* stem bark does not affect mitochondrial membrane integrity. This discovery suggests that CRMEPA may contain certain biologically active components that may be associated with pore components, leading to pore opening and hence apoptosis. In addition, the induction of the pore opening in concentration-dependent order with CRMEPA caused increase in the opening of the pore with increased fractions as seen in figure 4.3 with highest induction 6.3-fold at 140µg/ml in the absence of ca^{2+}.

In addition, evaluation of different concentrations of the three chloroform fractions, the *P. africanum* fraction, the *P. africanum* ethyl acetate *fraction and the P. africanum* methanol fraction (CFPA, EAFPA and MFPA) showed that a significant induction of pore opening was recorded using ethyl acetate and methanol fractions, nevertheless, with the chloroform fraction, no such activity was observed (figures 4.4, 4.6 and 4.8) respectively. However, EAFPA has been found to have the highest induction of 8.0-fold at µg/ml 180and this may suggest that the classes of phytochemicals present in EAFPA may be responsible for the induction.

MFPA was found to significantly induce mitochondrial pore opening with induction fold of 5.0 at 100µg/ml, but the induction was not as high as that of the ethyl acetate fraction. These studies have shown that the bioactive components present in the methanol extract (CRMEPA) and the fractions of *P. africanum* may be responsible for pore opening, with the ethyl acetate fraction (EAFPA) being the most effective with the highest induction coefficient, followed by methanol fraction while the addition of exogenous calcium further enhanced the calcium-induced opening. In contrast, chloroform produced no important effect on pore opening.

5.3 Ethyl acetate fraction of the stem bark of *P. africanum* modultaes apoptosis (*in vivo*)

Having observed the highest pore opening activity with EAFPA in an *in vitro* study, it was necessary to investigate if probably the same effects would be replicated *in vivo*. Studies have been conducted to achieve this because of the importance of the bioavailability of a compound throughout the plant, it is vital to develop a safe dosage schedule for the ethyl acetate component of P. africanum. The conclusion of different doses of EAFPA indicated a large increase in the induction of pore opening when compared with control, with the increase being dose-dependent (figure 4.14).

Therefore, the results of in vivo induction of mPT pore opening in mice liver by EAFPA complement the in vitro results and suggest that the presence of EAFPA triggered the induction on the membrane with induction of 2.5, 4.9 and 6.9 folds at 25, 50 and 100mg/kg body weight respectively. The result also showed that pore opening upon mPT induction increased with increasing fraction doses, making it dose dependent. Mitochondria are sites for the production of fuel necessary to maintain the activity of normal biological cells. They are good regulators and good cell death checkpoints that can be prescribed for cancer treatment, while the abnormal roles of mitochondria are associated with tumor cell survival and proliferation (Pustylnikov *et al*., 2018).

Upon further investigation, the crude methanol extract and its fractions were found to inhibit lipid peroxidation, with the chloroform fraction having the highest inhibition, suggesting that these fractions may protect cells from membrane damage caused by lipid peroxidation. Ferrous- induced lipid peroxidation inhibition in this study also showed that *P. africanum* has free radical scavenging potential as shown in figure 4.12. Therefore, the modulation of mPT pores detected may not as a result of ROS production, but for the available phytochemicals in the plant. Furthermore, thus, may suggest that *P. africanum* stem bark may play a role in protecting the physicochemical potential of membrane from severe free radical-induced cellular disfunction during undue apoptosis.

The LPO result showed a concentration-dependent enhancement of the Fe^{2+}-induced lipid peroxidation inhibition, showing that crude and fractions of *P. africanum* inhibit Fe^{2+} - induced lipid peroxidation, therefore, showing that *P. africanum* contains biologically active compounds, that act as free radical scavengers, and that mPT pore induction was not the result of membrane damage. All investigations done and characteristics established on stem bark fractions of P. africanum indicated that the ethyl acetate fraction of P. africanum was the most potent. In order to improve and establish the efficacy and activity of EAFPA, the effect of 14 days of intraperitoneal administration of several dosages - 25, 50 and 100 mg/kg body weight of EAFPA on MDA quantified revealed no substantial difference comparing to the control stimulating that P. africanum contains biologically active substances such as saponins, flavonoids, tannins etc capable of destroying free radicals.

Lipid peroxidation is a chain reaction initiated by hydrogen abstraction or addition of an oxygen radical leading to oxidative damage to polyunsaturated fatty acids (PUFA), and mitochondria have been recognized as one of the main sources of reactive oxygen species (ROS) production (Moldavsky and Moldovan, 2004; Ayala et al., 2014; Salemcity et al., 2023). Lipids, proteins, oxidative phosphorylation enzymes, and mtDNA are exposed to free radicals (Lobo *et al*., 2010) in mitochondria, and direct damage to these mitochondrial molecular structures reduces their binding or affinity for substrates or coenzymes, thereby minimizing their function (Skuratovskaya *et al.*, 2020).

Free radical chain reactions are involved in membrane lipid peroxidation, which is consistent with swelling and possible lysis of mitochondria and other cells such as microsomes, lysosomes (Peterson, 2017; Olowofolahan *et al*., 2020). Cytochrome c release owing to permeabilization of the mitochondrial pore is significant as it is regarded of as the point of no return for start of apoptosis (Chipuk et al., 2006; Ding et al., 2014 and Kuwana et al., 2020). The ethyl acetate fraction maximally liberated cytochrome c related with the crude methanol extract and other fractions, showing that mPT pore opening leads to cytochrome c release, and it is a necessary condition for the occurrence of apoptosis and this is in accordance with Olanlokun *et al*., (2022)

A concentration-dependent increase in the release of cytochrome c was observed when mitochondria were treated with crude methanol extract, chloroform, methanol and ethyl acetate fractions as revealed in figures 4.10, respectively, compared to control, while ethyl acetate had the highest cytochrome c release, confirming mPT pore induction opening with ethyl acetate, which has the highest induction multiplicity as it has been reported by Olowofolahan *et al*., (2020)

Research shows that, the main role of ATP synthase is in the synthesis of ATP, which can also be reversed under certain conditions, whether in pathological or physiological, the hydrolysis of ATP and deactivation of the mitochondrial inner membrane (Nicholls and Ferguson, 2013; Salemicity *et al*., 2023).

ATP synthase plays a crucial role not only in the depolarization of the inner membrane of mitochondria due to the permeabilization of mitochondrial membrane pores, nevertheless it also influences the response of mitochondrial permeability transition (mPT) to calcium, according to studies conducted by Giorgio *et al*., (2018). There has been a suggestion that the c-subunit, a critical component of ATP synthase integrated into the membrane, does not affect the mPT response to calcium, as demonstrated by the research of He *et al*. (2007). Interestingly, Bernadi Paolo delved even deeper to argue that the enzyme itself works as the pore (Bernadi, 2013). However, Zhou *et al*. (2016) questioned this technique and put up an other argument.

Furthermore, under pathological situations, the persistent opening of the pore leads to ATP hydrolysis and the release of inorganic phosphate (Pi), which eventually causes uncoupling of phosphorylation in mitochondria. Mnatsakanyan and Jonas (2020) remark that this mechanism leads to the alteration of metabolic processes, resulting in an increase in ATPase activity and phosphate accumulation. Consequently, mitochondrial activity is altered, ATP levels fall, and the structural and functional integrity of cells become impaired, leading to irreversible damage and cell death.

To measure ATPase activity, the researchers evaluated the release of inorganic phosphate, which is an indication of ATPase activity. The degree of mitochondrial ATPase activity was

evaluated in the crude methanol extract and different fractions of P. africanum, including CRMEPA, CFPA, EAFPA, and MFPA, using 2,4-dinitrophenol (DNP) as a reference (Alagbe *et al*., 2020). The results demonstrated a concentration-dependent increase in ATPase activity for both the crude methanol extract and its fractions, as proved by the release of inorganic phosphate.

Interestingly, among the examined fractions, the ethyl acetate fraction (EFPA) demonstrated the highest increase in ATPase activity, as indicated in figure 4.10. This research reveals that particular phytochemicals contained in CRMEPA, CFPA, EFPA, and MFPA may be connected with the formation of pores, leading to the opening of mPT pores following the release of cytochrome c. Moreover, this result coincides with the established notion that mPT promotes uncoupling of oxidative phosphorylation by reducing the absorption of inorganic phosphate (Bernard and Di Lisa, 2015).

Furthermore, the in vivo assessment of mitochondrial ATPase activity confirmed the results obtained in vitro. The ethyl acetate fraction (EAFPA) significantly enhanced mitochondrial ATPase activity compared to the control group, demonstrating a dose-dependent relationship. This data reveals that when the fractions of P. africanum climbed, there was a comparable rise in mitochondrial ATPase activity.

Subsequent permeabilization of the pore leads to cytochrome c release and caspases were activated (Brentnall *et al*., 2013; Olowofolahan *et al*., 2018). The activities of caspases 9 and 3 that were evaluated and showed that EAFPA caused a dose-dependent activation in the activities of caspases 9 and 3 (initiator and executor, respectively). These results indicate that EAFPA may have a modulating effect on mitochondrial-mediated apoptosis, due to the significant increase in the activities of initiator and executor caspases compared to control, thereby supporting mitochondrial pore opening by EAFPA both *in vitro* and *in vivo*. However, it was found that there was no induction in the colon of mice in all treated groups (figure 4.34).

5.4 Potential toxicity of *P. africanum*

Piptadeniastrum africanum, a plant thoroughly established in traditional herbal medicine, has been appreciated for its outstanding medicinal properties in soothing toothaches, treating malaria, and resolving digestive problems. Scientific studies have established the efficacy of the ethyl acetate fraction derived from this plant, exhibiting its capacity to stimulate the opening of mPT pores, enhance ATPase activity, and encourage the activation of caspase 9 and 3, eventually leading to the release of cytochrome c. Nonetheless, it is necessary to research the potential adverse outcomes connected with the use of EAFPA. To properly assess its toxicity, it becomes needed to discover the compound's toxicity profile and degree, frequently conducted by in vivo study employing entire organisms or in vitro studies utilizing isolated molecules or cells (Kharchoufa *et al*., 2020; Olojo *et al*., 2022).

Some compounds can cause acute and chronic toxicity, the consequences of which may not be serious or critical depending on the nature (Chinedu *et al*., 2013). An undesirable result(s) occurring within a short period of time following a single or repeated administration of a substance within a period of 24 hours is known as acute toxicity, while chronic toxicity occurs when used for a long period of time.

The vulnerability of animal models to toxins always leads to changes and disturbances in the hematological profile (Costa *et al*., 2004; Adedapo *et al*., 2007; Gbore *et al*., 2020). Leukocytes (leukocytes) protect the body from infections, and a decrease in the level of leukocytes indicates a violation of the immune system, so a high level of leukocytes can also be the cause of these diseases (Femi-Oloye *et al*., 2020).

The toxic effects were assessed using the hematological parameters, liver function indices enzymes (AST, ALP, ALT, total protein) and oxidative parameters such as lipid peroxidation, endogenous enzymes such as SOD, CAT, GST, and also the non-enzymatic antioxidant GSH. Oxidative stress is associated with a disease state due to an imbalance linking high levels of ROS production and inadequate antioxidant defense, leading to lipid peroxidation, cell membrane damage, protein degradation, and DNA damage (Pratiwi *et al*., 2021). The activities of liver enzymes, AST, ALT and ALP as well as total protein observed in the toxicant groups (DSS, BaP, and DSS+BaP) were significantly reduced by co-administration

of stigmasterol compared with control ($p < 0.05$) as being reported in figure 4.45 (Shittu *et al*., 2020). Serum AST, ALP, ALT, and total protein were higher in the toxicant groups (DSS, BaP, and DSS+BaP) compared normal and testedanimals, confirming colitis, colonic toxicity which was in agreement with Farombi *et al.*, (2013).

Nevertheless, the fraction separated from the sample, namely stigmasterol, greatly decreased the large surge in levels of enzymes present in the circulation (Feng et al., 2018). Stigmasterol, an excellent plant sterol commonly referred to as stigmasterin, provides a range of chemical properties that may be employed to build synthetic and semi-synthetic compounds for pharmaceutical manufacturing. Research studies have demonstrated that stigmasterol exhibits potential anticancer properties due to its ability to counteract reactive oxygen species, also known as free radicals, that are generated within the body through the oxidation of stressed cells upon cellular absorption (Bradford and Awad, 2007; Machelini *et al*., 2016).

Furthermore, the decrease in lipid peroxidation levels related with the rise of reduced glutathione, as illustrated in Figure 4.46, gives as confirmation of the antioxidant activity of stigmasterol (Singh *et al*., 2011; Ashraf and Bhatti, 2021). However, the anticancer potential of stigmasterol remains uncertain. Thus, the present study intends to examine the effects of stigmasterol on apoptotic regulation and colon disorders. A notable decline in the activity levels of superoxide dismutase (SOD), catalase (CAT), glutathione S-transferase (GST), and intracellular reduced glutathione (GSH) was noted in the groups exposed to toxicants when compared to the control group, as indicated in Figure 4.46.

This decline in enzyme activity can be related to enzyme inactivation. However, when mice were co-administered with the purified stigmasterol fraction, a considerable elevation in antioxidant enzyme levels was detected, which coincides with the findings of Oyedeji *et al* (2020). Glutathione, a tripeptide containing cysteine and carrying a reactive thiol group, is known to control intracellular redox status and shield cells from the harmful effects of free radicals and peroxides formed during oxidative stress (Adedara and Farombi, 2013; Olojo *et al*., 2023). GSH works as a non-enzymatic antioxidant for gut health and causes a response by interacting with reactive oxygen species through its thiol group (Ayer, 2010). Vital preventive processes undertaken by GSH against oxidative stress include the elimination of

hydroxyl radicals, direct quenching of singlet oxygen, and the conversion of antioxidant vitamins C and E into their active forms (Masella *et al*., 2005; Flora *et al.*,., 2008).

Furthermore, this study also indicated that among the rats exposed to DSS and BaP, a large increase in lipid peroxidation occurred in the colon. The migration of neutrophils into the colon can lead to elevated reactive oxygen species formation, thus boosting lipid peroxidation, oxidative stress, and finally compromising membrane integrity. Elevated levels of reactive oxygen species and lipid peroxidation induction are intimately related with the development of ulcerative colitis.

The major line of defense against these conditions is the activity of antioxidant enzymes such as SOD and CAT, which play a crucial role in neutralizing free radicals by both preventing their production and donating electrons to offset their detrimental effects. Other defensive strategies comprise the clearance of damaged or dysfunctional pro-oxidants at the molecular and cellular levels, including molecules like reduced glutathione (GSH), bilirubin, carotenoids, and more (Ighodaro and Akinloye, 2018; Krzystek-Korpacka *et al.*,., 2020).

The colitis induction by the administration of DSS and/or BaP significantly depleted the antioxidant system of the colon in an animal model, also, the colon tissue levels of SOD, CAT, GSH was sharply reduced in relation to the control group. Treatment with stigmasterol (200 and 400 mg/kg body weight P. *africanum)* protected against a reduction in the activity of all these enzymes and maintained their normal state (Farombi *et al*., 2013).

Acute induction of DSS colitis was accompanied by significant reduction of the colonic antioxidant system in rats (Vijayabharanthi *et al*., 2018). Catalase and GST activity in colon tissue was significantly reduced in DSS-treated rats compared to the corresponding group of control animals. Treatment with kolaviron or sulfasalazine prevented the depletion in the activity of these enzymes and remained insignificant in DSS-treated rats compared to controls (Farombi *et al*., 2013). Acute induction of DSS colitis was accompanied by significant reduction of the colonic antioxidant system in rats (Akinrinde *et al*., 2021). The activity of catalase and GST in colon tissue was significantly reduced in DSS-treated rats compared to the control of the corresponding animal group.

The results did not present any significant change in the EAFPA treated groups in relation to the control group. Some biologically active components of herbs perform various beneficial biological tasks. However, their pharmacological and physiological role is related to the presence of antioxidant and free radical properties with the regulation of detoxification enzymes (Sertel *et al*., 2011).

The EAFPA demonstrated antioxidant activity through its ability to increase GSH, SOD, CAT, total protein, and inhibit lipid peroxidation in experimental animals, while liver histopathological sections showed normal architecture compared to controls and increased when treated with the purified compound to increase antioxidant levels. Therefore, *P. africanum* does not have a toxic effect on the liver of experimental animals. In general, the plant extract and its fractions are non-toxic in nature and can tolerate a dose of 400 mg/kg body weight.

5.5 Bioactivity guided assays ascertianed ethyl acetate as the most potent

Through the use of bioactivity guided testing, it was proven that ethyl acetate (EA) displayed the most remarkable potency among a vast range of active EAFPA (Ethyl Acetate Fraction of Plant Extracts). The fundamental objective of exploring the bioactive substances and acquiring suitable assays to assess their biological activities, such as antioxidant and antibacterial capacities, was effectively accomplished by utilising relevant and significant methodologies (Mulinacci et al., 2004).

The isolation of EAFPA necessitated the deployment of a solvent-based approach that sorted the compounds according on their polarity (Altemimi et al., 2017). Subsequently, varied amounts of partially purified subfractions of EAFPA from each group were studied to evaluate their effect on mitochondrial-mediated cell death, specifically by modulating mitochondrial permeability transition (mPT). Notably, it was observed that the 100% EA section had the highest induction, exceeding other groups by a factor of 8.9. This induction was related to the opening of mitochondrial membrane pores, as seen in Figure 4.20. The discovery of bioactive compounds inside EAFPA capable of causing mitochondrial pore opening agrees with earlier results published by Olanlokun *et al* (2018).

5.6 Isolation of stigmasterol from purified *P. africanum* stem bark

Thus, the most efficient partially purified subfraction of 100% *P. africanum* EA was further purified, employing thin layer chromatography (TLC) after column chromatography (CC), and the pooled silica gel separated subfractions were viewed under short UV light. 254 nm and long UV-365nm, was eluted between various solvent ratios of chloroform and methanol, and the resulting pure compound was subjected to gas chromatography, mass spectroscopy (GC-MS) and nuclear magnetic resonance (NMR).

Analysis utilising gas chromatography-mass spectrometry (GC-MS) successfully found many physiologically active compounds during the purification of EAFPA. These compounds include 1,2-benzenedicarboxylic acid, butylcyclohexyl ether (present at 91%), 2-methyl-2-ethyl-3-hydroxy-2,2,4-trimethylpentyl ether (present at 78%), and the 2-methyl-2-ethyl-3-hydroxyhexyl ester of propanoic acid (present at 72%). Notably, the molecule 1,2-benzenedicarboxylic butylcyclohexyl ester, a benzoic acid ester, displays strong pharmacological activity such as antitumor, antibacterial, antiviral, and anticancer activities (Ram et al., 2020). Another molecule, propanoic acid 2-methyl-2-ethyl-3-hydroxy-2,2,4-trimethylpentyl ether, is an example of a non-steroidal anti-inflammatory medicine (NSAID), which is used in the treatment of inflammation-related tissue damage (Priyadarshin *et al*., 2018).

After intraperitoneal distribution of 125 mg/kg body weight of BaP to groups 3, 4, 5, and 6, biochemical assays, serum analysis, apoptotic analysis, and inflammatory analysis were undertaken. Following this, the colon was dissected, and samples were taken for proper examination, including immunohistochemistry. Furthermore, nuclear magnetic resonance testing verified the existence of stigmasterol. The presence of these bioactive compounds in EAFPA helps to the control of apoptosis (Forbes-Hernández *et al*., 2014).

Previous experiments by Young-Sang *et al* (2013) shown that stigmasterol produced from the marine microalgae Naviculaincerta induces apoptosis. Continuation of these assays demonstrated that a purified fraction of EAFPA containing stigmasterol could open the mitochondrial pore, suggesting its role in apoptosis induction. Stigmasterol belongs to the phytosterol family and is characterized by a side chain containing a double bond, consisting

of three cyclohexane rings and one cyclopentane ring, which efficiently causes apoptosis. Isolated from the marine microalgae Naviculaincerta, stigmasterol has a chemical formula of C29H48O and is part of the cholesterol family. Phytosterols of this kind are known to cause apoptosis in human breast, prostate, and colon cancers (Bradford and Award, 2007; Kim *et al*., 2014).

5.7 Apoptotic effect of isolated stigmasterol

Regarding the apoptotic activity of isolated stigmasterol, earlier research have established its potential to cause cell death mediated by mitochondria. Additionally, it has been demonstrated to prevent iron-induced lipid peroxidation, enhance ATPase activity, and have non-toxic effects. However, its impact on colon toxicity has not been explored. Thus, the current study attempts to examine the impact of the pure chemical (stigmasterol) on colon damage. indicators such as oxidative stress elimination, histological abnormalities, molecular and physiological immunological markers, and liver functions were evaluated. The results revealed that stigmasterol alleviated intestinal dysfunction coming from the injection of DSS and/or BaP.

Ulcerative colitis (UC) is a condition where the assessment of medicinal plants for treatment and management becomes crucial owing to the ineffectiveness and relapse of earlier therapeutic approaches. The symbiotic relationship between the gastrointestinal microbiota and the host immune system plays a critical role in sustaining the integrity of the gastrointestinal tract and managing inflammatory responses. Therefore, there is a need for drugs that can lower immune responses and oxidative stress to properly treat ulcerative colitis. The current study proved the anti-protective and anti-inflammatory properties of the isolated material (stigmasterol) derived from Piptadeniastrum africanum stem in the context of UC. Previous investigation has also showed the therapeutic efficacy of Piptadeniastrum africanum in the traditional treatment of stomach ulcers and wound healing (Mbiantcha *et al*., 2017).

The medicinal potential of *P. africanum* is explained by the manifestation of biologically active compounds in it, for instance, flavonoids, saponins, tannins, glycosides, sterols, as well as 1,2-benzenedicarboxylic acid, butylcyclohexyl ether (91%), propanoic acid, 2-methyl-, 2-

ethyl-3-hydroxy-2,2,4-trimethylpentyl ether (78%) and propanoic acid, 2-methyl,2-ethyl-3-hydroxyhexyl ether (72)% and stigmasterol isolated from *P. africanum* , they are well known and have pharmacological therapeutic properties such as antitumor, antioxidant, antiviral and anticancer potential as being revealed by previous researchers (Priyadarshin *et al*., 2018; Ram *et al* ., 2020). sIn the present study, intracellular ROS produced, were reduced by the purified fraction, and hence, protecting cells from apoptosis by increasing Bcl-2 levels (Pratiwi *et al*., 2021).

5.8 Isolated stimaterol attenuates inflammatory biomakers

Ulcerative colitis revealed as a solid connection amid lasting colon swelling, also cancer. It is a relapsing colon disorder that has been reported worldwide (Ajayi *et al*., 2015). A study of the effects of stigmasterol purified from *P. africanum* stem bark revealed pharmacological benefits of *P. africanum* in benzo{a}pyrene/dextran sulfate sodium (B{a}P/DSS) colitis in mice (Olojo *et al*., 2022).

Oral administration of dextran sulfate sodium is known to be a factor influencing both acute and chronic colitis in mice with the spread and development of many patterns of intestinal inflammation (Okayasu *et al.*, 1993; Deeleman *et al*., 1998; Farombi *et al.*, 2013). Ulcerative colitis (UC) is an example of inflammatory bowel disease (IBD) along with Crohn's disease (CD). Ulcerative colitis can be tiring, debilitating, severe, fatal, and dangerous with symptoms like diarrhea, rectal bleeding, fatigue, weight loss, and have a lifelong illness with profound psychological and social consequences (Farombi *et al*., 2013; Basson, 2019). DSS shows advantages due to its simplicity and similarity to human IBD compared to other animal models of colitis.

In this study, colitis was confirmed in animals in groups (2 {DSS}, 4 {DSS+BaP}, 5 {DSS+BaP+200 mg/kg *P. africanum}* and 6 {DSS+BaP+400 mg/kg *P.africanum }*) fed 4% DSS for ten (10) days, as evidenced by diarrhea from the fifth (5) day, a bloody spot in the anal area, and animals showed an increase in weight from the first (1) day to the fourth (4) on the day of the start of the experiments, with a decrease in weight observed from the fifth (5) day, but subsequently it was noted that the weight remained stable following the termination of DSS before the start of B{a}P (Adedara *et al*., 2017; Cochran *et al*., 2020

reported acute colonic inflammation after exposure of a mouse model to a 7-day administration of 3% DSS in drinking water, resulting in acute colonic inflammation followed by slow colonic epithelial turnover followed by chronic inflammation after DSS cessation.

Micrographs of the colon isolated for histology showed that the epithelium and glands of the control animals were not inflamed and the mucosa appeared normal and not infiltrated, whereas the mucosal epithelium of the DSS-only groups was poorly preserved, with lamina propria showing moderate fibrosis, while a few normal villi were lightly infiltrated with inflammatory cells. In the BaP groups, only mild inflammatory cell infiltration was observed, and atypical adenocarcinoma cells were found in the glandular epithelial cells compared to the control groups, which appeared normal and were not infiltrated. Administration of the DSS+BaP combination revealed the presence of a well-differentiated epithelial cell adenocarcinoma with moderate necrosis compared to the vehicle treated groups.

However, among the groups of harmful substances co-administered with P. africanum, we discovered the infiltration of inflammatory cells into the lamina propria, along with areas of glandular hyperplasia, but no adenomas were identified. Additionally, in the mucosal epithelium of the latter group, which obtained a bigger dosage of P. africanum, we discovered poorly sustained glandular hyperplasia without adenomas. The colon displayed indications of inflammation, injury, damage, and regeneration (Ivashkiv, 2018; Akinrinde *et al*., 2021). In the groups of hazardous substances that were injected with 200 mg/kg of body weight P. africanum, we detected partial healing defined by hyperplasia without adenomas.

Examining the micrographs of colon sections stained with hematoxylin and eosin (at 400x magnification) from the groups treated with 4% DSS in this experiment, we observed moderate infiltration of inflammatory cells, including lymphocytes, polymorphic cells, and plasma cells, in the lamina propria of the groups receiving DSS. The glands also exhibited considerable infiltration of inflammatory cells, and there was damage of the mucosal epithelium. In contrast, the lamina propria of the groups treated with the DSS + BaP combination demonstrated considerable infiltration of inflammatory cells, both internally and longitudinally (Ajayi *et al*., 2016; Perše and Cerar, 2020). Comparatively, the mucosa, epithelium, and glands of the control group remained normal and undisturbed by

inflammation. It is worth emphasising that the seven-day DSS model has been commonly applied to induce colitis in various investigations due to its propensity to change gut barrier function, resulting in increased permeability. This can mimic the experiences of numerous people, making it challenging to assess medicines focused at restoring barrier integrity (Ajayi *et al*., 2018; Cochran *et al*., 2020).

Benzo[a]pyrene (BaP) is a contaminant present in the environment and food, originating from both natural and man-made industrial activities, such as cigarette smoking, home waste incineration, and automotive emissions. It may also be formed by activities like grilling and roasting, where BaP is normally synthesised as a powder but may also be made as vapor at high temperatures (Ajayi *et al*., 2015). BaP has been proved to be non-carcinogenic but mutagenic when administered orally. However, in the setting of DSS-induced inflammation, BaP can contribute to tumor formation (Hakura *et al*., 2011).

The clinical manifestations of ulcerative colitis range from weight loss, diarrhea, bleeding, etc., and all of them were found in the present study that stigmasterol isolated from *P. africanum stem bark* significantly improved the prevalence of clinical manifestations that were noted in the model with sodium dextran sulfate in inflammatory bowel disease and preventive role of stigmasterol against the disorder-induced colonic dysfunction in Swiss mice was demonstrated in this study according to a report of Ke *et al.*, 2012. Micrograph of colon section by immunoassay (X400) showed abundant expression of interleukin 6 in DSS-only groups (160%) compared to control (15%), which was significantly altered by *P. africanum* (Hu *et al.*, 2018; Akinrinde *et al*., 2021).

However, the exact pathogenesis of IBD is ambiguous, studies also show that the secretion of inflammable chemokine leads not only to tissue damage, but also causes the activation of the inmate adaptive immune system, which can lead to increased exposure of minimal antigens to the colonic wall, causes the activation of both the innate and adaptive immune systems by stronger induction, which maintain an inflammatory state leading to chronic inflammation (Friedrich *et al.,* 2020). Ulcerative colitis showed elevated levels of pro-inflammatory cytokines (TNF-α and IL-6) compared to controls, and it can be seen that these cytokines were significantly reduced by stigmasterol treatment in colon tissues (Olojo *et al*., 2023).

Stigmasterol alleviates DSS+BaP colitis by modulating oxidative stress and inflammatory cytokines while maintaining the intestinal barrier Kiernan *et al.*, (2020) reported that pro-inflammatory cytokines (TNF-α and IL-6) could be a potential pharmacological agent.

CHAPTER SIX

Summary, Conclusion and Recommendations

6.1 Summary

This research authenticated that traditional plants are potential pharmaceutical agents when it comes to disease management. The study confirmed that *Piptadeniastrum africanum* (extract, fractions and subfractions) possesses some bioactive compounds that could make the plant a therapeutic agent in the control of diseases such as modulation of mitochondria mediated-cell death, increase in ATPase activity, inhibitory effect on lipid peroxidation the release of cytochrome c, DNA fragmentation, increase in caspases 9 and 3 activities in both in the test tube and in the living organism. Bioactivity guided assay through GC-MS and Nuclear Magnetic Resonance (NMR) revealed that Stigmasterol isolated from PA via modulation of mitochondria mediated-cell death attenuated the toxic effect of DSS/B(a)Pyrene on haematological profile.

It was observed that PA mitigated DSS/BaP- mediated increase in activity index restoration of body weight and reduction in diarrhea. The results also showed that PA attenuated DSS/BaP-induced toxicity by boosting antioxidant status while suppressing oxidative stress and pro-inflammatory biomarkers. Moreover, PA ameliorated DSS/BaP-induced histopatological lesions and destruction of colonic histological architecture in mice. However, stigmasterol has no inductive effect on the apoptotic biomakers. The ability of PA to maintain structurally and functionally colon in disease state demonstrated its chemopreventive potentials in the colon of the mice.

6.2 Conclusion

Purified fraction isolated from *Piptadeniasrtum africanum* modulated mitochondrial-mediated cell death by reducing chemokines levels in pro-apoptotic proteins (Bax, Bcl-2, etc.). The plant sterol (stigmasterol) contains favourable, promising and promising biologically active components that can be used in the prevention of liver and colon diseases. It also plays a protective role against oxidative stress-induced apoptosis. *P. africanum* extract and fractions modulate mPT pore opening in mouse liver. Various doses of *P. africanum* extract and fractions used in this study are non-toxic and induce mitochondria-mediated apoptosis in the liver.

However, cell death in the colon is not via mitochondria. The presence of colitis was observed in the DSS treated groups in terms of weight loss, blood smears and histological findings that improved with different doses of PA (BaP/DSS+200mg/kg and BaP DSS+400mg/kg), confirming therapeutic efficacy. *Piptadeniastrum africanum* expression of death-associated molecular patterns of pro-inflammatory cytokines (IL-6 and TNFα) due to loss of membrane integrity in mouse epithelial tissue that elicited inflammatory signals was reduced in mice treated with PA as reported in this present study, and this is consistent with studies in experimental animals and humans with ulcerative colitis (Papadakis and Targan, 2000, Hakura *et al.*, 2011, Farombi *et al.*, 2013). Stigmasterol could be a new regime for ulcerative colitis.

6.3 Recommendations

Based on the findings of the study, the following recommendations were made

1. Clinical application of stigmasterol could be an agent for dietary therapy for the treatment of ulcerative colitis
2. Stigmasterol should be compared with modern drugs on models to establish its remarkable potentials
3. Additional researches should be carried out for better understanding of the underlying techniques by which stigmasterol exerts its ameliorative effects.
4. It is reasonable that further pharmacological studies be conducted to assess the untapped potential of this bioactive agent.
5. However, this report can serve as a reference tool for other workers working with stigmasterol.

6.4 Contributions to knowledge

1. Modulatory effect of extract and fractions of *P. africanum* on mPT pore is demonstrated for the first time.
2. Mitigation of colon damage by ethyl acetate fraction of P. africanum stem bark is proven.
3. The following compounds are proven to be present in the first-time using GC-MS
   a. 1,2-Benzenedicarboxylic, butylcyclohexyl ester,
   b. Propanoic acid, 2-methyl-, 2-ethyl-3-hroxyl-2,2,4-trimethylpentyl ester,
   c. Propanoic acid, 2-methyl-, 2-ethyl-3-hroxylhexyl ester and
4 Nuclear Magnetic Resonance (NMR) result showed the presence of Stigmasterol, which mitigated pro-inflammatory cytokines (TNFα and IL-6).
5. Bioactivity-guided assay on the extract and fractions of PA showed that ethyl acetate exhibited the most potent causing the induction of mPTpore opening resulting in the release of cytochrome c, enhancement of mitochondrial ATPase activity and inhibition of mLPO in cells.
6. Stigmasterol remarkable antioxidant potentials are related to amelioration of ulcerative colitis resulted from DSS/BaP toxicants

REFERENCES

Abegunde, A. T., Muhammad, B. H., Bhatti, O. and Ali, T. (2016). Environmental risk factors for inflammatory bowel diseases: Evidence based literature review. *World journal of gastroenterology*, 22:6296–6317.

Abubakar, A. R. and Haque, M. (2020). Preparation of Medicinal Plants: Basic Extraction and Fractionation Procedures for Experimental Purposes. *Journal of Pharmacy and Bioallied Sciences*, 12:1-10.

Achem, J., Oyebode,O. T., Akinwole, M., Bolarin, O., Malgwi, J. M. and Olorunsogo, O. O.(2020). Solvent Fractions of Daniellia oliveri((Rolfe) Stem Bark Modulate Rat Liver Mitochondrial Permeability Transition Pore. *Archives of Basic and Applied MedicineI* 8:27-34.

Achille, L. S., Zhang, K., Eloge, K. M., Kouassi, C. J. A. and Michel, M. M. (2021). Influence of Spatial Distribution on the Regeneration of Piptadeniastrum africanum and Ocotea usambaernsis in Kalikuku, Lubero, North Kivu, Democratic Republic of Congo. *Open Journal of Ecology*, 11: 527-539.

Achir, B. and Atanasio P. (2018). Colorectal cancer and medicinal plants: Principle findings from recent studies. *Biomedicine & Pharmacotherapy*, 107:408-423.

Adedapo, A., Abatan, M. and Olorunsogo, O. (2007). Effects of some plants of the spurge family on haematological and biochemical parameters in rats. *Veterinarski Arhiv*. 77:29-38.

Adedara, I. A., Ajayi, B. O., Awogbindin, I. O. and Farombi, E. O. (2017). Interactive effects of ethanol on ulcerative colitis and its associated testicular dysfunction in pubertal BALB/c mice. *Alcohol*. 64: 65-75.

Adegbite, O. S., Akinsanya, Y. I., Kukoyi, A. J., Iyanda-Joel, W. O., Daniel, O. O. and Adebayo, A. H. (2015). Induction of rat hepatic mitochondrial membrane permeability transition pore opening by leaf extract of Olax subscorpioidea. *Pharmacognosy research*, 7: S63–S68.

Agarwal, A., Majzoub, A., Esteves, S., Ko, E., Ramasamy, R. and Zini, A. (2016). Clinical utility of sperm DNA fragmentation testing: practice recommendations based on clinical scenarios. *Translational Andrology And Urology*, 5:935-950.

Aguwa, C. N. and Lawal, A. M. (1988). Pharmacologic studies on the active principles of Calliandra portoticensis leaf extracts. *Journal of ethnopharmacology*, 22:63–71.

Ajayi, B. O, Adedara, I. A. and Farombi, E. O. (2016). Benzo(a)pyrene induces oxidative stress, pro-inflammatory cytokines, expression of nuclear factor-kappa B and deregulation of wnt/beta-catenin signaling in colons of BALB/c mice. *Food and Chemical Toxicology*. 95: 42-51

Ajayi, B. O., Adedara, I. A., Ajani, O. S., Oyeyemi, M. O. and Farombi, E. O. (2018) Gingerol modulates spermatotoxicity associated with ulcerative colitis and benzo[a]pyrene exposure in BALB/c mice" *Journal of Basic and Clinical Physiology and Pharmacology*, 29:247-256.

Ajayi, B. O., Adedara, I. A., and Farombi, E. O. (2015). Pharmacological activity of 6-gingerol in dextran sulphate sodium-induced ulcerative colitis in BALB/c mice. Phytotherapy research, 29:566-572.

Akinlami, O. O., Babajide, J. O., Demehin, A. I. and Famobuwa, O. E. (2012). Phytochemical screening and in–vitro antimicrobial effect of methanol bark extract of Piptadeniastrum africanum. *Journal of Science and Science Education*, Ondo. 3:93–96.

Akinrinde, A. S., Adekanmbi, A. O. and Olojo, F. O. (2022). Nigella sativa oil protects against cadmium-induced intestinal toxicity via promotion of anti-inflammatory mechanisms, mucin expression and microbiota integrity. *Avicenna journal of phytomedicine*, 12: 241–256.

Alagbe, J, O., Sharma, R., Ojo, E. A., Shittu, M. D. and Bello, K. A. (2020). Chemical evaluation of the proximate, minerals, vitamins and phytochemical analysis of Danielle oliveri stem bark. *International Journal of Biological, Physical and Chemical Studies (JBPCS)* 2:16-22

Alatise, I. O., Arigbabu, O. A., Lawal, O. L., Adesunkanmi, A. K., Agbakwuru, A. E., Ndububa, D. A. and Akinola, D. O (2009). Endoscopic hemorrhoidal sclerotherapy using 50% dextrose water: a preliminary report. *Indian Journal of Gastroenterology* 28:31-32

Alatise, O. I., Arigbabu, A. O., Agbakwuru, E. A., Lawal, O., O., Ndububa, D. A. and Ojo O. S. (2012). Spectrum of colonoscopy findings in Ile-Ife Nigeria. Niger Postgrad *Med J*. 19:219-224.

Alatise, O. I., Ayandipo, O. O. and Adeyeye, A. A. (2018). Symptom-based model to predict colorectal cancer in low-resource countries: results from a prospective study of patients at high risk for colorectal cancer. *Cancer*. 124:2766–73.

Albert von Kölliker, (1968). Würzburger histologist. *JAMA*. 206: 2111–2112. 1968.

Alexander, R. B.; Smith, R. A. and Schwarz, G. E. (2000). Effect of stream channel size on the delivery of nitrogento the Gulf of Mexico. *Nature* 403: 758– 761.

Altekruse, S. F., McGlynn, K. A.and Reichman, M. E. (2009). Hepatocellular carcinoma incidence, mortality, and survival trends in the United States from 1975 to 2005. *J Clin Oncol. 27*:1485–1491.

Algieri, V., Algieri, C., Costanzo, P., Fiorani, G., Jiritano, A., Olivito, F., Tallarida, M. A., Trombetti, F., Maiuolo, L., De Nino, A., and Nesci, S. (2023). Novel Regioselective Synthesis of 1,3,4,5-Tetrasubstituted Pyrazoles and Biochemical Valuation on F_1F_O-ATPase and Mitochondrial Permeability Transition Pore Formation. *Pharmaceutics*, 15: 498.

Anifowose, O. A., Olojo, F. O. and Bamigboye, A. Y. (2020) Phytochemical Aessentialnd Antimicrobial Potentials of the Methanolic Extracts of Rhizomes of Turmeric And Ginger. The Polytechnic, *Science and Engineer Perspectives* 15: 82-88.

Anwar, F., Latif, S., Ashraf, M., and Gilani, A. H. (2007). Moringa oleifera: A food plant with multiple medicinal uses. Phytotherapy Research: *An International Journal Devoted to Pharmacological and Toxicological Evaluation of Natural Product Derivatives*, 25:17–25.

Appiah, C. O., Singh, M., May, L., Bakshi, I., Vaidyanathan, A., Dent, P., Ginder, G., Grant, S., Bear, H. and Landry, J. (2023). The epigenetic regulation of cancer cell recovery from therapy exposure and its implications as a novel therapeutic strategy for preventing disease recurrence, Epigenetic Regulation of Cancer in Response to Chemotherapy, 337-385

Arome, D., and Chinedu, E. (2013). The importance of toxicity testing. *J. Pharm. BioSci*, 4, 146-148.

Arruebo, M., Vilaboa, N., Sáez-Gutierrez, B., Lambea, J., Tres, A., Valladares, M. and González-Fernández, Á. (2011). Assessment of the evolution of cancer treatment therapies. *Cancers*. 3:3279-3330.

Ashkenazi, A. and Dixit, V.M. (1998) Death Receptors Signaling and modulation. *Science*, 281: 1305-1308.

Assob, J. C., Kamga, H. L., Nsagha, D. S., Njunda, A. L., Nde, P. F., Asongalem, E. A., Njouendou, A. J., Sandjon, B., & Penlap, V. B. (2011). Antimicrobial and toxicological activities of five medicinal plant species from Cameroon traditional medicine. *BMC complementary and alternative medicine*, 11:70.

Ayala, A., Muñoz, M. F., & Argüelles, S. (2014). Lipid peroxidation: production, metabolism, and signaling mechanisms of malondialdehyde and 4-hydroxy-2-nonenal. *Oxidative medicine and cellular longevity*, 2014.

Bagyalakshmi, B., Nivedhitha, P., and Balamurugan, A. (2019). Studies on phytochemical analysis, antioxidant and antibacterial activity of Ficus racemosa L. leaf and fruit extracts against wound pathogens. *Vegetos*, 32:58-63.

Baines C. P., Kaiser R. A., Purcell N. H., Blair N. S., Osinska H., Hambleton M. A., et al. (2005). Loss of cyclophilin D reveals a critical role for mitochondrial permeability transition in cell death. *Nature* 434:658–662

Benda, C. (1898) "Ueber die Spermatogenese der Vertebraten und höherer Evertebraten, II. Theil: Die Histiogenese der Spermien" (On spermatogenesis of vertebrates and higher invertebrates, Part II: The histogenesis of sperm), *Archiv für Anatomie und Physiologie*, 73 : 393-398

Barry, M., Bleackley R. C. (2002). Cytotoxic T lymphocytes: all roads lead to death. Nature Reviews *Immunology* 2: 401-409.

Barsukova, A. G., Bourdette, D. and Forte, M. (2011). Mitochondrial calcium and its regulation in neurodegeneration induced by oxidative stress. *The European journal of neuroscience*, 34: 437–447.

Bernardi P., Penzo D. and Wojtczak L. (2002). Mitochondrial energy dissipation by fatty acids. Mechanisms and implications for cell death. *Vitam. Horm.* 65: 97–126

Bernardi P., Krauskopf A., Basso E., Petronilli V., Blachly-Dyson E., Di Lisa F., et al. (2006). The mitochondrial permeability transition from in vitro artifact to disease target. *FEBS J.* 273: 2077–2099

Bernardi, P. (2013) The Mitochondrial Permeability Transition Pore: A Mystery Solved? *Frontiers in Physiology*, 4:95.

Bernardi, P., and Di Lisa, F. (2015). The mitochondrial permeability transition pore : Molecular nature and role as a target in cardioprotection. *Journal of Molecular and Cellular Cardiology*, 78: 100–106

Bergmann, R. L., Richter, R., Bergmann, K. E. and Dudenhausen, J. W. (2010). Prevalence and risk factors forearlypostpartum anemia. *Eur J Obstet. Gynecol. Reprod. Biol.* 150: 126-31.

Beutner, G., Rück, A., Riede, B., Welte, W. and Brdiczka, D., (1996). Complexes between kinases, mitochondrial porin and adenylate translocator in rat brain resemble the permeability transition pore. 396:189-195.

Bian, Y., Li, L., Dong, M., Liu, X., Kaneko, T., Cheng, K., Liu, H, Voss, C., Cao, X., Wang, Y., Litchfield, D., Ye, M., Li, S.S.and Zou, H. (2016). Ultra-deep tyrosine phosphor proteomics enabled by a phosphor tyrosine superbinder. *Nat Chem Biol*. 12:959-966.

Blander, J. M. (2016) "Death in the intestinal epithelium-basic biology and implications for inflammatory bowel disease. *The FEBS journal.* 283:2720-30.

Blatt N. B., Bednarski J. J., Warner R. E., Leonetti F., Johnson K. M., Boitano A., et al. (2002). Benzodiazepine-induced superoxide signals B cell apoptosis: mechanistic insight and potential therapeutic utility. *J. Clin. Invest.* 110: 1123–1132

Boehm, M., Speck, U., Scheller, B., Abramjuk, C., Breitwieser, C., Dobberstein, J. and Hamm, B. (2006). Neointima in hibition: comparison effectiveness of non-stent-based local drug delivery and a drug-eluting stent in porcine coronary arteries. *Radiology*.240: 411-8.

Bortner, C. D., Oldenburg, N. B. and Cidlowski, J. A. (1995). The role of DNA fragmentation in apoptosis. Trends *Cell Biol.* 5:21-6.

Bourgonje, A. R., Feelisch, M., Faber, K. N., Pasch, A., Dijkstra, G.and Harry van Goor, H. (2020) Oxidative Stress and Redox-Modulating Therapeutics in Inflammatory Bowel Disease, *Trends in Molecular Medicine*, 26:1034-1046.

Bratton, D. L., Fadok, V. A., Richter, D. A., Kailey, J. M., Guthrie, L. A and Henson, P. M. (1997). Appearance of phosphatidylserine on apoptotic cells requires calcium-mediated nonspecific flip-flop and is enhanced by loss of the aminophospholipid translocase. *Journal. Biological. Chemistry*. 272:26159-26165.

Brentnall, M., Rodriguez-Menocal, L., De Guevara, R. L., Cepero, E., & Boise, L. H. (2013). Caspase-9, caspase-3 and caspase-7 have distinct roles during intrinsic apoptosis. *BMC cell biology*, *14*, 1-9.

Britannica, T. Editors of Encyclopaedia (2023). *liver*. *Encyclopedia Britannica*

Brunetti, L., Orlando, G., Ferrante, C., Chiavaroli, A., Vacca, M. and Peptide, Y. Y., (2005) inhibits dopamine and norepinephrine release in the hypothalamus. *Eur. J. Pharmacol*. 519:48–51.

Brunetti, L., Di Nisio, C., Recinella, L., Orlando, G., Ferrante, C., Chiavaroli, A., Leone, S., Di Michele, P., Shohreh, R. and Vacca, M. (2010) Obestatin inhibits dopamine release in rat hypothalamus. *Eur. J. Pharmacol.* 641:142–147.

Brunner, H. G., Nelson, M.R., VanZandvoort, P., Abeling,N. G., VanGennip, A. H., Olters, E. C., Kuiper, M. A., H. H. Ropers, H. H. and VanOost, B. A. (1993). x-linked borderline mental retardation with prominent behavioral disturbance: phenotype, genetic localization, and evidence for disturbed monoamine metabolism Am. *J.Hum*. *Genet.* 52:1032-1039

Brusotti, G., Tosi, S., Tava, A., Picco A.M., Grisoli P., Cesari I.and Caccialanza G. (2013). Antimicrobial and phytochemical properties of stem bark extracts from *Piptadeniastrum africanum* (Hook f.) *Brenan. Ind. Crops Prod.* 43:612–616.

Bucheler K., Adams V.,and Brdiczka D. (1991). Localization of the ATP/ADP translocator in the inner membrane and regulation of contact sites between mitochondrial envelope membranes by ADP. A study on freeze-fractured isolated liver mitochondria. *Biochim. Biophys. Acta* 1056:233–242

Bukowska, B., Mokra, K., and Michałowicz, J. (2022). Benzo[*a*]pyrene-Environmental Occurrence, Human Exposure, and Mechanisms of Toxicity. *International journal of molecular sciences*, *23*:63-48.

Burkill, H. M., (1985). Entry for CenchrusbiflorusRoxb. [family POACEAE]. In: The useful plants of West tropical Africa, Royal Botanic Gardens, Kew, UK 2.

Burkill, H.M. (1995) The Useful Plants of West Tropical African. Vol. 3, Families J-L., Royal Botanic Gardens, *Kew*, UK 3.

Burkill, H.M. (2014). The Useful Plants of West. *Journal of Environmental* Protection, 5: 12.

Brunetti, L., Leone, S., Orlando, G., Ferrante, C., Recinella, L., Chiavaroli, A., Di Nisio, C., Shohreh, R., Manippa, F. and Ricciuti, A.(2014). Hypotensive effects of omentin-1 related to increased adiponectin and decreased interleukin-6 in intra- thoracic pericardial adipose tissue. *Pharmacol. Rep.* 66: 991–995.

Brusotti G., Tosi S., Tava A., Picco A.M., Grisoli P., Cesari I. and Caccialanza G.(2013) Antimicrobial and phytochemical properties of stem bark extracts from Piptadeniastrum africanum (Hook f.) Brenan. *Ind. Crops Prod.;* 43:612–616.

Camano, S., Lazaro, A., Moreno-Gordaliza, E., Torres, A.M., de Lucas, C., Humanes, B., Lazaro, J.A., Gomez-Gomez, M.M., Bosca, L. and Tejedor, A. (2010). Cilastatin attenuates cisplatin-induced proximal tubular cell damage. *J. Pharmacol. Exp. Ther.*, 334:419–429.

Chassaing, B., Aitken, J. D., Malleshappa, M. and Vijay-Kumar, M. (2014). Dextran sulfate sodium (DSS)-induced colitis in mice. *Current protocols in immunology* 104: 15.25. 1-15.25. 14.

Chen, L., Deng, H., Cui, H., Fang, J., Zuo, Z., Deng J, Li, Y., Wang X. and Zhao L. (2018). Inflammatory responses and inflammation-associated diseases in organs. *Oncotarget*. 9:7204.

Chen, K. W., Demarco, B., Heilig, R., Shkarina, K., Boettcher, A., Farady, C. J., Pelczar, P., Broz, P. (2019). Extrinsic and intrinsic apoptosis activate pannexin-1 to drive NLRP3 inflammasome assembly. *EMBO J* 38:10.

Chen, L., Zeng, Y. and Zhou, S.-F. (2018). Role of Apoptosis in Cancer Resistance to Chemotherapy. *Interchopen.* Chapter 7. 80056

Chiara, F., Castellaro, D., Marin, O., Petronilli, V., Brusilow, W. S., Juhaszova, M., Sollott, S. J., Forte, M., Bernardi, P., & Rasola, A. (2008). Hexokinase II detachment from mitochondria triggers apoptosis through the permeability transition pore independent of voltage-dependent anion channels. *PloS one*, *3*: e1852.

Chiavaroli, A., Recinella, L., Ferrante, C., Locatelli, M., Macchione, N., Zengin, G., Leporini, L., Leone, S., Martinotti, S. and Brunetti, L. (2017) Crocus sativus, Serenoa repens and Pinus massoniana extracts modulate inflammatory response in isolated rat prostate challenged with LPS. *J. Boil. Regul. Homeost. Agents*. 31:531–541

Chinedu, E., Arome, D. and Ameh, F. S. (2013). A new method for determining acute toxicity in animal models. *Toxicol Int.* 20:224-226.

Chinsembu K.C Tuberculosis and nature's pharmacy of putative anti-tuberculosis agents. *Acta Trop* 153:46–56.

Chinnaiyan, A. M., Rourke, O., Tewari, K., Dixit, M. and FADD, V. D. (1995). A novel death domain-containing protein, interacts with the death domain of Fas and initiates apoptosis. *Cell.* 81:505-512

Chipuk, J., Bouchier-Hayes, L. & Green, D. Mitochondrial outer membrane permeabilization during apoptosis: the innocent bystander scenario. *Cell Death Differ* 13:1396–1402 (2006).

Chowdhury, A. A., Gawali, N. B., Bulani, V. D., Kothavade, P., Mestry, S. N., Deshpande, P. S. and Juvekar, A. R. (2018). In vitro antiglycating effect and in vivo neuroprotective activity of Trigonelline in d -galactose induced cognitive impairment. *Pharmacol. Rep.* 70:372–377.

Clipstone N. A. and Crabtree G. R. (1992). Identification of calcineurin as a key signalling enzyme in T-lymphocyte activation. *Nature* 357, 695–697

Cochran, K. E., Lamson, N. G., and Whitehead, K. A. (2020). Expanding the utility of the dextran sulfate sodium (DSS) mouse model to induce a clinically relevant loss of intestinal barrier function. *Peer Journal, 8*: e8681.

Cooper, H., Murthy, S. N. and Shah, R. S. (1993). Clinicopathologic study of dextran sulfate sodium experimental murine colitis. *Lab Invest.* 69:238–49.

Cooper, A. J. L and Hanigan, M. H. (2010). Enzymes Involved in Processing Glutathione Conjugates. *Comprehensive Toxicology*. 323–366.

Crompton M., Ellinger H., Costi A. (1988). Inhibition by cyclosporin A of a Ca^{2+}-dependent pore in heart mitochondria activated by inorganic phosphate and oxidative stress. *Biochem. J.* 255: 357–360

Cory, S. and Adams, J. M. (2002). The BCL2 family: regulators of the cellular life-or-deathswitch. *Nat Rev Cancer.* 2:647-656

Costa, A., Luoni, L., Marrano, C. A., Hashimoto, K., Köster, P., Giacometti, S., De Michelis, M. I., Kudla, J. and Bonza, M. C. (2017). Ca^{2+}-dependent phosphoregulation of the plasma membrane Ca^{2+}-ATPase ACA8 modulates stimulus-induced calcium signatures. *J Exp Bot.* 68:3215-3230.

Csukly K., Ascah A., Matas J., Gardiner P. F., Fontaine E. and Burelle Y. (2006). Muscle denervation promotes opening of the permeability transition pore and increases the expression of cyclophilin D. *J. Physiol*. 574: 319–327

Dall'Acqua S. and Aktumsek A. (2015) Investigation of Antioxidant Potentials of Solvent Extracts From Different Anatomical Parts of Asphodeline Anatolica

E. Tuzlaci: An Endemic Plant to Turkey. *Afr. J. Tradit. Complement. Altern. Med.* 11:481–488.

Damiano, D. L. (2006). Activity, Activity, Activity: Rethinking Our Physical Therapy Approach to Cerebral Palsy, *Physical Therapy*, 86: 1534–1540.

Dang, N.H., Van Thanh, N., Van Kiem, P., Huong, L. M., Van Minh, C. and Kim, Y. H. (2007). Two New Triterpene Glycosides from the Vietnamese Sea Cucumber*Holothuria scabra* . *Arch Pharm Res* 30, 1387–1391.

Dang, M., Henderson, R. E., Garraway, L. A.and Zon, L. I. (2016). Long-term drug administration in the adult zebrafish using oral gavage for Cancer preclinical studies. *DiseaseModels and Mechanisms.* 9:811–820.

David, S. and Hamilton, J. P. (2010). Drug-induced Liver Injury. *US gastroenterology & hepatology review*, *6*:73–80.

David, O. M., Olanlokun, J. O. and Owoniyi, B. E. ((2021). Studies on the mitochondrial, immunological and inflammatory effects of solvent fractions of Diospyros mespiliformis Hochst in Plasmodium berghei-infected mice. *Sci Rep* 11:6941 .

Davidson A. M. and Halestrap A. P. (1990). Partial inhibition by cyclosporin A of the swelling of liver mitochondria *in vivo* and *in vitro* induced by sub-micromolar [Ca^{2+}], but not by butyrate. Evidence for two distinct swelling mechanisms. *Biochem. J*. 268, 147–152

Dawé, A., Mbiantcha, M., Fongang, Y., Nana, W. Y., Yakai, F., Ateufack, G., Shaiq M. A., Lubna, I., Lateef, M. and Ngadjui, B. T. (2017). *Piptadenin*, a Novel 3,4-Secooleanane Triterpene and *Piptadenamide*, a New Ceramide from the Stem Bark of *Piptadeniastrum africanum*(Hook.f.). *Brenan. Chem. Biodivers*. 2:14

Delshad, M., Safaroghli-Azar, A., Pourbagheri-Sigaroodi, A., Poopak, B., Shokouhi, S., & Bashash, D. (2021). Platelets in the perspective of COVID-19; pathophysiology of thrombocytopenia and its implication as prognostic and therapeutic opportunity. *International immunopharmacology*, 99: 107-995.

De Marchi U., Basso E., Szabó I. and Zoratti M. (2006). Electrophysiological characterization of the Cyclophilin D-deleted mitochondrial permeability transition pore. *Mol. Membr. Biol*. 23: 521–530.

De Visser, K. E., Alexandra, E. and Lisa, M. C. (2006). Paradoxical roles of the immune system during cancer development. *Nat Rev Cancer;* 6:24-37

Devun, F., Walter, L., Belliere, J., Cottet-Rousselle, C., Leverve, X., and Fontaine, E. (2010). Ubiquinone analogs: a mitochondrial permeability transition pore-dependent pathway to selective cell death. *PloS one*, *5*:7 e11792.

Diamini, Z. C, Langa, R. L. S., Aiyegoro, O. A. and Okoh, A. L. (2017). Effects of probiotics on growthperformance, blood parameters, and antibody stimulation in piglets. South African. *J. Amin. Sci*. 47:6

Diamini, L. M., Tata, C. M., Djuidje, M. C. F., Ikhile, M. I., Nikolova, G. D., Karamalakova, Y. D., Gadjeva, V. G., Zheleva, A. M., Njobeh, P. B. and Ndinteh, D. T. (2019). Antioxidant and prooxidant effects of *Piptadeniastrum africanum* as the possible rationale behind its broad scale application in African ethnomedicine. *J Ethnopharmacol*. 231:429-437.

Diffoum J.B. (2012). Propriétés analgésiques et anti-inflammatoires de l'extrait aqueux des écorces de Piptadeniastrum africanum (Mimosaceae) chez le rat. *LAPHYPHA, UDs: Thèse de MASTER;* 94.

Ding, H., Sagar, V., Agudelo, M., Pilakka-Kanthikeel, S., Atluri, V. S. R., Raymond, A., ... & Nair, M. P. (2014). Enhanced blood–brain barrier transmigration using a novel transferrin embedded fluorescent magneto-liposome nanoformulation. *Nanotechnology*, *25*:055-101.

Dong, H., Wang, X., Huang, J., and Xing, J. (2016). Effects of post-harvest stigmasterol treatment on quality-related parameters and antioxidant enzymes of green asparagus (Asparagus officinalis L.). *Food additives & contaminants. Part A, Chemistry, analysis, control, exposure & risk assessment*, *33*:1785–1792.

Einem, L. T., Poirier, M. C. and Divi, R. L. (2011). The resveratrol analogue, 2,3',4,5'-tetramethoxystilbene, does not inhibit cyp gene expression, enzyme activity and benzo [a] pyrene-DNA adduct formation in MCF-7 cells exposed to benzo[a]pyrene. *Mutagenesis* 26: 629-635.

Elrod, W. J., Wong, R., Mishra, S., Vagnozzi, R. J., Sakthievel, B., Goonasekera, S. A., Karch, J., Gabel, S. Thomas, F., Brown, H. J., Murphy, E. and Molkentin, J. D (2010). Cyclophilin D controls mitochondrial pore-dependent Ca^{2+} exchange, metabolic flexibility, and propensity for heart failure in mice. *The American Society for Clinical Investigation*.120:3680-3687

El-Serag, H. B., Davila, J. A., Petersen, N. J., and McGlynn, K. A. (2003). The continuing increase in the incidence of hepatocellular carcinoma in the United States: an update. *Annals of internal medicine*, 139: 817–823.

El-Serag, B., Hashem, J. A., Marrero, L. R. and K Rajender Reddy (2008). Diagnosis and treatment of hepatocellular carcinoma. Gastroenterology 134:1752-1763.

Enari, M., Sakahira, H., Yokoyama, H., Okawa, K., Iwamatsu, A., Nagata, S. (1998). A caspase-activated DNase that degrades DNA during apoptosis, and its inhibitor ICAD. *Nature*. 391:43-50.

Engvall, E. and Perlmann, P. (1972). Enzyme-Linked Immunosorbent Assay, ELISA III. Quantitation of Specific Antibodies by Enzyme-Labeled Anti-Immunoglobulin in Antigen-Coated Tubes. *The Journal of Immunology*. 109:129- 135.

Fadok, V.F, Bratton, D.L Peter M. and Henson, P.M. (2001) Phagocyte receptors for apoptotic cells: recognition, uptake, and consequences. *The Journal of Clinical Investigation*10:108

Fan, Z., Beresford, P. J., Oh, D. Y., Zhang, D., and Lieberman, J. (2003). Tumor suppressor NM23-H1 is a granzyme A-activated DNase during CTL-mediated apoptosis, and the nucleosome assembly protein SET is its inhibitor. *Cell*, 112:659–672.

Fariss, M. W., and Zhang, J. G. (2003). Vitamin E therapy in Parkinson's disease. *Toxicology*, 189: 129–146.

Farombi E. O. and Owoeye O. (2011) Antioxidative and chemopreventive properties of Vernonia amygdalina and Garcinia biflavonoid. *Int J Environ Res Public Health*. 8:2533-55.

Farombi E. O., Adedara I. A., Ajayi B. O., Ayepola O. R. and Egbeme E. E. (2013). Kolaviron, a natural antioxidant and anti-inflammatory phytochemical prevents dextran sulphate sodium-induced colitis in rats. *Basic Clin Pharmacol Toxicol*. 113:49-55.

Farombi, E. O., Adedara, I. A., Ajayi, B. O., Ayepola, O. R. and Egbeme, E. E. (2013). Kolaviron, a Natural Antioxidant and Anti-Inflammatory Phytochemical Prevents Dextran Sulphate Sodium-Induced Colitis in Rats. *Basic Clin PharmacolToxicol*. 113:49-55.

Favaloro, B., Nerino, A., Vincenzo, G., Carmine, D., and Vincenzo, D. (2012). Role of apoptosis in disease. *Aging (Albany NY)*; 4:330-49.

Favazza L. A., Parseghian, C. M., Kaya, C., Nikiforova, M. N., Roy, S., Wald, A. I., Landau, M. S., Proksell, S. S., Dueker, J. M., Johnston, E. R., Brand, R. E., Bahary, N., Gorantla, V. C., Rhee, J, C., Pingpank, J. F., Choudry, H. A., Lee, K., Paniccia, A., Ongchin, M. C., Zureikat, A. H., Bartlett, D. L. and Singhi, A. D. (2020) KRAS

amplification in metastatic colon cancer is associated with a history of inflammatory bowel disease and may confer resistance to anti-EGFR therapy. *Mod Pathol*.33:1832-1843.

Feldman, E. L., Callaghan, B. C., Pop-Busui, R., Zochodne, D. W., Wright, D. E., Bennett, D. L., Bril, V., Russelli, F. W. and Viswanathan, V.(2019). Diabetic neuropathy. *Nat Rev Dis Primers* **5**: 41

Feng, S., Dai, Z., Liu, A., Wang, H., Chen, J., Luo, Z. and Yang, C. S. (2017). β-Sitosterol and stigmasterol ameliorate dextran sulfate sodium-induced colitis in mice fed a high fat Western-style diet. *Food Funct.* 8:4179-4186

Feng, S., Dai, Z., Liu, A. B., Huang, J., Narsipur, N., Guo, G., Kong, B., Reuhl, K., Lu, W., Luo, Z. and Yang, C. S. (2018). Intake of stigmasterol and β-sitosterol alters lipid metabolism and alleviates NAFLD in mice fed a high-fat western-style diet. *Biochim Biophys Acta Mol Cell Biol Lipids.*1863:1274-1284.

Ferrer, A., Altabella, T., Arró, M. and Boronat, A. (2017). Emerging roles for conjugated sterols in plants, *Progress in Lipid Research*, 67:27-37,

Field, M., McCourt, C., Toothaker, J., Bousvaros, A., Boston Children's Hospital Inflammatory Bowel Disease Center, Brigham and Women's Hospital Crohn's and Colitis Center, Shalek, A. K., Kean, L., Horwitz, B., Goldsmith, J., Tseng, G., Snapper, S. B., and Konnikova, L. (2020). Single-Cell Analyses of Colon and Blood Reveal Distinct Immune Cell Signatures of Ulcerative Colitis and Crohn's Disease. *Gastroenterology*, 159:591–608.e10.

Ferrante C., Recinella L., Ronci M., Menghini L., Brunetti L., Chiavaroli A., Leone S., Di Iorio L., Carradori S. and Tirillini B. (2016) et al. Multiple pharmacognostic characterization on hemp commercial cultivars: Focus on inflorescence water extract activity. *Food Chem. Toxicol.* ; 125:452–461.

Flora, S. J. S., Mittal, M. and Mehta, A. (2008). Heavy metal induced oxidative stress & its possible reversal by chelation therapy. *Indian Journal of Medical Research, 128*:501-523.

Flores-Romero, H., Ros, U., and Garcia-Saez, A. J. (2020). Pore formation in regulated cell death. *The EMBO journal*, 39a:e105753

Florio, R., De Lellis, L., Veschi, S., Verginelli, F., Di Giacomo, V., Gallorini, M., Perconti, S., Sanna, M., Mariani-Costantini, R.and Natale, A. (2018). Effects of dichloroacetate as single agent or in combination with GW6471 and metformin in paraganglioma cells. *Sci. Rep.* 8:13610.

Fontaine, E. and Bernardi, P. (1999). Progress on the mitochondrial permeability transition pore: regulation by complex I and ubiquinone analogs. *J. Bioenerg. Biomembr.* 31:335-345.

Forte M. and Bernardi P. (2006). The permeability transition and BCL-2 family proteins in apoptosis: co-conspirators or independent agents? *Cell Death Differ*. 13: 1287–1290

Fre, S. (2009). Notch signals control the fate of immature progenitor cells in the intestine. *Nature* 435:964–968.

Friedrich, M., Pohin, M. and Powrie, F. (2019). Cytokine Networks in the Pathophysiology of Inflammatory Bowel Disease. Immunity. 50:992–1006.

Furman, D., Campisi, J., Verdin, E., Carrera-Bastos, P., Targ, S. and Franceschi, C., (2019). Chronic Inflammation in the Etiology of Disease across the Life Span. *Nat. Med.* 25:1822–1832.

Garcia-Perez C., Roy S. S., Naghdi S., Lin X., Davies E. and Hajnoczky G. (2012). Bid-induced mitochondrial membrane permeabilization waves propagated by local reactive oxygen species (ROS) signaling. *Proc. Natl. Acad. Sci. U.S.A.* 109, 4497–4502

Gardai, S. J., Bratton, D. L., Ogden, C. A., and Henson, P. M. (2006). Recognition Ligands on Apoptotic Cells: a Perspective. J. *Leukoc. Biol*. 79:896–903.

Garrido, C., Galluzzi, L., Brunet, M., Puig, P. E., Didelot, C. and Kroemer, G. (2006). Mechanisms of cytochrome *c* release from mitochondria. *Cell Death Differ* 13:1423–1433.

Gbore, F. A., Adewole, A. M., Oginni, O., Adu, O. A., Akinnubi, T., Ologbonjaye, K. I., & Usaefat, A. (2020). Ameliorative Potential of Vitamins on Haematological and Biochemical Profiles of Clarias gariepinus Fed Diets Contaminated with Fumonisin B1. *International Journal of Advanced Biological and Biomedical Research*, *8*:388-402.

Gelberg H. (2018). Pathophysiological Mechanisms of Gastrointestinal Toxicity. *Comprehensive Toxicology*, 2018:139–178.

Gbore, F. A., Ologundudu, A., Arowosegbe, A. O., Ologun, T. M., Jolade, F. A. and Saliu, I. (2010). Assessment of haematological, serum biochemical and histopathological effects of subchronic dietary fumonisin B 1 in rats. *Journal of Bio-Science*, 18: 74-83

Giacomello, D. V., Chiavaroli, A., Orlando, G., Cataldi, A., Rapino, M., Di Valerio, V., Leone, S., Brunetti, L., Menghini, L.and Recinella, L. (2020). Neuroprotective and Neuromodulatory Effects Induced by Cannabidiol and Cannabigerol in Rat Hypo-E22 cells and Isolated Hypothalamus. *Antioxidants*. 9:71.

Gilbert, A., Mokam, E. C. D., Mbiantcha, M., Feudjio, R. B. D., David, N., Kamanyi, A. (2015). Gastroprotective and ulcer healing effects of Piptadeniastrum Africanum on experimentally induced gastric ulcers in rats. BMC Complement. *Altern. Med.* 15:2-14.

Giorgio V., Bisetto E., Soriano M. E., Dabbeni-Sala F., Basso E and Petronilli V. (2009). Cyclophilin D modulates mitochondrial F_OF_1-ATP synthase by interacting with the lateral stalk of the complex. *J. Biol. Chem*. 284, 33982–33988

Giorgio V., von Stockum S., Antoniel M., Fabbro A., Fogolari F., Forte M., *et al*.,(2013). Dimers of mitochondrial ATP synthase form the permeability transition pore. *Proc. Natl. Acad. Sci. U.S.A*. 110, 5887–5892

Giorgio, V., Burchell, V., Schiavone, M., Bassot, C., Minervini, G., Petronilli, V., Argenton, F., Forte, M., Tosatto, S., Lippe, G., and Bernardi, P. (2017). Ca^{2+} binding to F-ATP synthase β subunit triggers the mitochondrial permeability transition. *EMBO reports*, *18*:1065–1076.

Giorgio, V., Guo, L., Bassot, C., Petronilli, V. and Bernardi, P. (2018) Calcium and regulation of the mitochondrial permeability transition. *Cell Calcium* 70:56–63.

Green, D. R. (2019) the coming decade of cell death research: five riddles. *Cell*. 177:1094-10107.

Green, D. R and Kroemer, G. (2004). The pathophysiology of mitochondrial cell death. Science, 305: 626–629.

Grivennikov, S. I., Greten, F. R. and Karin, M. (2010). *Immunity, inflammation, and cancer*. 140: 883-899C.

Gurney, M. E., Pu, H., Chiu, A. Y., Dal Canto, M. C., Polchow, C. Y., Alexander, D. D., Caliendo, J., Hentati, A., Kwon, Y. W., & Deng, H. X. (1994). Motor neuron degeneration in mice that express a human Cu,Zn superoxide dismutase mutation. *Science (New York, N.Y.)*, *264*:1772–1775.

Hakura, A., Seki, Y., Sonoda, J., Hosokawa, S., Aoki, T., Suganuma, A., Kerns, W. D. and Tsukidate,K. (2011). Rapid induction of colonic adenocarcinoma in mice exposed to

benzo[a]pyrene and dextran sulfate sodium *Food and Chemical Toxicology,* 49:2997-3001.

Hassan, M., Hidemichi, W., Ali, A., Yusuke, O. and Noriaki, S. (2014). Apoptosis and molecular targeting therapy in cancer. *Biomed Res Int;* 2014:150-845

Hassan, A., Ijaz, S. S., Lal, R., Ali, S., Hussain, Q., Ansar, M., Khattak, R. H., and Baloch, M. S. (2016). Depth Distribution of Soil Organic Carbon Fractions in Relation to Tillage and Cropping Sequences in some Drylands of Punjab, Pakistan. *Land Degradation & Development* 27:1175-1185

Haworth R. A., Hunter D. R. (1979). The Ca^{2+}-induced membrane transition of rat liver mitochondria. II. Nature of the Ca^{2+} trigger site. *Arch. Biochem. Biophys*. 195, 460–467

He, J. (2017). Persistence of the mitochondrial permeability transition in the absence of subunit c of human ATP synthase. *Proc. Natl Acad. Sci. USA.* 114:3409–3414.

Heberle, H., Meirelles, G. V., Da Silva, F. R., Telles, G.P.and Minghim, R. (2015). InteractiVenn: A web-based tool for the analysis of sets through Venn diagrams. *BMC Bioinform.* 16:169.

He L. and Lemasters J. J. (2002). Regulated and unregulated mitochondrial permeability transition pores: a new paradigm of pore structure and function? *FEBS Lett*. 512, 1–7

Heldin, C. H., Lu, B., Evans, R. and Gutkind, J. S. (2016). Signals and Receptors. *Cold Spring Harb Perspect Biol.* 8:4.

Hengartner, M. (2000). The biochemistry of apoptosis. *Nature* 407:770–776

Henry, J. B. (1979) Clinical Diagnosis and Management by Laboratory Methods, (1), *W.B Saunders Company, Philadelphia*, PA, 1: 60.

Herick K., Krämer R., Lühring H. (1997). Patch clamp investigation into the phosphate carrier from *Saccharomyces cerevisiae* mitochondria. *Biochim. Biophys. Acta* 1321, 207–220

Heo, H. J., Kim, M. -J., Lee, J. -M., Choi, S. J., Cho, H. -Y., Hong, B., Kim, H. -K., Kim, E. and Shin, D. -H. (2004). Naringenin from Citrus junos Has an Inhibitory Effect on Acetylcholinesterase and a Mitigating Effect on Amnesia. *Dement. Geriatr. Cogn. Disord.* 17:151–157.

Hill, N. E., Castellino, D. R., Lansford, J. E., Nowlin, P., Dodge, K. A., Bates, J. E. and Pettit, G. S. (2004). Parent academic involvement as related to school behavior,

achievement, and aspirations: demographic variations across adolescence. *Child development, 75*:1491–1509.

Hitoshi, Y., Lorens, J., Kitada, S., Fisher, J., LaBarge, M., Ring, H. Z., Francke, U., Reed, J. C., Kinoshita, S. and Toso, G. P. N. (1998). A Cell Surface, Specific Regulator of Fas-Induced Apoptosis in T Cells, *Immunity*, 8: 461-471

Hostettmann, K., Marston, A., Ndojoko, K. and Wolfender, J. (2000). The potential of African plants as a source of drugs. Curr. Organic Chem. 4: 973-1010.

Hu, J., Feng, X., Valdearcos, M., Lutrin, D., Uchida, Y., Koliwad, S. K., & Maze, M. (2018). Interleukin-6 is both necessary and sufficient to produce perioperative neurocognitive disorder in mice. *British journal of anaesthesia*, 120, 537–545.

Huang, H., Xiao, X., Ghadouani, A., Wu, J., Nie, Z., Peng, C., Xu, X., and Shi, J. (2015). effects of natural flavonoids on photosynthetic activity and cell integrity in Microcystis aeruginosa. *Toxins*, *7*:66–80.

Hsu, H., Jessie, X. and David, V. G. (1995). The TNF Receptor I-Associated Protein TRADD Signals Cell Death and NF-KB Activation. *Cell*, 91: 495-504.

Hussain S, Khan AM, Rengel Z. (2019). Zincbiofortified wheat accumulates more cadmium in grains than standard wheat when grown on cadmium-contaminated soil regardless of soil and foliar zinc application. *Sci Total Environ*, 654: 402-408

Hussein, R. E., Amira A. and El-Anssary, A. A. (2018). Plants Secondary Metabolites: The Key Drivers of the Pharmacological Actions of Medicinal Plants, Herbal Medicine, *IntechOpen*. 2

Hüser, J., Rechenmacher, C. E. and Blatter, L. A. (1998). Imaging the Permeability Pore Transition in Single Mitochondria, *Biophysical Journal*, 74: 2129-2137

Huser, J. and Blatter, L. A. (1999). Fluctuations in mitochondrial membrane potential caused by repetitive gating of the permeability transition pore. *The biochemical journal*, 343: 311-317

Hutchinson, J. and Dalziel, J. M. (1963). Flora of West Tropical Africa. II. Millbank, London: *Crown Agents for Oversea Government and Administration* 4:435–436.

Hutchinson, J. and Dalziel, J.M. (2015). Flora of West Tropical Africa. *Crown Agente of the Colonies, London*. 2:14-18.

Ferrante C., Recinella L., Ronci M., Menghini L., Brunetti L., Chiavaroli A., Leone S., Di Iorio L., Carradori S. and Tirillini B.(2016) et al. Multiple pharmacognostic characterization on hemp commercial cultivars: Focus on inflorescence water extract activity. Food Chem. Toxicol. ; 125:452–461.

IARC Working Group on the Evaluation of Carcinogenic Risks to Humans (2012). Arsenic, metals, fibres, and dusts. *IARC monographs on the evaluation of carcinogenic risks to humans 100 (PT C*), 11.

Ighodaro O.M. and Akinloye O.A.(2018) First Line Defence Antioxidants-Superoxide Dismutase (SOD), Catalase (CAT) and Glutathione Peroxidase (GPX): Their Fundamental Role in the Entire Antioxidant Defence Grid. Alexandria *J. Med.*54:287–293.

Ivan, J. Fuss, W. S. and Ivashkiv L. B. (2018). signalling, epigenetics and roles in immunity, metabolism, disease and cancer immunotherapy. *Nat Rev Immunol.* 18:545-558.

Ivashkiv L. B. (2018). IFNγ: signalling, epigenetics and roles in immunity, metabolism, disease and cancer immunotherapy. *Nature reviews. Immunology*, *18*: 545–558.

Jacob, J. P. and Carter, C. A., (2008). Inclusion of buckwheat in organic broiler diets. J. Appl. Poult. Res., 17:522–528

James, A. M., Cochemé, H. M., Smith, R. A., and Murphy, M. P. (2005). Interactions of Mitochondria-targeted and Untargeted Ubiquinones with the Mitochondrial Respiratory Chain and Reactive Oxygen Species: Implications for the use of exogenous ubiquinones as therapies and experimental tools. *Journal of Biological Chemistry*, *280*:21295-21312.

Jan, R., and Chaudhry, G. E. (2019). Understanding Apoptosis and Apoptotic Pathways Targeted Cancer Therapeutics. *Advanced pharmaceutical bulletin*, 9:205–218.

Javadov, S., and Karmazyn, M. (2007). Mitochondrial permeability transition pore opening as an endpoint to initiate cell death and as a putative target for cardioprotection. *Cellular physiology and biochemistry : international journal of experimental cellular physiology, biochemistry, and pharmacology*, 20: 1–22.

Jetten, M. J. A., Kleinjans, J. C. S., Claessen, S. M., Chesné, C. and van Delft, J. H. M. (2013). Baseline and genotoxic compound induced gene expression profiles in HepG2 and HepaRG compared to primary human hepatocytes. *Toxicology in vitro* 27:2031-2040.

Jiofack, T.R.B. (2008). *Piptadeniastrum africanum* (Hook.f.) Brenan. Timbers Boisd'oeuvre. Retrievedfrom:Https??database.Prota.org/PROTAhtml/*Piptadeniastrum africanum_En.html. Accessed* [04-04- 2014]

Jiri Mestecky, Warren Strober, Michael W. Russell, Brian L. Kelsall, Hilde Cheroutre, Bart N. Lambrecht (2015). Mucosal Immunology (Fourth Edition), *Academic Press,* 1573-1612

Johnson, D. and Lardy, H. (1967) "Isolation of Rat Liver and Kidney Mitochondria," *Methods in Enzymology* 10:94-96.

Johnson, K. M., Chen, X., Boitano, A., Swenson, L., Opipari, A. W., J. R. and Glick G. D. (2005). Identification and validation of the mitochondrial F1F0-ATPase as the molecular target of the immunomodulatory benzodiazepine Bz-423. *Chem. Biol*. 12: 485–496

Johnson, C. A., Swedell, L. and Rothman, J. M., (2012). Feeding ecology of olive baboons (Papioanubis) in Kibale Nastional Park, Uganda: Preliminary results on diet and food selection. *African J. Ecol.,* 50:367-370

Joza, N., Susin, S. A., Daugas, E., Stanford, W. L., Cho, S. K., Li, C. Y., Sasaki, T., Elia, A. J., Cheng, H. Y., Ravagnan, L., Ferri, K. F., Zamzami, N., Wakeham, A., Hakem, R., Yoshida, H., Kong, Y. Y., Mak, T. W., Zúñiga-Pflücker, J. C., Kroemer, G., and Penninger, J. M. (2001). Essential role of the mitochondrial apoptosis-inducing factor in programmed cell death. *Nature,* 410:549–554.

Kaina, B. and Efferth, T. (2011) Toxicities by Herbal Medicines with Emphasis to Traditional Chinese Medicine. Current Drug Metabolism, 12:989-996.

Kataoka T, Schroter M, Hahne M, Schneider P, Irmler M, Thome M, Froelich C. J.and Tschopp J. FLIP (1998). prevents apoptosis induced by death receptors but not by perforin/granzyme B, chemotherapeutic drugs, and gamma irradiation. *J Immunol*. 161:3936–3942.

Kawamura, A., Kawamura, T., Riddell, M., Hikita, T., Yanagi, T., Umemura, H., & Nakayama, M. (2019). Regulation of programmed cell death ligand 1 expression by atypical protein kinase C lambda/iota in cutaneous angiosarcoma. *Cancer science, 110*:1780–1789.

Ke, F., Yadav P. K. and Ju, L.Z. (2012). Herbal medicine in the treatment of ulcerative colitis. Saudi *J Gastroenterol*. 18:3-10.

Kelly, G. L.and Strasser, A. (2020). Toward targeting antiapoptotic MCL-1 for cancer therapy. *Annu Rev Cancer Biol*.; 4:299–313.

Kerr, J. F., Whyllie, A. H., and Currie, A. R. (1972). Apoptosis: a basic biological phenomenon with wide-ranging implications in tissue kinetics. *British Journal of Cancer* 26:239-257.

Kharchoufa, L., Bouhrim, M., Bencheikh, N., El Assri, S., Amirou, A., Yamani, A., ... and Elachouri, M. (2020). Acute and subacute toxicity studies of the aqueous extract from Haloxylon scoparium Pomel (Hammada scoparia (Pomel)) by oral administration in rodents. *BioMed Research International*, *2020*.

Kim, M., Oh, H. S., Park, S. C., and Chun, J. (2014). Towards a taxonomic coherence between average nucleotide identity and 16S rRNA gene sequence similarity for species demarcation of prokaryotes. *Int. J. Syst. Evol. Micr*. 64:346–351.

Kim, Y. S., Li, X. F., Kang, K. H., Ryu, B., Kim, S. K. (2014). Stigmasterol isolated from marine microalgae Navicula incerta induces apoptosis in human hepatoma HepG2 cells. *BMB Rep*.;47:433-438.

Kim, E. K., Soo, H. K., Hye, S. J., Bo K. K., Min, K. M., Soo, L., Hak, C. J., Kyong, S. P. and Young M. C. (2019). The Effect of a Smartphone-Based, Patient-Centered Diabetes Care System in Patients with Type 2 Diabetes: A Randomized, Controlled Trial for 24 Weeks. *Diabetes Care,* 42:3-9.

Kobayashi, T., Siegmund, B. and Le Berre, C. (2020). Ulcerative colitis. *Nat Rev Dis Primers* 6:74.

Kohr M. J., Aponte A. M., Sun J., Wang G., Murphy E., Gucek M., et al. (2011). Characterization of potential S-nitrosylation sites in the myocardium. *Am. J. Physiol. Heart Circ. Physiol*. 300: H1327–H1335

Korshunova, A. Y., Blagonravov, M. L., Neborak, E. V., Syatkin, S. P., Sklifasovskaya, A. P., Semyatov, S. M., and Agostinelli, E. (2021). BCL2-regulated apoptotic process in myocardial ischemia-reperfusion injury (Review). *International journal of molecular medicine*, *47*:23–36.

Kothakota, S., Azuma, T., Reinhard, C., Klippel, A., Tang, J., Chu, K., McGarry, T. J., Kirschner M. W., Koths, K., Kwiatkowski and D. J., Williams, L. T. (1997). Caspase-3-generated fragment of gelsolin: effector of morphological change in apoptosis. *Science.* 278:294–298.

Kottke M., Adam V., Riesinger I., Bremm G., Bosch W., Brdiczka D., et al. (1988). Mitochondrial boundary membrane contact sites in brain: points of

hexokinase and creatine kinase location, and control of Ca^{2+} transport. *Biochim. Biophys. Acta* 935: 87–102.

Kowaltowski A. J., Castilho R. F. and Vercesi A. E. (2001). Mitochondrial permeability transition and oxidative stress. *FEBS Lett*. 495:12–15

Kroemer G, Galluzzi L. and Brenner C. (2007). Mitochondrial membrane permeabilisation in cell death. *Physiol Rev*. 87: 99-163

Kroemer, G., Galluzzi, L., Vandenabeele, P., Abrams, J., Alnemri, E. S., Baehrecke, E. K., Blagosklonny, M. V., El-Deiry, W. S., Golstein, P., and Green, D. R. (2009). Classification of cell death: *Recommendations of the Nomenclature Committee on Cell Death and Differentiation* 16:3-11.

Krzystek-Korpacka, M., Kempiński, R., Bromke, M. A., Neubauer, K. (2020). Oxidative Stress Markers in Inflammatory Bowel Diseases: Systematic Review. *Diagnostics (Basel)*. 10:601

Kuan, Y.S., Brewer-Jensen, P., Bai, W.L., Hunter, C., Wilson, C.B., Bass, S., Abernethy, J., Wing, J.S., Searles, L.L. (2009). Drosophila suppressor of sable protein [Su(s)] promotes degradation of aberrant and transposon-derived RNAs. *Mol. Cell. Biol.* 29: 5590--5603.

Kuwana, T., King, L. E., Cosentino, K., Suess, J., Garcia-Saez, A. J., Gilmore, A. P., and Newmeyer, D. D. (2020). Mitochondrial residence of the apoptosis inducer BAX is more important than BAX oligomerization in promoting membrane permeabilization. *The Journal of biological chemistry*, *295*: 1623–1636.

Lapidus, R.G. and Sokolove, P.M. (1993). Spermine inhibition of permeability transition of isolated rat liver mitochondria; An investigation of mechanism. *Arch Biochem Biophys*,306: 246-253.

Lavrik, I. N., Alexander, G. and Peter, H. K. (2005). Caspases: pharmacological manipulation of cell death. *J Clin Invest;* 115:2665-72.

Lenaz, G. (2001). The Mitochondrial Production of Reactive Oxygen Species: Mechanisms and Implications in Human Pathology. *IUBMB Life*, *52*:159–164.

Leung A. W. and Halestrap A. P. (2008). Recent progress in elucidating the molecular mechanism of the mitochondrial permeability transition pore. *Biochim. Biophys. Acta* 1777: 946–952.

Lesenefky, E. J., Slabe, T. J.., Stoll, M. S. K., Minkler, P. E. and Hoppel, C. L. (2001). Myocardial iscema selectively deplets cardiolipin in rabbit heart subsarcolemmal

mitochondria. *American Journal of Physiology- Heart and Circulatory Physiology*. 280:H2770-H2778.

Li, L., Clarice, R. W., Darden T. A. and Pedersen, L. G. (2001). Gene selection for sample classification based on gene expression data: study of sensitivity to choose of parameters of the GA/KNN method. *Bioinformatics* 17:1131-1142.

Li, J., Nicola, J. S., Jennifer, J., Michael, J. H., Sam, A. M., Danielle, D., Vanessa, C., Maria, H., Ryan, C., Dionysos, S., Rin, N., Luke, M., Siddharth, S., Elizabeth, L., Zhengmao, Y., Thomas, D. W., Teiko, S., Dimitry, D., Genee, Y. L., Klara, T., Diego, E., Isidro, H., John, R. J. and Teemu, T. J. (2017). Membrane-Proximal Epitope Facilitates Efficient T Cell Synapse Formation by Anti-FcRH5/CD3 and Is a Requirement for Myeloma Cell Killing. *Cancer Cell*; 31:383-395.

Lieberman, J. and Fan, Z. (2003). Nuclear war: the grandzyme A-bomb. *Curr. Opin. Immunol*

Liu J., Farmer J. D. J., Lane W. S., Friedman J., Weissman I., Schreiber S. L. (1991). Calcineurin is a common target of cyclophilin-cyclosporin A and FKBP-FK506 complexes. *Cell* 66:807–815

Liu, C. S., Tsai, C. S., Kuo, C. L., Chen, H. W., Lii, C. K., Ma, Y. S. and Wei, Y. H. (2003). Oxidative stress-related alteration of the copy number of mitochondrial DNA in human leukocytes. *Free Radic Res*.37:1307-1317.

Lobo, V., Patil, A., Phatak, A. and Chandra, N. (2010). Free radicals, antioxidants and functional foods: Impact on human health. *Pharmacogn Rev*. 4:118-126.

Locksley, R. M., Killeen, N. and Lenardo, M. J. (2001). The TNF and TNF receptor superfamilies: integrating mammalian biology. *Cell;* 104:487-501.

Lombardi, V. R., Etcheverría, I., Carrera, I., Cacabelos, R., and Chacón, A. R. (2012). Prevention of chronic experimental colitis induced by dextran sulphate sodium (DSS) in mice treated with FR91. *Journal of biomedicine & biotechnology*, 2012: 826178.

Lowry, O. H., Rosenbrough, N. J., Farr, A. L. and Randall, R. J. (1951). Protein measurement with Folin phenol reagent. *J Biol Chem*. 1051: 265-2.

Lopez, J. and Tait, S. W. G. (2015). Mitochondrial apoptosis: killing cancer using the enemy within. 112:957-62.

López D. V., Leger, B.S., Cox, K. J., Gill, S., Bishop, A. L., Scanlon, G. D., Walker, J. A., Gantz, V. M. and Choudhary, A. (2020). Small-Molecule Control of Super-Mendelian Inheritance in Gene Drives. *Cell Rep.* 31: 107841

Mahomoodally M.F.(2016). Characterization of phytochemical components of Ferula halophila extracts using HPLC-MS/MS and their pharmacological potentials: A multi-functional insight. *J. Pharm. Biomed. Anal.*; 160:374–382.

Manach, C., Williamson, G., Morand, C., Scarbert, A. and Rémésy, C. (2005). Bioavailability and bioefficacy of polyphenols in humans. I. Review of 97 bioavailability studies, *The American Journal of Clinical Nutrition*, 81: 230S–242S

Mandal, S., Guptan, P., Owusu-Ansah, E. and Banerjee, U. (2005). Mitochondrial regulation of cell cycle progression during development as revealed by the tenured mutation revealed in Drosophila. *Dev. Cell* 9: 843--854.

Mandal, T. K., Nildari S. and Das, N. S. (2010). Testicular toxicity in cannabis extract treated mice: association with oxidative stress and role of antioxidant enzyme systems, *Journal Toxicology and Industrial Health*. 26:11-23.

Margraf, A., and Perretti, M. (2022). Immune Cell Plasticity in Inflammation: Insights into Description and Regulation of Immune Cell Phenotypes. *Cells*, 11: 18-24.

Martel, C., Wang, Z., and Brenner, C. (2014). VDAC phosphorylation, a lipid sensor influencing the cell fate. *Mitochondrion*, *19*: 69-77.

Marzo I., Brenner C., Zamzami N., Susin S. A., Beutner G., Brdiczka D., et al. (1998). The permeability transition pore complex: a target for apoptosis regulation by caspases and bcl-2-related proteins. *J. Exp. Med*. 187:1261–1271

Mbiantcha, M., Almas, J., Shabana, S. U., Nida, D. and Aisha, F. (2017). Anti-arthritic property of crude extracts of *Piptadeniastrum africanum* (Mimosaceae) in complete Freund's adjuvant-induced arthritis in rats. *BMC complementary and alternative medicine*, 17: 1-16

Mbosso Teinkela, J. E., Siwe Noundou, X., Zeh Mimba, J. E., Meyer, F., Tabouguia, O. M., Assob Nguedia, J. C., Hoppe, H. C., Krause, R. W. M., Wintjens, R., & Azebaze, G. A. B. (2020). Compound isolation and biological activities of Piptadeniastrum africanum (hook.f.) Brennan roots. *Journal of ethnopharmacology*, *255*, 112-716

McKinnon, D. R., Graziella, P., James, A. I. J.r and Dubois-Dalcq M.(1993). A role for TGF-beta in oligodendrocyte differentiation. *The Journal of cell biology* 121:1397-1407.

Mengome, Line-E., Feuya, T., Guy, R., Eba, F. and Nsi-Emvo, E. (2009). Antiproliferative effect of alcoholic extracts of some gabonese medicinal plants on human colonic cancer cells. *Afr. J. Trad.* 6:112-117

Mensah, M., Komlaga, G., Donkor, Arnold, Caleb, A, Alexander and Dickson, Rita. (2019). Toxicity and Safety Implications of Herbal Medicines Used in Africa. *Intechopen*.10:7243

Meyer, A., Eskandari, S., Grallath, S. and Rentsch, D. (2006). AtGAT1, a high affinity transporter for gamma- aminobutyric acid in Arabidopsis thaliana. *J Biol Chem* 281:7197-204

Miller, P. K. and Ramos, S. K. (2001). Impact of cellular metabolism on the biological effects of Benzo[a]pyrene and related hydrocarbons†. *Drug metabolism reviews* 33 :1-35.

Miras, Moreno. B, Sabater, Jara. A. B., Pedreno, M. A and Almagro, L.(2016) Bioactivity of phytosterols and their production in plant in vitro cultures. *J Agric Food Chem* 64:7049–58.

Mirończuk-Chodakowska, I., Witkowska, A. M., Zujko, M. E.(2018). Endogenous Non-Enzymatic Antioxidants in the Human Body. *Adv. Med. Sci*. 63:68–78.

Mironova G. D., Gateau-Roesch O., Levrat C., Gritsenko E., Pavlov E., Lazareva A. V., et al. (2001). Palmitic and stearic acids bind Ca^{2+} with high affinity and form nonspecific channels in black-lipid membranes. Possible relation to Ca^{2+}-activated mitochondrial pores. *J. Bioenerg. Biomembr*. 33: 319–331

Mitchell P. (2011). Chemiosmotic coupling in oxidative and photosynthetic phosphorylation. 1966. *Biochim. Biophys. Acta* 18071507–1538

Mnatsakanyan, N. and Jonas, E. A. (2020). The new role of F_1F_o ATP synthase in mitochondria-mediated neurodegeneration and neuroprotection. *Experimental neurology*, 332:113-400.

Mohan, P. R. and Savithramma, N. (2019). Estimation of total phenol and tannin content present in the leaf, bark and fruits of an endemic semi-evergreen tree speciesTerminalia pallidaBrandis. *Pharma. Innovation*, 8:518-522.

Moujalled, D., Strasser, A. and Liddell, J. R. (2021). Molecular mechanisms of cell death in neurological diseases. *Cell Death Differ* 28: 2029–2044

Muganza D.M., Fruth B., Lami J.N., Mesia G., Kambu O., Tona G., Kanyanga R.C., Cos P., Maes L. and Apers S.(2016) In vitro antiprotozoal and cytotoxic activity of 33 ethonopharmacologically selected medicinal plants from Democratic Republic of Congo. *J.Ethnopharmacol*. 141:301–308.

Muhammad M. U., Kwazo H. A., Abubakar L. and Bagna E. A (2017). Nutritional profile and phytochemical composition of Gardenia sokotensis (Boscia of the rock) *African Journal of Food Science and Technology* 8: 108-112.

Myers, J. N., Harris, K. L., Rekhadevi, P. V., Pratap, S. and Ramesh, A. (2021). Benzo(a)pyrene-induced cytotoxicity, cell proliferation, DNA damage, and altered gene expression profiles in HT-29 human colon cancer cells. *Cell Biol Toxicol* 37:891–913.

Nagawa S, Xu T, Lin D, Dhonukshe P, Zhang X, Friml J, et al. (2012) ROP GTPase-Dependent Actin Microfilaments Promote PIN1 Polarization by Localized Inhibition of Clathrin-Dependent Endocytosis. *PLoS Biol* 10: e1001299.

Nandi, A, Yan, L. J., Jana, C. K., Das, N. (2019). Role of Catalase in Oxidative Stress- and Age- *Oxidative Medicine and Cellular Longevity.* 2019:19 pages

Newmeyer, D. D., Bossy-Wetzel, E., Kluck, R. M., Wolf, BB., Beere, H. M. and Green D. R. (2000). Bcl-Xl does not inhibit the function of Apaf-1. *Cell Death Differ*. 7:402-407.

Nicholls, D. G. and Ferguson, S. J. (2013). The Chemiosmotic Proton Circuit in Isolated Organelles: Theory and Practice. 4th edn,53–87. Nigeria".*International Journal of Advanced Research in Botany*, 5:1824.

Nimse, S. B. and Pal, D. (2015) Free Radicals, Natural Antioxidants, and Their Reaction Mechanisms. *RSCAdv.*;5:27986–28006.

Ning, X., Qi, H. and Li. (2017). Discovery of novel naphthoquinone derivatives as inhibitors of the tumor cell specific M2 isoform of pyruvate kinase. *Eur J Med Chem* 138:343-352.

Nissar, S., Sameer, A. S., Rasol, R., Chowdri, N. A. and Rashid, F. (2017). Glutathione S Transferases: Biochemistry, Polymorphism, Colorectal Carcinogenesis. *J Carcinog Mutagen* 8:286

Noté, O. P., Tapondjou, A. L., Mitaine-Offer, A.-C., Miyamoto, T., Pegnyemb, D. and Lacaille-Dubois M.-A.(2013) Triterpenoid saponins from *Piptadeniastrum africanum* (Hook. f.) Brenan. *Phytochem.* Lett. 6:505–510.

Nualkaew, S., Padee, P. and Talubmook, C. (2015). Hypoglycemic activity in diabetic rats of stigmasterol and sitosterol-3-O-Î²-D-glucopyranoside isolated from Pseuderanthemum palatiferum (Nees) Radlk. leaf extract. *Journal of Medicinal Plants Research*, 9: 629-635

Nualkaew, Somsak, Padee, Peerawit, Chusri and Talubmook. (2018). Hypoglycemic activity in Rhain B. Cope, in *Veterinary Toxicology* (Third Edition).

Nyananyo, B. L. (2006) Plants from the Niger Delta. *Onyoma Research Publications*, Port Harcourt, 403 pages

Obeng, J. (2021). "Diabetic Education for Nurses to Enhance Patient Outcomes". *Walden Dissertations and Doctoral Studies.* 11319.

Oda, E., Ohki R., Murasawa, H., Nemoto, J., Shibue, T., Yamashita, T., Tokino, T., Taniguchi, T., Tanaka, N and Noxa, a (2000) BH3-only member of the Bcl-2 family and candidate mediator of p53-induced apoptosis. *Science.*288:1053-1058

Ogboru, R. O., Okolie, P. L.and Agboje, I. (2015) Phytochemical Screening and Medicinal Potentials of the Bark of Dacryodes edulis (G. Don) HJ Lam. *J Environ Anal Chem* 2: 158.

Okayasu, I, Hatakeyama, S, Yamada, M, Ohkusa, T,Inagaki, Y and Nakaya, R (1990) "A novel method in the induction of reliableexperimental acute and chronic ulcerative colitis in mice," *Gastroenterology*, 98:694–702.

Okayasu, I., Hatakeyama, S., Ohkusa, T .(1990) A novel method in the induction of reliable experimental acute and chronic ulcerative colitis in mice. *Gastroenterology* . 98:694–702.

Olanlokun, O. J., Oyebode, T. O. and Olorunsogo, O. O. (2017). Effects of vacuum liquid chromatography (chloroform) fraction of the stem bark of Alstonia boonei on mitochondrial membrane permeability transition pore. *Journal of Basic and Clinical Pharmacy*; 8:22-29

Olanlokun, O. J., Oloke, K., Olorunsogo, O.O. (2020). Methanol extract and fraction of *Anchomanes difformis* root tuber modulate liver mitochondrial membrane permeability transition pore opening in rats. *Avicenna J Phytomed* ;10:190-201.

Olanlokun, O., Bodede, O., Prinsloo, G. and Olorunsogo, O. (2020). Comparative antimalarial, toxicity and mito-protective effects of Diospyros mespiliformis Hochst. ex A. DC. and Mondia whitei (Hook.f.) Skeels on Plasmodium berghei infection in mice. *Journal of Ethnopharmacology* 268:11-17.

Olanlokun, J. O., Balogun, F. A. and Olorunsogo, O. O. (2021). Chemotherapeutic and prophylactic antimalarial drugs induce cell death through mitochondrial-mediated apoptosis in murine models. *Drug and chemical toxicology*; 44:47-57.

Olanlokun, J. O., Ekundayo, M. T., Koorbanally, N. A. and Olorunsogo, O. O. (2022). Hexane fraction of Globimetula braunii induces mitochondria-mediated apoptosis in Plasmodium berghei-infected mice, *Toxicology Reports*.9:769-777

Olojo, F. O., Akinleye, S. A., Ogundairo, S. A. and Ubochi, V. C. (2023). *Arganosa spinosa* essential oil ameliorates colonic damage and extraintestinal alterations in a rat model of acetic acid-induced colitis by suppressing oxidative stress and inflammation. *Advances in Traditional Medicine* (in press)

Olojo, F. O., Anifowose, O. A., Ojo, E. A. and Adebayo, A. Q. (2022). Anti-malarial effect of the crude extract of the stem bark of *Piptadeniastrum africanum* (HOOK. F.) on hemosiderin level of the spleen. The Polytechnic, *Science and Engineer Perspectives* 16: 50-59

Olorunsogo O.O and Malomo S.O.(1985). Sensitivity of Oligomycin-inhibitedrespiration of isolated rat liver mitochondria to perfluidone, a fluorinated arylalkylsulfonamide. *Toxicology*, 35: 231-240.

Olorunsogo, O.O., Bababunmi, E.A. and Bassir, O. (1979). Uncoupling effect of N-phosphonomethylglycine at liver mitochondria. *Biochem. Pharm.,* 27:925-927

OlowofolahanA.O, Adeoye O.A, Offor G.N, Adebisi L.A and Olorunsogo O.O. (2015). Induction of Mitochondrial Membrane Permeability Transition Pore Opening and Cytochrome C Release by Fractions of Drymaria cordata. *Arch. Bas. App. Med*., 3: 135–144.

Olowofolahan, A. O., Adeoye, Y. D. and Olorunsogo, O. O. (2017). Induction of Mitochondrial-Mediated Apoptosis by Solvent Fractions of Methanol Extract of Heliotropium indicum in Rat Liver Cells. *Annual Research and Review in Biology*. 17: 1-15.

Olowofolahan, A. O., Bolarin, O. L. and Olorunsogo, O. O. (2020). In vitro and in vivo effect of 3-Para-fluorobenzoyl-propionic acid on rat liver mitochondrial permeability transition pore opening and lipid peroxidation. *Annals of Science and Technology*, *5*:39-44.

Olowofolahan, Adeola and Olorunsogo, O. (2020). Induction of apoptosis in rat liver cells via caspase activation by chloroform fraction of methanol extract of drymaria cordata. *European Journal of Biomedical and Pharmaceutical Sciences* 5. 73-83.

Olowofolahan, A. O. and Olorunsogo, O. O. (2021). Fractions of Ageratum conyzoides L.(Compositae) induce mitochondrial-mediated apoptosis in rats: Possible option in monosodium glutamate-induced hepatic and uterine pathological disorder. *Journal of Ethnopharmacology*, 277:114-192.

Owoeye, E., Rachel, Ogboru, Bakpolor, V., and Omobude, D. (2018). phytochemical screening and proximate analysis of the bark of Piptadeniastrum africanum hook (fabaceae). 19:135-141.

Oyebode, O. T., Odejide, T. T., Kukoyi, A. J., Adebisi, L. A. and Olorunsogo, O. O. Effects of different fractions of Calliandra portoricensis root bark on isolated ratliver mitochondrial membrane permeability transition pore. *Afr J Med Med Sci*., 2012; 41: 399–409.

Oyebode O. T., Abolaji A. O., Oluwadare J. O., Adedara A. O. and Olorunsogo (2020) Apigenin ameliorates D-galactose-induced lifespan shortening effects via antioxidative activity and inhibition of mitochondrial-dependent apoptosis in Drosophila melanogaster. *Journal of Functional Foods*.;69:103-957.

Oyebode, O. T., Akinyelu, J. O., Oamen, E. A., and Olorunsogo, O. O. (2018). Methanol fraction of *Calliandra portoricensis* root bark activates caspases via alteration in mitochondrial viability in vivo. *Journal of Herbmed Pharmacology*, *7*:251-258.

Oyedeji, T. A., Onireti, D. O., Lasisi, O. S., Akobi, C. I. and Olorunsogo, O. O.(2021) Stigmasterol isolated from the chloroform fraction of *Adenopus breviflorus* Benth fruit induces mitochondrial-dependent apoptosis in rat liver. *J Complement Integr Med.* 18:737-744

Osei, E., Der, J., Owusu, R., Kofie, P. and Axame, w. K. (2017). The burden of HIV on Tuberculosis patients in the Volta region of Ghana from 2012 to 2015: implication for Tuberculosis control. *BMC Infect Dis* 17, 504

Pandey, P., Bajpai, P., Siddiqui, M. H., Sayyed, U., Tiwari, R.and Shekh, R.. (2019) Elucidation of the chemopreventive role of stigmasterol against Jab1 in gall bladder carcinoma. *Endocr Metab Immune Disord Drug Targets* 19:826–837.

Papadakis, K. A., and Targan, S. R. (2000). The role of chemokines and chemokine receptors in mucosal inflammation. *Inflammatory bowel diseases*, *6*(4), 303–313.

Pardo, J., Bosque, A., Brehm, R., Wallich, R., Naval, J., Müllbacher, A., Anel, A and Simon M. M. (2004). Apoptotic pathways are selectively activated by granzyme A and/or granzyme B in CTL-mediated target cell lysis. *J Cell Biol.*167:457-468.

Parone, P. A., Da Cruz, S., Han, J. S., McAlonis-Downes, M., Vetto, A. P., Lee, S. K., Tseng, E., and Cleveland, D. W. (2013). Enhancing mitochondrial calcium buffering capacity reduces aggregation of misfolded SOD1 and motor neuron cell death without extending survival in mouse models of inherited amyotrophic lateral

sclerosis. *The Journal of neuroscience : the official journal of the Society for Neuroscience*, 33: 4657–4671.

Parrott, J. M., Redus, L. and O'Connor J. C. (2016). Kynurenine metabolic balance is disrupted in the hippocampus following peripheral lipopolysaccharide challenge. *J. Neuroinflammation.* 13:1-25.

Pastorino, J. G., Shulga, N. and Hoek, J. B. (2002). Mitochondrial binding of hexokinase II inhibits Bax-induced cytochrome c release and apoptosis. *The Journal of biological chemistry*, 277;7610–7618.

Pathak, D., Gandhi, D., & Gupta, A. (2019). Self-supervised exploration via disagreement. In *International conference on machine learning* 97:5062-5071

Pavlov E., Zakharian E., Bladen C., Diao C. T., Grimbly C., Reusch R. N., et al. (2005). A large, voltage-dependent channel, isolated from mitochondria by water-free chloroform extraction. *Biophys. J*. 88:2614–2625

Payab, M., Hasani - Ranjbar, S., Shahbal, N., Qorbani, M., Aletaha, A. and Haghi-Aminjan, H. (2019). Effect of the herbal medicines in obesity and metabolic syndrome: a systematic review and meta-analysis of clinical trials. *Phytother. Res.* 34:526–545.

Payab, M., Shirin, H., Nazila, S., Mostafa, Q., Azadeh, A., Hamed, H., Akbar, S., Fatemeh, K., Shekoufeh, N., Shokoufeh, H., Mohammad, A. and Bagher, L. (2020). Effect of the herbal medicines in obesity and metabolic syndrome: A systematic review and meta-analysis of clinical trials. *Phytother Res;* 34:526-545.

Pellegrino-Coppola D.(2020). Regulation of the mitochondrial permeability transition pore and its effects on aging. *Microb Cell.*7:222-233.

Peoples, J. N., Saraf, A. and Ghazal, N., (2019). Mitochondrial dysfunction and oxidative stress in heart disease. *Exp Mol Med* 51:1–13

Perše, M, and Cerar, A. (2012). "Dextran Sodium Sulphate Colitis Mouse Model*: Traps and Tricks*", s 2012: 13 pages

Pessayre, D., Fromenty, B., and Mansouri, A. (2004). Mitochondrial injury in steatohepatitis. *European journal of gastroenterology & hepatology*, 16:1095–1105.

Peter, M. E and Krammer, P. H. (1998) Mechanisms of CD95 (APO-1/Fas)- mediated apoptosis. *Curr Opin Immunol.*10:545-551.

Peters, J. P., Jannie, B., Viola, O., Minoru, F., O Krähenbühl, Jurg Tschopp, Jan W Slot and Hans J Geuze (1991). Cytotoxic T lymphocyte granules are secretory lysosomes,

containing both perforin and granzymes. *The Journal of experimental medicine* 173:1099-1109.

Petersen, R.C. (2017). Free-radicals and advanced chemistries involved in cell membrane organization influence oxygen diffusion and pathology treatment. *AIMS Biophys.*4:240-283.

Pistritto, G., Trisciuoglio, D., Ceci, C., Garufi, A., D'Orazi, G. (2016). Apoptosis as anticancer mechanism: function and dysfunction of its modulators and targeted therapeutic strategies. *Aging (Albany NY).* 4:603-619.

Porter, R. J., Kalla, R. and Ho, G. T. (2020). Ulcerative colitis: Recent advances in the understanding of disease pathogenesis. *F1000 Faculty Rev*- 9: 294.

Potęga, A. (2022). Glutathione-Mediated Conjugation of Anticancer Drugs: An Overview of Reaction Mechanisms and Biological Significance for Drug Detoxification and Bioactivation. *Molecules.*;27:5252.

Pratiwi, R., Nantasenamat, C., Ruankham, W., Suwanjang. W., Prachayasittikul, V., Prachayasittikul S. and Phopin K. (2021). Mechanisms and Neuroprotective Activities of Stigmasterol Against Oxidative Stress-Induced Neuronal Cell Death via Sirtuin Family. *Front Nutr.* 12:648-995

Priyadarshini, Medha & Kotlo, Kumar & Dudeja, Pradeep & Layden, Brian. (2018). Role of Short Chain Fatty Acid Receptors in Intestinal Physiology and Pathophysiology. 10.1002/cphy.c170050.

Pustylnikov, S., Costabile, F. and Beghi, S., Facciabene, A. (2018). Targeting mitochondria in cancer: current concepts and immunotherapy approaches. *Transl Res.* 202:35-51.

Raaflaub, J. (1953). Die schwellung isolierter leberzellmitochondrien und ihre physikalisch-chemische beeinflussbarkeit. *helvetica physiologica et pharmacologica acta*, 11: 142-156.

Rahman, M. d., Tanvir, M. d., Abdus Sobur, M. d., Saiful Islam, Samina Ievy, M. d., Jannat Hossain, M. E., El Zowalaty, A. M. M., Taufiquer, R. and Hossam M. A. (2020). "Zoonotic Diseases: Etiology, Impact, and Control" *Microorganisms* 8: 1405

Rai, N. K,, Tripathi, K., Sharma, D. and Shukla, V. K. (2005). Apoptosis: a basic physiologic process in wound healing. *International Journal of Lower Extremity Wounds*, 4: 138-144.

Ram, S., Mitra, M., Shah, F., Tirkey, S, R. and Mishra, S. (2020). Bacteria as an alternate biofactory for carotenoid production: A review of its applications, opportunities and challenges, *Journal of Functional Foods*, 67: 103-867

Ramprasath, V. R. and Awad, A. B. (2015). Role of phytosterols in cancer prevention and treatment. *J AOAC Int* 98:735–738.

Rasola A. and Bernardi P. (2007). The mitochondrial permeability transition pore and its involvement in cell death and in disease pathogenesis. *Apoptosis* 12:815–833

Rasola A., Sciacovelli M., Chiara F., Pantic B., Brusilow W. S. and Bernardi P. (2010). Activation of mitochondrial ERK protects cancer cells from death through inhibition of the permeability transition. *Proc. Natl. Acad. Sci. U.S.A.* 107:726–731

Redza-Dutordoir, M. and Averill-Bates, D. A. (2016). Activation of apoptosis signalling pathways by reactive oxygen species, Biochimica et Biophysica Acta (BBA) - *Molecular Cell Research,* 1863:2977-299.

Reed JC: (1997) Bcl-2 family proteins: regulators of apoptosis and chemoresistance in haematologic malignancies. *Semin Haematol* 34: 9-19.

Ricchelli F., Šileikyte J. and Bernardi P. (2011). Shedding light on the mitochondrial permeability transition. *Biochim. Biophys. Acta* 1807: 482–490.

Rosenberg, N., Mor-Cohen, R., Sheptovitsky, V. H., Romanenco, O., Hess, O. and Lahav, J. (2019). Integrin-mediated cell adhesion requires extracellular disulfide exchange regulated by protein disulfide isomerase. *Experimental Cell Research.* 381:77-85

Kroemer G, Galluzzi L. and Brenner C. (2007). Mitochondrial membrane permeabilisation in cell death. *Physiol Rev*. 87: 99-163

Rosenberg, D. W., Huakang, H., Oladimeji, A., Takayasu, I., Charle,s G. and Lee, M. E. (2019). Inhibition of PGE2/EP4 receptor signaling enhances oxaliplatin efficacy in resistant colon cancer cells through modulation of oxidative stress. *Scientific reports* 9: 1-11.

Rubio-Moscardo, F., Blesa, D., Mestre, C., Siebert, R., Balasas, T., Benito, A., Rosenwald, A., Climent, J., Martinez, J. I., Schilhabel, M., Karran, E. L., Gesk, S., Esteller, M., deLeeuw, R., Staudt, L. M., Fernandez-Luna, J. L., Pinkel, D., Dyer, M. J., Martinez-Climent, J. A. (2005). Characterization of 8p21.3 chromosomal deletions in B-cell lymphoma: TRAIL-R1 and TRAIL-R2 as candidate dosage-dependent tumor suppressor genes. *Blood.*106:3214–22

Russell, J. H. and Ley, T. J. (2002). Lymphocyte mediated cytotoxicity. *Annual Review of Immunology,* 20: 323-370.

Sarna, K. S. (1991). Physiology and pathophysiology of colonic motor activity: Part one of two. *Digestive diseases and sciences* 36:827-862.

Salami, O. A., Fafunso, M. A., Choudhary, M. Iqbal. and Atta-Ur-R. Toxicological Screening of the Ethanol Root Bark Extracts of Two Anthocleista Species (2015). *World Applied Sciences Journal* 33: 1164-1170.

Salaudeen, I. A., Olojo, F. O., Rasheed-Adeleke, A. A., Onye, I. and Ogunbusola, S. G. (2023). Evaluation of the Nephroprotective and Hypoglycemic effect of aqueous extract of leaf and root of *Thaumatococcus danielli* on Alloxan-induced Diabetic Rats. *International journal of Innovative Research and Development.*12: 78-83.

Salemcity, A. J., Olanlokun, J. O., Adegoke, A. O., Olojo, F. O. and Olorunsogo, O. O (2023). Reversal of mitochondrial permeability transition pore and pancreas degeneration by chloroform fraction of *Ocimum gratissimum* leaf extract in type 2 diabetic rat model. *Frontiers in Pharmacology* (in press)

Sander, R. G. and Powell, C. B. (2004). Expression of notch receptors and ligands in the adult gut. *Journal of Histochemistry & Cytochemistry* 52: 509-516.

Satheeshkumar, N., Mukherjee, P. K., Bhadra, S.and Saha, B. (2010). Acetylcholinesterase enzyme inhibitory potential of standardized extract of Trigonella foenum graecum L and its constituents. *Phytomedicine*; 17:292–295.

Szabo, S. J., Sullivan, B. M., Peng, S. L. and Glimcher, L. H. (2003). Molecular mechanisms regulating Th1 immune responses. *Annual review of immunology*, 21:713–758.

Scaffidi, C., Schmitz, I., Krammer, P.H., ***and*** Peter, M.E. ***(1999).*** The role of c-FLIP in modulation of CD95-induced apoptosis. *J Biol Chem*; 274:1541–1548**.**

Schinzel A. C., Takeuchi O., Huang Z., Fisher J. K., Zhou Z., Rubens J., et al. (2005). Cyclophilin D is a component of mitochondrial permeability transition and mediates neuronal cell death after focal cerebral ischemia. *Proc. Natl. Acad. Sci. U.S.A.* 102, 12005–12010

Scholtysek, C., Krukiewicz, A.A., Alonso, J.L., Sharma, K.P., Sharma, P.C., and Goldmann, W.H. (2009). Characterizing components of the Saw Palmetto Berry Extract (SPBE) on prostate cancer cell growth and traction. *Biochem Biophys Res Commun* 379:795–798.

Schuler., M., and Green, D.R. (2001). Mechanisms of p53-dependent apoptosis. *Biochem Soc Trans;* 29:684-688.

Scorrano L., Penzo D., Petronilli V., Pagano F. and Bernardi P. (2001). Arachidonic acid causes cell death through the mitochondrial permeability transition. Implications for tumor necrosis factor-α apoptotic signaling. *J. Biol. Chem*. 276:12035–12040

Scorrano, L., Oakes, S. A., Opferman, J. T., Cheng, E. H., Sorcinelli, M. A. Pozzan, T. and Korsmeyer, S. J (2003). Bax and Bak Regulation of endoplasmic reticulum Ca^{2+}:A control point for apoptosis *Science* 300:135-139

Sertel, S., Eichhorn, T., Plinkert, P.K., and Efferth, T. (2011). Chemical composition and antiproliferative activity of essential oil from the leaves of a medicinal herb, Levisticum officinale, against UMSCC1 head and neck squamous carcinoma cells. *Anticancer Res,* 31:185–191.

Seenivasan, R., Indu, H., Archana, G. and Geetha, S. (2010). Antibacterial activity of some marine algae from South East coast of India. *Journal of Pharmacy Research*. 3:1907-1912.

Shahzad, N., Khan, W., M. d., S., Ali, A., Saluja, S.S., and Sharma, S. (2017). Phytosterols as a natural anticancer agent: Current status and future perspective. *BioMed Pharmacother* 88:786–794.

Shi, Y. (2002). Mechanisms of caspase activation and inhibition during apoptosis. Mol Cell; 9:459-70.

Shoshan-Barmatz, V. and Ben-Hail, D. (2012). VDAC, a multi-functional mitochondrial protein as a pharmacological target. *Mitochondrion, 12*: 24–34.

Siemen D. and Ziemer M. (2013). What is the nature of the mitochondrial permeability transition pore and what is it not? *IUBMB Life* 65:255–262

Singh, R., Letai, A. and Sarosiek, K. ***(2019).*** Regulation of apoptosis in health and disease: the balancing act of BCl-2 family *proteins;* 20:175-93.

Singh, R.P., Dhania, G.., Sharma, A., Jaiwal, P.K., (2007). Biotechnological approaches to improve phytoremediationefficiciency for environment contaminants. In: Environmental bioremediation technologies, Singh, S.N. Tripahti, R.D. (Eds) *Springer,* 223-258

Singh, K., Zouhar, M., Mazakova, J., ***and*** Rysanek, P. (2014). Genome wide identification of the immunophilin gene family in Leptoshaeriamaculans:

a casual agent of blackleg disease in oilseed rape (Brassicanapus). *OMICS* 18:645-657.

Singh, P., Jain, M., Saxena, V., Sharva, V., Boddun, M., & Jain, N. (2019). Evaluation of local–delivery system containing 80% aloe vera gel used as an adjunct to scaling and root planning in chronic periodontitis: A clinical study. *Dent Oral Maxillofac Res, 5*: 1-5.

Sivakumar and Balasubramanian, 2020. A Review on Some Folk Medicinal Plants and Their Common Uses. *Research Biotica*, 3: 131- 134.

Skuratovskaya, E. and Yurakhno, Violetta and Chesnokova, Irina. (2020). Biochemical response of two fish species of Gobiidae (Gobiiformes) to Cryptocotyle (Opisthorchiida, Heterophyidae) metacercariae infection from the mouth of the river Chernaya (Black Sea). *Ecologica Montenegrina.* 38: 158-165.

Šileikyte, J., Blachly-Dyso,n E., Sewell, R., Carpi, A., Menabo, R., Di Lisa, F., Ricchelli, F., Bernardi, P. and Forte, M. (2015). Regulation of the Mitochondrial Permeability Transition Pore by the Outer Membrane does not Involve the Peripheral Benzodiazepine Receptor (TSPO). *J. Biol. Chem.*

Slee, E. A., Harte, M. T., Kluck, R. M., Wolf, B. B., Casiano, C. A., Newmeyer, D. D., Wang, H. G., Reed, J. C., Nicholson, D. W., Alnemri, E. S., Green, D. R., and Martin, S. J. (1999). Ordering the cytochrome c-initiated caspase cascade: hierarchical activation of caspases-2, -3, -6, -7, -8, and -10 in a caspase-9-dependent manner. *The Journal of cell biology*, 144: 281–292.

Slee, E. A., Colin, A. and Seamus, J. M. (2001). Executioner caspase-3,-6, and-7 perform distinct, non-redundant roles during the demolition phase of apoptosis. *Journal of biological Chemistry* 276 7320-7326.

Sofowora, A., Ogunbodede, E., & Onayade, A. (2013). The role and place of medicinal plants in the strategies for disease prevention. *African journal of traditional, complementary, and alternative medicines : AJTCAM*, 10:210–229.

Sokolove P. M. and Shinaberry R. G. (1988). Na^+-independent release of Ca^{2+} from rat heart mitochondria. Induction by adriamycin aglycone. *Biochem. Pharmacol*. 37, 803–812

Sorgato M. C., Keller B. U. and Stühmer W. (1987). Patch-clamping of the inner mitochondrial membrane reveals a voltage-dependent ion channel. *Nature* 330:498–500.

Spainhour, C. (2007). 6 Gastrointestinal.Toxicology of the Gastrointestinal Tract, 135.

Strobel, A., Gutknecht, L., Rothe, C., Reif, A., Mössner, R., Zeng, Y., Brocke, B. and Lesch, K-P.(2003). Allelic variation in 5-HT1A receptor expression is associated with anxiety- and depression-related personality traits. *Journal of neural transmission* 110 :12.

Su, L. J., Zhang, J. H., Gomez, H., Murugan, R., Hong, X., Xu, D., Jiang, F., and Peng, Z. Y. (2019). Reactive Oxygen Species-Induced Lipid Peroxidation in Apoptosis, Autophagy, and Ferroptosis. *Oxidative medicine and cellular longevity*, 2019:5080843.

Sultan A. and Sokolove P. M. (2001). Free fatty acid effects on mitochondrial permeability: an overview. *Arch. Biochem. Biophys*. 386,:52–61

Susin, S.A., Daugas, E., Ravagnan, L., Samejima, K., Zamzami, N., Loeffler, M., Costantini, P., Ferri, K.F., Irinopoulou, T., Prevost, M.C., Brothers, G., Mak, T.W., Penninger, J., Earnshaw, W.C., and Kroemer G (2000). Two distinct pathways leading to nuclear apoptosis., 192: 571-580

Suttiarporn, P., Chumpolsri, W., Mahatheeranont, S., Luangkamin, S., Teepsawang, S., and Leardkamolkarn, V. (2015). Structures of phytosterols and triterpenoids with potential anti-cancer activity in bran of black non-glutinous rice. *Nutrients* 7:1672–87.

Suzan, O., and Adnan, A. (2021) "LIPID PEROXIDATION" In the book:Accenting Lipid Peroxidation. Intechopen, Chapter 1:1-11

Swaminathan, V., Reddy, S. K., and Dommer, S. L. (2012). Spillover effects of ingredient branded strategies on brand choice: A field study. *Marketing Letters*, *23*, 237-251

Swarup, R., Kargul, J., Marchant, A., Zadik, D., Rahman, A., Mills, R., ... and Bennett, M. J. (2004). Structure-function analysis of the presumptive Arabidopsis auxin permease AUX1. *The Plant Cell*, 16: 3069-3083..

Takahashi N., Hayano T. and Suzuki M. (1989). Peptidyl-prolyl cis-trans isomerase is the cyclosporin A-binding protein cyclophilin. *Nature* 337:473–475

Tamara, Y., Forbes-Hernández, Francesca, G., Massimiliano, G., Luca, M., José, L. Q., José, M., and Alvarez-Suarez, M. B. (2014). The effects of bioactive compounds from plant foods on mitochondrial function: A focus on apoptotic mechanisms, *Food and Chemical Toxicology*, 68:154-182.

Tanaka, T. (2012). Development of an inflammation-associated colorectal cancer model and its application for research on carcinogenesis and chemoprevention. *International journal of inflammation* 2012.

Tapan, K. P., and Smruti R. M. (2015). Caspases: An apoptosis mediator *J. Adv. Vet. Anim. Res*., 2: 18-22

Tatiana, A. N. D. (2008). Ethnobotany and traditional medicine of pygmies baka. *Medicinal Chemistry and Pharmaceutical Technology.* 2:129-133.

Testa, U. and Riccioni, R . (2007). Deregulation of apoptosis in acute myeloid leukemia. *Haematological* 92:81-94.

Thavasu, P. W. *et al*. (1992) Measuring cytokine levels in blood. Importance of anticoagulants, processing, and storage conditions. *J Immunol Methods* 153:115–124.

Thavasu, P. W., Longhurst, S., Joel, S. P., Slevin, M. L., & Balkwill, F. R. (1992). Measuring cytokine levels in blood. Importance of anticoagulants, processing, and storage conditions. *Journal of immunological methods*, *153*(1-2), 115–124.

The Toxicologist, 56th Annual Meeting and ToxExpo™ Baltimore, Maryland | March 12–16, 2022

Thun, M. J., DeLancey, J. O., Center, M. M., Jemal, A. and Ward, E.M. (2010). "The global burden of cancer: priorities for prevention," *Carcinogenesis*.31:100–110,.

Traber, M. G. and Stevens, J. F. (2011) Vitamins C and E: beneficial effects from a mechanistic perspective. *Free Radic Biol Med*. 51:1000-1013.

Tungmunnithum, D., Thongboonyou, A., Pholboon, A., and Yangsabai, A. (2018). Flavonoids and Other Phenolic Compounds from Medicinal Plants for Pharmaceutical and Medical Aspects: An Overview. *Medicines (Basel, Switzerland)*, *5*:93

Tungmunnithum, D., Thongboonyou, A., Pholboon, A., Yangsabai, A. (2017). Ulcerative Colitis with Serum-Derived Bovine Immunoglobulin Added to the Standard Treatment Regimen. *Case Rep Gastroenterol*; 11:335-343.

Turdo, A., Veschi, V., Gaggianesi, M., Chinnici, A., Bianca, P, Todaro, M and Stassi, G. (2019). Meeting the Challenge of Targeting Cancer Stem Cells. *Frontiers in Cell and Developmental Biology*. 7:2019

Urbani, A., Giorgio, V., Carrer, A., Franchin, C., Arrigoni, G., Jiko, C., Abe, K., Maeda, S., Shinzawa-Itoh, K., Bogers, J. F. M., McMillan, D. G. G., Gerle, C., Szabò, I., & Bernardi, P. (2019). Purified F-ATP synthase forms a Ca^{2+}-dependent high-conductance channel matching the mitochondrial permeability transition pore. *Nature communications*, 10: 4341.

Ungaro, R., Colombel, J. F., Lissoos, T., and Peyrin-Biroulet, L. (2019). A Treat-to-Target Update in Ulcerative Colitis: A Systematic Review. *The American journal of gastroenterology*, 114:874–883.

van Delft Joost, H. M., Karen, M., Yvonne, C. M S., Marcel H. M. van Herwijnen., Karen, J. J. B., André, B. and Jos, C. S. K. (2010). Time series analysis of benzo [A] pyrene-induced transcriptome changes suggests that a network of transcription factors regulates the effects on functional gene sets. *Toxicological Sciences* 117:381-392.

Vaseva A. V., Marchenko N. D., Ji K., Tsirka S. E., Holzmann S. and Moll U. M. (2012). p53 opens the mitochondrial permeability transition pore to trigger necrosis. *Cell* 149: 1536–1548

Vianello, A., Casolo, V., Petrussa, E., Peresson, C., Patui, S., Bertolini, A., Passamonti, S., Enrico Braidot, E. and Zancani, M. (2012). The mitochondrial permeability transition pore (PTP) — An example of multiple molecular exaptation?, *Biochimica et Biophysica Acta (BBA) - Bioenergetics*, 1817:2072-2086.

Vernon, H., Wehrle, C. J., Alia, V. S. K. and Kasi, A. (2022). Anatomy, Abdomen and Pelvis: Liver. In *StatPearls*. Publishing.

Virtanen, R.(2023). *Claude Bernard*. *Encyclopedia Britannica*.

von Einem, J. C., Peter, S., Günther, C., Volk, H. D., Grütz, G., Salat, C., Stoetzer, O., Nelson, P. J., Michl, M., Modest, D. P., Holch, J. W., Angele, M., Bruns, C., Niess, H. and Heinemann, V. (2017). Treatment of advanced gastrointestinal cancer with genetically modified autologous mesenchymal stem cells - TREAT-ME-1 - a phase I, first in human, first in class trial. *Oncotarget*, *8*:80156–80166.

Wallace, D. C., Fan, W., & Procaccio, V. (2010). Mitochondrial energetics and therapeutics. *Annual review of pathology*, *5*:297–348.

Walsh C. T., Zydowsky L. D., McKeon F. D. (1992). Cyclosporin, A, the cyclophilin class of peptidylprolyl isomerases, and blockade of T cell signal transduction. *J. Biol. Chem*. 267:13115–13118

Wang P. and Heitman J. (2005). The cyclophilins. *Genome Biol*. 6:226.1–226.6

Wang, G., Zhang, J., He, R., Liu, C., Ma, T. and Bao, Z. (2017). Runoff Sensitivity to Climate Change for Hydro-Climatically Different Catchments in China. *Stoch. Environ. Res. Risk Assess.* 31:1011–1021.

Weydert, C. J. and Cullen, J. J. (2010). Measurement of superoxide dismutase, catalase and glutathione peroxidase in cultured cells and tissue. *Nat Protoc.* 5:51-66

WHO, (2012). IARC Working Group on the Evaluation of Carcinogenic Risks to Humans. (2012). "Biological agents A review of human carcinogens." *IARC monographs on the evaluation of carcinogenic risks to humans* 100:1-441.

Whyllie, A. H., Kerr, J. F. and Currie, A. R. 1980 Cell death: the significance of apoptosis. *International Review of Cytology* 68:251-306.

Woodfield, K. Y., Price, N. T. and Halestrap, A. P. (1997). cDNA cloning of rat mitochondrial cyclophilin. *Biochimica et Biophysica Acta (BBA)-Gene Structure and Expression*, 1351:27-30.

World Health Organization. (2018). World health statistics: monitoring health for the SDGs, sustainable development goals. World Health Organization.978:92-94

Woyengo, T. A., Ramprasath, V. R., Jones, P. J. (2009) Anticancer effects of phytosterols. *Eur J Clin Nutr* 63: 813–820.

Wu, Chin-Chung Mei-Ling Chan, Wen-Ying Chen, Ching-Yi Tsai, Fang-Rong Chang and Yang-ChangWu. MCT-05-0027. Published August 2005

Wu, H. J., Wu, E. (2012) The role of gut microbiota in immune homeostasis and autoimmunity. *Gut Microbes*. 3:4-14.

Wu, K., Diqing, S., Jinming, L., Renata, S. and Jian-Ping, W. (2019). Magnetic nanoparticles in nanomedicine: a review of recent advances. *Nanotechnology;* 30: 2003.

Xiang, W., Yang, C.-Y., and Bai, L. (2018). MCL-1 inhibition in cancer treatment. *Onco. Targets Ther*. 11:7301–7314.

Xu, X., Lai, Y., and Hua, Z. C. (2019). Apoptosis and apoptotic body: disease message and therapeutic target potentials. *Bioscience reports*, *39*: BSR20180992.

Yang, E., Zha, J., Jockel, J., Boise, L. H., Thompson, C. B., and Korsmeyer, S. J. (1995). Bad, a heterodimeric partner for Bcl-XL and Bcl-2, displaces Bax and promotes cell death. *Cell* (80) 285–291.

Zamzami N. and Kroemer G. (2001). The mitochondrion in apoptosis: how Pandora's box opens. *Nat. Rev. Mol. Cell. Biol*. 2, 67–71

Zengin, G., Uysal, A., Diuzheva, A., Gunes, E., Jekő, J., Cziáky, Z., and Mahomoodally, M. F. (2018). Characterization of phytochemical components of Ferula halophila extracts using HPLC-MS/MS and their pharmacological potentials: A multi-

functional insight. *Journal of Pharmaceutical and Biomedical Analysis*, *160*:374-382.

Zha, J., Harada, H., Yang, E., Jockel, J.and Korsmeyer, S. J. (1996) Serine phosphorylation of death agonist BAD in response to survival factor results in binding to 14-3-3 not BCL-X(L). *Cell*. 87:619-28.

Zhang, H., Jin-Jiao, H., Ruo-Qiu, Fu., Xin, Liu., Yan-Hao, Zhang., Jing, Li., Lei, Liu., Yu-Nong, L., Q, Qing-Song Luo, Qin Ouyang and Ning Gao (2018). Flavonoids inhibit cell proliferation and induce apoptosis and autophagy through downregulation of PI3Kγ mediated PI3K/AKT/mTOR/p70S6K/ULK signaling pathway in human breast cancer cells. *Sci Rep*, 8:11-255.

Zhong, Q-Y, Gelaye, B., Zaslavsky, A. M., Fann, J. R., Rondon, M. B. and Sánchez, S. E., (2015) Diagnostic Validity of the Generalized Anxiety Disorder - 7 (GAD-7) among Pregnant Women. *(Hook.f.) Brenan and Cathormionaltissimum (Hook.f.)* PLoS ONE 10:4

Zhou, B. R., Feng, H., Ghirlando, R., Li, S., Schwieters, C.D., Bai, Y. (2016). A Small Number of Residues Can Determine if Linker Histones Are Bound On or Off Dyad in the Chromatosome. J. Mol. Biol. 428(20): 3948--3959.

Zhou, B., Caudal, A., Tang, X., Chavez, J. D., McMillen, T. S., Keller, A., Villet, O., Zhao, M., Liu, Y., Ritterhoff, J., Wang, P., Kolwicz, S. C. Jr., Wang, W., Bruce, J. E. and Tian, R.(2022). Upregulation of mitochondrial ATPase inhibitory factor 1 (ATPIF1) mediates increased glycolysis in mouse hearts. *J Clin Invest.* 132:10.

Zhu, Z., Cai, T., Fan, L., Lou, K., Hua, X., Huang, Z., & Gao, G. (2020). Clinical value of immune-inflammatory parameters to assess the severity of coronavirus disease 2019. *International Journal of Infectious Diseases*, 95: 332-339.

Zoratti M., Szabó I. and De Marchi U. (2005). Mitochondrial permeability transitions: how many doors to the house? *Biochim. Biophys. Acta* 1706: 40–52.

Yuan, R., Young, S., Liang, J., Schmid, M., Miego, A. and Stupack, D. (2011). Caspase-8 isoform 6 promotes death effector filament formation independent of microtubules. *Apoptosis : an international journal on programmed cell death* 17:229-235

Zwick, M., Esposito, C., Hellstern, M. and Seelig, A. (2016). How Phosphorylation and ATPase Activity Regulate Anion Flux though the Cystic Fibrosis Transmembrane Conductance Regulator (CFTR). *J Biol Chem*. 291:14483-14498

APPENDICES

Standard Protein Curve

This was determined by preparing various standard solutions which are then assayed for their values.

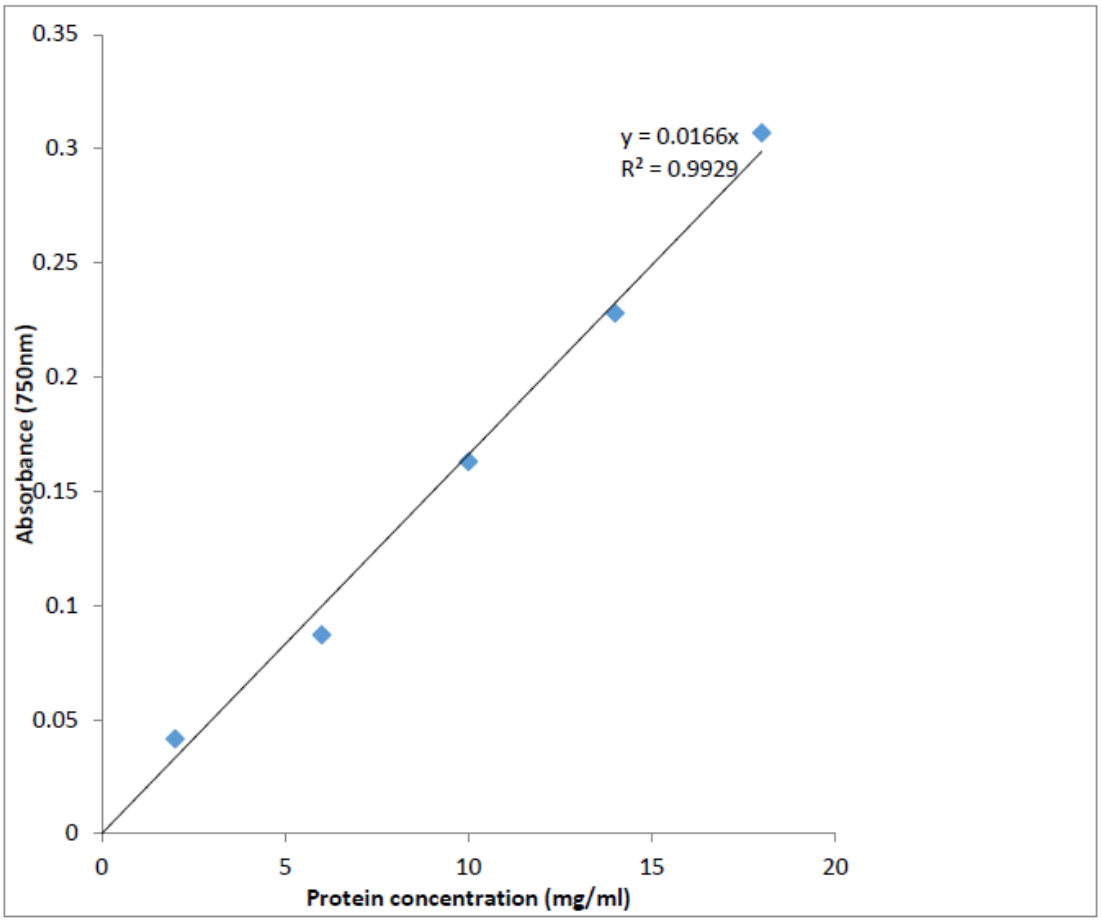

Protein curve

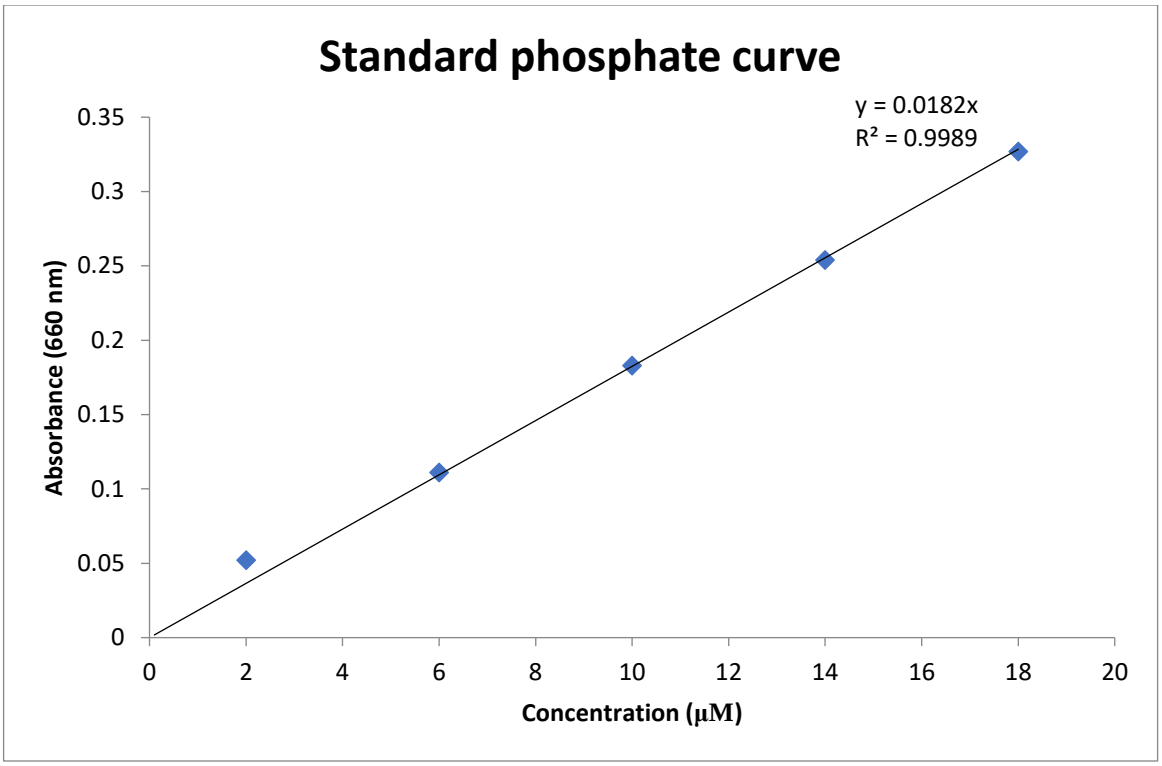

Standard Phosphate curve